Worcester Polytechnic Institute
Digital WPI

Major Qualifying Projects (All Years) | Major Qualifying Projects

April 2013

Microfabrication of 3D Tissue Engineering Scaffolds Using a Low-Cost 3D Printer

Elizabeth Laura Mayor
Worcester Polytechnic Institute

Jesse Daniel Halter
Worcester Polytechnic Institute

Nicholas Patrick Trabucco
Worcester Polytechnic Institute

Thomas Sung Butler
Worcester Polytechnic Institute

Follow this and additional works at: https://digitalcommons.wpi.edu/mqp-all

Repository Citation
Mayor, E. L., Halter, J. D., Trabucco, N. P., & Butler, T. S. (2013). *Microfabrication of 3D Tissue Engineering Scaffolds Using a Low-Cost 3D Printer*. Retrieved from https://digitalcommons.wpi.edu/mqp-all/348

This Unrestricted is brought to you for free and open access by the Major Qualifying Projects at Digital WPI. It has been accepted for inclusion in Major Qualifying Projects (All Years) by an authorized administrator of Digital WPI. For more information, please contact digitalwpi@wpi.edu.

Worcester Polytechnic Institute, Biomedical Engineering Department

Microfabrication of 3D Tissue Engineering Scaffolds Using a Low-Cost 3D Printer

MQP Project Advised by: Professor Domhnull Granquist-Fraser

& Co-advised by: Professor Sakthikumar Ambady

Student Authors: Thomas S. Butler, Jesse D. Halter, Elizabeth L. Mayor, Nicholas P. (Musselman) Trabucco

Submitted on April 25, 2013

Project Unique ID # DGF-111B

Abstract

Bone tissue engineering has many potential applications including healing bone after trauma, repairing and bone defects associated with cancer. However tissue scaffolds are required to create 3D cultures in vitro. Current scaffold fabrication techniques do not allow for adequate control over the internal pore network. With the advent of rapid prototyping fully customized pore structures are feasible. Here we describe the process for creating a biomorphic bone tissue engineering Poly-lactide scaffold using a low cost 3D extrusion printer. We have developed a scaffold that is built fully using a 3d printer and successfully seeded with mouse osteoblast cells using a collagen hydrogel. We have determined that this scaffold has biomimetic geometry and preserves cellular bio-functionality.

Authorship

Abstract:	Elizabeth Mayor
Introduction:	Nicholas Trabucco
Literature Review:	Jesse Halter
Project Strategy:	All
Alternative designs:	All
Design Verification:	Elizabeth Mayor
Discussion:	Tom Butler and Elizabeth Mayor
Final Design Validation:	Jesse Halter
Conclusions:	Nick Trabucco

Acknowledgements

We would like to thank Professor Fraser and Professor Ambady for their continued advice and help throughout this project. We would also like to thank the other MQP team working on this project DGF 111-A for their collaboration. Thank you to Professor Potami and Professor Hera for all their help with mathematical modeling and computational fluid dynamics. Many thanks to Industrial Motions Engineering for donating their time and energy to help us with manufacturing the micro-bore holes within the custom printer nozzles free of charge. Also thank you to MakerBot Industries, for authorizing and distributing their stock nozzle CAD SolidWorks file and working with our team as we attempted to modify our MakerBot Replicator to satisfy the aims of this project. Thank you to Lisa Wall for all her help as lab manager. Also thank you to Hans Snyder for all his help teaching the team how to perform histology. Thank you to all the other professors and students and who helped us take this project from an idea to practice, and our friends and family for all their love and support along the way.

Table of Contents

Abstract 1
Authorship 2
Acknowledgements 3
Table of Contents 4
Chapter 1: Introduction 10
Chapter 2: Literature Review 13
2.1 Clinical Need 13
2.2 Manufacturing Tissue Engineering 3D Scaffolds 15
2.2.1 Traditional manufacturing technologies 16
2.2.2 Prior scaffold manufacturing technologies 16
2.2.3 Rapid prototyping manufacturing technologies 16
2.2.4 Tissue engineering scaffolds manufactured with rapid prototyping technologies 19
2.3 Nature inspired biomimetic functional geometry scaffold designs 19
2.4 Mathematically modelable scaffold design 20
2.5 Bone tissue parameters for 3D tissue engineering scaffold designs 20
Chapter 3: Project Strategy 22
3.1 Client Statement: 22
3.2 Constraints 22
3.3 Objectives 23
3.3.1 Low Cost 25
3.3.2 Rapidly Manufactured (Rapid) 25
3.3.3 Biocompatible Material (Biocompatible) 25
3.3.4 Biomorphic 26
3.3.5 Permeable 27
3.3.6 Degradable 27
3.4 Revised client statement 28
3.5 Project Approach 28
Chapter 4: Alternative Designs 30
4.1 Needs Analysis 30
4.2 Functions & Specifications 31
4.2.1 Promote cell adhesion 31

4.2.2 Promote cell proliferation and differentiation 31
4.2.3 Diffuse nutrients uniformly 31
4.3 Design Alternatives 32
4.3.1 Minimal Surfaces Modeling 34
4.3.2 2D Stacked or 3D Space Filling Fractals 37
4.3.3 2D Stacked Mesh 38
4.3.4 Simple Unit Cells 39
4.3.5 Other Design Considerations 40
4.4 Conceptual Tentative Final Design 45
4.5 Feasibility Study & Experiments Methodology 46
4.5.1 Feasibility studies 46
4.5.2 Experiments Methodology 48
4.6 Preliminary Data 48
4.6.1 Nozzle resolution improvement feasibility study 48
Chapter 5: Design Verification: 51
5.1 Small scale printing 51
5.1.1 Initial testing 51
5.1.2 Nozzle fabrication 51
5.1.3 New nozzle testing and stretching 54
5.2 Culture System Verification 56
5.2.1 MC 3T3 E1 Differentiation 57
5.2.2 Collagen gel system 58
5.2.3 MC 3T3 E1 in collagen 59
5.3 Final testing 59
5.3.1 Methodology 60
5.3.2 Results 60
Chapter 6: Discussion 63
6.1 Biocompatibility: Cyto-toxicity 63
6.2 Biomorphic: Geometric biomorphism to provide functional biomimetic 63
6.2.1Biomorphism: Pore size and geometry 64
6.2.2 Functional Biomimetics: Calcium production and differentiation 64
6.3 Customizable using a low cost printer 64

6.4 Constraints 65
Economic impact 65
Environmental impact 66
Societal influence 66
Ethical concerns 66
Health and safety issues 67
Manufacturability 67
Sustainability 67
Chapter 7: Final Design & Validation 68
Chapter 8: Conclusions & Recommendations 75
8.1 Conclusions 75
8.2 Recommendations 76
8.2.1 Modifying the overall shape of the scaffold 76
8.2.2 Improved material 76
8.2.3 Bio flow chamber for better nutrient flow 77
8.2.4 Cancerous testing 77
References 78
Appendix A: Mathematical models used 82
Gyroid inverse of thickened cube 82
Gyroid thickness bounded with cylinder: 82
Gyroid filled one pore structure: 82
Diamond TPMS thickened: 82
Diamond TPMS filled one pore structure: 82
Gyroid thicked cube: 82
Thin Wall Gyroid: 83
High Resolution Thin Wall Gyroid - 10 x 10 x 10 ratio: 83
High Resolution Thin Wall Gyroid - 10 x 10 x 3 ratio: 83
Final Testing - 10x10x3: 83
Appendix B: Makerbot ReplicatorG Settings 84
Appendix C: Cell Seeding Protocol 85
Appendix D: Determination of Cell Seeding Density 86
Appendix E: SolidWorks CAD Drawings 87

Appendix F: Esprit CAM Software Settings Used to Manufacture Nozzles..... 97
Appendix G: Nozzle & Small Printing Test Measurement Images 140

Table of Figures

Figure 1 – Example of 2D tissue culture techniques 14
Figure 2 – Representative image for need of live 3D tissue engineering 15
Figure 3 – Objectives Tree Structure for 3D Printed Tissue Scaffold 24
Figure 4 – Pair-wise Comparison Chart for the 3D Printed Scaffold Project 24
Figure 5 – Functions-Means Chart 33
Figure 6 – Morphological Chart 34
Figure 7 – Example of a TPMS Structure 35
Figure 8 – Example of a Thickened TPMS Structure 36
Figure 9 – Examples of 2D Layered Space Filling Fractals 38
Figure 10 – (a)2D Mesh Lattice (45° angle) & 2D Layers can be Stacked into (b)3D Block Structures (iso)39
Figure 11 – Simple Unit Cells and 4x4x4 Cubes of Each Unit Cell Concept 40
Figure 12 – Selection / Evaluation Matrix Chart 45
Figure 13 – Comparison of Original 0.4mm Nozzle (left) to Possible 0.1mm Nozzle (right) Designs 49
Figure 14 – Custom nozzles stretching extruded filament size 56
Figure 15 – Close up image of scaffold printed with 200µm nozzle with stretch 56
Figure 16 – Differentiation at different seeding densities in standard tissue culture plastic 57
Figure 17 – Alizarin red staining of paraffin embedded gel 59
Figure 18 – Hoechst staining of scaffolds at day 6 61
Figure 19 – Day 19 Hoechst staining 61
Figure 20 – Alizarin red staining in full scaffold system 62
Figure 21 – Image of final printed scaffold design surface 74

Table of Tables

Table 1 – Micro-drilling results 53
Table 2 – Actual bore sizes 54
Table 3 – Filament stretching in custom nozzles 55

Chapter 1: Introduction

Tissue engineering is an emerging field with a relatively broad range of medical applications, including advanced wound healing and organ replacement. Bone repair has long been considered a practice that involves the fixation of the injury while allowing the body to reconstruct itself, or if the injury is severe enough sometimes implants are required. With the dawn of tissue engineering another option is on the rise. The possibility of creating a biologically compatible implant that allows complete recovery of injuries which might not be possible from using other previous methods can be highly valuable to those suffering moderate to severe bone damage.

Three dimensional manufacturing can be used to create a scaffold that, in conjunction with cell seeding, can create similar implants but until recently normal practices have been either highly expensive or unable to control the internal structure reliably. Such methods include gas foaming, salt leeching and electro-spinning, which allow the control of the pore size and porosity but are somewhat difficult to control the interconnectivity of the pores. Rapid 3D printing is a relatively recent process that allows the manufacturing of scaffolds with the ability to control the internal structure. The problem that arises from the use of this technology is that high-end printers are still expensive. Our goal for this project was to develop a method of using an inexpensive 3D printer to produce a scaffold that can be used to seed cells and allow them to create a potential bone implant.

In order to accomplish such a task there are several factors that needed to be considered, the first being the actual printer that would be used. The Makerbot Replicator is an inexpensive commercially sold printer that is designed to be used for personal printing in one's home. In order to get this kind of printer to create a scaffold that can be used for cell seeding there are several hurdles to overcome. The positioning resolution of the Replicator is accurate enough to get the size and definition that would be needed but the extrusion diameter was too large to effectively produce the structure. The filament chosen to become the material used for the scaffold needed to be both biocompatible and able

to be printed with accurately. Aside from the printer's capabilities the other aspects including the designed shape of the scaffold and the method of getting cells to attach within the entirety of the scaffold. Throughout this project we sought the solutions to these problems.

The key to finding a correct morphology that we could use involved finding a shape that we could easily model that had the desired porosity, surface area to volume ratio and in many senses provide an environment for the cells that would mimic nature. Using computer modeling, a triply periodic minimal surface based shape was chosen to be the general structure. Since it was modeled using a mathematical formula, it was possible to customize the size of the structure and its pores as well as the surface area to volume ratio to match the desired porosity. This model was able to be transferred to the Makerbot software in order to print.

The printing of the model itself was also looked into in order to maximize its success as a cell scaffold. The Replicator is built to handle both PLA (poly-lactide) and PVA (poly-vinyl alcohol), but taking into account the degradation time of PLA would allow for cell culturing while PVA would not, PLA was chosen. With the material chosen the next step was to achieve the printing accuracy to produce structures of the desired size. This required the extrusion nozzle of the printer to be significantly smaller, which was accomplished by creating new nozzles using micro-drills. Several sized nozzles were created and after testing to see the extruded filament size, the nozzle measuring close to half the diameter of the standard nozzle. To get even smaller print sizes we adopted the concept of stretching the filament while printing by programming the printer to extrude less material while traveling at the same rate. The print speed was also lowered to a fraction of the normal speed in order to reduce the defects that can occur during the process. The final testing models were printed to the size of a 10mm x 10mm x 3mm squares.

Cell seeding was the next obstacle that was looked into in order to discover a way to allow the cells to enter the scaffold in a uniform density and attach to the walls of the scaffold itself. The concept of using a collagen gel mixed with the desired concentration of cells was accepted and after testing a couple forms of collagen, the group settled on a rapid setting collagen called PureCol EZ Gel. The idea behind using this was to create the collagen/cell mixture, inject it onto the samples and allow it to wick into the porous structure of the scaffold.

The effectiveness of our design was tested during a two week time span. Testing was designed so that scaffolds seeded with bone tissue cells were evaluated for their location in the scaffold and their ability to differentiate at many time points. These sections were then imaged for cell presence and calcium deposits for which the results were promising.

Chapter 2: Literature Review

2.1 Clinical Need

There is a clinical demand for method(s) to produce custom 3D living tissue structures rapidly and cost-effectively (Moroni, L. *et al*, 2008; Fielding, G. A. *et al*, 2012; Kapfer, S. C. *et al*, 2011). There are numerous medical applications and end-goals for replacement 3D living tissue found in-progress within recent research literature. Some example tissue engineering applications include replacement skin for burn victims (Supp, D. *et al*, 2012), replacement organs such as kidneys, lungs, liver, and heart (Atala, A. *et al*, 2012; Bronzino, D. (editor), 2006) to address diseases or trauma, disease free replacement coronary arteries (Tiwari, A. *et al*, 2003) to address heart attacks, bone tissue replacement to address trauma or total joint replacement revision surgeries where patients bone is damaged and unsuitable to house the replacement artificial joint components (Teraoka, F. *et al*, 2010; Terrier, A. *et al*, 2009), as well as numerous other research and clinical purposes within the fields of tissue engineering and regenerative medicine.

Traditional cell culture techniques, as illustrated in Figure 1 below, used within industry to date involve two-dimensional (2D) tissue growth in Petri-dishes, well-plates, or other 2D cell culture containers. These 2D techniques have been found to have limited applicability in the realm of functional thick 3D tissue engineering applications, such as the 3D tissue example illustrated in Figure 2 further below. Cutting edge research involving 3D tissue engineering typically involves more complex equipment such as 3D tissue bio-reactors and one of two common strategies or a mix of both: complex cellular self assembly and artificial scaffold based approaches (Rolle, M. W., 2012; “Methods in Bioengineering: 3D Tissue Engineering”, 2010; Yeong, W. Y. *et al*, 2004; Yoo, D. *et al*, 2012).

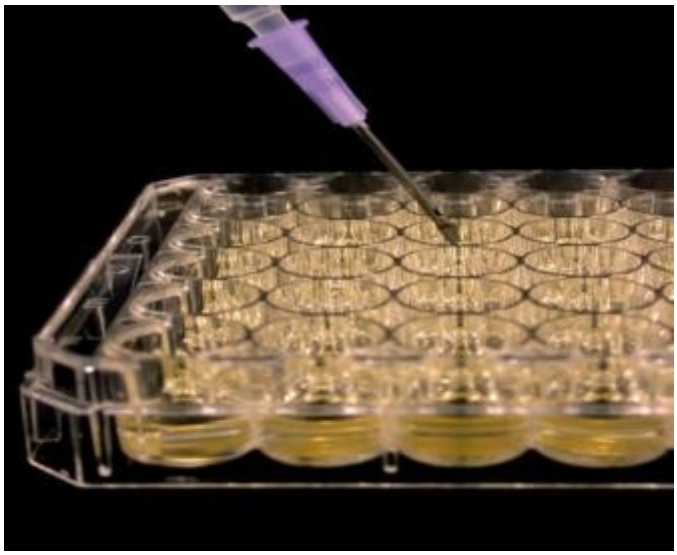

Figure 1 – Example of 2D tissue culture techniques ("Needle & Plate", www.flickr.com, 2013)

Many researchers believe the best solution is to learn how living tissues originally develop and the bio-signals and controls native within the body to signal this development, in order to re-create the natural process in an induced tissue engineering application to regenerate or replace damaged tissues (Gwyther, T. A., *et al*, 2011; Rolle, M. W., 2012). This approach is best described as self-assembled 3D tissue engineering. While this approach has many merits due to its aim of recreating an already existing natural 3D tissue generation process, there are numerous complex interactions and ongoing research to address various existing knowledge gaps and challenges between fetal 3D tissue generation and adult replacement 3D tissue generation that must be addressed prior to widespread application of self-assembled 3D tissue engineering (Gwyther, T. A., *et al*, 2011; Rolle, M. W., 2012). There are also limitations to self-assembly 3D tissue engineering techniques, such as in development of structural tissues, such as bone and cartilage of adult patients. In these applications patients need artificial means of providing the necessary structural support while the regenerative or replacement tissue develops, until the tissue is capable of withstanding the structural support needed.

A shorter-term solution to 3D tissue engineering applications involves utilizing artificial biocompatible 3D tissue scaffolds to guide cells into the needed 3D tissue shapes. These tissue scaffolds can be either non-degrading permanent biocompatible replacement tissue scaffold materials, or short or long-term degrading biocompatible materials. While there are numerous applications for non-structural tissue applications, the use artificial tissue scaffolds for structural tissue have a distinct advantage over self-assembly approaches, in that they can be designed to provide the necessary structural integrity needed until the 3D replacement tissue has developed enough to provide the structural support on its own (Amirkhani, S. *et al*, 2012; Becker, S. T. *et al*, 2009; Fang, Z. *et al*, 2005; Fisher, J. *et al*, 2009; Goonoo, N. *et al*, 2013; Guarino, V., *et al*, 2008; Pandithevan, P. , *et al*, 2009; Roshan-Ghias, A. F., *et al*, 2011; Terrier, A., *et al*, 2009).

Figure 2 – Representative image for need of live 3D tissue engineering ("Organ-Regeneration-Ear-615.Jpg." wikispaces, 2013)

2.2 Manufacturing Tissue Engineering 3D Scaffolds

Tissue engineering 3D scaffold designs have only recently begun to be researched and developed in the past decade or two, as manufacturing technology and design control of designs for tissue engineering applications were previously lacking. Significant advances in the equipment and manufacturing techniques have been made in recent decades allowing much improved control of

designs and obtaining the necessary order of magnitude necessary, micro- and nano- scales, for tissue engineering applications.

2.2.1 Traditional manufacturing technologies

Traditional manufacturing techniques such as drilling, machining, and molding processes involve subtractive processes, where bulk material in near-net shapes are obtained and modified to generate the necessary end-product. These techniques are inadequate for tissue engineering applications, as there is no ability to control the internal structure on the micro-scale to create the internal pore networks needed for tissue engineering purposes. Other manufacturing techniques were necessary for pioneering tissue engineering applications to produce controlled internal porous structures.

2.2.2 Prior scaffold manufacturing technologies

Techniques such as gas foaming and salt leaching were commonly utilized for early tissue engineering scaffold designs, producing scaffold designs with internal porous structures and some control of the resulting internal pore size, porosity void fraction, and pore interconnectivity through tightly controlled manufacturing techniques. These designs still lack the necessary internal pore design control to produce consistent relevant pore sizes and highly interconnected internal pore structures that are beneficial to enhanced cellular in-growth and proliferation (Amirkhani, S., *et al*, 2012; Hsu, Y., *et al*, 2007; Moroni, L., *et al*, 2008; Nachtrab, S., *et al*, 2012; Pham, Q. P., *et al*, 2006; Zeltinger, J., *et al*, 2001).

2.2.3 Rapid prototyping manufacturing technologies

Newly developing rapid prototyping technologies utilizing additive processes, built layer by layer, have been utilized extensively in recent 3D scaffold tissue engineering research. These relatively new manufacturing techniques offer much greater control of the internal pore size and pore interconnectivity than prior manufacturing techniques (Amirkhani, S., *et al*, 2012; Armillotta, A., *et al*, 2007; Becker, S., *et al*, 2009; Cheah, C. M., *et al*, 2003 Part 1 & 2; Kapfer, S. C., *et al*, 2011; Maher, P.S., *et*

al, 2009; Moroni, L., *et al*, 2008; Noritomi, P., *et al*, 2009; Pang, L., *et al*, 2007; Phattanaphibul, T., *et al*, 2011; Sachlos, E., *et al*, 2003; Woesz, A., 2008; Yeong, W. Y., *et al*, 2004). There are numerous types of rapid prototyping equipment broadly grouped into the following categories, including granular material binding technologies, photolithography technologies, and fused deposition modeling technologies.

Granular material binding technologies take highly controlled and precision sized powder substances and roll out over a building surface in thin layers. Various technologies are then utilized to bind specific regions of the building surface together to build the desired structure, with subsequent layers added above and bound to the prior layers to generate a 3D structure. These granular material binding technologies can utilize metal, plastic, or ceramic materials depending on the binding technology used, with some available biocompatible materials available for tissue engineering scaffold applications. Selective Laser Sintering (SLS) utilizes lasers to sinter or micro-melt materials together at the site of the laser focus, while others use liquid dispensed binding agents, such as chemically reactive reagents or adhesives to bind the granular material base into the desired structures (Cheah, C. M., *et al*, 2003 – Part 1 & 2; Rajagopalan, S., *et al*, 2006; Teraoka, F., *et al*, 2010; Woesz, A., 2008).

Photolithography based rapid prototyping techniques utilize photo-sensitive liquids that cure or solidify when light energy is focused above threshold energy or intensity levels. Subsequent liquid layers are added and selectively solidified to generate the layer-by-layer 3D structure. The primary materials used for this technology are polymeric based, with some biocompatible material formulations available for tissue engineering scaffold applications (Amirkhani, S., *et al*, 2012; Melchels, F. P., *et al*, 2010; Yoo, D., July 2012).

Fused deposition modeling (FDM) rapid prototyping technologies involves continuous melt extrusion of small plastic filaments layer-by-layer with binding to the prior layer to generate the desired 3D structure. There are limited stock materials available for FDM based printing, with most commonly

available materials being acrylonitrile-butadiene-styrene (ABS) and poly-lactide (PLA) ("3 Dimensional Printers Below $20,000 - Comparison Chart." Castle Island Co., 2013). PLA is a biocompatible material, and many other biocompatible materials could also be utilized with this technology for tissue engineering scaffold applications (El-Amin, S. F. *et al*, 2006).

Significant advances in these relatively recent additive process rapid prototyping technologies occur on a regular basis, improving manufactured part resolutions, adding new compatible materials, and reducing costs of the equipment with higher manufacturing volumes and industrial and commercial utilization. The cost of some rapid prototyping technologies is becoming low enough to be considered cost effective for small office use and personal in-home 3D printing (MakerBot Industries, 2013). These low costs could also significantly increase the volume of tissue engineering research and development applications, as prior generation and more expensive equipment justification cost limitations are becoming less and less burdensome within the industry. However, it must first be determined if these low-cost 3D printing technologies are capable of producing functional 3D tissue engineering scaffolds at adequate resolutions and with biocompatible materials that the prior much more expensive rapid prototyping technologies had previously proven feasible.

A rapid prototyping comparison website exists to compare and contrast all available or soon-to-be-available technologies under $20,000 ("3 Dimensional Printers Below $20,000 - Comparison Chart." Castle Island Co., 2013). From the comparison chart compiled on this website, it can be seen that that majority of these low-cost 3D printing technologies are FDM-based. While FDM processes are continuously improving and reducing the printed part resolution, these technologies remain on the edge as potential applications for tissue engineering scaffold designs having biomimetic pore size and porosity void fraction ratios. A currently unavailable, but promising 3D printer based on photo-lithography technology having an adequate minimum feature resolution for tissue engineering applications, called

the Form1, is reported to be available in the late spring to early summer of 2013 from Form Labs in Massachusetts ("Formlabs – the Form 1", 2013). Details of the product material utilized and the potential availability of biocompatible materials for tissue engineering scaffold applicability in the future remains unknown at the time of this report.

2.2.4 Tissue engineering scaffolds manufactured with rapid prototyping technologies

There are numerous recent tissue engineering 3D scaffold design research and development efforts involving rapid prototyping technologies. A large portion of these prior rapid prototyping 3D tissue engineering scaffold design efforts have involved basic layered grids, unit cells, or gas foaming/salt leach techniques (Amirkhani, S., *et al*, 2012; Armillatta, A., *et al*, 2007; Becker, S. T., *et al*, 2009; Bucklen, A., *et al*, 2009; Cheah, C. M., *et al*, 2003 – Part 1 & 2; Fang, Z., *et al*, 2005; Fielding, J. A., *et al*, 2012; Fisher, J., *et al*, 2009; Freed, L. E., *et al*, 1994; Guarino, V., *et al*, 2008; Hsu, Y. H., *et al*, 2007; Maher, P. S., *et al*, 2005; Moroni, L., *et al*, 2008; Nachtrab, S., *et al*, 2012; Phattanaphibul, T., *et al*, 2011; Woesz, A., 2008; Yeong, Y. W., *et al*, 2004; Zeltinger, J., *et al*, 2001), with only a few developments involving more complex and uniquely designed biomimetic shapes (Bártolo, P., *et al*, 2009; Hockaday, L. A., *et al*, 2012; Kapfer, S. C., *et al*, 2011; Melchels, F. P., *et al*, 2010; Pandithevan, P., *et al*, 2009; Rajagopalan, S., *et al*, 2006; Vozzi, G., *et al*, 2004; Yoo, D., June 2012; Yoo, D., July 2012). While there is some precedence for complex 3D tissue engineering scaffold designs being manufactured using rapid prototyping technologies, there appears to be a lack of research into available low-cost rapid prototyping technologies for 3D tissue engineering scaffold designs having complex biomimetic designs.

2.3 Nature inspired biomimetic functional geometry scaffold designs

Nature has evolved living tissue designs over millions of years to become optimized for specific functional tasks. Examples of nature's evolutionary design optimization can be found in numerous plant and animal species. Many trees have space filling growing and outreaching branches to maximize the

available surface area of their leaves exposed to solar energy. Many various tissues, such as sea corals, and internal lung tissue have continuous folded and repetitive structures and micro-structures to maximize their surface area exposed to their environment to provide optimal nutrient and waste exchange. Natural bone tissues have highly interconnected porous structures that allow for internal nutrient and waste diffusion, while also maintaining high structural rigidity and support through more dense exterior shells, while using the same basic building material throughout.

Biomimetic design concepts inspired by applicable natural evolutionary processes can yield highly optimized designs without need for iterative trial and error based design approaches, potentially saving significant time and expenses in the process (Hsu, Y. H., *et al*, 2007; Rajagopalan, S., *et al*, 2006). This project aims to utilize nature inspired biomimetic functional geometrical designs to generate 3D bone tissue engineering scaffold designs.

2.4 Mathematically modelable scaffold design

There are numerous advantages to creating complex designs based on mathematically models. Mathematical based structural model designs can be utilized to perform structural evaluations and simulations of complex shaped designs to determine design strengths in various planes or at specific critical design locations. Mathematical based designs are also easily adjustable to fit various specifications or conditions to provide customized designs (Melchels, F. P., *et al*, 2010; Kapfer, S. C., *et al*, 2011). Due to the many advantages of mathematically modelable designs, this project aims to utilize a mathematically based 3D tissue engineering scaffold design that maintains a highly biomorphic design to natural bone structure.

2.5 Bone tissue parameters for 3D tissue engineering scaffold designs

Bone tissue has numerous features and typical specifications that apply to 3D tissue engineering scaffold designs. As identified in various prior literatures, bone tissue in-growth and proliferation is

typically optimized if the pore size of the scaffold is maintained in the 200-400 micron range (Hsu, Y. H. *et al*, 2007; Teraoka, F. *et al*, 2010). This pore size range, along with a continuous surface and highly interconnected pores provides conditions conducive to nutrient and waste permeability throughout the scaffold design (Hsu, Y. H. *et al*, 2007; Teraoka, F. *et al*, 2010). Natural bone tissues typically have porosity void fractions of up to 90+%, while maintaining structural integrity (Hsu, Y. H. *et al*, 2007; Teraoka, F. *et al*, 2010). An adequate balance in the 3D tissue engineering scaffold design must be found that is capable of providing adequate permeability, structural integrity while also allowing rapid cellular in-growth and proliferation throughout the scaffold.

Chapter 3: Project Strategy

Here we examined the potential of a 3D extrusion printer to build scaffolds for tissue engineers. These scaffolds are designed to structurally support cell cultures in a three dimensional environment that mimics the setting *in vivo*. The ability to culture cells in three dimensions allows tissue engineering to tackle problems such as designing organ replacements or wound healing systems (Supp *et al* 2011; Bronzino *et al* 2005). 3d printers have recently become a viable option for completely custom, low cost projects (Fang 2005; Maher 2009). The extrusion printers we had available, the Makerbot Thing-O-matic or the Makerbot replicator, each cost under ~$2500. These printers use established biocompatible materials, Polylactide (PLA) and polyvinyl alcohol (PVA), and so are applicable for printing tissue scaffolds (Bronzino *et al* 2005). Since the structure and morphology of these scaffolds can be completely controlled, scaffolds can be built with a highly biomorphic structure that mimics the natural extracellular matrix (Ratner 2005). Here we established the goals of our design, through refining our client statement. Objectives, functions, and constraints of this design were incorporated in the client statement to establish the scope of the design space.

3.1 Client Statement:

From our meeting with our advisors, we established this initial client statement:

> "Design, build and evaluate a tissue engineering scaffold using 3D extrusion printing technology."

This gave us a starting point to move forward in establishing goals for this project.

3.2 Constraints

There are four major constraints that govern project. It must be biocompatible, printable, sterilizable and within the budget. Being biocompatible is listed as both a constraint and an objective because there are different degrees of biocompatibility. Our constraint states that it must allow cell growth, in any capacity. As an objective, we plan to maximize biocompatibility. The material chosen

must be a printable material. The budget also constrains the project. We have approximately a $500 budget to make any changes to the printer, print the scaffold and any prototypes needed, and test that the scaffold. The scaffold has to be sterilizable. This means we need to pick a material that can be sterilized in a way that is non- toxic to cells.

The scaffold must be produced using safe techniques and materials. Proper personal protective equipment (PPE) should be determined for any unsafe processes and worn at all times by all involved in carrying out these processes. The team will need to sterilize and test the scaffold with proper PPE's and other safety equipment and use proper bio-hazard and sharps disposal practices to ensure the safety of our team as well as others utilizing the lab space.

3.3 Objectives

The project objectives and constraints were determined through research and several meetings with the project advisors and the project teams members. It was determined that the 3D printed tissue scaffold high level objectives are: low cost, rapidly manufactured, biocompatible material, biomorphic, permeable, and degradable. The objectives tree structure generated for this project is below in Figure 3 for reference.

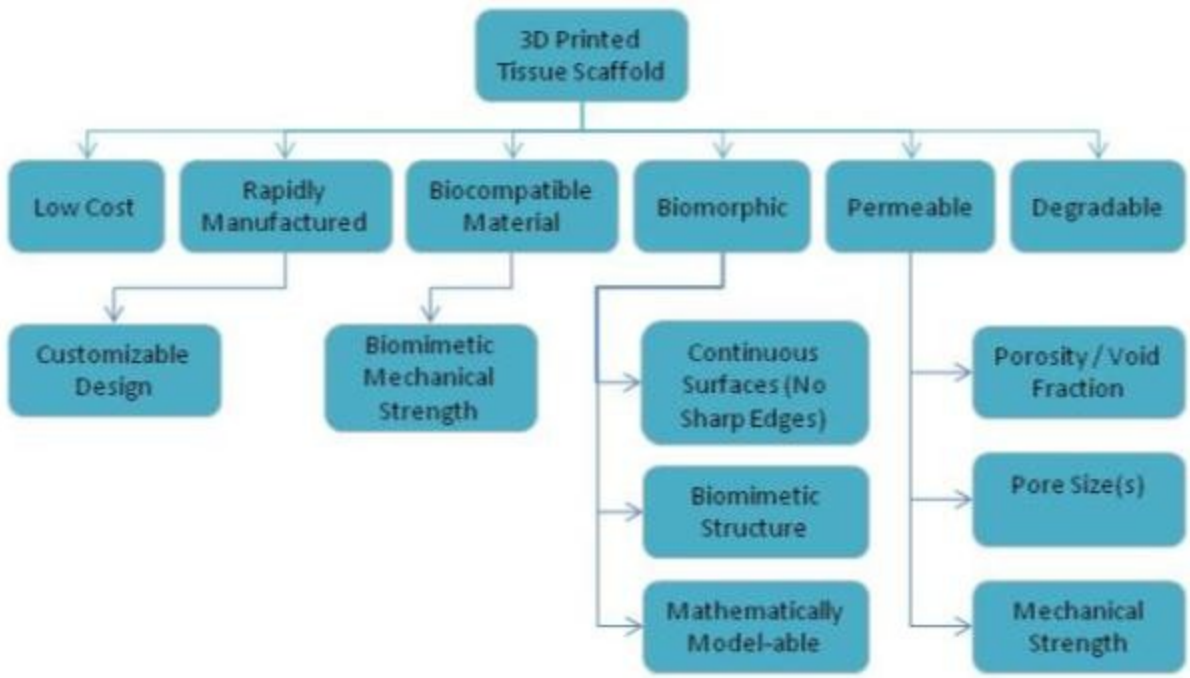

Figure 3 – Objectives Tree Structure for 3D Printed Tissue Scaffold

Utilizing the highest level of the objectives tree, a pairwise comparison chart (PCC) was developed to rank the importance of each of the primary objectives for this project. The resultant PCC is shown below in Figure 4 for reference.

	Low Cost	Rapid	Biocompatible	Biomorphic	Permeable	Degradable	**Totals**
Low Cost	XXXXXXX	1	0	0	0	0	**1**
Rapid	0	XXXXXXX	0	0	0	0	**0**
Biocompatible	1	1	XXXXXXX	0	0	1	**3**
Biomorphic	***1***	***1***	***1***	***XXXXXXX***	***0.5***	***1***	***4.5***
Permeable	***1***	***1***	***1***	***0.5***	***XXXXXXX***	***1***	***4.5***
Degradable	1	1	0	0	0	XXXXXXX	**2**

Figure 4 – Pair-wise Comparison Chart for the 3D Printed Scaffold Project

As shown above in Figure 4, for this project the biomorphic and permeable objectives are tied for the highest importance, with each of these scoring a 4.5 out of 5 possible points. The biocompatible material objective is ranked third. The remaining and least important objectives for this project each scored 2 or less points out of 5 possible points (degradable, low cost, and rapidly manufactured).

3.3.1 Low Cost

The low cost objective is intended to satisfy both the WPI MQP budget allowance for this project, as well as to create affordable scaffolds in an attempt to minimize costs associated with any procedures and products utilizing the scaffold designs. Additionally, this project is utilize a low-cost 3D printer, in an attempt to determine if functional tissue scaffold designs are printable, which could indicate a potential prior limiting barrier may now be eliminated and allow broader adoption and utilization of 3D printing technology within the tissue engineering and clinical industries. By aiming to minimize costs throughout the development process, we can help to minimize end product costs, making them more affordable and more applicable to the general public.

3.3.2 Rapidly Manufactured (Rapid)

The rapidly manufactured objective is intended to allow for a single rapid prototyping system being utilized within a laboratory setting to be capable of producing patient-specific scaffold products in a timely manner. The envisioned finished process involves not only manufacturing the scaffold, but also includes post-manufacture sterilization, cellular seeding and proliferation processes. Minimizing the time to manufacture and down-time reduces the overall cost of equipment required and thus helps to minimize end-product costs.

3.3.3 Biocompatible Material (Biocompatible)

The biocompatible material objective involves developing scaffolds utilizing materials that are already established as implantable and resorbable by tissues in-vitro/vivo. While rapid prototyping techniques utilize numerous materials, there are few materials established as implantable and

biocompatible which are compatible with the MakerBot 3D printers. The biomaterials already in existence in the proper form for the Replicator are poly-lactide (PLA) and poly-vinyl alcohol (PVA). There are numerous other biocompatible materials that could be processed into the necessary form to be utilized by the Replicator, a 1.75mm extruded filament coiled onto a spool.

A secondary aim within the biocompatible material objective is to use a material that has biomimetic mechanical properties as the target tissue being replaced by the scaffold. This objective is to create permanent or temporary, if the material is resorbed, structural integrity within the scaffold design until the replacement tissue can take over the structural loads, by picking a material having similar mechanical properties to the target tissue being replaced.

3.3.4 Biomorphic

The biomorphic objective aims to provide a continuous surface free of sharp edges, a biomimetic structure to the native tissue being replaced by the scaffold design, and a mathematically modelable scaffold design.

The natural tissue internal design is free of sharp edges. Using a design similar to the native structure will maximize cellular in-growth and proliferation within the scaffold design, as these designs have already been optimized through evolution over millions of years for their intended environment. Utilizing some form of biomimetic design, the design will already include many of nature's functional optimizations and reduce iterative design processes and the time and costs associated with them.

The aim to be mathematically modelable is intended to provide easier calculations and modeling to mechanically evaluate the scaffold design. For example a mathematical model can be used to evaluate the scaffolds structural strength under simulated loading within a structure or fluid flow through a structure, and gives a means to easily compare design variations. Additionally mathematically based scaffold models have the ability to be easily customized should minor design changes be deemed necessary.

3.3.5 Permeable

The permeable objective is intended to provide the proper internal porosity void fraction, pore size(s), and mechanical strength needed within the scaffold structure to withstand biological forces. The porosity void fraction is the ratio of empty space versus filled space within a scaffold design. Proper porosity is a key to effective nutrient and waste diffusion through the scaffold. Without proper nutrient diffusion and waste removal within the scaffold, the in-growing and proliferating cells can die due to toxicity or a lack of required nutrients.

Various prior studies have aimed to determine proper scaffold structural porosity void fraction and pore size(s) for specific cell/tissue types. This objective aims to use prior research findings to optimize the projects scaffold designs for the proper range of properties (porosity void fraction, pore size(s), as well as structural strength, etc.) that promote proper nutrient diffusion and waste removal to allow cellular in-growth and proliferation.

3.3.6 Degradable

The degradable objective aims to create a complete wound healing solution, where the scaffold material can be slowly and safely resorbed and degraded by cellular tissue in-vitro or in-vivo and replaced by proliferating cells and extra cellular matrix. Biocompatible materials have a wide range of degradation times, from the relatively quick PVA taking as little as a few hours, to slower resorbing materials such as PLA taking months to several years to degrade, or even non-resorbing materials such as titanium or stainless steel. This objective aims to identify the proper mix of specific biocompatible material(s) that have the necessary degradation properties needed for the specific replacement tissue. The selected material(s) will provide the initial structural support and integrity needed for natural loads the replacement tissue scaffold will see within in-vitro or in-vivo environments, while allowing natural cellular replacement by tissue to eventually handle this structural support role when fully developed.

3.4 Revised client statement

After reviewing the state of the literature, and interviewing stakeholders, and establishing objectives, functions, and constraints for our design, we incorporated this information into our revised client statement:

"Design, build and evaluate a low cost, under $20, biocompatible bone tissue engineering scaffold using 3D extrusion printing technology that can be fabricated rapidly. Scaffold must be sterilizable, degradable, with biomimetic morphology as determined by mathematical modeling. Scaffold must have customizable sizes and shapes, and be adaptable to different materials and printers. Scaffold must promote cell proliferation, adhesion, and transport waste and nutrients throughout the entire scaffold. "

This client statement narrowed our design space, and helped establish goals for the project.

3.5 Project Approach

The project began with a client statement proposed by our advisors; use a 3D printer to create a tissue scaffold that could be used for biomedical applications. We gained access to a 3D printer called the Makerbot Replicator and searched the literature for previous attempts at similar projects. Various organizational tools were used to define the design space, including a Gantt chart, a pair-wise comparison chart (see Figure 4), and an objectives tree (see Figure 3). This refined information was incorporated into the revised client statement.

Next, we established alternative design concepts by individual and group brainstorming. The potential concepts were evaluated and ranked to identify the best designs, and the top few ideas were conceptually developed further while the overall best was selected for the project testing phase.

The structural design was created on a free-ware mathematical visualization software, called K3DSurf, then exported as an .obj file that could be imported into graphic design (i.e. Autodesk 3DS Max software) or CAD based software (i.e. SolidWorks). Once imported the model can be converted to the

printer-friendly and compatible file type known as a .stl file. Once the model existed as a .stl file, it can be loaded into the 3D printer software to prepare and print the model on the 3D printer. With the 3D printed model scaffold design, the scaffold can be evaluated in a variety of ways, including seeding cells to observe the efficiency as a working tissue scaffold, imaging the material produced at various levels of magnifications, validating the accuracy of the final printed scaffold, and measuring the printed porosity void fraction and pore sizes. Numerous versions of mathematical models were evaluated and visualized using the K3DSurf software, and these various model equations are included in “Appendix A: Mathematical models used” for reference.

Chapter 4: Alternative Designs

The overall goal of this project is to design a scaffold for bone tissue engineering using a low cost 3D printer. Scaffolding is a common technique in tissue engineering to provide structure to 3D tissue cultures to control the in-growth and proliferation of seeded cells. As discussed previously, using a 3D printer allows for fully controlled micro- and macro-structures of the scaffold, unlike traditional scaffolding techniques where the internal pore size, distribution, and pore interconnectivity are limited (Yeong *et al* 2004). Within this section of the report, we will establish the functions and associated specifications of the scaffold design, and generate design alternatives based on these guiding criteria. These design alternatives can then be ranked and feasibility of the various designs can be assessed so that a final design can be selected and fully evaluated as part of this project.

4.1 Needs Analysis

Tissue engineering of bone tissue requires specific features in scaffolds for effective cell in-growth and proliferation within the scaffold designs. The most important features are related to the physical structure of the scaffold and the intrinsic material properties of the scaffold. The scaffold needs promote proliferation, which can be achieved by a variety of methods. By promoting cellular proliferation and ingrowth, the scaffold will create a successful piece of tissue engineered bone—a construct made almost entirely of cells and cell derived matrix. This relates back to the issues of porosity, pore size and interconnectivity discussed in our objectives. However, given our constraints on scaffold fabrication (we must use a MakerBot 3D printer) the feasibility of the printing adequate resolution to achieve proper pore sizes and porosity void fraction ratio must be assessed. The structure of any potential design must balance the feasibility of printing and the optimum morphology and material properties for promoting cellular growth.

Any scaffold must also mimic the mechanical structural supporting role of the target tissue to be replaced, therefore becoming another major function of our design. We have determined that a

mathematical model-based scaffold design is advantageous, as it yields a means of easily controlling the pore size and porosity void fraction of the model, and also can provide a means for simulation or evaluation of mechanical loading or internal fluid flow characteristics of the scaffold design.

4.2 Functions & Specifications

4.2.1 Promote cell adhesion

Cell adhesion is the ability of cells to attach and distribute themselves within the scaffold design once seeded. This is extremely important to a tissue scaffold because without cell adhesion and distribution of the cells within the scaffold, the cellular tissue will not proliferate and in-grow within the scaffold. The ability of a scaffold material to attach to the seeded cells allows for more rapid in-growth into the structure. We plan to focus mainly on the uniform distribution of the cells throughout the scaffold for evaluation purposes. We specify our seeding design will uniformly distribute cells throughout the scaffold structure, such that cells are present within all regions of the scaffold when evaluated after testing is completed.

4.2.2 Promote cell proliferation and differentiation

Our scaffold will promote cell proliferation, meaning that cells that are seeded into the scaffold will proliferate and differentiate into osteoblast-like cells producing calcium deposits within the scaffold structure. Regarding the cell proliferation and differentiation specification for our scaffold, we expect to find significant calcium deposits throughout all regions of the scaffold to indicate the cells have converted into osteo-blast like cells and are producing calcium throughout.

4.2.3 Diffuse nutrients uniformly

Since we are dealing with a 3 dimensional scaffold that will have numerous pores running through it, the aspect of having a uniform flow to allow for the effective diffusion of nutrients is necessary. Without a uniform flow, certain areas of the scaffold would get more or less nutrients and removal of waste than other regions. This can lead to dead zones within tissues which can cause severe

problems within the host organism that receives the tissue implant. Uniform diffusion throughout the scaffold can be seen by the effects that it has, such as the absence or quantitatively different concentration of cells after the seeding process or lessened differentiated cells within a region. We specify that the scaffold design will not show indications of highly necrotic cells, indicating the nutrient and waste diffusion through the scaffold is adequate to promote proliferation and differentiation of the cells within the seeded scaffold.

4.3 Design Alternatives

The design aspect of this project consists primarily of a major design of the morphology of the scaffolding, along with numerous modifications to optimize the scaffold, which are independent of the shape selected. In addition, these design aspects of the project also must conform to the objectives, constraints and functions of the overall project.

The project team utilized a functions-means chart as shown in Figure 5 below and a morphologic chart shown in Figure 6 further below to assist in the brainstorming and generation of design alternatives for this project.

Functions	Means			
Promote/allow cell proliferation/adhesion	biocompatible material	pore sizes	porosity	material surface treatments/coatings
Printing biomorphic pore/porosity sizes	standard nozzle bore / extruder assembly	customized smaller nozzle bore / extruder assembly	optimizing 3D printer settings	
Generate / manipulate mathematical models to be biomorphic to bone tissue data	K3DSurf	MATLAB		
Customize model to fit near-net shape/size	CAD software (SolidWorks, ProE, etc.)	animation software (3DS Max, Maya, etc.)	K3DSurf / MATLAB	combo of any / all software available

Figure 5 – Functions-Means Chart: major functions for our structure design (the morphology of the scaffold) are included on the left most column. The means listed in the other columns are high level concepts of the many ways or options these functions can be accomplished. This is broken down more specifically within the morphological chart shown in Figure 6

Various design alternatives were developed for the designed shape and style of the scaffold itself. As shown in the above morphological chart across the porosity (biomorphic) goal row, these major design alternatives for the structure shape and style of the scaffold include: minimal surfaces modeling, 2D stacked or 3D space-filling fractal modeling, 2D stacked mesh, and simple unit cells. The remainder of the design options listed in the above functions-means and morphologic chart will be grouped and discussed later in this report within the section identified as “4.3.5 Other Design Considerations”.

Goals	Option 1	Option 2	Option 3	Option 4
allow adhesion	plasma treat with O2, N2, or ammonia gas	surface coat with collagen or hydroxyapatite (HA)	rely on intrinsic properties of the material	
primary material (biocompatibility)	PLA	PVA	ABS	
porosity (biomorphic)	minimal surfaces modeling	use 2D stacked or 3D space filling fractals	2D stacked mesh	simple unit cells
vary porosity (biomorphic)	use a gradient of pore sizes (linear, radial etc.)	use a stepwise function to vary layers of pore sizes	no pore variation	
withstand printing	use one nozzle and no support material	use one nozzle with supports of the same material that are removed in post processing	use 2 materials, one scaffold material, one support material that is removed	

Figure 6 – Morphological Chart: the morphological chart gives specific design alternatives for achieving different design goals (both functions and objectives) each row begins with a header that describes the goal and is followed in subsequent columns with several means of accomplishing it. This includes all project goals, not just the design for the scaffold morphology.

4.3.1 Minimal Surfaces Modeling

The minimal surface modeling design alternative is based on pioneering work performed in tissue engineering studies such as those performed by Rajagopalan *et al* in 2006. These efforts, involving triply periodic minimal structures (TPMS), are more easily described as repetitive minimal surface patterns that extend continuously in each direction of 3D space, and have been inspired by mathematicians and scientists observing and attempting to mimic complex naturally structures over the past several hundred years. To date, TPMS scaffold structures show promise of increased cell proliferation and enhanced cell in-growth in comparison to the then-current simple mesh/grid type scaffold simple shapes most commonly utilized in tissue engineering scaffolds (Kapfer *et al* 2011). An

example of a TPMS shape is shown below in Figure 7 as a visual reference to the core of the design concept.

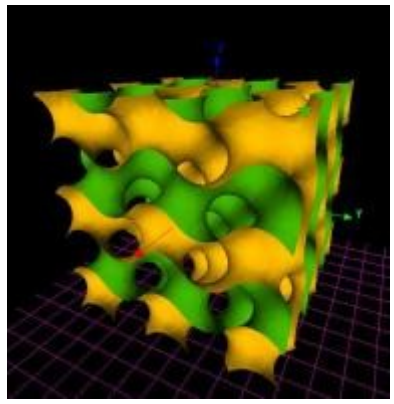

Figure 7 – Example of a TPMS Structure, (visualized by K3DSurf v0.6.2 Software)

As shown in the above example image, a TPMS surface inherently has an infinitely small wall thickness with void-space between these continuous thin walls of the 3D structure. Utilizing the MakerBot Replicator 3D printer, the basic TPMS structure shown above must be modified, as the printer nozzle resolution dictates the smallest wall thickness possible. The TPMS structure must be modified to thicken the walls and thus adjusting the pore to void space ratio known as porosity void fraction. The K3DSurf V0.6.2 Software program (Taha, 2012), is capable of visualizing mathematical models, such as the above figure of a 'Gyroid' TPMS structure defined mathematically as:

(Equation 1) $$S_{(surface)} = \cos(x) * \sin(y) + \cos(y) * \sin(z) + \cos(z) * \sin(x).$$

Using simple mathematical principles, the TPMS structure can be varied by affecting both the amplitude and period of the sine and cosine wave components of the above mathematical expression. These amplitude and period variables, while important, are less critical than the ability to vary the thickness of the wall, and the porosity of the overall structure. Other mathematical manipulation is

available to create a 'thickness' from the TPMS thin-wall concept, as illustrated in the below K3DSurf image, Figure 8, and mathematical equation (Equation 2 below).

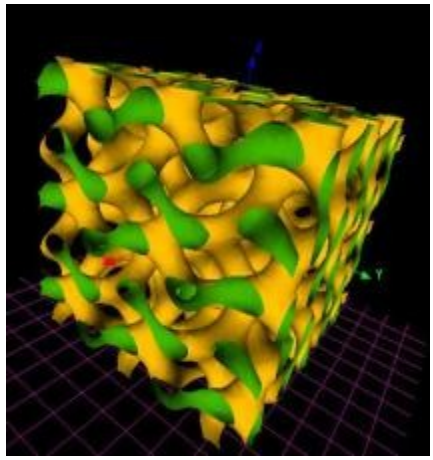

Figure 8 – Example of a Thickened TPMS Structure (Visualized by K3DSurf V0.6.2 Software)

The above image is defined mathematically as:

(Equation 2) $S_{(surface)} = 1-(\cos(x) * \sin(y) + \cos(y) * \sin(z) + \cos(z) * \sin(x))^2$

As shown, the newly generated thickened TPMS structure now has enclosed tubes and hollow porous void space between these tubes. This model can now be manipulated further to optimize the structure to fit the biomorphic structure of bone tissue, by manipulating the ratio of tube thickness to hollow region and scaling the structure to meet the size of the overall replacement bone scaffold geometry section to be printed.

The above examples of modified TPMS 3D structures are not intended to represent the optimized design selected for this project, and are instead just an example of how mathematical manipulation of the TPMS structures can be achieved using the K3DSurf V0.6.2 Software to adjust a scaffold design to generate biomimetic tissue scaffold designs.

As indicated above, the size of the pores and the porosity void fraction can be controlled to generate a best fit to the biomorphic nature of the bone tissue structure that is capable of being printed on the MakerBot Replicator 3D Printer (minimum extruded filament size is the smallest possible wall

thickness. The outer shape of the scaffold can also be manipulated to enclose the model to any mathematically defined shape; cubes are shown in the above K3DSurf example images for convenience. The resultant block of 3D TPMS-based scaffold structure design can be exported from K3DSurf to an .obj file type commonly used in graphic design and CAD software. An ideal end goal would be export the mathematical scaffold model into CAD software, where it can be conformed to the outer boundaries of any final replacement tissue shape and size needed. Once shaped, the CAD model can be exported into a format compatible for printing on the MakerBot 3D printer, a .stl file type. As our team lacks experienced CAD operators, this end goal is unlikely to be addressed within the scope of this project.

4.3.2 2D Stacked or 3D Space Filling Fractals

This concept is based on recent efforts performed in tissue engineering studies to incorporate fractals, which are naturally occurring structures, into tissue engineering efforts (Pandithevan, P., et. al., 2009). Some examples of fractals in human anatomy included blood vessel distribution within the body and internal lung bronchial pathways. Other biologic examples of fractal geometries include tree branch and leaf vein patterns. Fractals are a useful, evolution derived tool for efficiently delivering nutrients by maximizing interfacing surface area. Examples of 2D space filling fractal designs are depicted below in

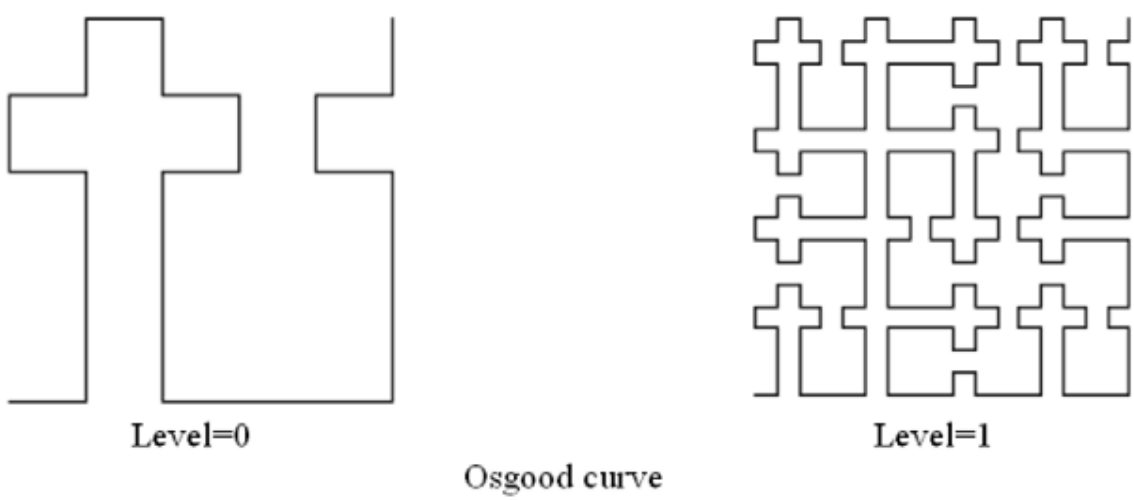

Figure 9. These 2D layers (or other fractal based 2D layer designs) could be stacked into 3D blocks to generate the desired 3D bone tissue scaffold structure.

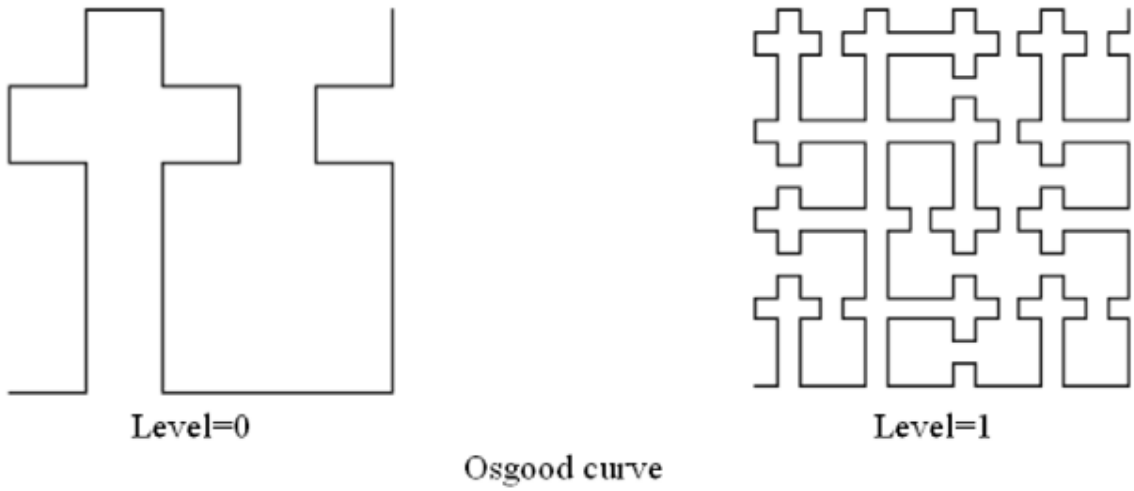

Figure 9 – Examples of 2D Layered Space Filling Fractals (images from Kumar et. al. (2009))

Another fractal design concept is to utilize 3D space filling fractal designs. An introductory meeting was coordinated with a WPI academic computing applications scientist specializing in mathematical fractal modeling, Adriana Hera, Ph.D., to gather additional background and availability of tools to mathematically model 3D space filling fractals. Dr. Hera mentioned 3D space filling fractals are complex that manipulating the fractals to fill 3D space to create a bone tissue scaffolding design is a highly risky task, especially with our team having limited experience with programming and MatLab. She mentioned stacking 2D fractals was much more practical for our project goals if fractal designs are to be utilized.

4.3.3 2D Stacked Mesh

Using a simple stacked mesh is another alternative for generating a scaffold. Simple 2D meshes can be stacked into 3D blocks, such as stacking several lattice structures depicted in Figure 10 below. These stacked 2D mesh designs are the easiest design concept to print in the printer, but are limited in their biomorphic properties, as these designs do not produce continuous internal surfaces with no sharp corner features that alternative scaffold designs provide. Additionally, simple stacked 2D mesh designs have been previously printed on low-cost 3D printers, indicating this scaffold approach has already been

completed for various tissue scaffolds, and would be repetitive of existing performed research in the field of tissue engineering.

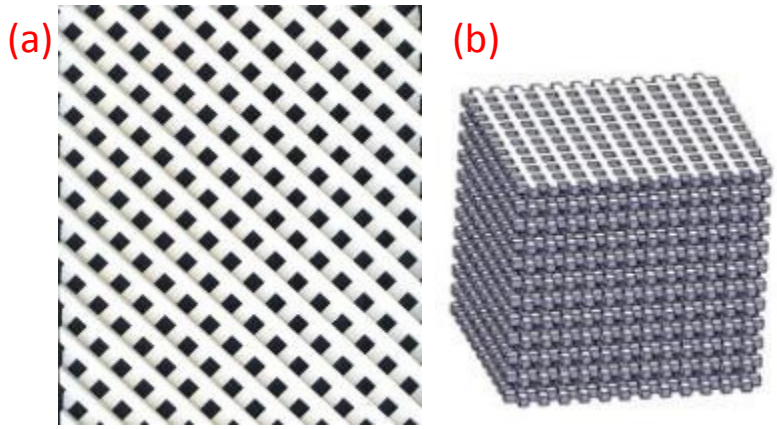

Image from Decorativecomponents.com Image from Amirkhani et. al., 2012

Figure 10 – (a) 2D Mesh Lattice (45° angle) & 2D Layers can be Stacked into (b) 3D Block Structures (iso)

The printed tube of extruded plastic is printed with a hollow spacing between printed tubes and upon completion of one layer, the design is printed at a rotated angle on the next and successive layers, such that the 2D grids are stacked into a 3D structure having consistent tube and hollow pore structures throughout.

The porosity void fraction and pore size can be easily manipulated to generate this approaches best fit to the biomorphic nature of the bone tissue structure. A basic repeating block design of stacked 2D mesh could be easily generated and exported to the 3D printer, and again, this has already been accomplished in prior research.

4.3.4 Simple Unit Cells

Simple unit cell scaffold designs are based on generating an appropriately sized unit cell shape concept, and repeating this cell in 3D space to fill the outer boundaries of any final replacement tissue shape and size needed. Examples of a few unit cell designs are below in Figure 11 for reference.

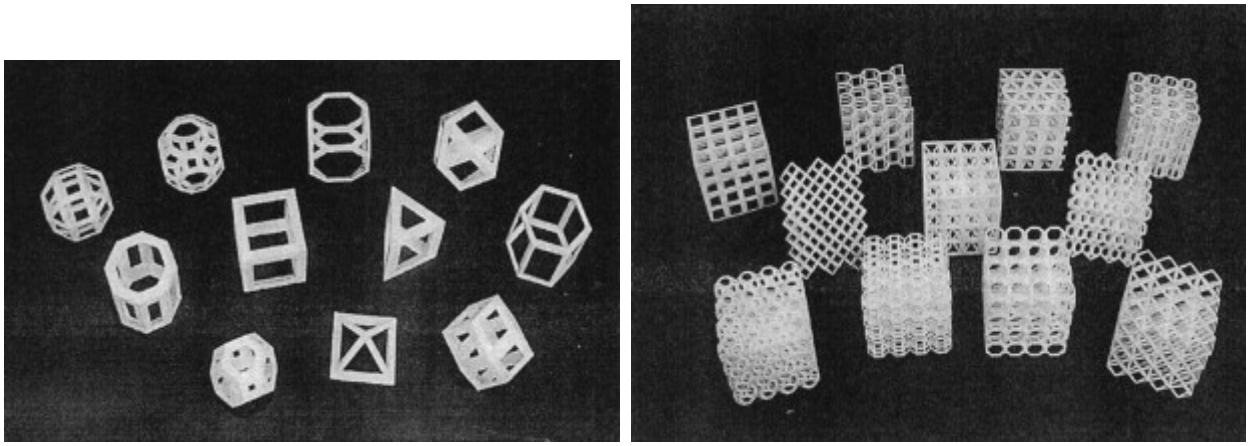

Figure 11 – Simple Unit Cells and 4x4x4 Cubes of Each Unit Cell Concept (images from Cheah, 2003)

The size of the pores and the porosity can be controlled to generate a best fit to the biomorphic nature of the bone tissue structure. As with the layered mesh this design could be completely modeled in CAD software before exporting to the printer. The limitations of the unit cell designs include the potential for unutilized secondary pore structures, sharp corner features, and a non-continuous surface, each reducing the scaffold design biomorphic, permeable, and cell adhesion properties relative to alternative scaffold designs considered.

4.3.5 Other Design Considerations

In addition to the primary design alternative variation for this project, shape/concept for the scaffold geometry, there are numerous additional design considerations involved in order to meet the objectives, constraints and functions of the overall project. The following sub-sections of this report detail these additional design considerations.

4.3.5.1 Biocompatible Material Selection

The MakerBot Replicator 3D Printer has a dual-nozzle capable design (MakerBot Industries, 2012). The dual-nozzle design of this 3D printer is typically utilized for printing designs of two colors during a printing operation, and can also be utilized to print two separate materials that require

fully independent printing parameters (i.e. extrusion temperature, material extruder feed-rate & nozzle printing speeds) (MakerBot Industries, 2012). A single nozzle design typically results in sagging and warping of the extrude tube over longer unsupported regions of the design (MakerBot Industries, 2012). For the design of a bone scaffold, the design is purposely porous; intentionally leaving numerous regions unsupported during the print operation, and thusly, results in a design with potential for significant variances in as-designed versus as-printed scaffolding of the overhanging regions sag prior to solidifying. The MakerBot Replicator's dual-nozzle design and available material selection offers a unique solution to this problem. By utilizing a primary material for the scaffold solid portion of the design, and a removable support material to temporarily fill the areas of the scaffold design intended to be porous, the supported dual-nozzle printed scaffold design may be a more accurate match the as-designed scaffold design, as there are little to no unsupported regions in the dual-nozzle printed design. An additional processing step is necessary for dual-nozzle printed designs, in order to remove the temporary support material from within the printed scaffold design (MakerBot Industries, 2012), as well as the printing process taking much longer, as the entire volume of the scaffold bounding box is to be printed, versus only the walls printed in a single material and single nozzle print.

The available printing materials compatible with the MakerBot Replicator 3D Printer are currently limited to acrylonitrile butadiene styrene (ABS), polylactic acid (PLA), and polyvinyl alcohol (PVA) (MakerBot Industries, 2012). For the purposes of this project, all materials to be selected will be of the natural filament color, as there is no information available to determine if the coloring dyes utilized are biocompatible.

The ABS material is not biocompatible, and therefore is eliminated as a potential material choice for use in this project (eliminated from both a primary and a secondary support material choice).

The remaining available biocompatible materials are PLA and PVA. The PVA material is rapidly water soluble, indicating a scaffold design printed with this material as the primary material would

rapidly dissolve in aqueous solutions, such as cell culture media (MakerBot Industries, 2012). PVA is therefore not an applicable primary material for printing the bone tissue scaffold designs for this project, however, its material properties (rapidly dissolving in water) have potential for utilization as a removable secondary support material as described above, if there is noticeable sagging of printed designs at overhanging regions of the printed scaffold design.

The only remaining available stock material that is both printer compatible and biocompatible is PLA. The PLA material degrades within an adequate time-period to be applicable for bone tissue scaffolding application of this project, as it generally takes months to years for PLA to biodegrade in-vitro and in-vivo (depending on the specific design and biological tissue environment the material is utilized within) (Roshan-Ghias, et. al., 2011). PLA is also a commonly utilized material for biocompatible applications, including various tissue engineering scaffold applications, such as the intent of this project (Roshan-Ghias, et. al., 2011).

4.3.5.2 MakerBot Replicator Compatible Nozzles/Extruder Assemblies

The standard nozzle bore of the MakerBot Replicator 3D Printer is 0.4mm (400μm) (MakerBot Industries, 2012). Bone tissue in-growth and proliferation has been shown to be optimized in scaffold designs having pore sizes that range from 200-400μm in size, designs having greater than 50% porosity void fraction, and (Hsu, et. al., 2011; Taraoka, et. al., 2010). For this project, the current MakerBot Replicator nozzle bore size and desired bone tissue pore sizes would result in scaffold designs with an upper porosity void fraction limit estimate of roughly 66 & 50% (for designs having pore sizes of 200 & 400μm respectively). This indicates the current nozzle bore of the MakerBot Replicator is a limitation for the project objective of designing bone tissue scaffold structures with optimized cellular in-growth and proliferation designs. Further, initial printed extrusions and the actual nozzle bore hole size were measured using microscope imaging, and it was determined that there is some extrusion die swell, enlarging the printed extrusion filament above the upper threshold limit of 400 microns. Additional

solutions to reduce the printed extrusion filament size are necessary to achieve our minimum goal of printing 400 micron sized pores with an estimated 50% porosity void fraction. There is potential to identify existing off-the-shelf commercially available and compatible nozzles for the MakerBot Replicator 1 printer, as well as the potential to manufacture custom nozzles having smaller extrusion bore hole sizes. All of these alternative design options will be further considered, in order to achieve the goals of this project.

4.3.5.3 Biomimetic Pore Size Gradients

Natural human bone has pore size and porosity gradients throughout the cancellous and cortical portions of the anatomical bone structure (Hsu, et. al., 2011; Taraoka, et. al., 2010). These variable pore size and porosity gradients that occur in natural bone are the result of the bone tissue biomechanical physiological response to strain and applied loads applied to the local bone structure that occur during normal use (Hsu, et. al., 2011; Taraoka, et. al., 2010).

The option of applying gradients of pore size and porosity to various regions of the scaffold design may be applicable to this project to achieve a higher level of biomimetic morphology within the final design. Each of the four identified alternative designs for the scaffold shape is capable of being modified to apply gradients in pore size and porosity. However, the extruded plastic filament size is again a potential limitation and/or bottleneck to this portion of the design. The stock MakerBot Replicator nozzle extruded filament bore size, as described earlier in the design alternatives portion of this report, currently results in an overall porosity design upper limit of roughly 50%, which is already lower than desirable to optimize cellular in-growth and proliferation of the printed scaffold design. If the nozzle extruded filament bore size is not capable of being significantly lowered (i.e. to ~0.1- 0.15mm / ~100-150μm), applying a pore size or porosity gradient would only further lower the overall porosity of the design, and further impede cellular in-growth and proliferation of the overall design. Due to this limitation, application of pore size and porosity gradients is not recommended for this project unless the

nozzle extruded filament size of a customized/replacement nozzle can reach the range of 0.1-0.15mm (100-150μm).

4.3.5.4 Surface Treatments to Enhance Cell Adhesion and Proliferation

The performed literature review for this project identified journal articles describing tissue engineering scaffold design improvements for cellular adhesion, in-growth, and proliferation that result from enhancing the cellular interfacing material surface properties of the material of the scaffold design (Li, Y. H., *et al*, 2007; Yang, *et al*, 2002; Pang, *et al*, 2007).

The surface of a scaffold design can be enhanced to improve adhesion by performing a plasma treatment process and then coating the plasma treated surface with a thin layer of collagen (Yang, et. al., 2002). This combined surface treatment process notably enhanced the cellular adhesion, in-growth, and proliferation of seeded cells in comparison to collagen coating the surface without first plasma treating the surface (Yang, *et al*, 2002).

A final considered potential surface treatment applicable particularly to bone tissue scaffold designs is application of a hydroxyapatite coating to the scaffold material (Pang, *et al*, 2007). The hydroxyapatite coating has very similar material properties to natural bone ceramic-like tissue, and is considered a good tissue engineering material for bone tissue applications as it promotes osteoblastic in-growth and proliferation (Pang, *et al*, 2007). There are multiple methods to generate hydroxyapatite coatings on material surfaces, including a relatively simple and low-temperature process to coat various material surfaces as implemented by Pang *et al* (2007).

The application of these surface treatments to this project are dependent on if the required materials and equipment is available to process within WPI laboratory setting, and if these surface modification techniques/processes are affordable within the schedule and limited budget available to the project. As these techniques/processes are a secondary design improvements, these design enhancements will only be considered if adequate schedule and budget remain after first fulfilling the

primary objectives and functions of the project. If these surface modification design enhancements are not able to be evaluated as part of this project, these would be a great starting-point to consider future developments for a follow-on project.

4.4 Conceptual Tentative Final Design

The initial conceptual tentative final design was determined from a weighted evaluation selection matrix/chart, as shown below in Figure 12 for this project. This selection matrix evaluates only the primary design alternative of scaffold shape/geometry, and results in weighted scores for each design alternative, with the highest score being the recommended final design path to evaluate further.

	objectives and constraints	Minimal Surfaces	Space Filling Fractals	Mesh	Simple Unit Cells
constraints	biocompatible				
	printable	?	?		
	within budget				
	sterilizable				
	safe				
objectives	low cost (2)	16	16	20	16
	rapid (1)	8	8	10	8
	cell adhesion compatibility (6)	54	48	36	30
	biomorphic (9)	90	90	45	54
	permeable (9)	90	81	72	63
	degradable (4)	28	28	28	28
total score		**286**	**271**	**211**	**199**

Figure 12 – Selection / Evaluation Matrix Chart: Each of the above listed objectives contain a weighting value within parentheses. These weighting values were derived from the earlier Pair-Wise Comparison Chart from Chapter 3 of this report by scaling the weighing values to a scale of 1-10, with each design alternative being scored from 1-10 within each objective category. The resultant weighted values are shown in each cell and totaled for each design alternative, with the Minimal Surfaces design alternative receiving the highest score of 286 weighted points

The selection evaluation matrix above helped the team determine which design would best fulfill our objectives, and if any alternatives should be eliminated due to conflicts from constraints. As indicated by the question marks (?) in the above selection / evaluation matrix chart, the more complex Minimal Surfaces and Space Filling Fractals alternative designs may be prone to additional as-designed versus as-printed design errors, as the nozzle size limitation and complexity of the printed layer designs

may cause an increase in error compared to the more easily printable design alternatives of Mesh and Simple Unit Cell alternative designs.

The two top ranked design alternatives outscored the remaining two design alternatives in each category with the exception of the low cost and rapid objectives (least important weighting multiplier), where the only the Mesh design alternative scored modestly higher due to the potential of this scaffold design being printed using only a single material and single nozzle, unlike the other designs. Subsequent small scale printing determined the small overhanging distances associated with this projects goal 200-400 micron pore sizes and estimated porosity void fraction between 50-66% range result in limited sagging. This indicates each design is capable of being printed with a single nozzle and a single material, equalizing the minor advantage the mesh design alternative had in this one weighted category.

Each of the design alternatives will be modified/scaled to provide a pore size of roughly 200-400 microns, provided adequate 3D printer nozzle bore size and extruded filament size can also be printed in this 200-400 micron size range. Each design alternative will be modified/scaled to achieve the best possible printable pore size and porosity void fraction given the design constraints, controlled by the final nozzle used.

4.5 Feasibility Study & Experiments Methodology

4.5.1 Feasibility studies

There were experiments done to test the feasibility of each feature of the design before continuing to a final design. These feasibility studies looked at single aspects of the model to specifically examine their effectiveness; these tests included testing the biocompatibility of the material in a 2D culture to verify there are no cyto-toxic reactions to indicate the PLA material is biocompatible. The small-scale printing tested the available custom nozzles and the printer setting optimizations to reduce the printed extrusion filament size.

Regarding the biocompatibility of the material being used for the scaffold, the ability for cells to grow on an unmodified normal piece of PLA was tested. This was done by printing a flat piece of PLA, seed cells onto it using 2D tissue culture techniques and recording whether or not there was cellular growth after a period of time. During these tests, there were no identified biocompatibility issues in the time-frames evaluated for the PLA material, however, after several days contamination was noticed within the 2D culture dish. This indicates either the PLA material placed in the culture dish was not properly sterilized, or that accidental non-sterile cell culture techniques had resulted in contaminated culture dishes. The piece of PLA used had no specific biomorphic shape since this was only to test the material alone and get a base-line to evaluate potential for cell growth and proliferation.

Before proceeding with printing a functional modeled scaffold, the actual capabilities of the printer need to be assessed as to make sure that it can handle the printing of our design. The feasibility of creating certain designs as well as the nozzle requirements were focused on. Due to the low cost of the material we were able to do a trial and error method by first attempting to print our model using ABS. Although ABS is not a biocompatible material these tests were just to judge the ability of the printer to form the shape. This was the first test done so we had to simply load our designs onto the printer and since we had yet to switch from factory default ABS to our ordered PLA, we started test prints. The test print was a scaled up version of the design using one nozzle, which allowed us to see how well overhangs and curves are handled. The analysis of the test prints was by a purely visual method, in which we looked for if the shape held during the process and where mistakes were made on the part of the printer.

Before evaluating the printed functional model scaffolds, additional cell culture system design testing and sterilization method evaluations were performed to further optimize the potential for successful evaluations for this project. There were various identified sterilization methods considered, with the simplest and easiest method being selected for continued evaluations, sterilization in 70%

ethanol for a prolonged time-period of 2+ hours, followed by drying the printed scaffolds in the bio-safety cabinet (BSC) utilizing an ultraviolet light for an additional 2+ hours. The cell culture system designs and techniques used for this project continued to change and be further optimized up until the final evaluation testing began.

4.5.2 Experiments Methodology

Once all of the individual tests were completed, an in vitro experiment using the finished scaffold as a whole was performed to assess its functionality. These tests were done with the purpose of measuring how well the finished design performs, which include checking for the correct pore size using a microscope to measure the resultant pore-size using a free-ware program called ImageJ.

4.6 Preliminary Data

4.6.1 Nozzle resolution improvement feasibility study

The MakerBot manufacturer was contacted to determine if smaller nozzle bore options exist. In response, the manufacturer stated they are not aware of any smaller nozzle designs that are directly compatible with their MakerBot Replicator. However, also in response to our email, they submitted their standard nozzle CAD design and authorized us to modify the standard nozzle design to have custom nozzles manufactured for our evaluation purposes.

A customized nozzle or a replacement compatible extruder assembly compatible with the MakerBot Replicator 3D Printer is desired to achieve the desired printed filament resolution for our models. A replacement compatible nozzle or extruder assembly with a nozzle printed filament size of 100-200 microns (if possible/available) could result in bone tissue scaffold designs with an upper void fraction of 66-80%, significantly better than at the upper limit of 400 micron pore size.

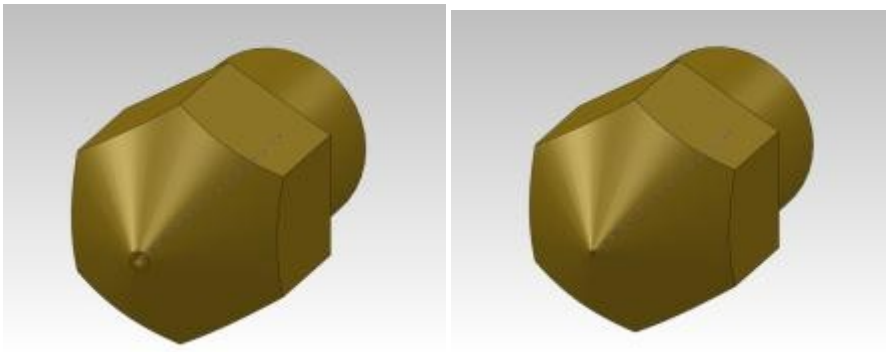

Figure 13 – Comparison of Original 0.4mm Nozzle (left) to Possible 0.1mm Nozzle (right) Designs: note the change in angle of the new design, and the need for high tolerances to develop this new nozzle

The replacement commercial-off-the-shelf components currently identified as available and partially or fully compatible (partial compatibility requires additional replacement extruder assembly components) with the MakerBot Replicator, potentially have nozzle bore sizes as small as 0.25mm (250μm). One manufacturer of potentially compatible components, MakerGear.com, listed an experimental nozzle having a bore size of 0.15mm (150μm) however, this component does not appear to be currently available and these nozzles were determined to not be compatible with the MakerBot Replicator 3D printer.

The literature review performed also identified a research paper relating to the various design considerations and the process of utilizing computational fluid and thermal dynamic modeling to design and optimize a custom nozzle for a RepRap 3D Printer having a smaller nozzle bore size (Ju and Roxas, 2008). The RepRap 3D Printer has numerous similar and/or partially compatible design components to the MakerBot Replicator 3D. The research indicated the back-pressure build-up within the nozzle design increases significantly with smaller nozzle bore designs, and this may bottleneck due to design limitations within the extruder assembly design of the 3D printer (Ju and Roxas, 2008). Attempts were made to generate a computational fluid dynamics (CFD) model using available Fluent software on the WPI campus. The model generated required numerous critical and limiting assumptions, as the material properties of the solid and melted (phase change) PLA material, as well as the relatively unknown

pressures generated within the nozzle made it too difficult to determine theoretical evaluations of the nozzle design with any expected accuracy or realistic results. Therefore, it was proved necessary to manufacture custom nozzles to determine their printing effectiveness experimentally.

Custom nozzles were manufactured in the WPI machine shop using an automated lathe tool and Esprit CAD/CAM software tool available in the machine shop lab space. With assistance from WPI's machinist staff, particularly Torbjorn Bergstrom and Adam Sears, the custom nozzles were manufactured from brass hex-stock available in the machine shop, having all features except the final micro-drill bore holes. The WPI machine equipment was incapable to reliably aligning the tool head with the needed precision to drill centered and properly aligned extrusion bore holes. To complete the final bore hole drilling needed to manufacture functional custom nozzles to test with the MakerBot Replicator 1 3D printer, a machine shop, Industrial Motions Engineering of Woburn MA was contacted. The machinists at IME, Mike Mangum and Joe Fustolo agreed to perform the micro-drilling of the nozzles for our project at no charge. Of the 16 nozzles submitted, 14 nozzles were returned, and at least 1 nozzle of each size, 150, 200, 250, and 300 micron nominal bore size were inspected and found to be adequately machined for functional evaluation testing of these custom nozzles. The remainder of the nozzles returned had defects or failures making them unusable for evaluation testing purposes. This low yield of manufactured custom nozzles is believed to be due to the limited budget for machining tools resulting is utilization of very cheap and inappropriate micro-drills to result in consistent and high-yield nozzles. Further evaluation of alternative manufacturing techniques for custom nozzles is necessary to properly evaluate and determine if improved nozzle quality and yield is possible with available micro-machining techniques.

Chapter 5: Design Verification:

In order to verify our final design we needed to first verify both our printing capabilities with the Replicator with our modifications as well as our cell culture model system. We developed protocols for testing small scale printing through stretching the filament and through incorporating customized nozzles using small test patterns. We also verified a procedure for differentiating MC-3T3 murine fibroblast cells into osteoblastic like cells. After these studies we were able to move on to testing our scaffolds ability to support osteoblast growth.

5.1 Small scale printing

Small scale printing testing was conducted on the Replicator 1 printer by modifying printer settings and modifying the printer itself. This allowed us to verify that we could create scaffolds with pore sizes in the necessary range for osteoblastic growth (200µm-400µm) and the necessary void fraction (a minimum of above 50%). This necessitates that the fiber size must be smaller than the pore size in the final model, indicating we needed to decrease the fiber size until it is below (200µm-400µm).

5.1.1 Initial testing

Our first attempt at filament testing involved changing the G language numerical tool path for the printer head (GCode), by changing the travel rate of the nozzle and the feed rate. We attempted to implement a post extrusion filament stretching technique by modifying the feed-rate and travel-rate settings. This was thought to modify the ratio of the nozzle travel speed and the filament feed rates. However upon observation and further investigation into the GCode it was established that these parameters have no effect on stretching. We therefore determined that a new method for decreasing the filament thickness would be necessary.

5.1.2 Nozzle fabrication

When our initial stretching protocol proved ineffective we determined that a new method for decreasing filament size was needed. After a short design evaluation we decided to fabricate custom nozzles for the printer with smaller bore sizes than the standard Replicator nozzle. We decided to use

micro-drills to create the smaller bore size as they were the least expensive alternative and readily available. The specialized equipment and experience knowledge-base to manufacture the custom nozzles with the purchased micro-drills was lacking within our team and available WPI resources, therefore, an outside vendor machine shop, Industrial Motions Engineering of Woburn MA graciously agreed to drill the nozzle bores for us at no charge for our academic project use.

5.1.2.1 Methodology

Our team manufactured the custom nozzles from hexagonal Brass stock; the same material standard nozzles are made from. Using Esprit CAD/CAM software the nozzle "blanks" were manufactured using an automated lathe. These blanks contained all the features of the final nozzle with the exception of the nozzle bore hole. This hole was fabricated using micro-drills of sizes 150µm, 200µm, 250µm, and 300µm. this type of drilling was outside the scope of our team and the WPI manufacturing labs; however Industrial Motions Engineering of Woburn MA offered to donate their time and expertise to drilling these holes for us. 16 total blanks were sent to Industrial Motions Engineering, with the assumption that 4 blanks would be used for each size nozzle bore (i.e. 4 blanks for the 150µm drill bit, 4 blanks for the 200µm drill bit etc.)

5.1.2.2 Results

The nozzle fabrication protocol had a 60% yield on usable nozzles. The initial lathing of the outer nozzle form was effective resulting in no defective parts; however the micro-drilling procedure proved much more difficult. Of the 16 nozzles 2 nozzles were deemed defective by Industrial Motions Engineering and were not returned to us, and upon microscopic evaluation 4 more nozzles were deemed defective. Please see appendix F for detailed information regarding lathing and manufacturing. Below you can see the evaluation matrix for the nozzles in table 1.

Table 1 – Micro-drilling results: this shows the qualitative evaluation of the micro-drilled nozzles as viewed under a stereoscope. Red indicates Nozzle was deemed unusable, yellow indicates a nozzle that may be usable and green indicates the most successful nozzle, and the one that was used in further testing. "Not returned" indicates a nozzle deemed defective by Industrial Motions Engineering. Images are provided for the nozzles used in testing.

No.	150 Micron	200 Micron	250 Micron	300 Micron	400 Micron (Std)
1	Bore closed	good	Bad	off center	
2	burr-OK	Irregular shape	burr-off center	Good	
3	good(off center)	burr	burr-off center	burr-off center	
4	Not returned	Not returned	Good	Bad	
	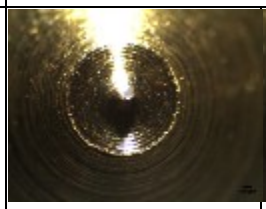	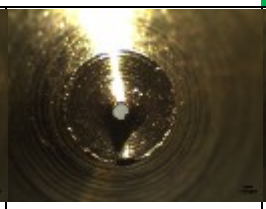	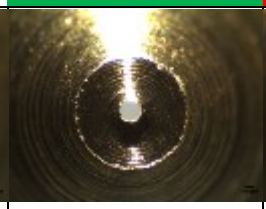	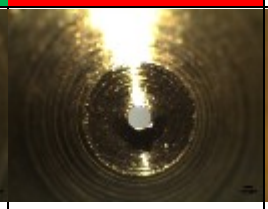	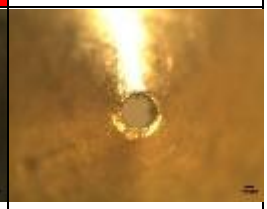
	Nozzle 3	**Nozzle 1**	**Nozzle 4**	**Nozzle 2**	**Standard Nozzle**

The chosen nozzles, 1 of each bore size, were then further evaluated through measuring of the actual bore size using ImageJ. It was found for most micro-drilled nozzles that the bore size was actually smaller than the intended drill size. The standard nozzle however was slightly larger than the stated 400µm bore size. For clarity the nozzles will still be referred to by their intended bore size (i.e. 150µm, 200µm, 250µm, 300µm, 400µm). The results of this analysis are shown in table 2 below. Please see appendix G for images detailing how measurements were made.

Table 2 – Actual bore sizes: this shows the actual bore sizes of the custom and standard nozzles as determined under a stereoscope. The title indicates the intended size for the nozzle bore and the average and STD deviation of the actual size of the bore are given at the bottom.

	150µm	200µm	250µm	300µm	400µm (Std)
	119µm	188µm	249µm	274µm	417µm
	117µm	180µm	251µm	284µm	419µm
		183µm	246µm	274µm	411µm
					406µm
Average	118.00µm	183.67µm	248.67µm	277.33µm	413.25µm
Standard Dev.	1.41µm	4.04µm	2.52µm	5.77µm	5.91µm

5.1.3 New nozzle testing and stretching

5.1.3.1 Methodology

When the initial stretching protocol proved ineffective we determined that modifications to the printer and settings needed to be made. We decided to implement a new stretching protocol by changing the filament size in the GCode (tool path code for Replicator). For a detailed image of the settings used please see Appendix B) this indicates to the Replicator to decrease the flow rate of PLA through the nozzle, while maintaining the nozzle travel rate. We used a filament stretch of only approximately 25% increase in volumetric flow rate, in order to avoid jamming of the printer. We printed the test pattern shown below either stretched or un-stretched with each of the custom nozzles.

5.1.3.2 Results

We successfully printed our test pattern with all custom nozzles. Please see appendix E for CAD drawings detailing the test patterns used. The stretching protocol proved effective in reducing the printed filament size in all nozzles except the 150µm nozzle. Table 3 below shows qualitatively the

effectiveness of the stretching protocol with representative images for each nozzle. Please see appendix G for images detailing how measurements were made.

Table 3 – Filament stretching in custom nozzles: Standard images correspond to the standard printing conditions, with no stretching. The stretched images correspond to the 25% volumetric stretching described above. The scale bars are 100µm

	150 Micron	200 Micron	250 Micron	300 Micron	400 Micron (Std)
Standard					
Stretched					

The graph below, in figure 14, shows the measured filament size changes in all custom nozzles. A T-test was done for statistical significance to compare the stretched to the un-stretched, and the stretching proved significant with and α=.10 for all nozzles except the 150µm nozzle. There was also evidence of die swell, swelling of the filament after extrusion in all nozzles and in both protocols.

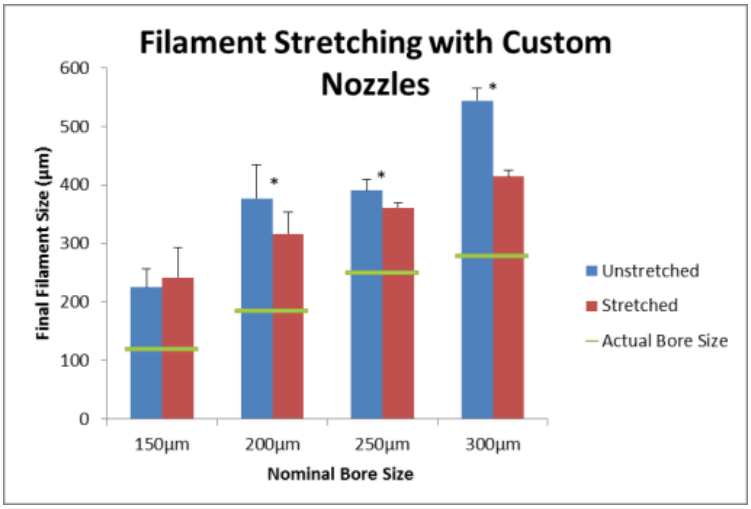

Figure 14 – Custom nozzles stretching extruded filament size. Here the blue bars, (un-stretched) represent the standard printing protocol, and red bars represent a 25% volumetric stretch. As described above, the actual nozzle bore size is different from the nominal bore size, and the green bars represent the actual bore size. Error bars are standard deviation and a * indicates statistical significance with an α of .10

As the 150µm nozzle was able to produce filament sizes of 225±30.74µm it was initially used in order to maximize porosity. However in longer term printing (i.e. printing of scaffolds) the nozzle caused the printer to jam. Therefore the 200µm nozzle with the 25% volumetric stretch (filament size: 316.25±37.11µm) was used for the remaining tests. Figure 15 shows a close up image of the printed scaffold created using the 200µm nozzle

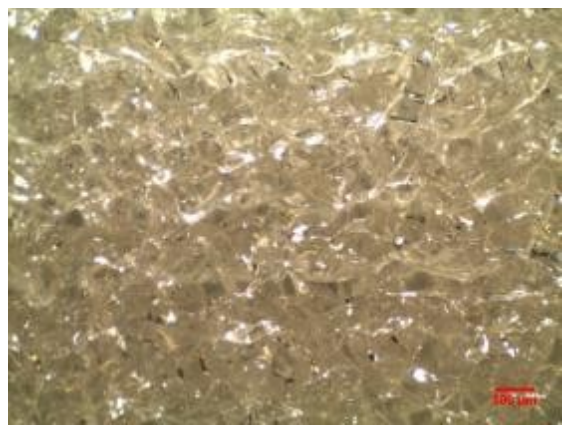

Figure 15 – Close up image of scaffold printed with 200µm nozzle with stretch

5.2 Culture System Verification

In order to test the scaffolds support of osteoblastic cells we used a murine osteoblastic precursor cell line from the ATCC, MC 3T3-E1. This cell line has been used previously to evaluate osteoblast response to the culture environment (Wang et al, 2008). We first verified the differentiation protocol described for these cells in both standard culture conditions and our experimental culture

system. We also used MC 3T3-E1 proliferation during differentiation in standard 2D Cultures to determine an effective seeding density.

5.2.1 MC 3T3 E1 Differentiation

5.2.1.1Methodology

In order to verify our cell line we tested the differentiation potential of MC3T3 fibroblasts. Based on the recommendations from the ATCC, to induce differentiation we used Ascorbic acid, and β-glycerophosphate. We also briefly studied the cell density per surface area to determine its impact on differentiation. We seeded cells at several different densities in a 12-well plate in order to determine the amount of confluency that leads to the greatest number of differentiated cells. In order to verify differentiation we looked for calcium deposition after 14 days. Calcium deposition is a hallmark of osteoblast cells, as it is the main component of the bone matrix they lay down. We also checked for cellular proliferation at several time points between 0 and 14 days in differentiation media to determine if proliferation was correlated to differentiation.

5.2.1.2 Results

To stain for the calcium deposits in the 12 well plates we used Alizarin red. Cells were initially plated at densities of 10,000 cells/well, 50,000 cells/well, and 80,000 cells/ well (1 well= 1.9cm^2 surface area). Representative images of each seeding density can be seen below in figure 16.

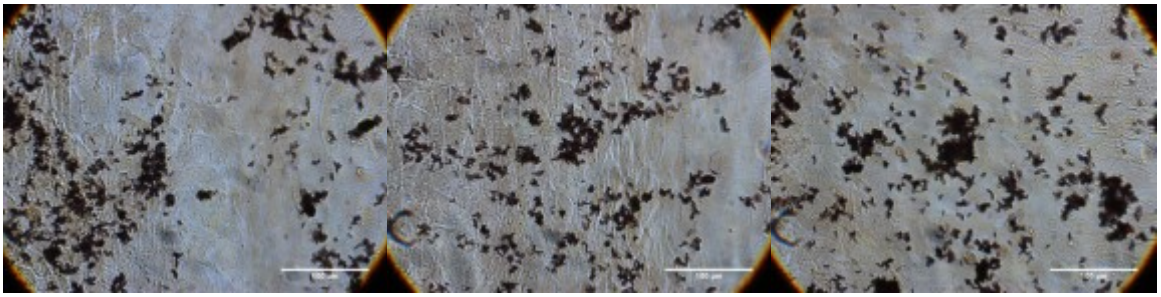

Figure 16 – Differentiation at different seeding densities in standard tissue culture plastic: alizarin red staining at different seeding densities. From left to right: 10,000 cells/well, 50,000 cells/well, and 80,000 cells/well. Black deposits were stained strongest, indicating high concentrations of calcium. Images were white balanced, under initial observation calcium deposits appeared red.

5.2.2 Collagen gel system

In order to seed cells onto our scaffold we chose to use a gel to evenly distribute cells throughout the scaffold. We chose to use a type I collagen gel as it is the most prominent type of collagen in natural bone. For this application we needed a highly viscous gel, almost a solid, with a relatively fast gelation time, to prevent significant cell settling. We also needed the pre-gelled solution to be able to wick into the pores of the scaffold. We attempted to use two different collagen gels for this purpose.

5.2.2.1 PureCol

We initially planned to use a pure collagen solution and induce gelation with raised temperatures as recommended by the manufacturer. The collagen (PureCol 3.47mg/mL) was brought to a pH of 7.4 using NaOH and mixed with 10X culture media at a ratio of 8 parts collagen to 1 part media as per manufacturer's instructions. When placed on to a scaffold in a 4 well plate the gel fully wicked into the pores of the PLA scaffold. However, after 48 hours the gel had not solidified in either the scaffold or the control well. As this gel was deigned to solidify in less than 2 hours it was deemed unusable for this purpose.

5.2.2.2 PureCol EZ gel

We settled on PureCol EZ gel which uses a much simpler procedure and has a faster gelation time. This gel was tested for gelation time and solidity in the same way as the previous purely collagen gel, seeding both an empty well (to create a gel slab) and a scaffold (to verify the ability of collagen to permeate scaffold). Pelleted cells were re-suspended in a very small amount of culture media (less than 100µm) and mixed with the PureCol EZ gel. This solution was than seeded into the appropriate well, and transferred to and incubator at 37C to induce gelation. After 45 minutes of observation the gel appeared fully solidified, and by the 1 hour indicated by the protocol it was certainly fully solidified. The gel also wicked into the pores of the scaffold fairly effectively. Initially gel solution pooled on top of the scaffold,

after the incubation time there was no longer a pool on top of the scaffold, nor any collagen gel visible in the well. This was deemed a suitable gel for our purposes and was used in further testing.

5.2.3 MC 3T3 E1 in collagen

5.2.3.1 Methodology

Once the seeding method in the collagen gel had been determined, the cell differentiation in the collagen gel also needed to be verified. We seeded MC-3T3-E1 fibroblasts into a pure slab of collagen gel the same size as our final scaffold. We determined the seeding density in the based on the most successful differentiation density from the 2d testing. The gel was seeded into a containment chamber made of PLA that was 10 mm X 10 mm X 3mm, then covered in differentiation media and cultured for up to 18 days. The gels and containment chambers were then embedded in paraffin and sectioned on a microtome. Sections were stained with alizarin red to identify calcium deposits in the collagen gel, indicating differentiation of the fibroblasts.

5.2.3.2 Results

At 12 days there were positive results from alizarin red staining. It was difficult to collect data as the containment chambers were difficult to section using the microtome, and few sections remained attached to the microscope slides even at multiple attempts. A representative image of the Alizarin red staining at 12 days is shown in Figure 17.

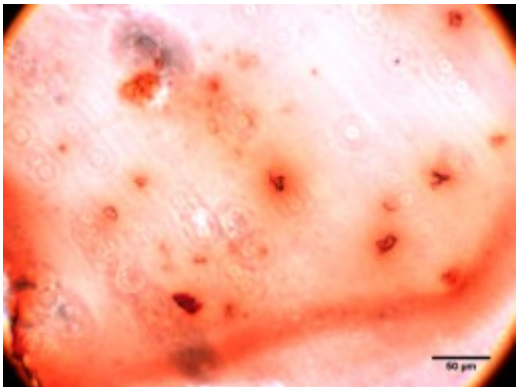

Figure 17 – Alizarin red staining of paraffin embedded gel: this shows the positive response to alizarin red for MC 3T3-E1 cultured in a collagen gel. The line at the edge of this image is the edge of the collagen gel the concentrated red indicate areas of high calcium concentration

5.3 Final testing

After all the verification of pretesting conditions we were able to test our full scaffold seeding protocol. All steps were followed as determined by the above results. The scaffolds were seeded with the collagen gel and cells numbers determined by the differentiation testing

5.3.1 Methodology

The thick wall “sheet solid” Gyroid model described in chapter 4 was used for these tests. This model was determined mathematically to have The final size of the scaffold samples was MC-3T3 cells were re-suspended in a PureCol EZ gel as described above and seeded into a PLA scaffold, these scaffolds were cultures for either 6, 12, or 19 days. Detailed procedure can be found in appendix C. Data collection was then done by paraffin embedding the scaffolds and sectioning on the microtome. These sections were stained for cell presence (Hoechst staining) and differentiation potential (Alizarin red staining)

5.3.2 Results

Overall we found that cells were successfully seeded and maintained in the scaffold. We also established positive differentiation results in the scaffolds.

5.3.2.1 Hoechst Staining

In order to verify that the cell seeding into our scaffolds was successful we used the Hoechst nuclear stain. This staining also allowed us to visualize all the components of our scaffold (collagen, PLA, MC-3t3 cells). We found that there were cells visible in the scaffold at all levels indicating a successful seeding procedure. We also found that the collagen created a matrix within the PLA pores that appears to be supporting the osteoblasts. Representative images of cells seeded in a scaffold are available in figure 18.

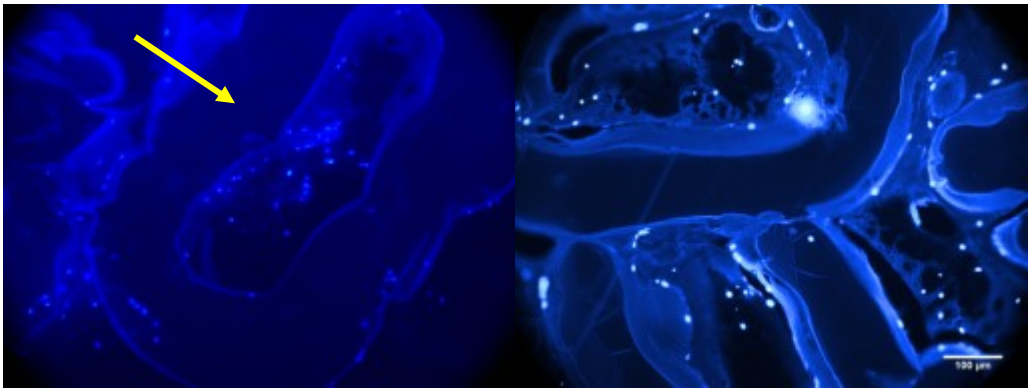

Figure 18 – Hoechst staining of scaffolds at day 6: these two images summarize the successful seeding of cells into the PLA/collagen complex. The image on the left shows one full pore of the PLA scaffold. Here can be seen the point where two pore channels come together, with the PLA fibers indicated by the yellow arrow. On the right is an image where all three components of the cell seeding system are easily visualized. As in the image on the left the large tube structures absent of cells are the PLA fibers. The smaller fibers within the pores are the collagen gel, which clearly is forming some sub pores in the structure. In both images the nucleus of cells is indicated by the highly fluorescent marks.

Unfortunately none of the day 12 samples produced successful sections on the microtome, and are not reported here. Day 19 samples were more successful, but the results may indicate cells were not seeded fully into the scaffold as they were concentrated on the outside edges. This can be seen in figure 19.

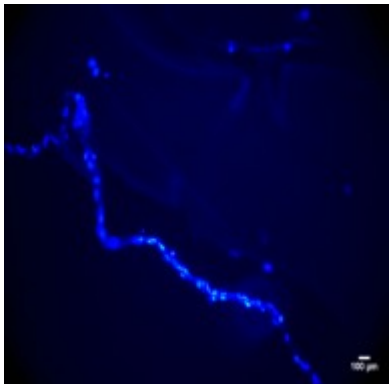

Figure 19 – Day 19 Hoechst staining. This image shows the edge of the scaffold in the section concentrated with cell

5.3.2.2 Alizarin Red

Once again alizarin red was used to evaluate differentiation potential of these cells in this culture system. We found here that by day 12 cells had a positive reaction to alizarin red with results that appear comparable to culture in collagen slab gel. Figure 20 is a representative image of alizarin red staining that clearly indicates calcium deposits.

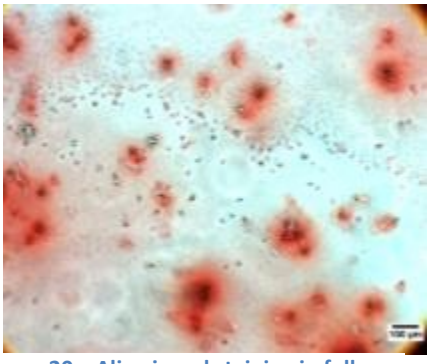

Figure 20 – Alizarin red staining in full scaffold system: note red deposits indicating differentiated cells

Chapter 6: Discussion

Overall we found this system to be a highly successful method for 3 dimensional cultures of osteoblastic cells. We found that our scaffold system is biocompatible biomorphic, and allows for cellular bio-functionality, our osteoblastic cell line, successfully cultured, behaved in the manner expected, and the scaffold had biomorphic geometry. Our scaffold fabrication process was also shown to be a viable option. The modifications to printer were found to be relatively simple and cost effective and the low cost printer was capable of printing at resolutions necessary for creating scaffolds. We found that this system fully meets our client statement requiring our system be a biocompatible, biomorphic, and customizable for permeability, rapidly manufactured and rapidly manufactured using an affordable 3d printer.

6.1 Biocompatibility: Cyto-toxicity

We determined that our combination of PLA and Collagen Type I is non cyto-toxic and biocompatible. Our PLA is biocompatible material, is therefore non cyto-toxic, as determined by our long term study in the scaffold. We were able to establish that cells were differentiated within the scaffold after 12 days indicating that they were still metabolically active. This was determined from the positive results of the Alizarin red staining indicating that cells were producing calcium, a hallmark of differentiated osteoblasts and not undifferentiated fibroblasts. As these cells were metabolically active they are therefore still living. The full biocompatibility of this material needs to be assessed further, but for the purposes of this experiment the cyto-toxicity was found to be a non-factor.

6.2 Biomorphic: Geometric biomorphism to provide functional biomimetic

There are two major points to the claim that our scaffold system is biomorphic. First, we have established a biomorphic geometry that is fully printable, and second we established the entire system provides functional biomimetic, meaning the system maintains the cellular functionality they are expected to have.

6.2.1Biomorphism: Pore size and geometry

We established earlier that our scaffold needed a pore size of 200-400µm as this was optimal for osteoblastic growth. (Hsu, Y. H., 2007; Teraoka, F., 2010) We manufactured a 200µm bore nozzle to print our scaffold inside the 200-400 um pore size, while maintaining porosity above 50%. In order to accomplish this we needed to maintain a filament thickness smaller than that of the pores. This nozzle, the 200µm bore size with a 25% volumetric stretching procedure enabled created a filament thickness 316µm allowing us to use pore sizes within our range to maintain cell growth. As discussed in the literature review our choice of the Gyroid based sheet solid model allowed us to ensure that our design has similar structure to bone with fully continuous surface. It also maximizes the surface area of the structure allowing for the greatest amount of surface for cell adhesion.

6.2.2 Functional Biomimetics: Calcium production and differentiation

We measured the bio-functionality of our cells by measuring the production of calcium by our osteoblastic line. The calcium production was validated by the alizarin red stain for calcium at 12 days, which came back positive. Since the calcium production was not impeded in our system, we can assume that our cells have maintained the differentiated functionality, i.e. they have not remained in the proliferative fibroblastic state. We can also say that our PLA does not appear to affect Bio-functionality, as the calcium production of cells in a collagen slab is comparable to the culture of cells in collagen and PLA together. In the future this indicated that our PLA/collagen system is effective for the culture of osteoblast cells. Though we only measured production of one factor here, with further testing of cell morphology and metabolic activity

6.3 Customizable using a low cost printer

The successful modification of this printer and the mathematical model to produce scaffold places this system in a position to combine 3d printing technology, tissue engineering, and clinical applications. The capability of this low cost printer makes the barrier for researchers to enter this field

very low, as the cost is fairly low. Including the cost of the custom manufactured nozzles there is a slight increase in price but it is not comparable to most high resolution printing technologies such as stereo-lithography and laser sintering. The inner design of the pore structure can be easily edited to incorporated different cell types for future tissue engineering purposes. The macro-structure of this scaffold is also easily controlled through manipulating the bounding geometry. This could in the far future become applicable for creating scaffolds that are customized to a patients wound or defect shape.

6.4 Constraints

Along with the objectives we detailed above our design fell well within the constraints we established for the system. We determined this must be sterilizable, rapidly manufactured less than 24 hours, and fall within our time and budget. We successfully sterilized the scaffold by established methods (70% ethanol soak and UV exposure) and the full manufacturing process, including sterilization and seeding but not including cell culture only required 8hours of total time. Our entire design process was conducted within the necessary budget and time constraints.

Economic impact

The economic impact of this project as it currently stands clinically are minimal. Clinical applications of tissue engineered constructs and this construct in particular are very new, and few products exist on the market today. However the impact of this project on tissue engineering research is great. We have shown that a low cost 3d printer is capable of creating tissue engineering scaffolds, greatly lowering the barrier of entry to future researchers who wish to use this technology. The price of rapid prototyping technology has possibly prevented tissue engineers from considering it for their application, but these results obtained with a low cost printer with standard low cost PLA make this a much more affordable option.

Environmental impact

Our current scaffold and process will not have a large environmental impact. The material of the scaffold is fully biodegradable, and is not intended to be discarded in large quantities. There is little to no use of harmful chemicals in the manufacturing or seeding process. Tissue engineering as a whole has an environmental impact due to the use of many single use containers (bottles, Tissue culture plates, pipettes etc.) however this impact can be mitigated by proper cell culture techniques. In the future scaling up and moving away from such single use containers would help limit any environmental impact of this project.

Societal influence

This project may contribute to the creation of fully customized bone tissue engineering constructs for patients with bone trauma or defects. However there would need to be many major changes to the current mentality surrounding bone treatment before this is a possibility, aside from the regulation and verification of such an implant. The safety and affordability of such a product would need to be explained thoroughly to ant potential patients as well as the risks and benefits associated with implants that contain living tissue. From a research standpoint, this project could have an impact on opening the doors to smaller or less well funded labs to participate in exploring rapid prototyping in tissue engineering, as the cost of high resolution 3d printers may have impacted research decisions.

Ethical concerns

Any ethical concerns surrounding this project are those concerning tissue engineering and using live cells in medical devices. For example, though we do not envision continuing to use cell lines in the final product there are several concerns with using non-terminal cells; immortalized cell lines that continued to proliferate in the body have the potential to form cancers and teratomas, and widespread use of a single cell line in multiple patients could create a situation where the implant unwittingly infected many people with a virus that had not previously been identified. These factors are mitigated

by use of the patients own cells whenever possible as is done in many of the currently available tissue engineering treatments

Health and safety issues

Currently this product has few health and safety risks associated with it as it is in the early stages of research, and no part of the manufacturing or testing process is overtly dangerous to laboratory professionals. Down the line if this product is to be commercialized, all potential safety risks need to be evaluated according to all FDA regulations and ISO standards to ensure a functional and safe product. Some potential issues include: PLA interactions with existing tissue both healthy and diseased, the safety of using laboratory differentiated cells in an implant (because of the potential for other cell types to arise), and the healing time associated with using a product like this.

Manufacturability

This project focused on the manufacturing aspect of this scaffold; it is highly manufacturable and could be scaled up fairly easily. MakerBot replicators are readily available and can easily be used to create the scaffold. The manufacturability of the custom nozzles has been assessed here and found to have a fairly low yield, in the future it may be beneficial to explore a new method for nozzle bore creation, i.e. moving away from micro-drilling. The tissue culture portion could become partially automated in a manufacturing setting but an experienced tissue culturist would likely need to be available for seeding an implant. Overall we believe this project could be scaled up without much issue regarding manufacturability.

Sustainability

As discussed in the environmental impact this process is highly sustainable as it used few highly limited resources. The largest sustainability issues arise from disposable lab equipment, which can be mitigated.

Chapter 7: Final Design & Validation

Tissue engineering is a rapidly expanding field of medical and clinical research and development with promise of delivering much needed solutions to numerous clinical problems without adequate treatments. Tissue engineering traditionally splits into two related disciplines for 3D tissue development: scaffold-based and self-assembly. While many of the tissue engineering applications would be best solved by mimicking the human body's natural development path (infancy & early development) of self-assembly, this solution path is currently not available to create functional 3D tissues and numerous hurdles remain for many of the clinical applications of self-assembled tissue engineering technology. A shorter-term solution, scaffold-based tissue engineering, has significant promise to solve near-term clinical needs, as well as to solve tissue engineering applications requiring structural support, such as the bone tissue application focused on within this project.

Design projects commonly utilize a task-breakdown approach based on solving a given or developed project statement. This project was given a very broad initial client statement to utilize existing low-cost 3D printer technology to create 3D tissue engineering scaffolds. A primary aim of this project statement was to determine if the existing low-cost printing technology is capable of delivering functional scaffolds for tissue engineering applications, and to assess the advantages and limitations of existing low-cost 3D printing technology for tissue engineering purposes. The initial problem statement was expanded through client interviews and initial research into the field scaffold-based tissue engineering to better understand the clinical applications and current needs. The development of a revised problem statement led to a tighter scope of this project, providing objectives, functions and constraints to guide and evaluate the progress throughout the project.

Various tools were utilized to prioritize and better define specific project goals, as described within Chapter 3 – Project Strategy of this report. This project strategy led to development and preliminary evaluations of several potential design alternatives to achieve the goals of this project, as described

within Chapter 4 – Alternative Designs. Research was performed to identify optimal bone tissue properties, with the aim of developing a tissue scaffold design that closely mimics natural bone tissue. The team performed a down-select process as outlined within Chapter 4 to select the generalized scaffold design to be generated and evaluated as part of this project; a triply-periodic minimal structure (TPMS) based scaffold design. The advantages of this design include having a highly continuous internal surface and interconnected pores and having variable pore size and porosity void fraction through mathematical manipulations to the formula – both of which allow this design to be customizable in order to closely mimic the structure within natural bone tissue, as identified within the performed research of this project.

Next, the project team acquired a MakerBot Industries Replicator 1 3D printer. This low-cost (~$2500) 3D printer was utilized for the remainder of this project. The Replicator 1 was selected due to it having the current best stock printing resolution (0.4mm extrusion nozzle) available for low-cost 3D printers, the printer being a very common and customizable 3D printing platform within the industry, and due to offering two biocompatible feedstock materials, Poly-lactide (PLA) and polyvinyl alcohol (PVA). Of the two available stock materials, PLA was selected for its longer term degradation time (6-24+months) which allows time for the bone tissue to integrate into the scaffold while the PLA withstands the structural loads, until the integrated bone tissue begins to absorb and handle the structural loads (while the PLA slowly degrades and is resorbed).

The MakerBot Replicator 1 extrusion nozzle (0.4mm bore size) when printed actually prints larger filaments, as there is extrusion die swell during the printing process. As the nozzle printed extrusion size exceeded the acceptable maximum pore size to print functional bone tissue scaffold (400 microns), various alternatives were considered to reduce the overall printed extrusion size. Commercial available nozzles having significantly smaller bore sizes were not available from MakerBot Industries or other 3D

printer manufacturers that could be easily compatible with the Replicator 1 3D printer. An available QU-BD company nozzle advertised as being compatible with the MakerBot Replicator 1 printer had an extrusion bore size of 0.35mm, and these nozzles were purchased as a small improvement over the stock MakerBot nozzle, however, were not selected for the final design as another alternative design was more successful in reducing the printed extrusion size. As there were no available off-the-shelf nozzles to significantly reduce the printed extrusion size, custom manufactured nozzles were manufactured. Micro-drills were obtained to create nominal nozzle bore sizes of 0.15mm, 0.20mm, 0.25mm, and 0.30mm. MakerBot Industries authorized and distributed their SolidWorks CAD model of their existing standard nozzle for our project, allowing our team to modify the CAD file and manufacture the custom nozzles to test for smaller printed extrusion sizes. Each of the custom nozzles were manufactured (all features except the final bore hole were manufactured at the WPI Manufacturing Lab, with assistance from Torbjorn Bergstrom and Adam Sears; final nozzle bore holes were drilled by Industrial Motions Engineering of Woburn MA, by machinists Mike Mangum and Joe Fustolo) and tested, with each nozzle successfully printing the simple filament test pattern having a concentric circle and square pattern with the circle intersecting each corner of the square. The custom nozzle bore sizes and the printed test pattern extruded filament sizes were each measured by collecting microscope images on the same microscope with the same zoom objective, and then utilizing ImageJ free-ware tool to perform the image analysis measurements of the bore size and filament size features from the collected microscope images. The smallest nozzle (0.15mm), while producing the smallest printed extrusion size, proved to be unreliable during long-term print testing, with the next smallest printed extrusion size coming from the 0.2mm nozzle, which was functional during all testing with no noticed abnormal behavior during printing. This custom 0.2mm nozzle was selected for all subsequent testing of this project.

Using the ReplicatorG software that is compatible with the MakerBot Replicator 1 3D printer, the settings of the printer were optimized in an attempt to further reduce the extruded filament size as much as possible. After testing and researching the available settings and their purposes within the software, the settings were optimized by changing the filament diameter setting of the ReplicatorG software user interface. The default setting of the software for the Replicator 1 printer using 1.75mm filament feedstock was 1.8mm. By changing this default value to a value of 2.0mm, the software believes there is ~25% more volumetric material entering the nozzle per extruder step of the feed motor, therefore, the printer feeds the material ~25% slower into the extruder nozzle during the printing process. This software setting change resulted in significant reduction in printed extrusion size, while no noticed side-effects during printing were identified. This optimized printer setting was tested throughout the project, and was determined to be recommended for the final configuration of this project. Results of the circle-square test prints at standard and optimized printer settings and of the custom nozzle bore imaging can be found in Appendix G for reference. The ReplicatorG software setting screenshots utilized for this project are available in Appendix B for reference.

Existing free-ware, K3DSurf Software, was selected and utilized to visualize the TPMS geometry of the bone tissue engineering structure and to export this geometry to a common file type, .obj file, which is capable of being imported into design & CAD software. The final selected mathematical formula based on the TPMS structure and optimized to create bone tissue mimetic pore size and porosity void fraction capable of being printed with the MakerBot Replicator 1 3D printer selected has the following formula: $S_{(Surface)} = - (0.4 - (0.81*\cos(2*x) * \sin(2*y) + 0.81*\cos(2*y) * \sin(2*z) + 0.81*\cos(2*z) * \sin(2*x))^2)$.

A free student-edition of the Autodesk 3DS-Max design software was then utilized to import the K3DSurf generated .obj file of the final scaffold design, where the model was then converted to a .still file compatible with the MakerBot Replicator 1 3D printer utilized for this project.

Once in the .stl file format, the software provided by MakerBot to interface with their 3D printer, ReplicatorG, was utilized to import and scale the .stl file structure to the final design size selected, 10mm X 10mm X 3mm, and to align the base of the structure to be printed with the print platform. The ReplicatorG printer settings were optimized for the custom 0.2mm sized nozzle bore and the 2.0mm filament size setting to print a reduced filament size within the acceptable 0.2-0.4mm pore size determined to be optimal for bone tissue in-growth and proliferation from the performed research.

Once the ReplicatorG software was used to place the imported .stl model of the scaffold design on the center of the 3D printer platform and scaled to produce a scaffold design having the desired pore size, the ReplicatorG software was used to generate a G-Code machine programming language output file, containing all the printer-specification settings, along with the layer-by-layer path instructions needed to construct the structure on the 3D printer. The ReplicatorG software generated G-Code file was then converted to a .s3g file and transferred to a SD card, which could be plugged into the card-reader port of the Replicator 1 3D printer. Using the Replicator 1 3D printer user interface, the .s3g file to be printed was selected, and the printing process was carried out by the MakerBot Replicator 1 3D printer. The final printed scaffolds were imaged using a microscope and confirmed the final extruded print size resulted in acceptable pore size (~0.3-0.4mm) and calculated porosity void fraction (~50%).

To further evaluate the printed final scaffold design, the scaffolds were prepared for cell culturing. The preparation included sterilizing the scaffolds in 70% ethanol for 2+ hours, followed by drying of the scaffolds within a bio-safety cabinet (BSC) while utilizing ultraviolet (UV) light for 2+ hours. The cells chosen to evaluate the scaffold design were mouse fibroblast cells, MC3T3-E1, which are osteoblast precursor cells that can be differentiated into osteoblast-like cells producing calcium deposits when exposed to differentiation factors within the culture medium. The MC3T3-E1 cells were grown in tissue culture flasks to obtain an adequate number of cells to seed the scaffold designs with 4.38x10^6 cells

per mL. To ensure the cells were incorporated into the scaffold structure during the seeding procedure, the cells were mixed with a viscous collagen type 1 gel and placed on top of the scaffold and allowed to naturally wick into the scaffold structure while scaffold and cells suspended in the collagen gel were incubated to cure and solidify the gel. A brief video was generated to summarize the cell seeding procedure onto the scaffolds, and is included within the electronic documentation package submitted with this report to the project advisors.

In addition to seeding cells onto the scaffold design, cells were also seeded into a collagen type 1 slab having the same overall thickness as the scaffold design. This was intended as a control to verify whether or not cells seeded into a collagen type 1 suspension thick slab are capable of proliferating and differentiation into calcium producing osteoblast-like cells. Additionally, cells were plated onto 2D flat PLA plates printed with the MakerBot Replicator 1, to ensure the PLA material printed caused no adverse effects to the MC3T3-E1 cells. These control tests were intended to help isolate potential sources of failure should cells not be capable of 3D seeding, proliferating, and differentiation within the final testing 3D printed scaffold designs.

The cell culture testing was conducted with various time-points to monitor cellular activity over the tested time-periods. The cell culture testing and subsequent cell staining with alizarin red resulted in verification that the collagen type 1 slab control and the scaffold designs had allowed the cells to proliferate and differentiate into osteoblast-like cells, as evident by presence of significant calcium deposits present within the microtome sliced sections from the center region of test samples. . The cell culture testing and subsequent cell staining Hoechst 33342 resulted in verification that the cells seeded into the slab and scaffold designs had been well mixed and that cells were present within microtome sliced sections from the center region of test samples.

The performed evaluations for this project succeeded in verifying the goals set forth within the revised client statement had each been met by the final design bone tissue engineering scaffold (having bone tissue mimetic pore size and porosity void fraction, and a continuous interconnected internal pore structure) printed in the biocompatible PLA material by the low-cost MakerBot Replicator 1 3D printer and its custom manufactured 0.2mm bore nozzle.

A photograph of the final design printed scaffold is below for reference. The green color filter was applied to provide enhanced contrast vs. standard white-light images for visualization purposes only.

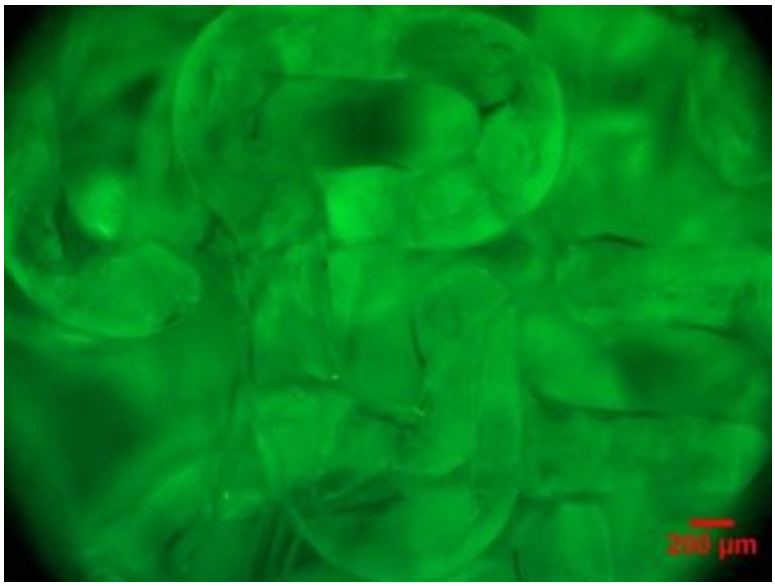

Figure 21 – Image of final printed scaffold design surface showing pore size and printed filament size at 5X objective magnification of Zeiss Axiovert 40 CFL microscope

Chapter 8: Conclusions & Recommendations

8.1 Conclusions

Based on the progress of our MQP, we have followed our initial goal of creating a 3D scaffold with all of the original properties that we set out to achieve initially. The result of the project is the creation of a scaffold that allows cells to attach and function towards forming actual bone, using the kind of printer that is so comparatively cheap that it could be found inside a residential house. Our work shows that the chosen scaffold design can be accurately printed to size on a cheap printer, seeded with a collagen/cell mixture and after allowing differentiation, show live cells attached to the internal structure that are producing calcium formations.

The major accomplishment of this project is the lack of expensive equipment in the creation of this scaffold. Creating and modifying the design of the scaffold was done using free software that anyone would have access to which is relatively easy to use. The printer that creates the physical scaffold from the design is many times cheaper than other printers capable of accomplishing the same task and though a small alteration in the nozzle size needs to be made, it is still inexpensive. The final price range of creating our scaffold would be on the magnitude of allowing even small local hospitals to produce this scaffolds when needed.

The results of the testing show that at some levels within the scaffold, cells are attaching to the walls. This not only allows the cells to differentiate and produce calcium formations within the structure but could also prove useful in the formation of channels within the potentially formed bone tissue that would provide nutrient flow to the inner layers.

Through the process of trying to print our scaffold to a smaller size than could normally be printed, our team manufactured a nozzle half the size of the standard nozzle. This allowed the printer, which already has high positioning resolution, to create structures at almost half the size that it could normally with the standard nozzle.

8.2 Recommendations

Since this project had a limited amount of time that could be dedicated to it, there are several recommendations for future experimentation that could be done to improve upon what was accomplished. These recommendations were considered to be valuable yet unrealistic to additionally achieve within the time period or outside the desired scope of the project.

8.2.1 Modifying the overall shape of the scaffold

During experimentation scaffolds were printed in 10 mm squares, 3mm tall and although these proved to be able to allow testing of its efficiency, this shape is impractical for actual implantation within a patient. Developing a way to print the scaffold in a required shape for the individual patients needs would allow practical use of the bone scaffold. Potentially computer modeling could be used in conjunction with medical imaging to obtain a shape that could then be used to print a scaffold to fit in the needed area.

8.2.2 Improved material

The current material that was used to print the scaffold is PLA which is a biocompatible material that has proven to work in our testing, yet improvement on its functionality would be beneficial. Since it is not medical grade PLA, further testing should be done on how it can be treated before or after printing to increase its efficiency regarding cellular attachment and

proliferation. (Park *et al,* 1998, Mainil-Varlet *et al*, 1997, Itthichaisri *et al*, 2007, Fisher *et al,* 2009)

Degradation time of the scaffold after seeding was not fully tested since the estimated time for PLA to degrade within a biological environment was much longer than available. A study showing the effects that the scaffolds degradation has on the attached cells should be done to see what would happen within one that has been inserted into the body. Treatments to affect the lifespan of the material should be considered to obtain optimal results.

8.2.3 Bio flow chamber for better nutrient flow

Cell death within the scaffold can occur when there is improper flow throughout the pore structure preventing fresh media from reaching deeper cells as well as preventing waste from leaving. In order to provide an even distribution of nutrients throughout the scaffold a bio flow chamber should be considered. Although we were unable to quantify insufficient nutrient perfusion and waste removal, it is suggested that a chamber be used to prevent potential cell death especially on larger scaffolds.

8.2.4 Cancerous testing

As with most processes that involve the use of manipulated cells, the danger of cancerous masses forming is a major concern. An assessment on the cancer risks should be done by monitoring scaffolds with desired cells for a long period of time with the intent of observing unwanted and potentially cancerous cell behavior. To reduce cancer risks within an in-vivo environment it would most likely be best to use the patient's own cells, for which testing should be done in the more distant future on live test subjects such as lab rats.

References

"3 Dimensional Printers Below $20,000 - Comparison Chart." Castle Island Co., http://www.additive3d.com/3dpr_cht.htm.

"Formlabs - the Form 1." http://formlabs.com/pages/our-printer.

"Makerbot® Filament - Natural Pla, 1kg Spool." MakerBot Industries, http://store.makerbot.com/filament#pla.

"Makerbot® Industries - Store." http://wiki.makerbot.com/.

"Makerbot® Replicator™." MakerBot Industries, http://store.makerbot.com/replicator.html.

"Makerbot® Water Soluble Pva - 1kg Spool- 1.75mm / 1.8mm - Pva - Plastic." MakerBot Industries, http://store.makerbot.com/makerbotr-water-soluble-pva-1kg-spool-1-75mm.html.

"Needle and Plate." http://www.flickr.com/photos/ajt23/437925500/.

"Organ-Regeneration-Ear-615.Jpg." wikispaces, https://hsgeometryadventure.wikispaces.com/file/view/organ-regeneration-ear-615.jpg/202415166/organ-regeneration-ear-615.jpg.

Tissue Engineering and Artificial Organs. Tissue Engineering and Artificial Organs. edited by J. D. Bronzino3 vols: CRC Press, 2006. doi:doi:10.1201/9781420003871.fmatt

Amirkhani, S., R. Bagheri, and A. Z. Yazdi. "Effect of Pore Geometry and Loading Direction on Deformation Mechanism of Rapid Prototyped Scaffolds." [In English]. *Acta Materialia* 60, no. 6-7 (Apr 2012): 2778-89.

Armillotta, A., and R. Pelzer. "Modeling of Porous Structures for Rapid Prototyping of Tissue Engineering Scaffolds." [In English]. *The International Journal of Advanced Manufacturing Technology* 39, no. 5-6 (2008/11/01 2007): 501-11.

Atala, A. "Tissue Engineering of Reproductive Tissues and Organs." *Fertil Steril* 98, no. 1 (Jul 2012): 21-9.

Bártolo, P., and H. Almeida. "The Use of Periodic Minimal Surfaces for Scaffolds Design." In *Innovative Developments in Design and Manufacturing*: CRC Press, 2009.

Becker, S. T., T. Douglas, S. Galonska, E. Sherry, S. Sivananthan, I. N. Springer, M. Steiner*, et al.* "Rapid Prototyping: Porous Titanium Alloy Scaffolds Produced by Selective Laser Melting for Bone Tissue Engineering." [In English]. *Tissue Engineering, Part C: Methods* 15 (2009/06// // 2009): 115+.

Bucklen, A., C. Liebschner, and Wettergreenm B. "Scaffold Micro-Architecture Optimization Based on Bio-Mimetic Principles." In *Innovative Developments in Design and Manufacturing*: CRC Press, 2009.

Cheah, C. M., C. K. Chua, K. F. Leong, and S. W. Chua. "Development of a Tissue Engineering Scaffold Structure Library for Rapid Prototyping. Part 1: Investigation and Classification." [In English]. *The International Journal of Advanced Manufacturing Technology* 21, no. 4 (2003/02/01 2003): 291-301.

Cheah, C. M., C. K. Chua, K. F. Leong, and S. W. Chua. "Development of a Tissue Engineering Scaffold Structure Library for Rapid Prototyping. Part 2: Parametric Library and Assembly Program." [In English]. *The International Journal of Advanced Manufacturing Technology* 21, no. 4 (2003/02/01 2003): 302-12.

El-Amin, S. F., E. Botchwey, R. Tuli, M. D. Kofron, A. Mesfin, S. Sethuraman, R. S. Tuan, and C. T. Laurencin. "Human Osteoblast Cells: Isolation, Characterization, and Growth on Polymers for Musculoskeletal Tissue Engineering." *J Biomed Mater Res A* 76, no. 3 (Mar 1 2006): 439-49.

Fang, Z., B. Starly, and W. Sun. "Computer-Aided Characterization for Effective Mechanical Properties of Porous Tissue Scaffolds." *Computer-Aided Design* 37, no. 1 (1// 2005): 65-72.

Fielding, G. A., A. Bandyopadhyay, and S. Bose. "Effects of Silica and Zinc Oxide Doping on Mechanical

and Biological Properties of 3d Printed Tricalcium Phosphate Tissue Engineering Scaffolds." *Dent Mater* 28, no. 2 (Feb 2012): 113-22.

Fisher, J., D. Dean, J. Wallace, A. Mikos, and K. Kim. "Stereolithographic Rendering of Low Molecular Weight Polymer Scaffolds for Bone Tissue Engineering." In *Innovative Developments in Design and Manufacturing*: CRC Press, 2009.

Fisher, R. J., and R. A. Peattie. "Controlling Tissue Microenvironments: Biomimetics, Transport Phenomena, and Reacting Systems." Chap. 18 In *Tissue Engineering Ii*, edited by Kyongbum Lee and David Kaplan. Advances in Biochemical Engineering/Biotechnology, 1-73: Springer Berlin Heidelberg, 2007.

Freed, L. E., G. Vunjak-Novakovic, R. J. Biron, D. B. Eagles, D. C. Lesnoy, S. K. Barlow, and R. Langer. "Biodegradable Polymer Scaffolds for Tissue Engineering." *Biotechnology (N Y)* 12, no. 7 (Jul 1994): 689-93.

Gabryś, E., M. Rybaczuk, and A. Kędzia. "Fractal Models of Circulatory System. Symmetrical and Asymmetrical Approach Comparison." *Chaos, Solitons & Fractals* 24, no. 3 (5// 2005): 707-15.

Goonoo, N., A. Bhaw-Luximon, G. L. Bowlin, and D. Jhurry. "An Assessment of Biopolymer- and Synthetic Polymer-Based Scaffolds for Bone and Vascular Tissue Engineering." *Polymer International* 62, no. 4 (2013): 523-33.

Guarino, V., F. Causa, P. Taddei, M. di Foggia, G. Ciapetti, D. Martini, C. Fagnano, N. Baldini, and L. Ambrosio. "Polylactic Acid Fibre-Reinforced Polycaprolactone Scaffolds for Bone Tissue Engineering." *Biomaterials* 29, no. 27 (Sep 2008): 3662-70.

Gwyther, T. A., J. Z. Hu, A. G. Christakis, J. K. Skorinko, S. M. Shaw, K. L. Billiar, and M. W. Rolle. "Engineered Vascular Tissue Fabricated from Aggregated Smooth Muscle Cells." *Cells Tissues Organs* 194, no. 1 (2011): 13-24.

Hockaday, L. A., K. H. Kang, N. W. Colangelo, P. Y. Cheung, B. Duan, E. Malone, J. Wu*, et al.* "Rapid 3d Printing of Anatomically Accurate and Mechanically Heterogeneous Aortic Valve Hydrogel Scaffolds." *Biofabrication* 4, no. 3 (Sep 2012): 035005.

Hsu, Y. H., I. G. Turner, and A. W. Miles. "Fabrication of Porous Bioceramics with Porosity Gradients Similar to the Bimodal Structure of Cortical and Cancellous Bone." [In English]. *J Mater Sci Mater Med* 18, no. 12 (Dec 2007): 2251-6.

Itthichaisri, C., M. Wiedmann-Al-Ahmad, U. Huebner, A. Al-Ahmad, R. Schoen, R. Schmelzeisen, and N. C. Gellrich. "Comparative in Vitro Study of the Proliferation and Growth of Human Osteoblast-Like Cells on Various Biomaterials." *J Biomed Mater Res A* 82, no. 4 (Sep 15 2007): 777-87.

Kapfer, S. C., S. T. Hyde, K. Mecke, C. H. Arns, and G. E. Schroder-Turk. "Minimal Surface Scaffold Designs for Tissue Engineering." *Biomaterials* 32, no. 29 (Oct 2011): 6875-82.

Li, Y. H., and Y. D. Huang. "The Study of Collagen Immobilization on Polyurethane by Oxygen Plasma Treatment to Enhance Cell Adhesion and Growth." [In English]. *Surface & Coatings Technology* 201, no. 9-11 (Feb 26 2007): 5124-27.

Maher, P. S., R. P. Keatch, K. Donnelly, R. E. Mackay, and J. Z. Paxton. "Construction of 3d Biological Matrices Using Rapid Prototyping Technology." [In en]. *Rapid Prototyping Journal* 15, no. 3 (29/05/2009 2009): 204-10.

Mainil-Varlet, P., R. Curtis, and S. Gogolewski. "Effect of in Vivo and in Vitro Degradation on Molecular and Mechanical Properties of Various Low-Molecular-Weight Polylactides." *Journal of Biomedical Materials Research* 36, no. 3 (1997): 360-80.

Melchels, F. P., K. Bertoldi, R. Gabbrielli, A. H. Velders, J. Feijen, and D. W. Grijpma. "Mathematically Defined Tissue Engineering Scaffold Architectures Prepared by Stereolithography." *Biomaterials* 31, no. 27 (Sep 2010): 6909-16.

Nat Mater 11, no. 9 (Sep 2012): 768-74.

Moroni, L., J. R. de Wijn, and C. A. van Blitterswijk. "Integrating Novel Technologies to Fabricate Smart

Scaffolds." *J Biomater Sci Polym Ed* 19, no. 5 (2008/01/01 2008): 543-72.

Nachtrab, S., S. C. Kapfer, D. Rietzel, D. Drummer, M. Madadi, C. H. Arns, A. M. Kraynik, G. E. Schroder-Turk, and K. Mecke. "Tuning Elasticity of Open-Cell Solid Foams and Bone Scaffolds Via Randomized Vertex Connectivity." [In English]. *Advanced Engineering Materials* 14, no. 1-2 (Feb 2012): 120-24.

Noritomi, P., F. A. Lixandro, H. Lipson, P. Cheung, H. Kang, J. da Silva, J. Butcher*, et al.* "Construction and Adaptation of an Open Source Rapid Prototyping Machine for Biomedical Research Purposes: A Multinational Collaborative Development." In *Innovative Developments in Design and Manufacturing*: CRC Press, 2009.

Pandithevan, P., and G. Kumar. "Fractal Tool Paths for Layered Manufacturing of Scaffolds with Matched Bone Properties." In *Innovative Developments in Design and Manufacturing*: CRC Press, 2009.

Pang, L., Y. Hu, Y. Yan, L. Liu, Z. Xiong, Y. Wei, and J. Bai. "Surface Modification of Plga/B-Tcp Scaffold for Bone Tissue Engineering: Hybridization with Collagen and Apatite." *Surface and Coatings Technology* 201, no. 24 (10/15/ 2007): 9549-57.

Park, A., B. Wu, and L. G. Griffith. "Integration of Surface Modification and 3d Fabrication Techniques to Prepare Patterned Poly(L-Lactide) Substrates Allowing Regionally Selective Cell Adhesion." *J Biomater Sci Polym Ed* 9, no. 2 (1998/01/01 1998): 89-110.

Pham, Q. P., U. Sharma, and A. G. Mikos. "Electrospinning of Polymeric Nanofibers for Tissue Engineering Applications: A Review." [In en]. *Tissue Eng* 12, no. 5 (May 2006): 1197-211.

Phattanaphibul, T., and P. Koomsap. "Investigation of Pla-Based Scaffolds Fabricated Via Svm Rapid Prototyping." [In English]. *Journal of Porous Materials* 19, no. 4 (2012/08/01 2011): 481-89.

Rajagopalan, S., and R. A. Robb. "Schwarz Meets Schwann: Design and Fabrication of Biomorphic and Durataxic Tissue Engineering Scaffolds." *Med Image Anal* 10, no. 5 (Oct 2006): 693-712.

Ratner, B. D. *Biomaterials Science : An Introduction to Materials in Medicine* [in English]. Amsterdam; Boston: Elsevier Academic Press, 2004.

Rolle, M. W. "Electrospun Pet-Pu Cuffs for Tissue Tube Anchoring." 1. Worcester, MA USA: Worcester Polytechnic Institute, 2012.

Roshan-Ghias, A., F. M. Lambers, M. Gholam-Rezaee, R. Muller, and D. P. Pioletti. "In Vivo Loading Increases Mechanical Properties of Scaffold by Affecting Bone Formation and Bone Resorption Rates." *Bone* 49, no. 6 (Dec 2011): 1357-64.

Roxas, M., and S. Ju. "Fluid Dynamics Analysis of Desktop-Based Fused Deposition Modeling Rapid Prototyping - 265.Pdf." University of Toronto, 2008.

Sachlos, E., N. Reis, C. Ainsley, B. Derby, and J. T. Czernuszka. "Novel Collagen Scaffolds with Predefined Internal Morphology Made by Solid Freeform Fabrication." *Biomaterials* 24, no. 8 (4// 2003): 1487-97.

Taha, A "K3dsurf : 3d Surface Generator." SourceForge.Net, http://k3dsurf.sourceforge.net/.

Supp, D. M. "Skin Substitutes for Burn Wound Healing: Current and Future Approaches." [In English]. *Expert Review of Dermatology* 6 (2011/04// // 2011): 217+.

Teraoka, F., M. Hara, M. Nakagawa, and T. Sohmura. "Fabrication of Sintered Porous Poly(L-Lactide) Scaffold with Controlled Pore Size and Porosity." *Journal of Applied Polymer Science* 117, no. 3 (2010): NA-NA.

Terrier, A., M. Sedighi-Gilani, A. Roshan Ghias, L. Aschwanden, and D. P. Pioletti. "Biomechanical Evaluation of Porous Biodegradable Scaffolds for Revision Knee Arthroplasty." *Comput Methods Biomech Biomed Engin* 12, no. 3 (Jun 2009): 333-9.

Tiwari, A., C. DiSalvo, R. Walesby, G. Hamilton, and A. M. Seifalian. "Mediastinal Fat: A Source of Cells for Tissue Engineering of Coronary Artery Bypass Grafts." *Microvasc Res* 65, no. 1 (Jan 2003): 61-4.

Vozzi, G., A. Previti, G. Ciaravella, and A. Ahluwalia. "Microfabricated Fractal Branching Networks." *J Biomed Mater Res A* 71, no. 2 (Nov 1 2004): 326-33.

Wang, J., J. de Boer, and K. de Groot. "Proliferation and Differentiation of Mc3t3-E1 Cells on Calcium Phosphate/Chitosan Coatings." *J Dent Res* 87, no. 7 (Jul 2008): 650-4.

Wang, J., J. de Boer, and K. de Groot. "Proliferation and Differentiation of Osteoblast-Like Mc3t3-E1 Cells on Biomimetically and Electrolytically Deposited Calcium Phosphate Coatings." *J Biomed Mater Res A* 90, no. 3 (Sep 1 2009): 664-70.

Wang, M., Y. Li, J. Wu, F. Xu, Y. Zuo, and J. A. Jansen. "In Vitro and in Vivo Study to the Biocompatibility and Biodegradation of Hydroxyapatite/Poly(Vinyl Alcohol)/Gelatin Composite." *J Biomed Mater Res A* 85, no. 2 (May 2008): 418-26.

Woesz, A. "Rapid Prototyping to Produce Porous Scaffolds with Controlled Architecture for Possible Use in Bone Tissue Engineering." Chap. 9 In *Virtual Prototyping & Bio Manufacturing in Medical Applications*, edited by Bopaya Bidanda and Paulo Bártolo, 171-206: Springer US, 2008.

Yang, J., J. Bei, and S. Wang. "Enhanced Cell Affinity of Poly (D,L-Lactide) by Combining Plasma Treatment with Collagen Anchorage." *Biomaterials* 23, no. 12 (Jun 2002): 2607-14.

Yeong, W. Y., C. K. Chua, K. F. Leong, and M. Chandrasekaran. "Rapid Prototyping in Tissue Engineering: Challenges and Potential." *Trends Biotechnol* 22, no. 12 (Dec 2004): 643-52.

Yoo, D. "Heterogeneous Minimal Surface Porous Scaffold Design Using the Distance Field and Radial Basis Functions." *Med Eng Phys* 34, no. 5 (Jun 2012): 625-39.

Yoo, D. "New Paradigms in Internal Architecture Design and Freeform Fabrication of Tissue Engineering Porous Scaffolds." *Med Eng Phys* 34, no. 6 (Jul 2012): 762-76.

Zeltinger, J., J. K. Sherwood, D. A. Graham, R. Mueller, and L. G. Griffith. "Effect of Pore Size and Void Fraction on Cellular Adhesion, Proliferation, and Matrix Deposition." *Tissue Eng* 7, no. 5 (Oct 2001): 557-72.

Appendix A: Mathematical models used

These are the mathematical models explored using K3d surf. The 'if' statements represent the boundaries of the model.

Gyroid inverse of thickened cube

```
if((x^10 + y^10 +z^10 < 9*10^8),

-(.5-(.81*(cos(x)*sin(y)+cos(y)*sin(z)+cos(z)*sin(x)))^2),

(x^10 + y^10 +z^10 -9*10^8))
```

Gyroid thickness bounded with cylinder:

```
if((((x/10)^2 + (y/10)^2)< 1),

(1-(.9*cos(x) * .9*sin(y) + .9*cos(y) * .9*sin(z) + .9*cos(z) * .9*sin(x))^2),

(((x/10)^2 + (y/10)^2 -1)))
```

Gyroid filled one pore structure:

```
if((x^10 + y^10 +z^10 < 900000000),

(.9*cos(x) * .9*sin(y) + .9*cos(y) * .9*sin(z) + .9*cos(z) * .9*sin(x)),

(x^10 + y^10 +z^10 -900000000))
```

Diamond TPMS thickened:

```
if((x^10 + y^10 +z^10 < 900000000),

(1-(1.5*sin(x) *sin(y) *sin(z) +1.5*sin(x) * cos(y) * cos(z) +1.5*cos(x) * sin(y) * cos(z) + 1.5*cos(x) * cos(y)
* sin(z))^2),

(x^10 + y^10 +z^10 -900000000))
```

Diamond TPMS filled one pore structure:

```
if((x^10 + y^10 +z^10 < 900000000),

(1.5*sin(x) *sin(y) *sin(z) +1.5*sin(x) * cos(y) * cos(z) +1.5*cos(x) * sin(y) * cos(z) + 1.5*cos(x) * cos(y) *
sin(z)),

(x^10 + y^10 +z^10 -900000000))
```

Gyroid thicked cube:

```
if((x^10 + y^10 +z^10 < 10^8),

(1-(cos(x)*sin(y) +cos(y)*sin(z) +cos(z)*sin(x))^2),

(x^10 + y^10 +z^10 -10^8))
```

Thin Wall Gyroid:

```
if((x^10 + y^10 +z^10 < 10^8),

-(.1-(.9*cos(x) * .9*sin(y) + .9*cos(y) * .9*sin(z) + .9*cos(z) * .9*sin(x))^2),

(x^10 + y^10 +z^10 -10^8))
```

High Resolution Thin Wall Gyroid - 10 x 10 x 10 ratio:

```
if((x^100 + y^100 + z^100 <10^99),

-(.2-(.9*cos(2*x) * .9*sin(2*y) + .9*cos(2*y) * .9*sin(2*z) + .9*cos(2*z) * .9*sin(2*x))^2),

(x^100 + y^100 + z^100-10^99))
```

High Resolution Thin Wall Gyroid - 10 x 10 x 3 ratio:

```
if((x^100 + y^100 + z^170 <10^99),

-(.2-(.9*cos(2*x) * .9*sin(2*y) + .9*cos(2*y) * .9*sin(2*z) + .9*cos(2*z) * .9*sin(2*x))^2),

(x^100 + y^100 + z^170-10^99))
```

Final Testing - 10x10x3:

```
if((x^100 + y^100 + z^200 <10^97),

-(.4-(.9*cos(2*x) * .9*sin(2*y) + .9*cos(2*y) * .9*sin(2*z) + .9*cos(2*z) * .9*sin(2*x))^2),

(x^100 + y^100 + z^200-10^97))
```

Appendix B: Makerbot ReplicatorG Settings

Here are screenshots of the settings used to print the final model with the 200µm nozzle and 25% stretch.

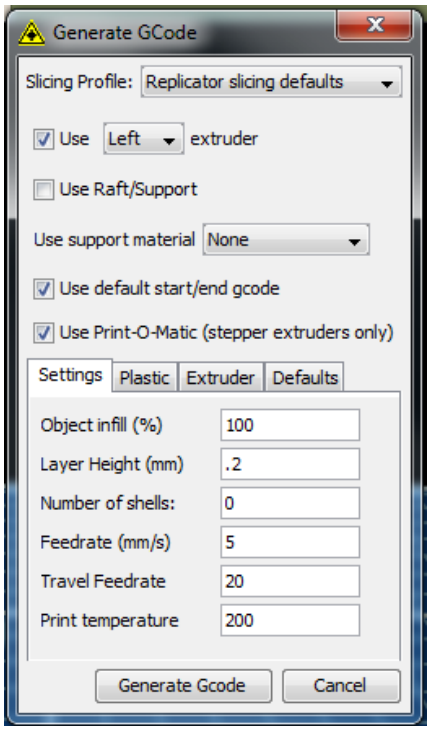

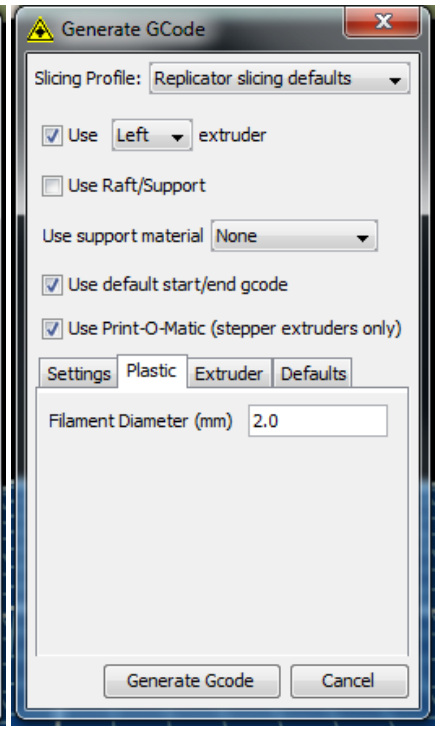

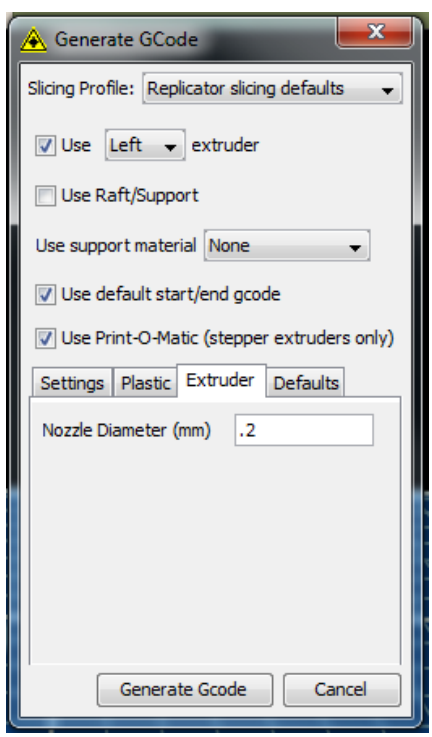

Appendix C: Cell Seeding Protocol

1. Place printed scaffolds in 70% ethanol for a minimum of 2 hours

2. Using sterile forceps move the scaffolds into a sterile tissue culture plate, allow to sit in a biosafety hood under UV light for at least 2 hours to complete sterilization and allow ethanol to evaporate.

3. again using sterile forceps relocate scaffolds from tissue culture plate into the PDMS seeding chamber. (this chamber is formed to the outer boundary of the sample scaffold in order to minimize gel loss during gelation)

4. Place EZ col gel on ice in the hood

5. trypsinize cells to be seeded and count. pellet in a 15mL conical tube

6. resuspend pellet in small (less than 200µl) amount of differentiation media

7. add collagen to resuspended cells to create a concentration of 2.5 $*10^6$ cells/mL

8. pipette 380µm of cell/collagen mixture onto the scaffold (note this number is accurate for the 10mm x10mm x3mm sample)

9. cover the entire PDMS seeding chamber with the sterile aluminum foil from autoclaving and relocate to 37C incubator for 1 hour

10. unwrap chamber in BSC and using sterile forceps move the scaffold into a cell culture plate(12 well or 4 well plate recommended).

11. cover scaffold with appropriate media and culture using standard culture methods.

Appendix D: Determination of Cell Seeding Density

After alizarin red staining on a 2d plate we determined 50,000 cells/well was the optimum for differentiation, using a cell thickness of 60µm as observed in imaging. All our collagen and scaffolds had a thickness of 3mm.

2d plate culture surface =1.9cm^2

60µm thick layers of cells/3mm=**50 layers**

50,000 cells/layer *50 layers=**2.5 *10^6 cells/50 layers**

50 layers in 24 well plate .3cm tall:

1.9cm^2 * .3cm = .570cm^3=.570mL

Final cell concentration **4.38x10^6 cells/mL**

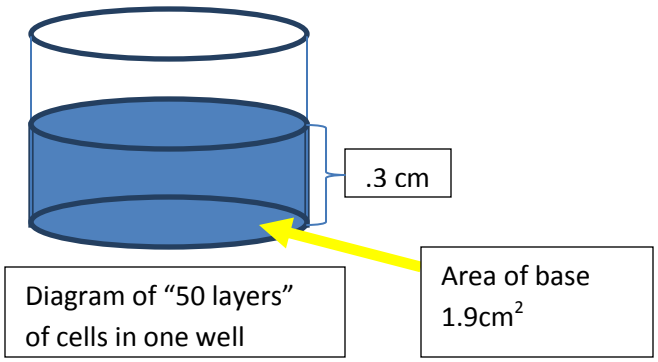

Appendix E: SolidWorks CAD Drawings

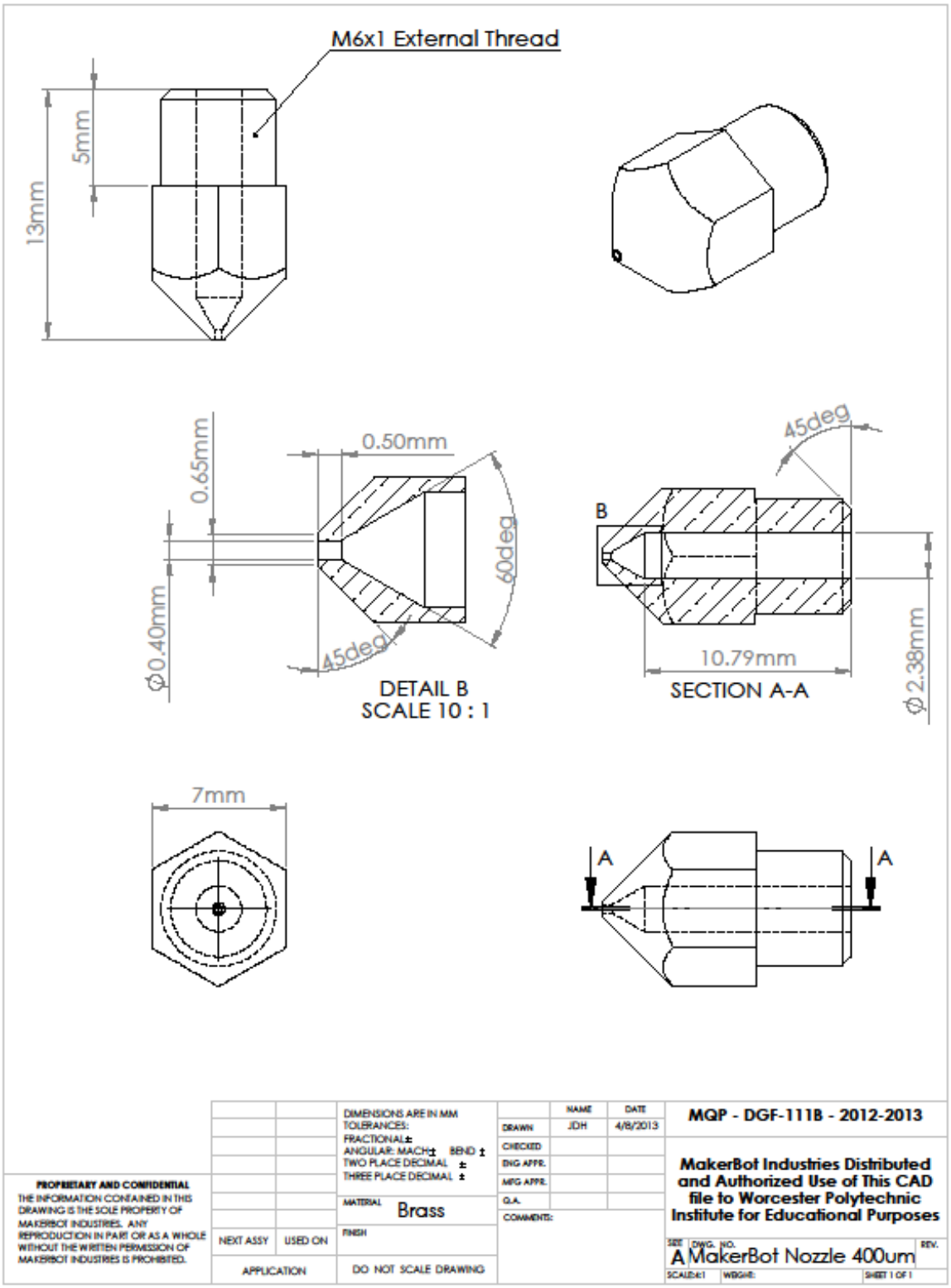

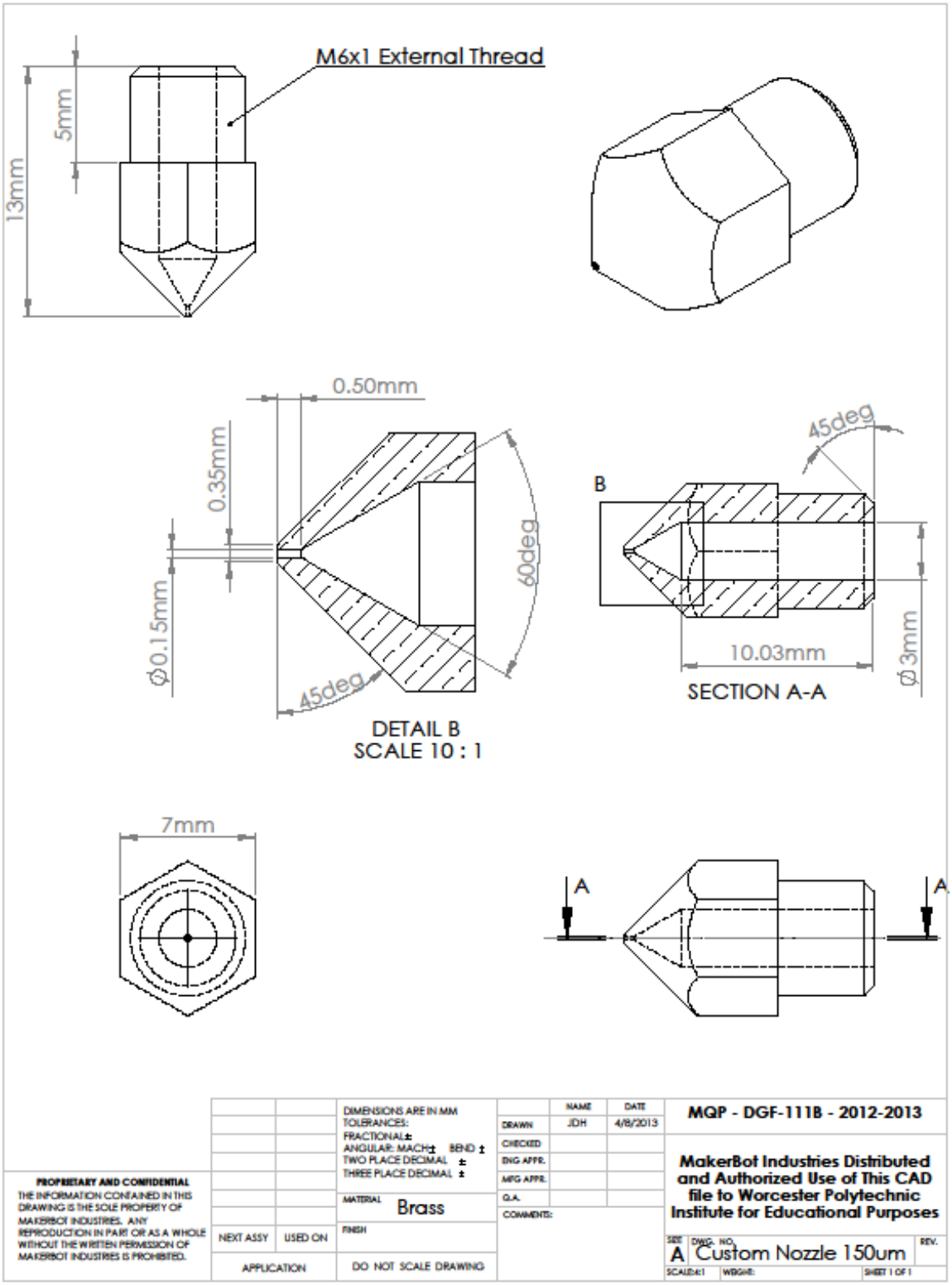
M6x1 External Thread
5mm
13mm
0.50mm
0.35mm
Ø0.15mm
60deg
45deg
DETAIL B
SCALE 10 : 1
B
45deg
10.03mm
Ø3mm
SECTION A-A
7mm
A
A
PROPRIETARY AND CONFIDENTIAL
THE INFORMATION CONTAINED IN THIS DRAWING IS THE SOLE PROPERTY OF MAKERBOT INDUSTRIES. ANY REPRODUCTION IN PART OR AS A WHOLE WITHOUT THE WRITTEN PERMISSION OF MAKERBOT INDUSTRIES IS PROHIBITED.
NEXT ASSY
USED ON
APPLICATION
DIMENSIONS ARE IN MM
TOLERANCES:
FRACTIONAL ±
ANGULAR: MACH ± BEND ±
TWO PLACE DECIMAL ±
THREE PLACE DECIMAL ±
MATERIAL Brass
FINISH
DO NOT SCALE DRAWING
NAME
DATE
DRAWN JDH 4/8/2013
CHECKED
ENG APPR.
MFG APPR.
Q.A.
COMMENTS:
MQP - DGF-111B - 2012-2013
MakerBot Industries Distributed and Authorized Use of This CAD file to Worcester Polytechnic Institute for Educational Purposes
SIZE A
DWG. NO. Custom Nozzle 150um
REV.
SCALE:1:1
WEIGHT:
SHEET 1 OF 1

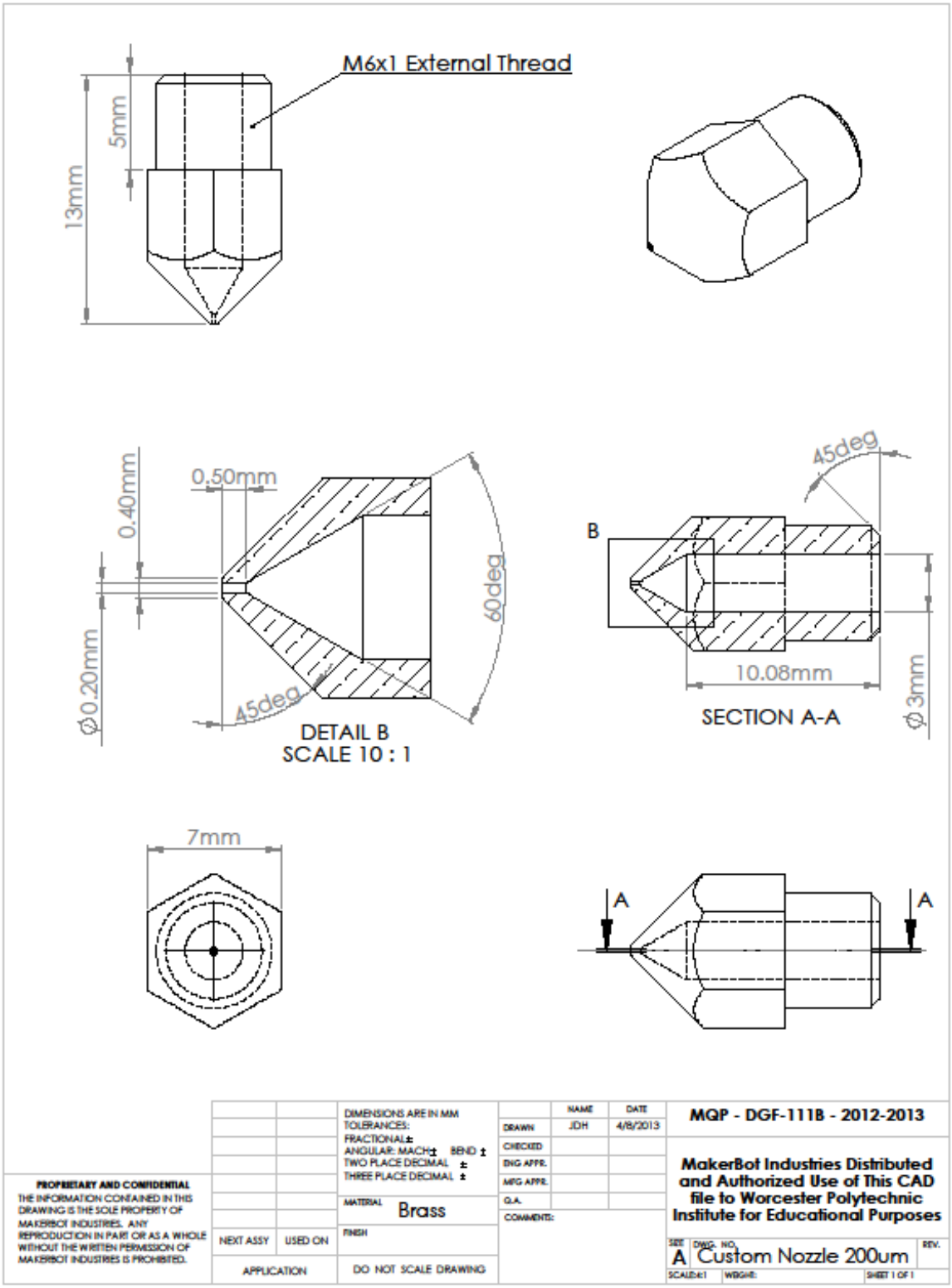
M6x1 External Thread
5mm
13mm
0.50mm
0.40mm
60deg
45deg
Ø0.20mm
DETAIL B
SCALE 10 : 1
45deg
B
10.08mm
Ø3mm
SECTION A-A
7mm
A
A
PROPRIETARY AND CONFIDENTIAL
THE INFORMATION CONTAINED IN THIS DRAWING IS THE SOLE PROPERTY OF MAKERBOT INDUSTRIES. ANY REPRODUCTION IN PART OR AS A WHOLE WITHOUT THE WRITTEN PERMISSION OF MAKERBOT INDUSTRIES IS PROHIBITED.
NEXT ASSY
USED ON
APPLICATION
DIMENSIONS ARE IN MM
TOLERANCES:
FRACTIONAL ±
ANGULAR: MACH ± BEND ±
TWO PLACE DECIMAL ±
THREE PLACE DECIMAL ±
MATERIAL
Brass
FINISH
DO NOT SCALE DRAWING
NAME
DATE
DRAWN
JDH
4/8/2013
CHECKED
ENG APPR.
MFG APPR.
Q.A.
COMMENTS:
MQP - DGF-111B - 2012-2013
MakerBot Industries Distributed and Authorized Use of This CAD file to Worcester Polytechnic Institute for Educational Purposes
SIZE
A
DWG. NO.
Custom Nozzle 200um
REV.
SCALE:1:1
WEIGHT:
SHEET 1 OF 1

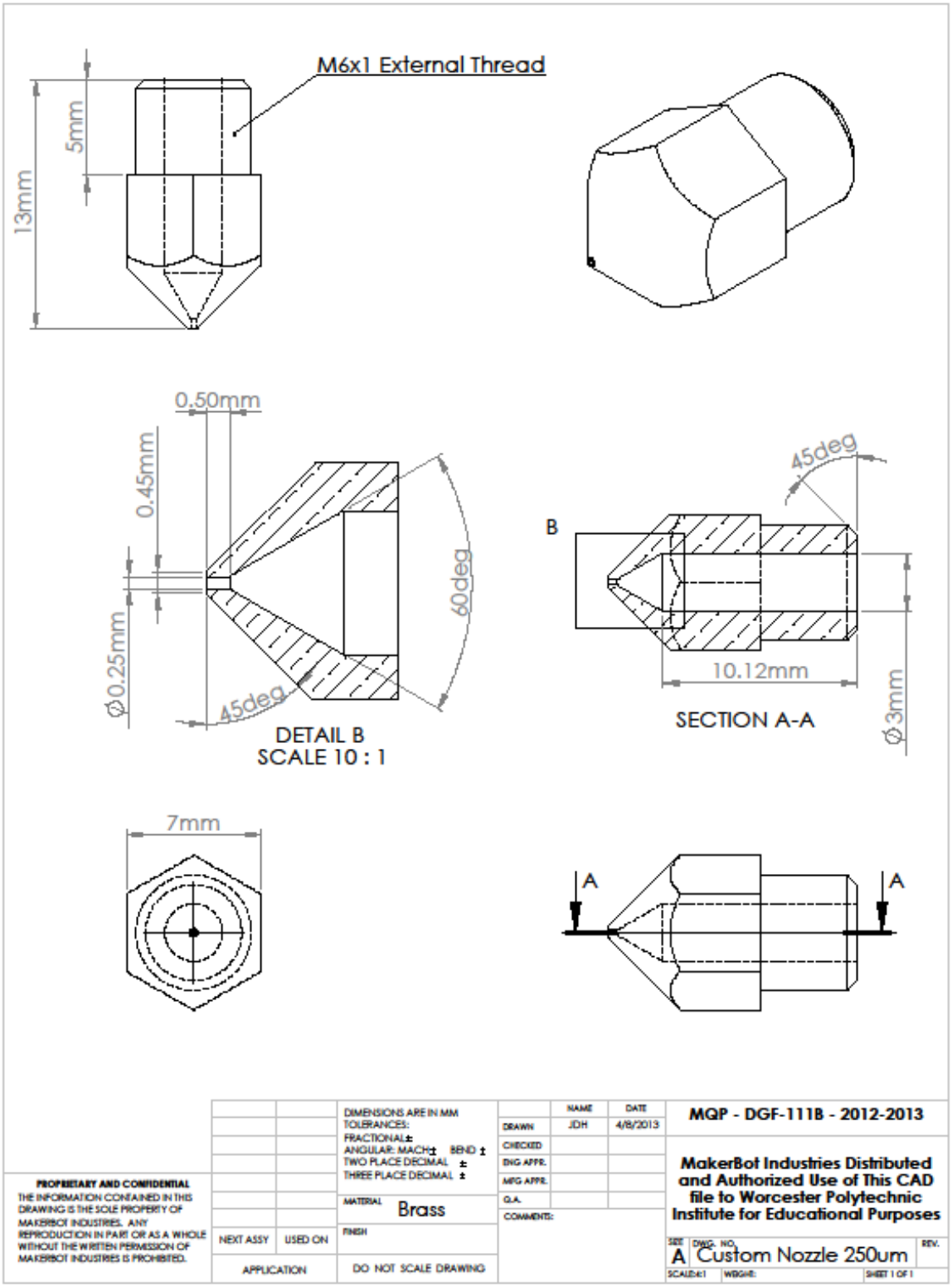
M6x1 External Thread
5mm
13mm
0.50mm
0.45mm
Ø0.25mm
60deg
45deg
DETAIL B
SCALE 10 : 1
B
45deg
10.12mm
Ø3mm
SECTION A-A
7mm
A
A
PROPRIETARY AND CONFIDENTIAL
THE INFORMATION CONTAINED IN THIS DRAWING IS THE SOLE PROPERTY OF MAKERBOT INDUSTRIES. ANY REPRODUCTION IN PART OR AS A WHOLE WITHOUT THE WRITTEN PERMISSION OF MAKERBOT INDUSTRIES IS PROHIBITED.
NEXT ASSY
USED ON
APPLICATION
DIMENSIONS ARE IN MM
TOLERANCES:
FRACTIONAL ±
ANGULAR: MACH ± BEND ±
TWO PLACE DECIMAL ±
THREE PLACE DECIMAL ±
MATERIAL Brass
FINISH
DO NOT SCALE DRAWING
NAME
DATE
DRAWN JDH 4/8/2013
CHECKED
ENG APPR.
MFG APPR.
Q.A.
COMMENTS:
MQP - DGF-111B - 2012-2013
MakerBot Industries Distributed and Authorized Use of This CAD file to Worcester Polytechnic Institute for Educational Purposes
SIZE A
DWG. NO. Custom Nozzle 250um
REV.
SCALE:1:1
WEIGHT:
SHEET 1 OF 1

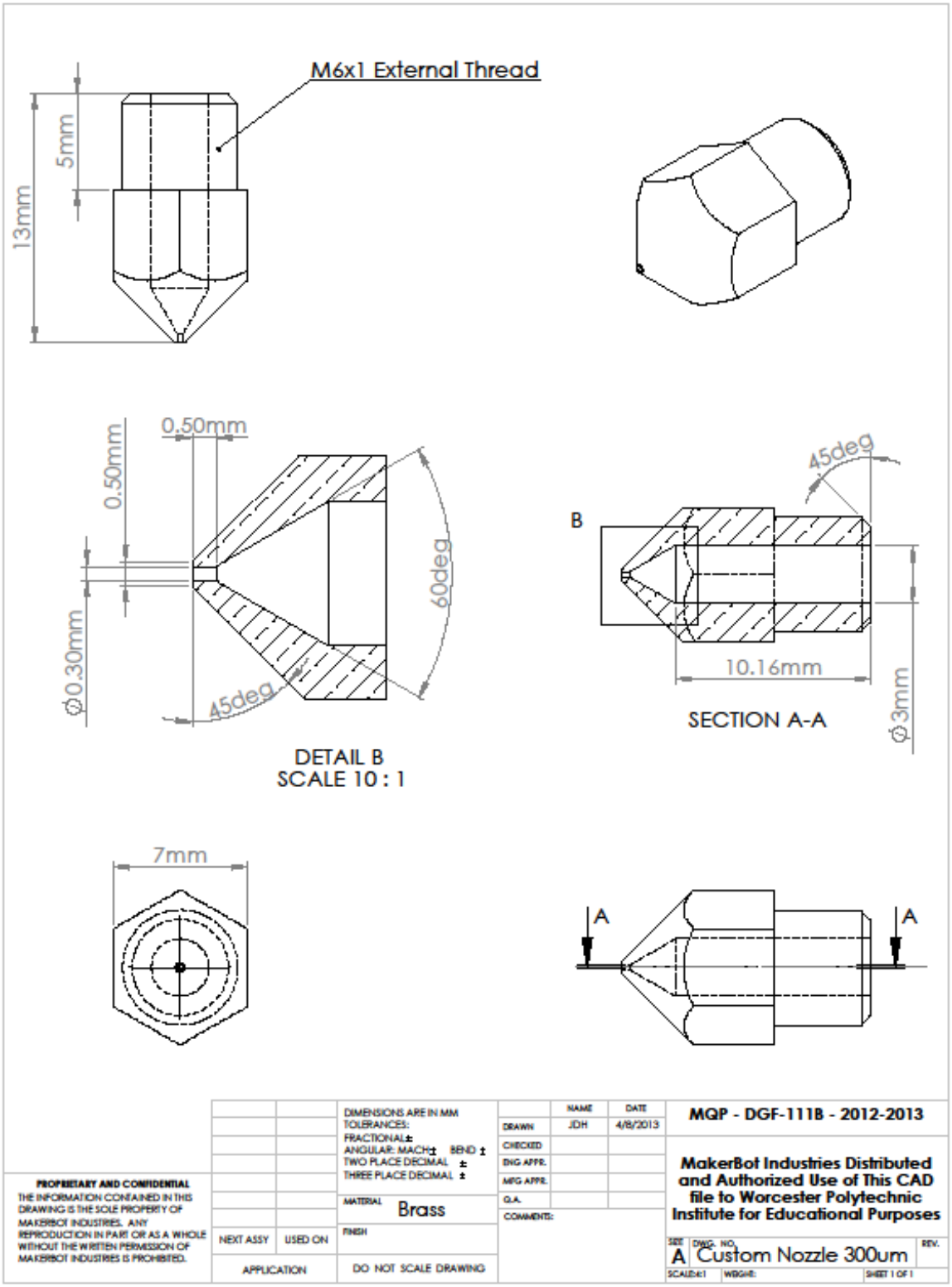
M6x1 External Thread
5mm
13mm
0.50mm
0.50mm
Ø0.30mm
60deg
45deg
DETAIL B
SCALE 10 : 1
B
45deg
10.16mm
Ø3mm
SECTION A-A
7mm
A
A
PROPRIETARY AND CONFIDENTIAL
THE INFORMATION CONTAINED IN THIS DRAWING IS THE SOLE PROPERTY OF MAKERBOT INDUSTRIES. ANY REPRODUCTION IN PART OR AS A WHOLE WITHOUT THE WRITTEN PERMISSION OF MAKERBOT INDUSTRIES IS PROHIBITED.
NEXT ASSY
USED ON
APPLICATION
DIMENSIONS ARE IN MM
TOLERANCES:
FRACTIONAL ±
ANGULAR: MACH ± BEND ±
TWO PLACE DECIMAL ±
THREE PLACE DECIMAL ±
MATERIAL
Brass
FINISH
DO NOT SCALE DRAWING
NAME
DATE
DRAWN
JDH
4/8/2013
CHECKED
ENG APPR.
MFG APPR.
Q.A.
COMMENTS:
MQP - DGF-111B - 2012-2013
MakerBot Industries Distributed and Authorized Use of This CAD file to Worcester Polytechnic Institute for Educational Purposes
SIZE
A
DWG. NO.
Custom Nozzle 300um
REV.
SCALE:1:1
WEIGHT:
SHEET 1 OF 1

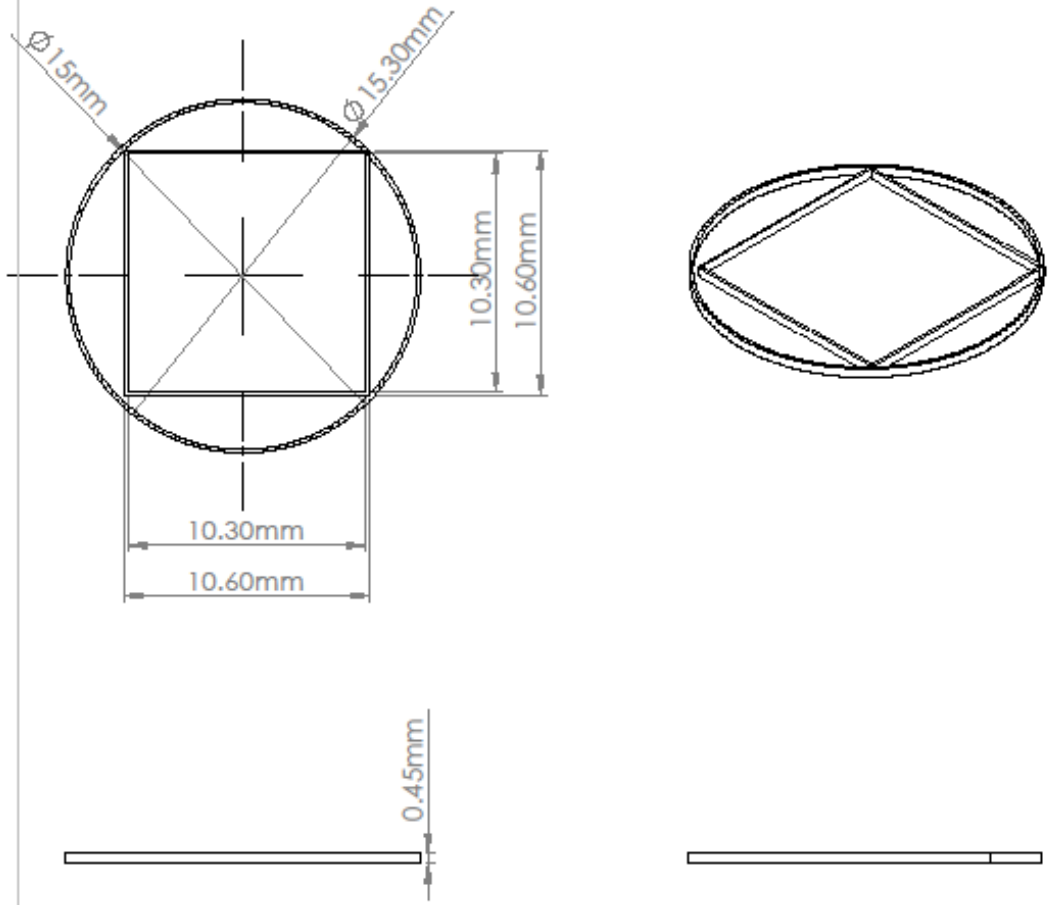

				NAME	DATE	Worcester Polytechnic Institute
		DIMENSIONS ARE IN MM TOLERANCES: FRACTIONAL ± ANGULAR: MACH ± BEND ± TWO PLACE DECIMAL ± THREE PLACE DECIMAL ±	DRAWN	JDH	4/8/2013	
			CHECKED			MQP - DGF-111B - 2012-2013
			ENG APPR.			
			MFG APPR.			
		MATERIAL Poly-lactide - 1.75mm Filament	Q.A.			
			COMMENTS:			
NEXT ASSY	USED ON	FINISH Printed by MakerBot Replicator				SIZE A DWG. NO. circle-square 150um REV.
APPLICATION		DO NOT SCALE DRAWING				SCALE:6:1 WEIGHT: SHEET 1 OF 1

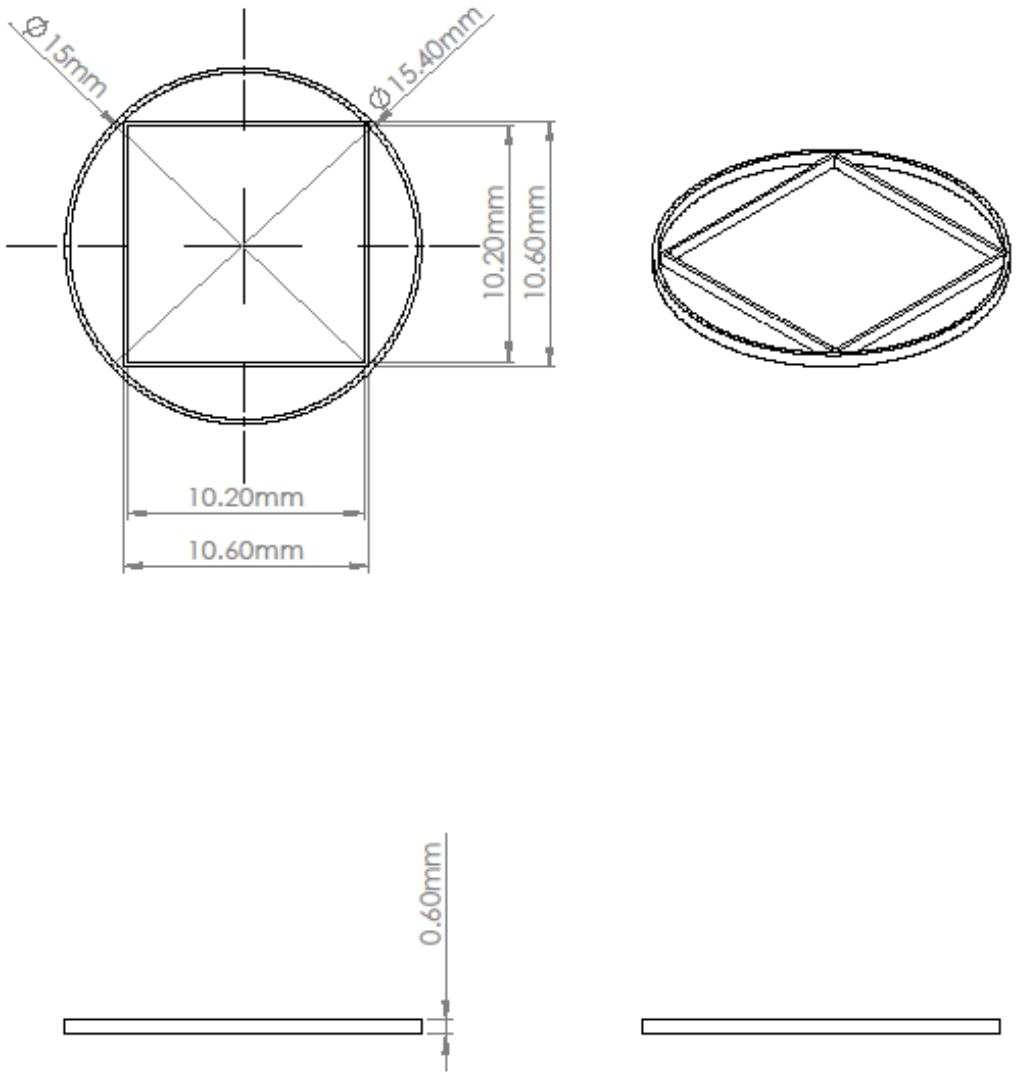

		DIMENSIONS ARE IN MM TOLERANCES: FRACTIONAL ± ANGULAR: MACH ± BEND ± TWO PLACE DECIMAL ± THREE PLACE DECIMAL ±		NAME	DATE
			DRAWN	JDH	4/8/2013
			CHECKED		
			ENG APPR.		
			MFG APPR.		
		MATERIAL Poly-lactide - 1.75mm Filament	Q.A.		
			COMMENTS:		
NEXT ASSY	USED ON	FINISH Printed by MakerBot Replicator			
APPLICATION		DO NOT SCALE DRAWING			

Worcester Polytechnic Institute

MQP - DGF-111B - 2012-2013

SIZE A | DWG. NO. circle-square 200um | REV.

SCALE:1:1 | WEIGHT: | SHEET 1 OF 1

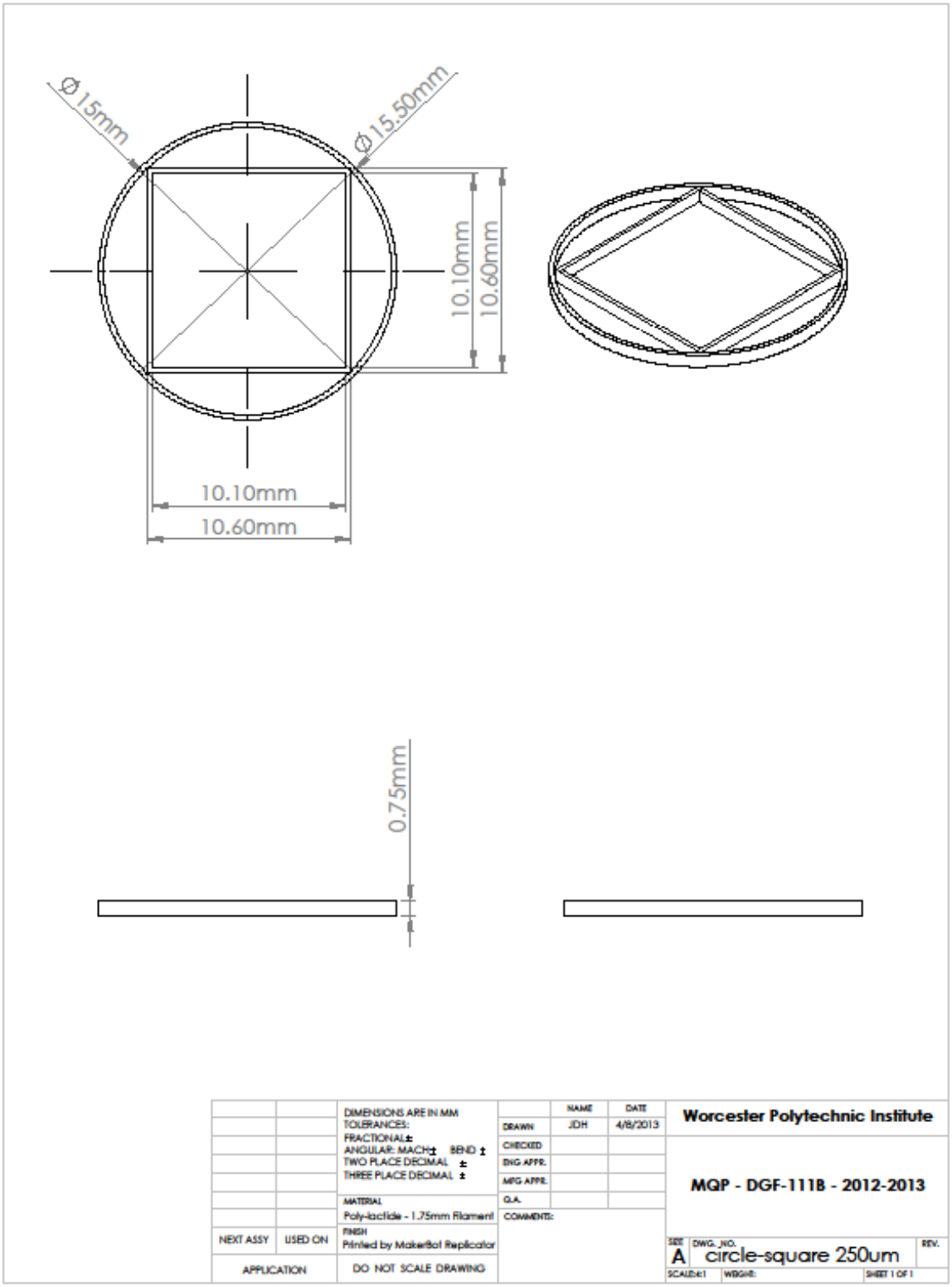
Ø15mm
Ø15.50mm
10.10mm
10.60mm
10.10mm
10.60mm
0.75mm
DIMENSIONS ARE IN MM
TOLERANCES:
FRACTIONAL ±
ANGULAR: MACH ± BEND ±
TWO PLACE DECIMAL ±
THREE PLACE DECIMAL ±
MATERIAL
Poly-lactide - 1.75mm Filament
FINISH
Printed by MakerBot Replicator
NEXT ASSY
USED ON
APPLICATION
DO NOT SCALE DRAWING
NAME
DATE
DRAWN
JDH
4/8/2013
CHECKED
ENG APPR.
MFG APPR.
Q.A.
COMMENTS:
Worcester Polytechnic Institute
MQP - DGF-111B - 2012-2013
SIZE
A
DWG. NO.
circle-square 250um
REV.
SCALE:1:1
WEIGHT:
SHEET 1 OF 1

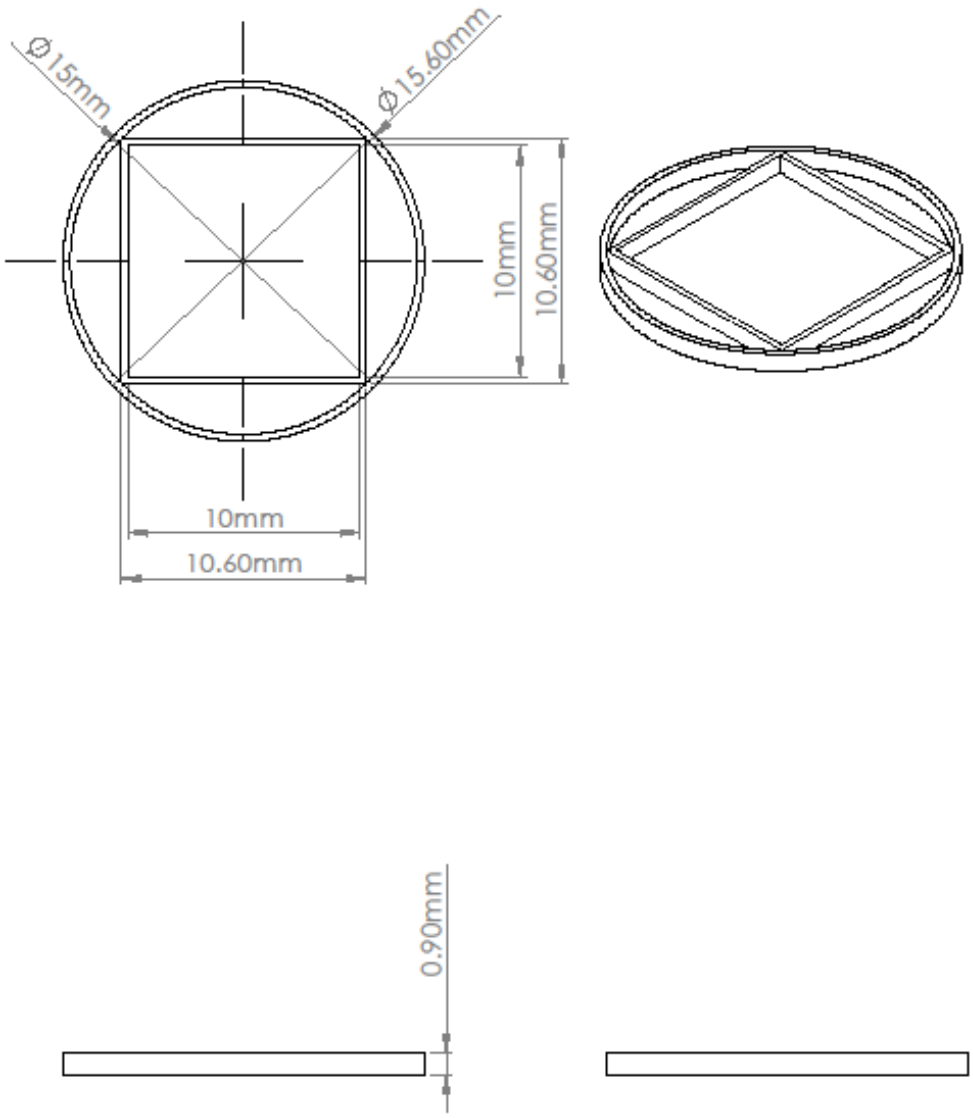

		DIMENSIONS ARE IN MM TOLERANCES: FRACTIONAL ± ANGULAR: MACH ± BEND ± TWO PLACE DECIMAL ± THREE PLACE DECIMAL ±		NAME	DATE
			DRAWN	JDH	4/8/2013
			CHECKED		
			ENG APPR.		
			MFG APPR.		
		MATERIAL Poly-lactide - 1.75mm Filament	Q.A.		
			COMMENTS:		
NEXT ASSY	USED ON	FINISH Printed by MakerBot Replicator			
APPLICATION		DO NOT SCALE DRAWING			

Worcester Polytechnic Institute

MQP - DGF-111B - 2012-2013

SIZE A | DWG. NO. circle-square 300um | REV.

SCALE:1:1 | WEIGHT: | SHEET 1 OF 1

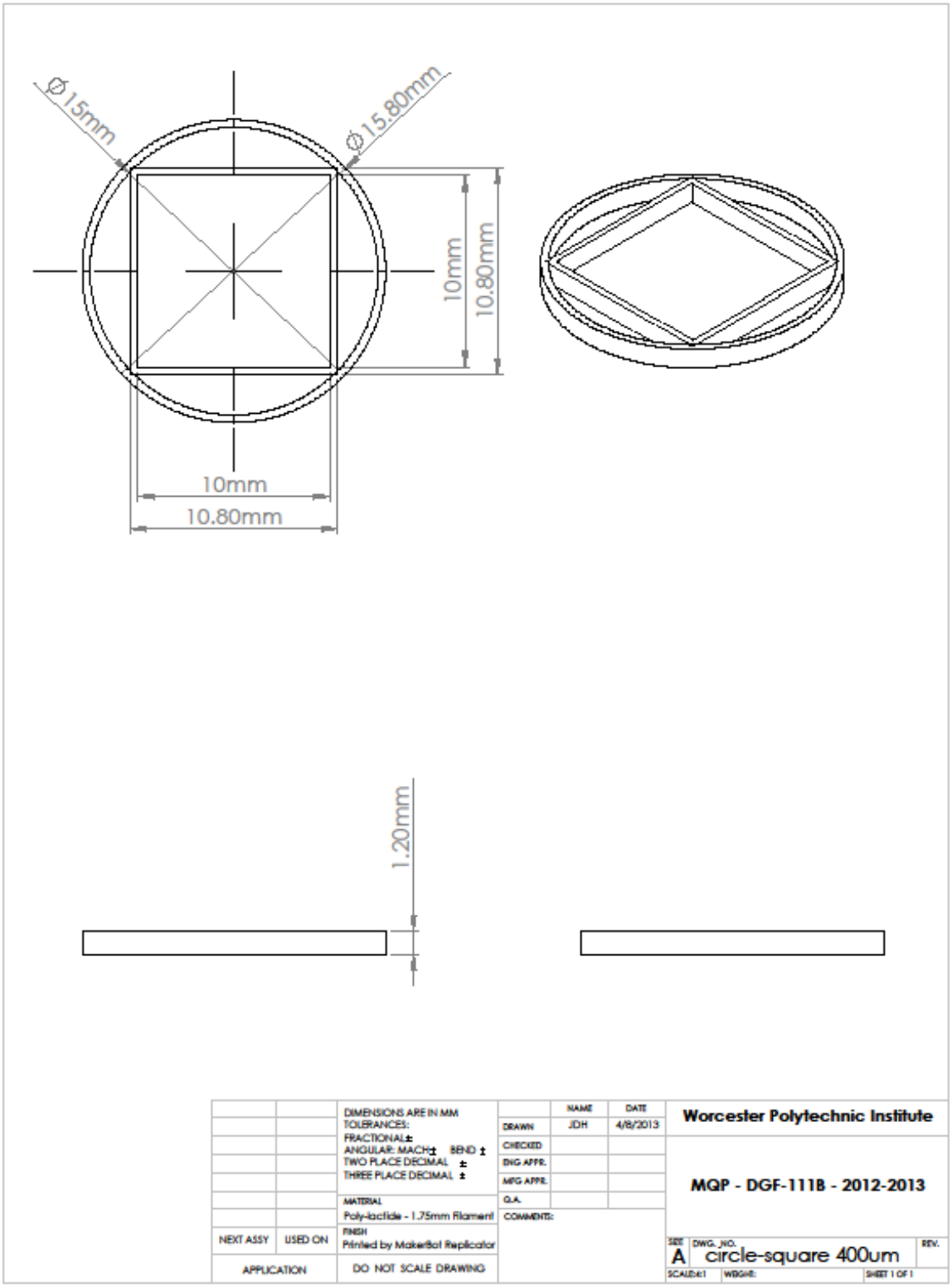
Ø15mm
Ø15.80mm
10mm
10.80mm
10mm
10.80mm
1.20mm
DIMENSIONS ARE IN MM
TOLERANCES:
FRACTIONAL ±
ANGULAR: MACH ± BEND ±
TWO PLACE DECIMAL ±
THREE PLACE DECIMAL ±
MATERIAL
Poly-lactide - 1.75mm Filament
FINISH
Printed by MakerBot Replicator
NEXT ASSY
USED ON
APPLICATION
DO NOT SCALE DRAWING
NAME
DATE
DRAWN
JDH
4/8/2013
CHECKED
ENG APPR.
MFG APPR.
Q.A.
COMMENTS:
Worcester Polytechnic Institute
MQP - DGF-111B - 2012-2013
SIZE
A
DWG. NO.
circle-square 400um
REV.
SCALE:1:1
WEIGHT:
SHEET 1 OF 1

Appendix F: Esprit CAM Software Settings Used to Manufacture Nozzles

McMASTER-CARR

609-689-3000
609-259-3575 (fax)
nj.sales@mcmaster.com

Receipt

Purchase Order	1118JHALTER
Paid	$84.60
Invoice	41182424
Invoice Date	11/19/12

Billed to
ATTENTION: JESSE D HALTER
WRIGHT GROUP, INC.
125 REAR STANPHYL RD.
REAR RED BUILDING
UXBRIDGE MA 01569

Shipped to
Wright Group, Inc.
125 Rear Stanphyl Rd.
Rear Red Building
Uxbridge MA 01569

Information About Your Payment

Credit Card	MasterCard Ending- 6751
Date	11/20/12
Name on Card	Jesse D Halter
Your Account	99883100

Jesse Halter placed this order.

Line		Product	Ordered	Shipped	Balance	Price	Total
1	2951A11	High-Speed Steel Micro-Size Drill Bit, .0059" Size, 3/4" Overall Length, .04" Drill Depth	3 Each	3	0	9.56 Each	28.68
2	2951A22	High-Speed Steel Micro-Size Drill Bit, .0098" Size, 3/4" Oal, .09" Drill Depth	3 Each	3	0	5.47 Each	16.41
3	2951A16	High-Speed Steel Micro-Size Drill Bit, .0079" Size, 3/4" Overall Length, .08" Drill Depth	3 Each	3	0	6.88 Each	20.64
4	2951A27	High-Speed Steel Micro-Size Drill Bit, .0118" Size, 3/4" Overall Length, .09" Drill Depth	3 Each	3	0	4.72 Each	14.16

Merchandise	79.89
Shipping	4.71
Total	$84.60
Payment Received 11/20/12	(84.60)
Balance Due	$0.00

Packing List	Shipped	Weight	Carrier	Tracking
4138230-01	11/19/2012	1 lb	UPS Ground	1Z0835200345510164

Federal ID 36-1458720 McMaster-Carr Supply Company

Purchased micro-drills to manufacture custom bore nozzles compatible with the MakerBot Replicator.

HOME / HOLEMAKING / CENTER DRILLS (COMBINATION DRILL & COUNTERSINKS) & SPOTTING DRILLS / SPOTTING DRILLS & SETS / SPOTTING DRILLS / #89698955

Spotting Drills | Body Diameter (mm): 3.00 | Drill Point Angle: 60

MSC Part #:	89698955
Big Book Page #:	191
Brand:	Accupro

Write the first review

Share this product 0

Order Qty:	Order Qty of 1 = (1) Piece
In Stock:	61
Price:	$15.61 ea.
Quantity:	1

TOTAL: $16.81

Add to My List
Create a CMI Label

Description | Alternate Items | Item Notes | Reviews

Spotting Drills | Body Diameter (mm): 3.00 | Drill Point Angle: 60 | Flute Length (mm): 12.00 | Overall Length (mm): 38.00 | Spotting Drill Material: Solid Carbide | Spotting Drill Finish/Coating: Bright

Product Specifications

Body Diameter (mm)	3.00
Drill Point Angle	60
Flute Length (mm)	12.00
Overall Length (mm)	38.00
Spotting Drill Material	Solid Carbide
Spotting Drill Finish/Coating	Bright
Drill Bit Grade	High Performance
Cutting Direction	Right Hand
Tapered (Yes/No)	No

Purchased 60 degree 3mm spot drill specialty drill bit to drill nozzle filament extrusion melt chamber.

WPI Machine Shop Esprit Computer Aided Manufacturing (CAM) Software used to manufacture nozzles.

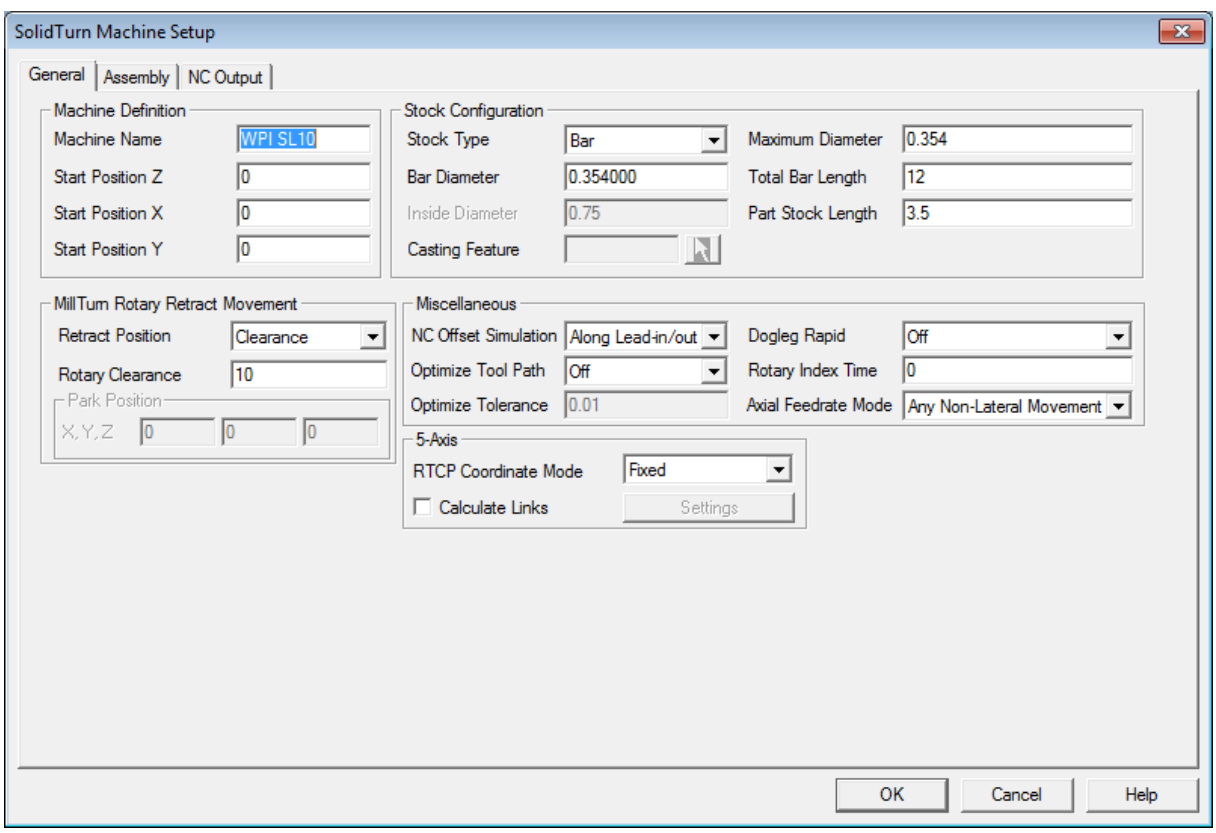

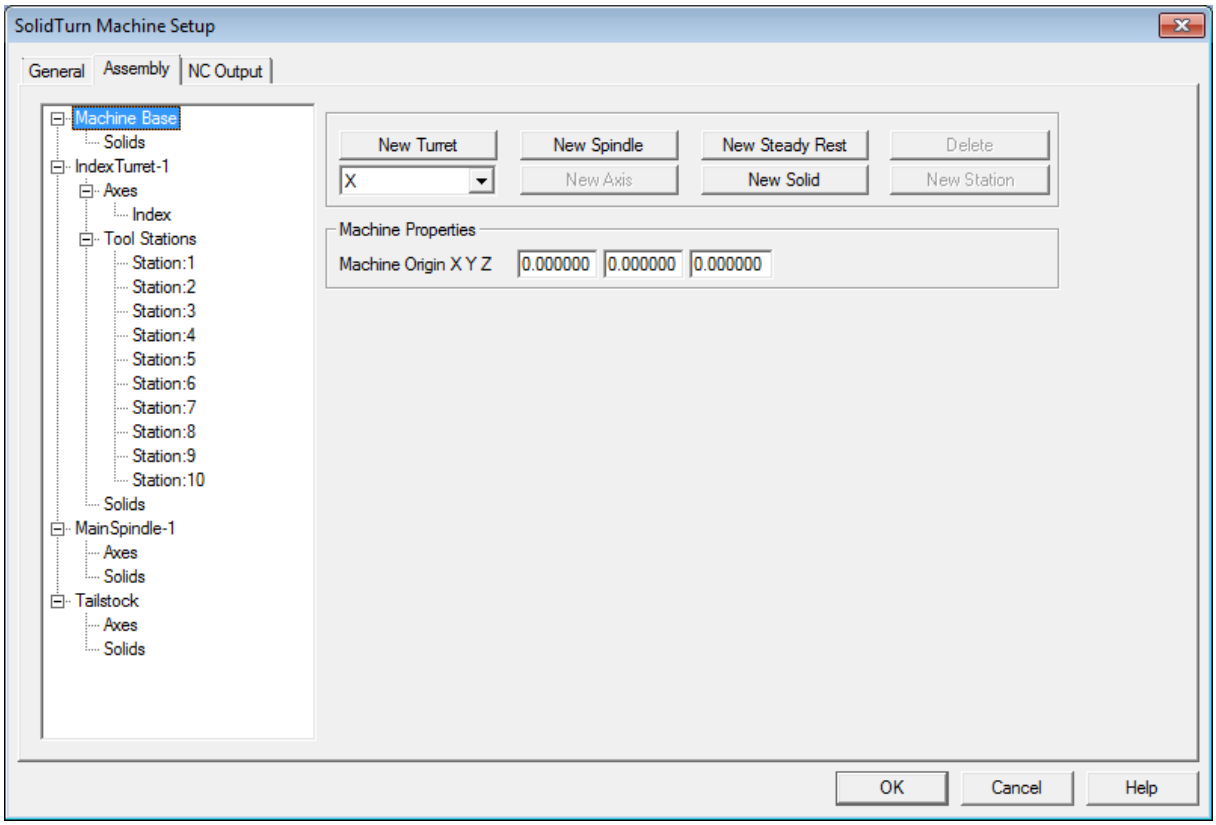
SolidTurn Machine Setup
General
Assembly
NC Output
Machine Base
Solids
IndexTurret-1
Axes
Index
Tool Stations
Station:1
Station:2
Station:3
Station:4
Station:5
Station:6
Station:7
Station:8
Station:9
Station:10
Solids
MainSpindle-1
Axes
Solids
Tailstock
Axes
Solids
New Turret
New Spindle
New Steady Rest
Delete
X
New Axis
New Solid
New Station
Machine Properties
Machine Origin X Y Z
0.000000
0.000000
0.000000
OK
Cancel
Help

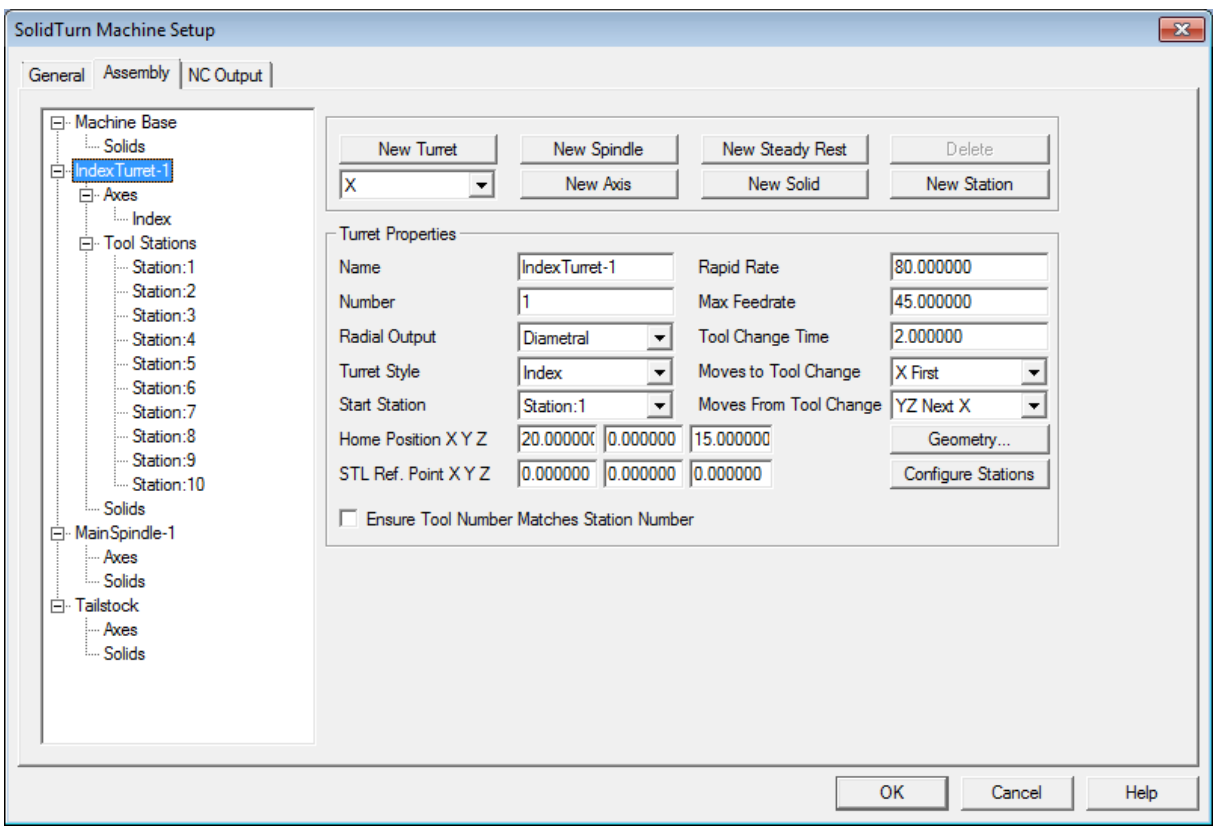
SolidTurn Machine Setup
General
Assembly
NC Output
Machine Base
Solids
IndexTurret-1
Axes
Index
Tool Stations
Station:1
Station:2
Station:3
Station:4
Station:5
Station:6
Station:7
Station:8
Station:9
Station:10
Solids
MainSpindle-1
Axes
Solids
Tailstock
Axes
Solids
New Turret
New Spindle
New Steady Rest
Delete
X
New Axis
New Solid
New Station
Turret Properties
Name
IndexTurret-1
Rapid Rate
80.000000
Number
1
Max Feedrate
45.000000
Radial Output
Diametral
Tool Change Time
2.000000
Turret Style
Index
Moves to Tool Change
X First
Start Station
Station:1
Moves From Tool Change
YZ Next X
Home Position X Y Z
20.00000(
0.000000
15.000000
Geometry...
STL Ref. Point X Y Z
0.000000
0.000000
0.000000
Configure Stations
Ensure Tool Number Matches Station Number
OK
Cancel
Help

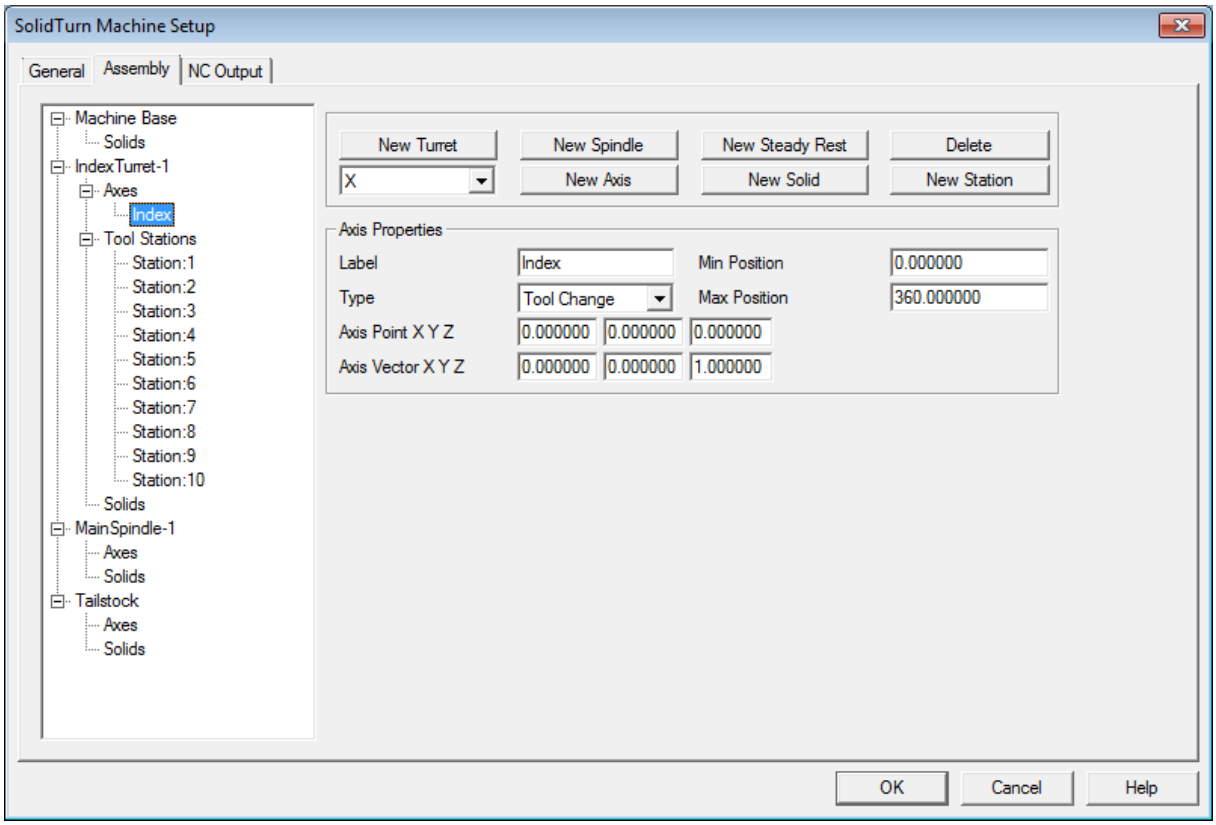
SolidTurn Machine Setup
General
Assembly
NC Output
Machine Base
Solids
IndexTurret-1
Axes
Index
Tool Stations
Station:1
Station:2
Station:3
Station:4
Station:5
Station:6
Station:7
Station:8
Station:9
Station:10
Solids
MainSpindle-1
Axes
Solids
Tailstock
Axes
Solids
New Turret
New Spindle
New Steady Rest
Delete
X
New Axis
New Solid
New Station
Axis Properties
Label
Index
Min Position
0.000000
Type
Tool Change
Max Position
360.000000
Axis Point X Y Z
0.000000
0.000000
0.000000
Axis Vector X Y Z
0.000000
0.000000
1.000000
OK
Cancel
Help

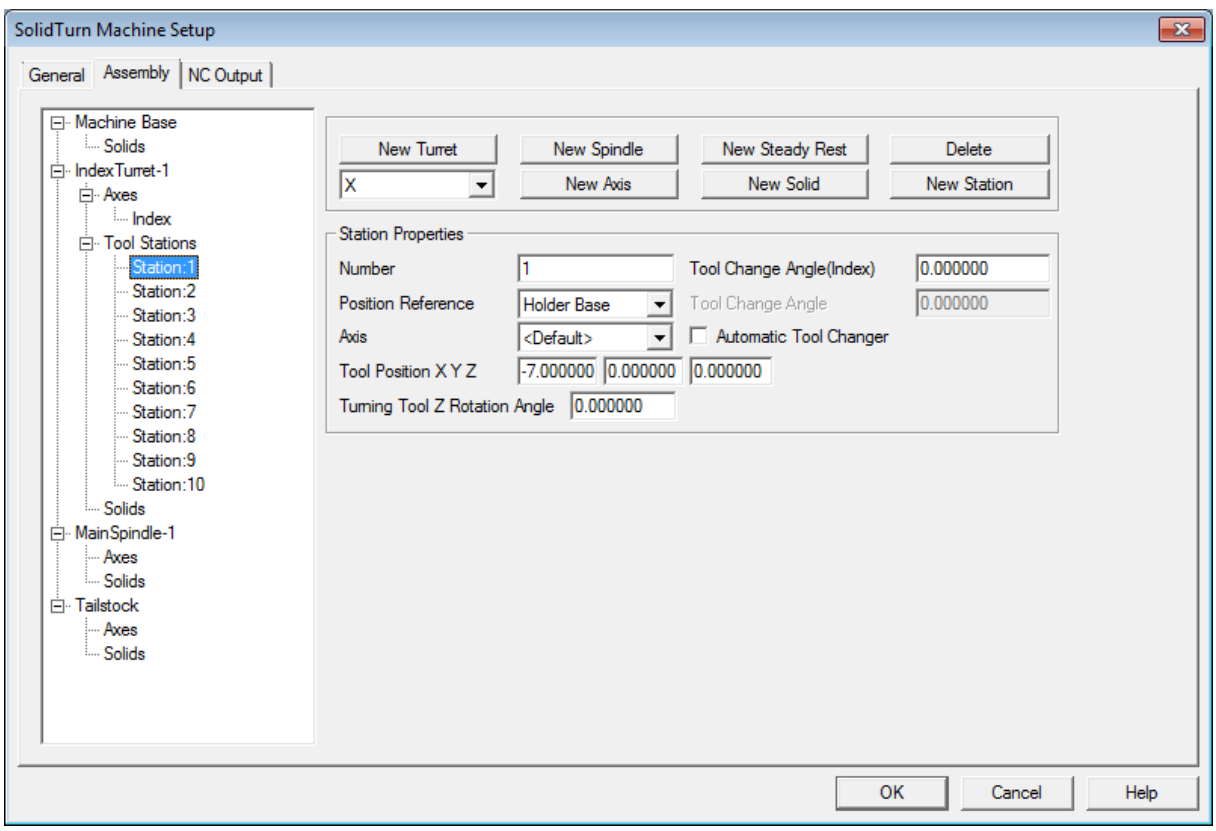
SolidTurn Machine Setup
General
Assembly
NC Output
Machine Base
Solids
IndexTurret-1
Axes
Index
Tool Stations
Station:1
Station:2
Station:3
Station:4
Station:5
Station:6
Station:7
Station:8
Station:9
Station:10
Solids
MainSpindle-1
Axes
Solids
Tailstock
Axes
Solids
New Turret
New Spindle
New Steady Rest
Delete
X
New Axis
New Solid
New Station
Station Properties
Number
1
Tool Change Angle(Index)
0.000000
Position Reference
Holder Base
Tool Change Angle
0.000000
Axis
<Default>
Automatic Tool Changer
Tool Position X Y Z
-7.000000
0.000000
0.000000
Turning Tool Z Rotation Angle
0.000000
OK
Cancel
Help

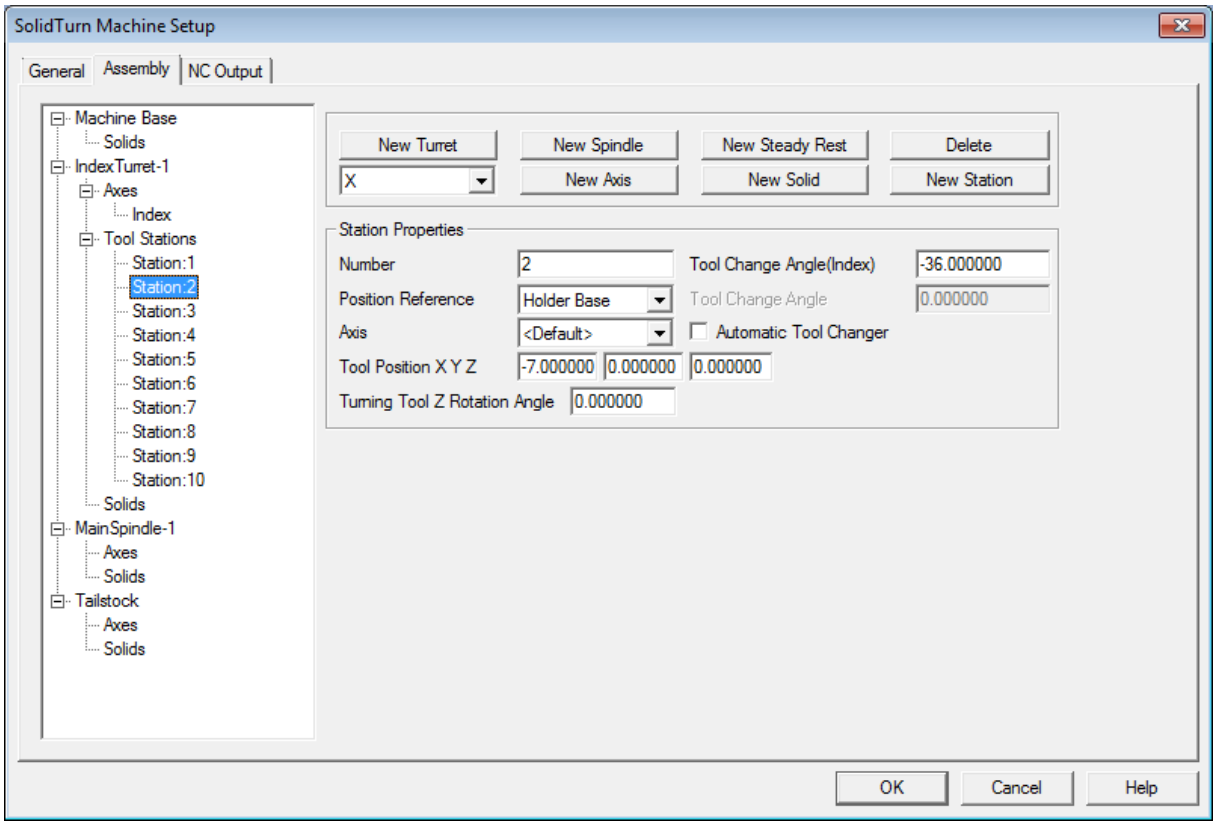
SolidTurn Machine Setup
General
Assembly
NC Output
Machine Base
Solids
IndexTurret-1
Axes
Index
Tool Stations
Station:1
Station:2
Station:3
Station:4
Station:5
Station:6
Station:7
Station:8
Station:9
Station:10
Solids
MainSpindle-1
Axes
Solids
Tailstock
Axes
Solids
New Turret
New Spindle
New Steady Rest
Delete
X
New Axis
New Solid
New Station
Station Properties
Number
2
Tool Change Angle(Index)
-36.000000
Position Reference
Holder Base
Tool Change Angle
0.000000
Axis
<Default>
Automatic Tool Changer
Tool Position X Y Z
-7.000000
0.000000
0.000000
Turning Tool Z Rotation Angle
0.000000
OK
Cancel
Help

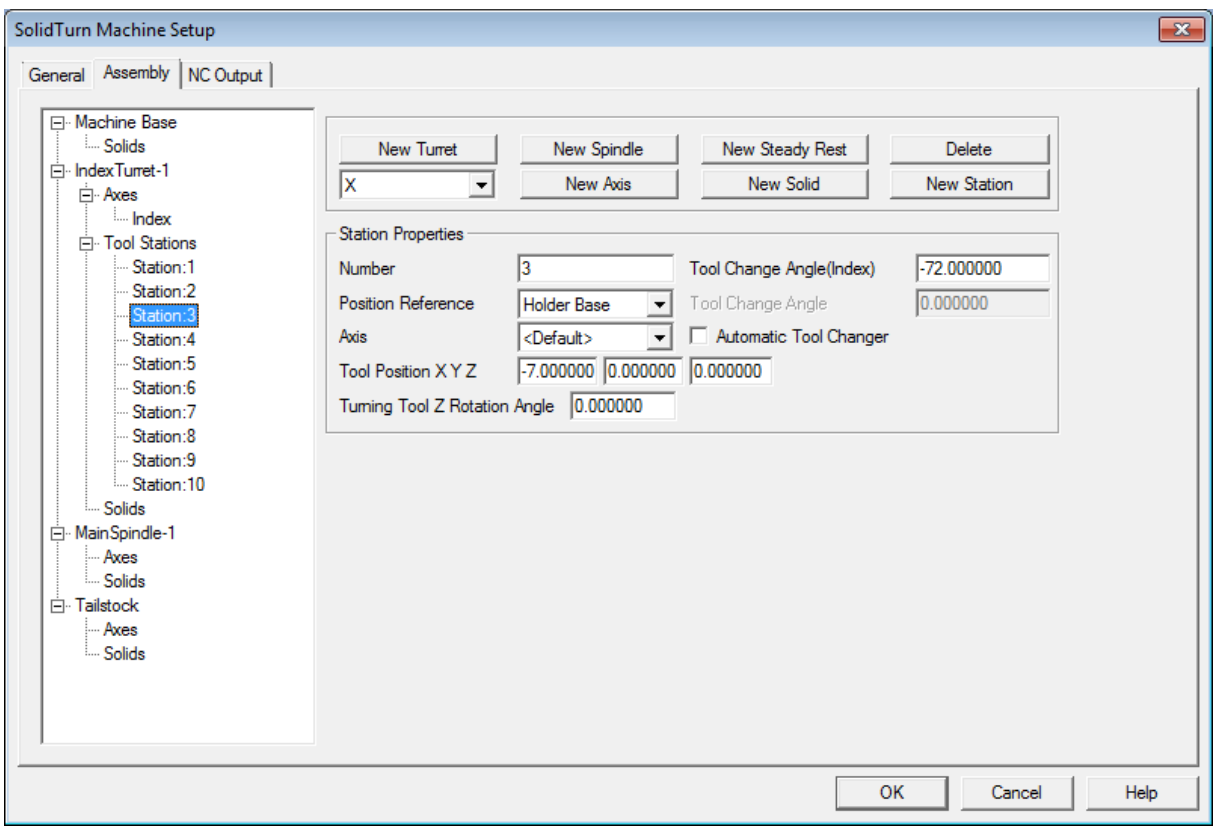
SolidTurn Machine Setup
General
Assembly
NC Output
Machine Base
Solids
IndexTurret-1
Axes
Index
Tool Stations
Station:1
Station:2
Station:3
Station:4
Station:5
Station:6
Station:7
Station:8
Station:9
Station:10
Solids
MainSpindle-1
Axes
Solids
Tailstock
Axes
Solids
New Turret
New Spindle
New Steady Rest
Delete
X
New Axis
New Solid
New Station
Station Properties
Number
3
Tool Change Angle(Index)
-72.000000
Position Reference
Holder Base
Tool Change Angle
0.000000
Axis
<Default>
Automatic Tool Changer
Tool Position X Y Z
-7.000000
0.000000
0.000000
Turning Tool Z Rotation Angle
0.000000
OK
Cancel
Help

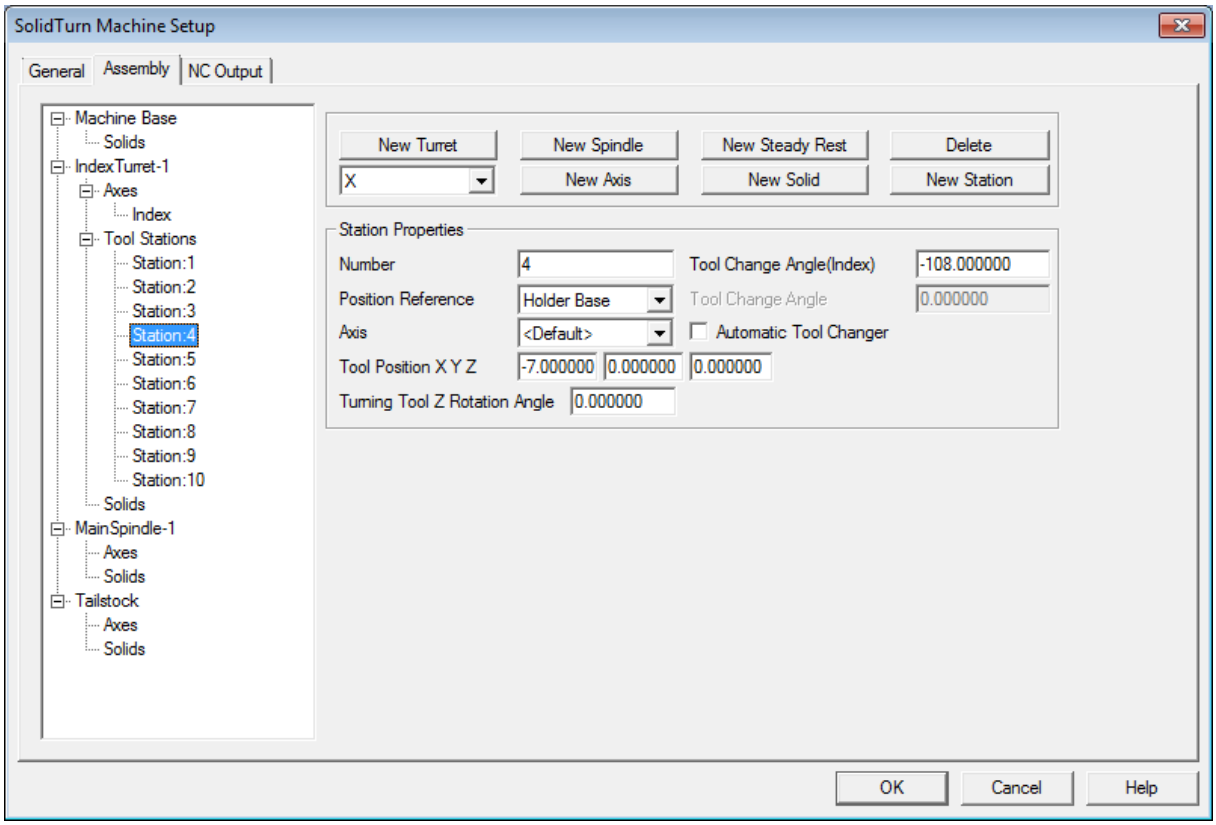
SolidTurn Machine Setup
General
Assembly
NC Output
Machine Base
Solids
IndexTurret-1
Axes
Index
Tool Stations
Station:1
Station:2
Station:3
Station:4
Station:5
Station:6
Station:7
Station:8
Station:9
Station:10
Solids
MainSpindle-1
Axes
Solids
Tailstock
Axes
Solids
New Turret
New Spindle
New Steady Rest
Delete
X
New Axis
New Solid
New Station
Station Properties
Number
4
Tool Change Angle(Index)
-108.000000
Position Reference
Holder Base
Tool Change Angle
0.000000
Axis
<Default>
Automatic Tool Changer
Tool Position X Y Z
-7.000000
0.000000
0.000000
Turning Tool Z Rotation Angle
0.000000
OK
Cancel
Help

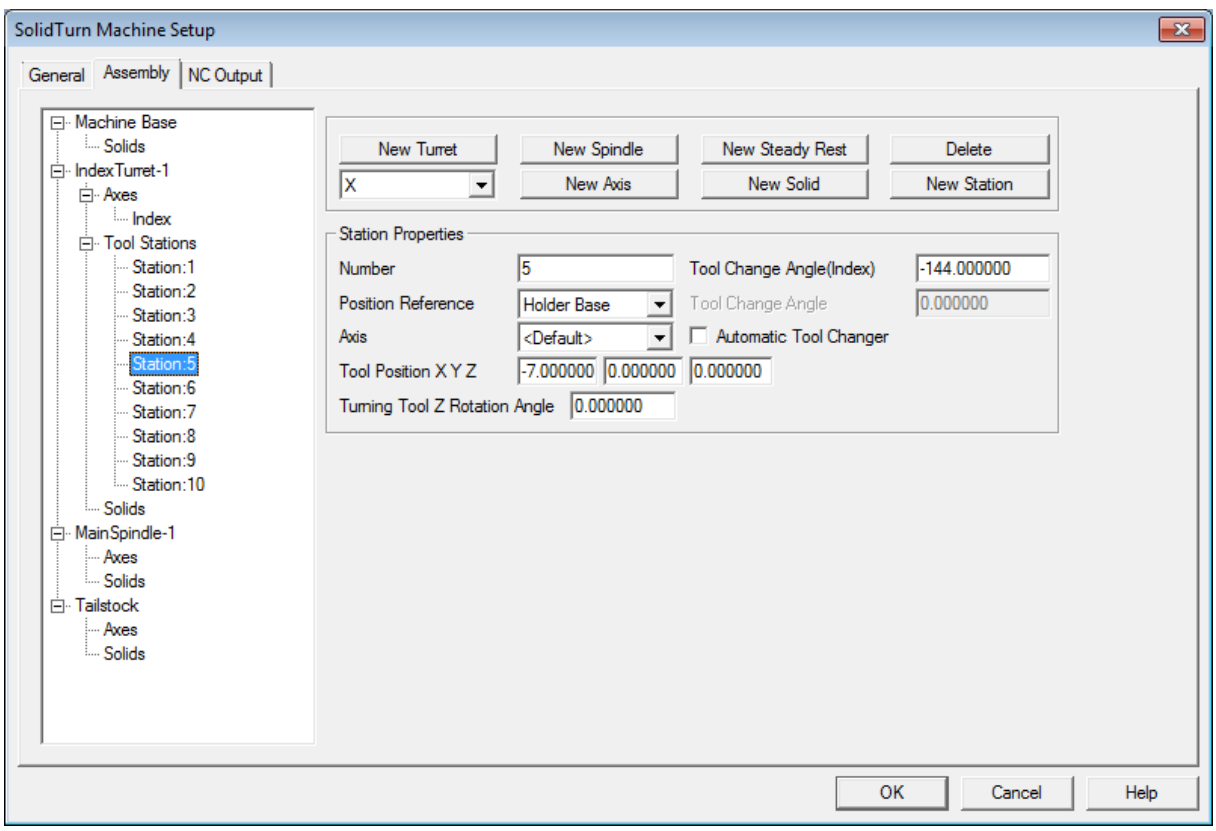
SolidTurn Machine Setup
General
Assembly
NC Output
Machine Base
Solids
IndexTurret-1
Axes
Index
Tool Stations
Station:1
Station:2
Station:3
Station:4
Station:5
Station:6
Station:7
Station:8
Station:9
Station:10
Solids
MainSpindle-1
Axes
Solids
Tailstock
Axes
Solids
New Turret
New Spindle
New Steady Rest
Delete
X
New Axis
New Solid
New Station
Station Properties
Number
5
Tool Change Angle(Index)
-144.000000
Position Reference
Holder Base
Tool Change Angle
0.000000
Axis
<Default>
Automatic Tool Changer
Tool Position X Y Z
-7.000000
0.000000
0.000000
Turning Tool Z Rotation Angle
0.000000
OK
Cancel
Help

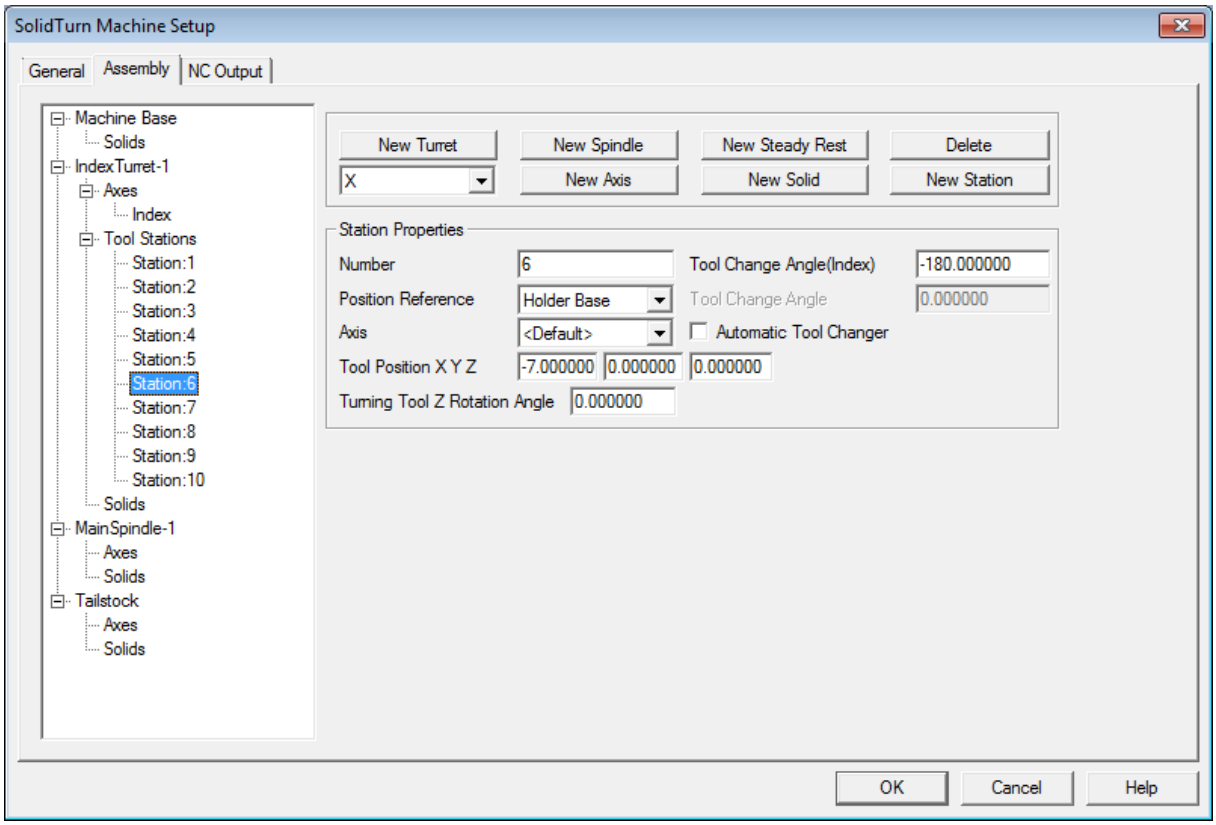
SolidTurn Machine Setup
General
Assembly
NC Output
Machine Base
Solids
IndexTurret-1
Axes
Index
Tool Stations
Station:1
Station:2
Station:3
Station:4
Station:5
Station:6
Station:7
Station:8
Station:9
Station:10
Solids
MainSpindle-1
Axes
Solids
Tailstock
Axes
Solids
New Turret
New Spindle
New Steady Rest
Delete
X
New Axis
New Solid
New Station
Station Properties
Number
6
Tool Change Angle(Index)
-180.000000
Position Reference
Holder Base
Tool Change Angle
0.000000
Axis
<Default>
Automatic Tool Changer
Tool Position X Y Z
-7.000000
0.000000
0.000000
Turning Tool Z Rotation Angle
0.000000
OK
Cancel
Help

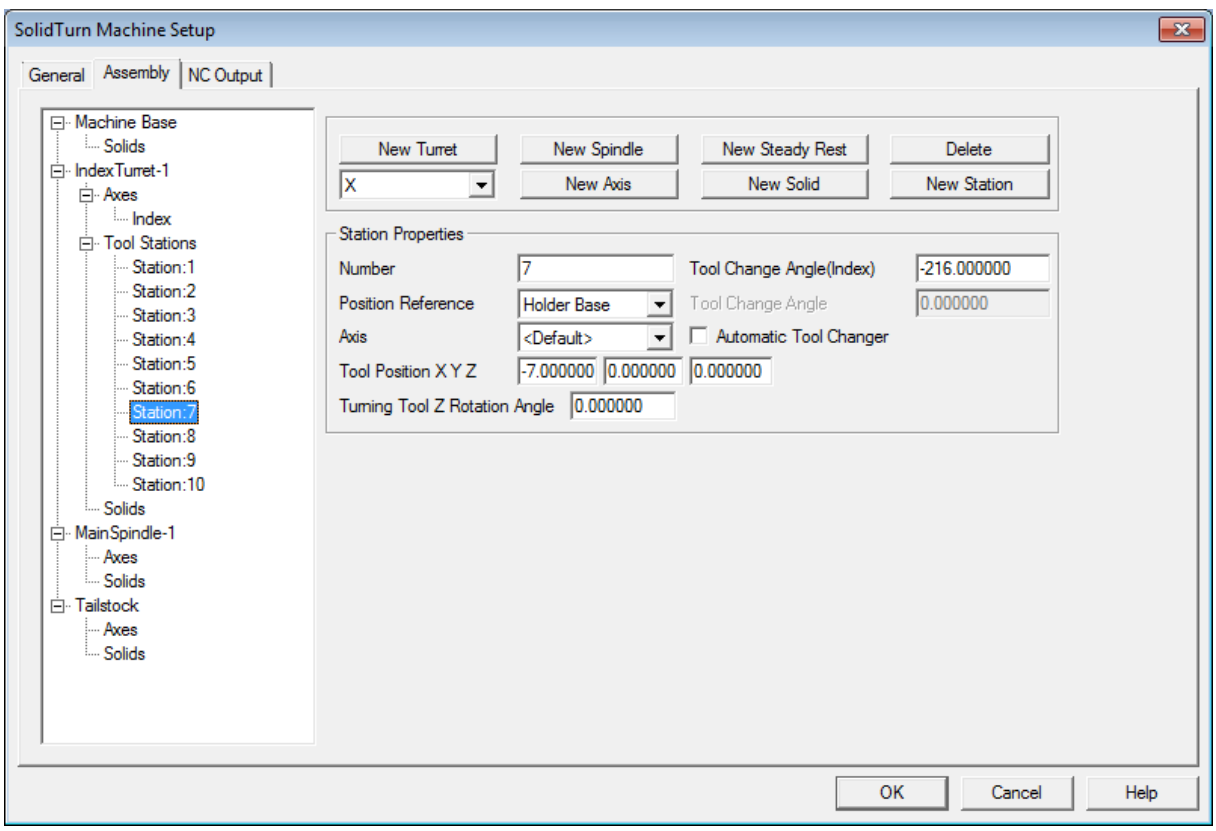
SolidTurn Machine Setup
General
Assembly
NC Output
Machine Base
Solids
IndexTurret-1
Axes
Index
Tool Stations
Station:1
Station:2
Station:3
Station:4
Station:5
Station:6
Station:7
Station:8
Station:9
Station:10
Solids
MainSpindle-1
Axes
Solids
Tailstock
Axes
Solids
New Turret
New Spindle
New Steady Rest
Delete
X
New Axis
New Solid
New Station
Station Properties
Number
7
Tool Change Angle(Index)
-216.000000
Position Reference
Holder Base
Tool Change Angle
0.000000
Axis
<Default>
Automatic Tool Changer
Tool Position X Y Z
-7.000000
0.000000
0.000000
Turning Tool Z Rotation Angle
0.000000
OK
Cancel
Help

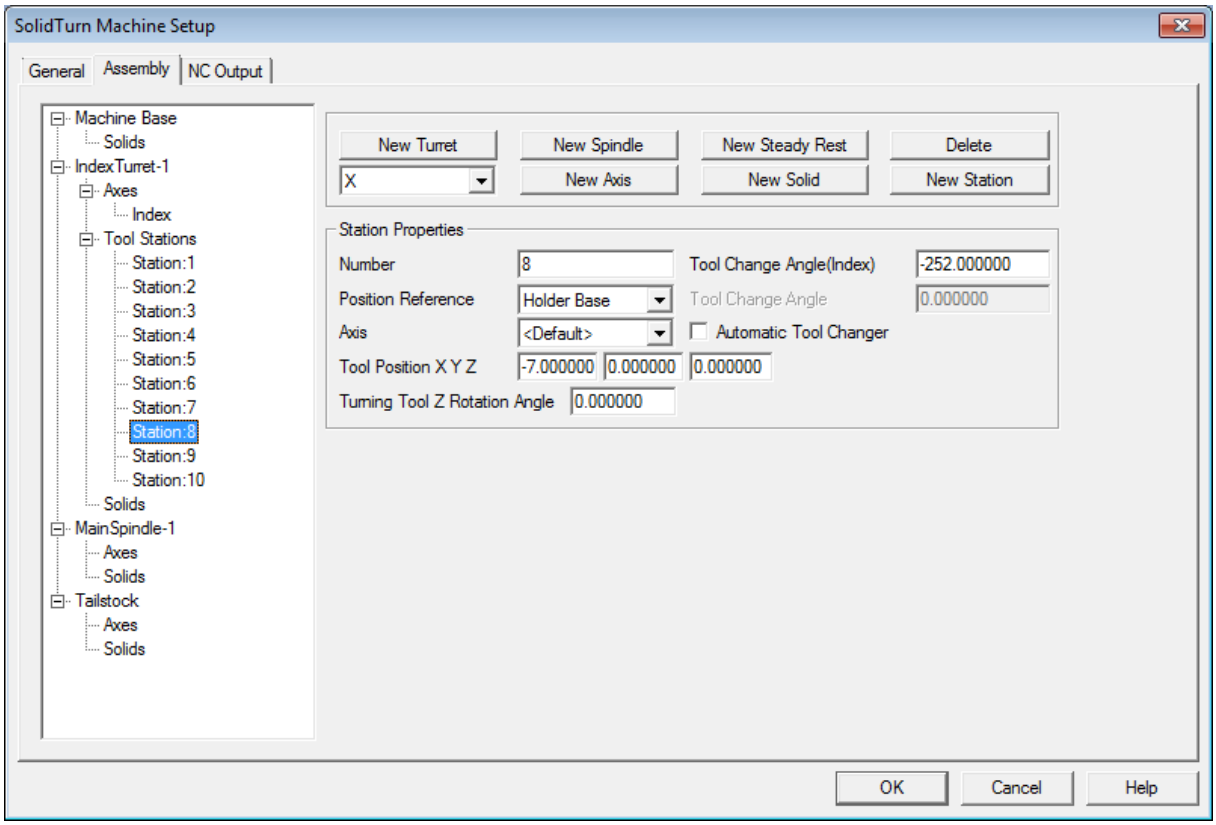
SolidTurn Machine Setup
General
Assembly
NC Output
Machine Base
Solids
IndexTurret-1
Axes
Index
Tool Stations
Station:1
Station:2
Station:3
Station:4
Station:5
Station:6
Station:7
Station:8
Station:9
Station:10
Solids
MainSpindle-1
Axes
Solids
Tailstock
Axes
Solids
New Turret
New Spindle
New Steady Rest
Delete
X
New Axis
New Solid
New Station
Station Properties
Number
8
Tool Change Angle(Index)
-252.000000
Position Reference
Holder Base
Tool Change Angle
0.000000
Axis
<Default>
Automatic Tool Changer
Tool Position X Y Z
-7.000000
0.000000
0.000000
Turning Tool Z Rotation Angle
0.000000
OK
Cancel
Help

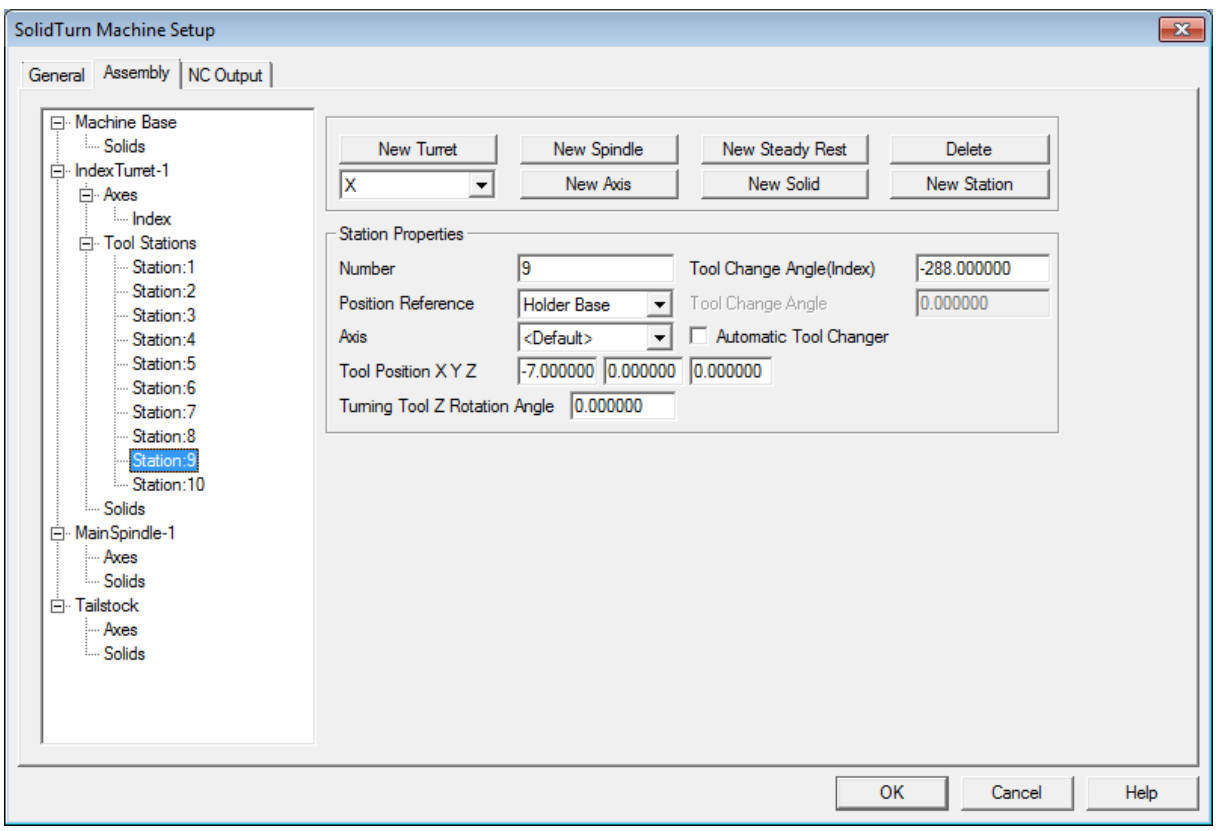
SolidTurn Machine Setup
General
Assembly
NC Output
Machine Base
Solids
IndexTurret-1
Axes
Index
Tool Stations
Station:1
Station:2
Station:3
Station:4
Station:5
Station:6
Station:7
Station:8
Station:9
Station:10
Solids
MainSpindle-1
Axes
Solids
Tailstock
Axes
Solids
New Turret
New Spindle
New Steady Rest
Delete
X
New Axis
New Solid
New Station
Station Properties
Number
9
Tool Change Angle(Index)
-288.000000
Position Reference
Holder Base
Tool Change Angle
0.000000
Axis
<Default>
Automatic Tool Changer
Tool Position X Y Z
-7.000000
0.000000
0.000000
Turning Tool Z Rotation Angle
0.000000
OK
Cancel
Help

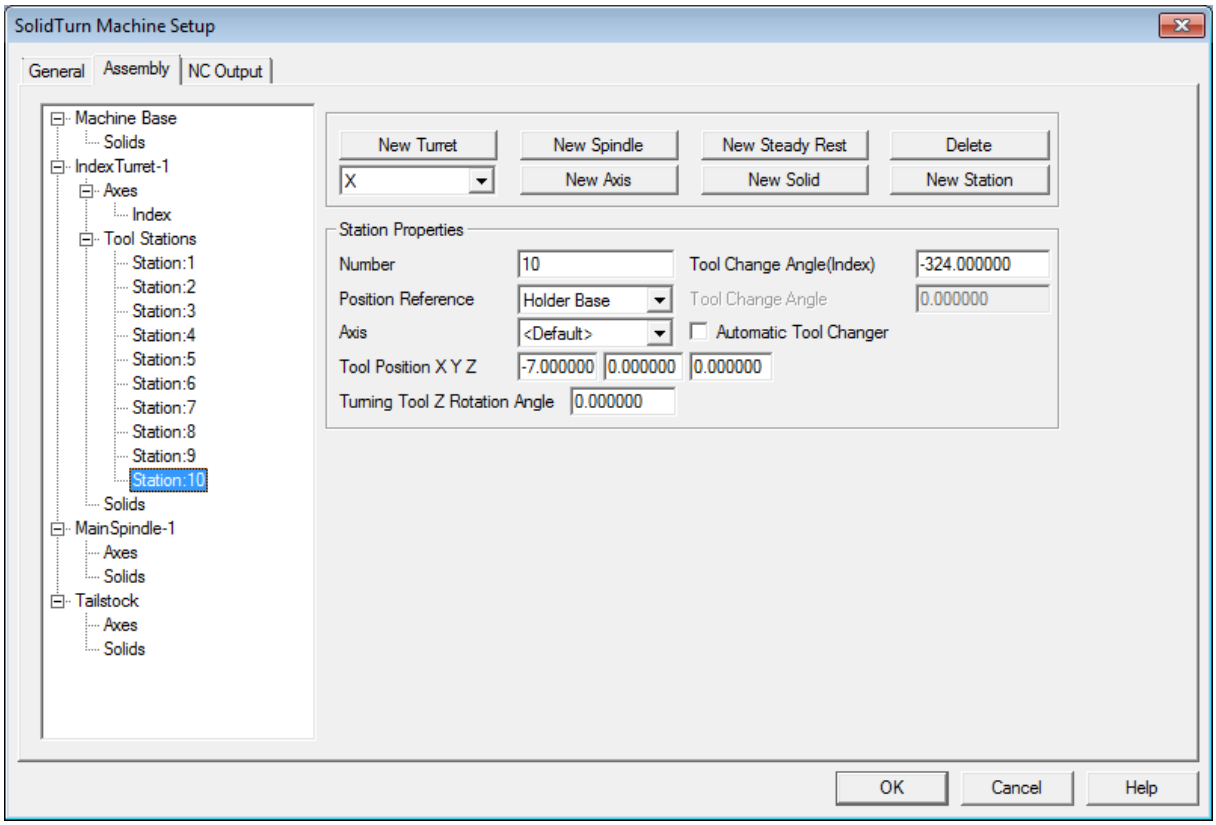
SolidTurn Machine Setup
General
Assembly
NC Output
Machine Base
Solids
IndexTurret-1
Axes
Index
Tool Stations
Station:1
Station:2
Station:3
Station:4
Station:5
Station:6
Station:7
Station:8
Station:9
Station:10
Solids
MainSpindle-1
Axes
Solids
Tailstock
Axes
Solids
New Turret
New Spindle
New Steady Rest
Delete
X
New Axis
New Solid
New Station
Station Properties
Number
10
Tool Change Angle(Index)
-324.000000
Position Reference
Holder Base
Tool Change Angle
0.000000
Axis
<Default>
Automatic Tool Changer
Tool Position X Y Z
-7.000000
0.000000
0.000000
Turning Tool Z Rotation Angle
0.000000
OK
Cancel
Help

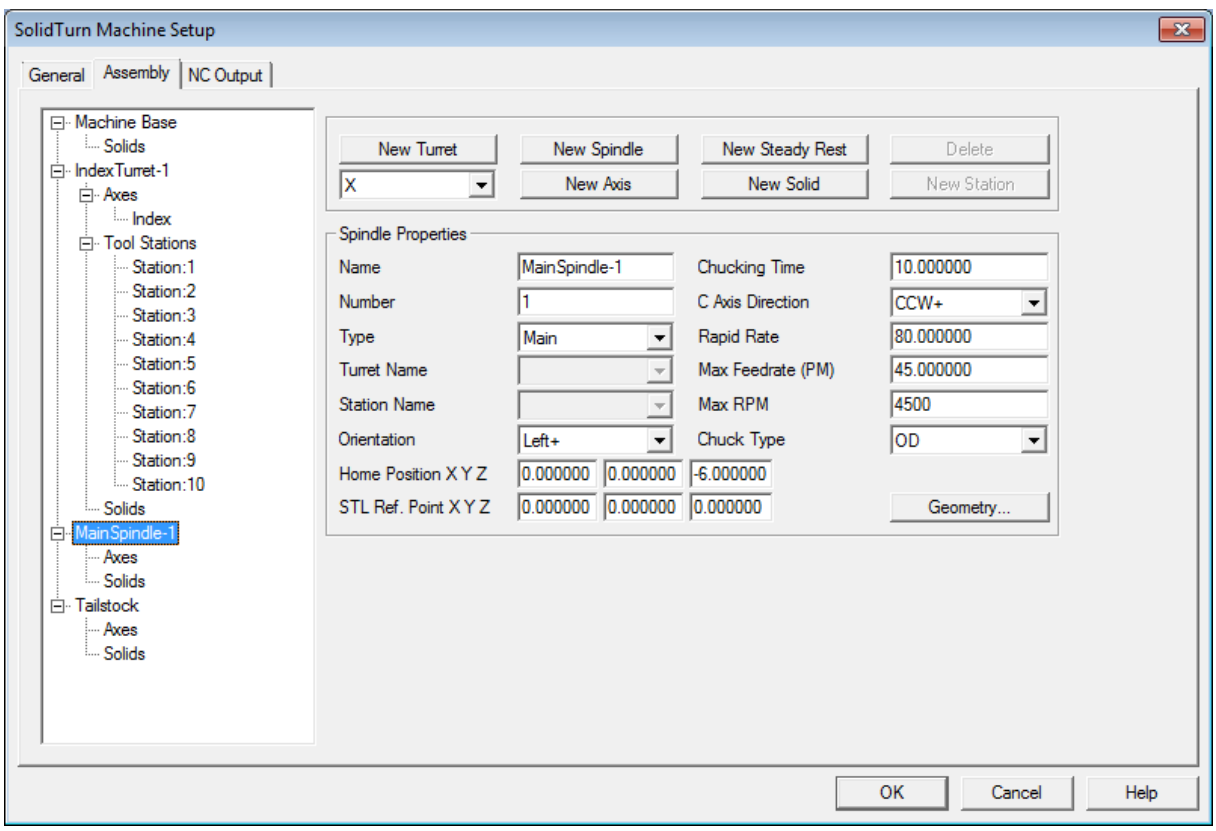
SolidTurn Machine Setup
General
Assembly
NC Output
Machine Base
Solids
IndexTurret-1
Axes
Index
Tool Stations
Station:1
Station:2
Station:3
Station:4
Station:5
Station:6
Station:7
Station:8
Station:9
Station:10
Solids
MainSpindle-1
Axes
Solids
Tailstock
Axes
Solids
New Turret
New Spindle
New Steady Rest
Delete
X
New Axis
New Solid
New Station
Spindle Properties
Name
MainSpindle-1
Chucking Time
10.000000
Number
1
C Axis Direction
CCW+
Type
Main
Rapid Rate
80.000000
Turret Name
Max Feedrate (PM)
45.000000
Station Name
Max RPM
4500
Orientation
Left+
Chuck Type
OD
Home Position X Y Z
0.000000
0.000000
-6.000000
STL Ref. Point X Y Z
0.000000
0.000000
0.000000
Geometry...
OK
Cancel
Help

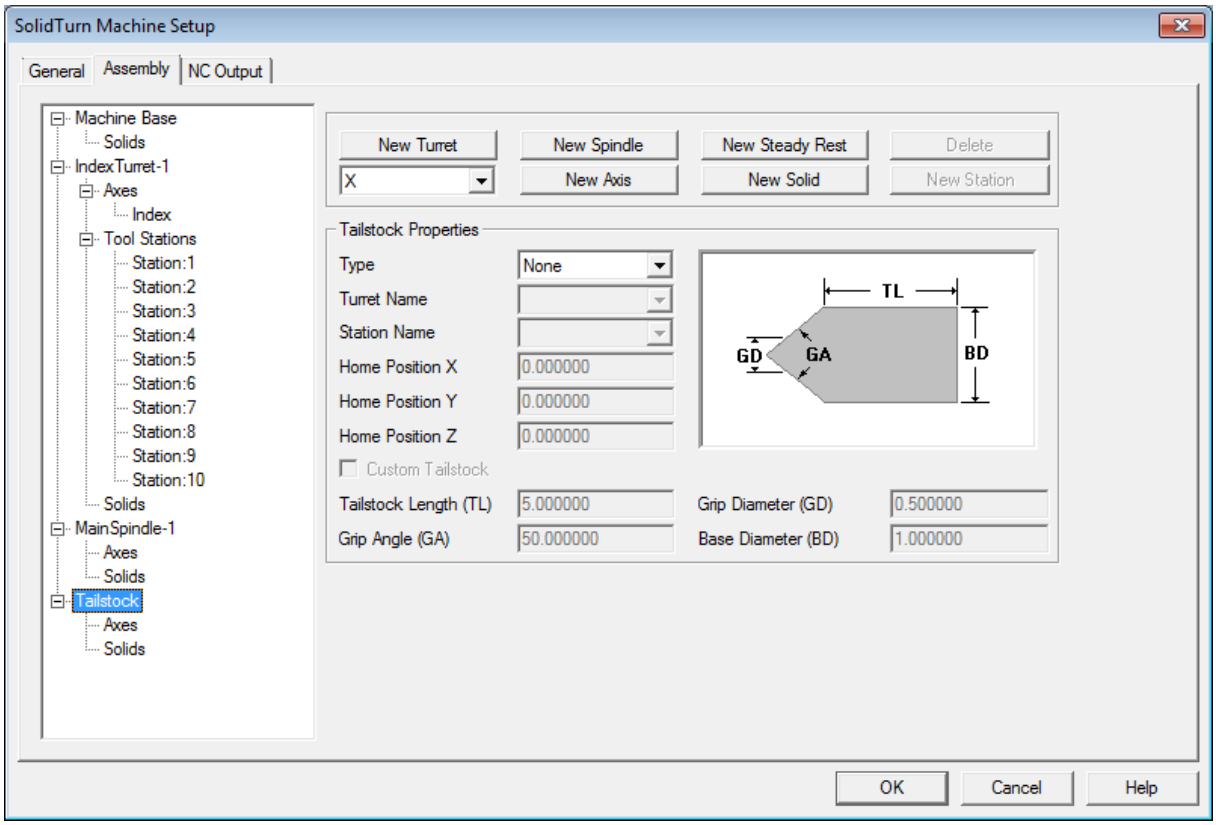

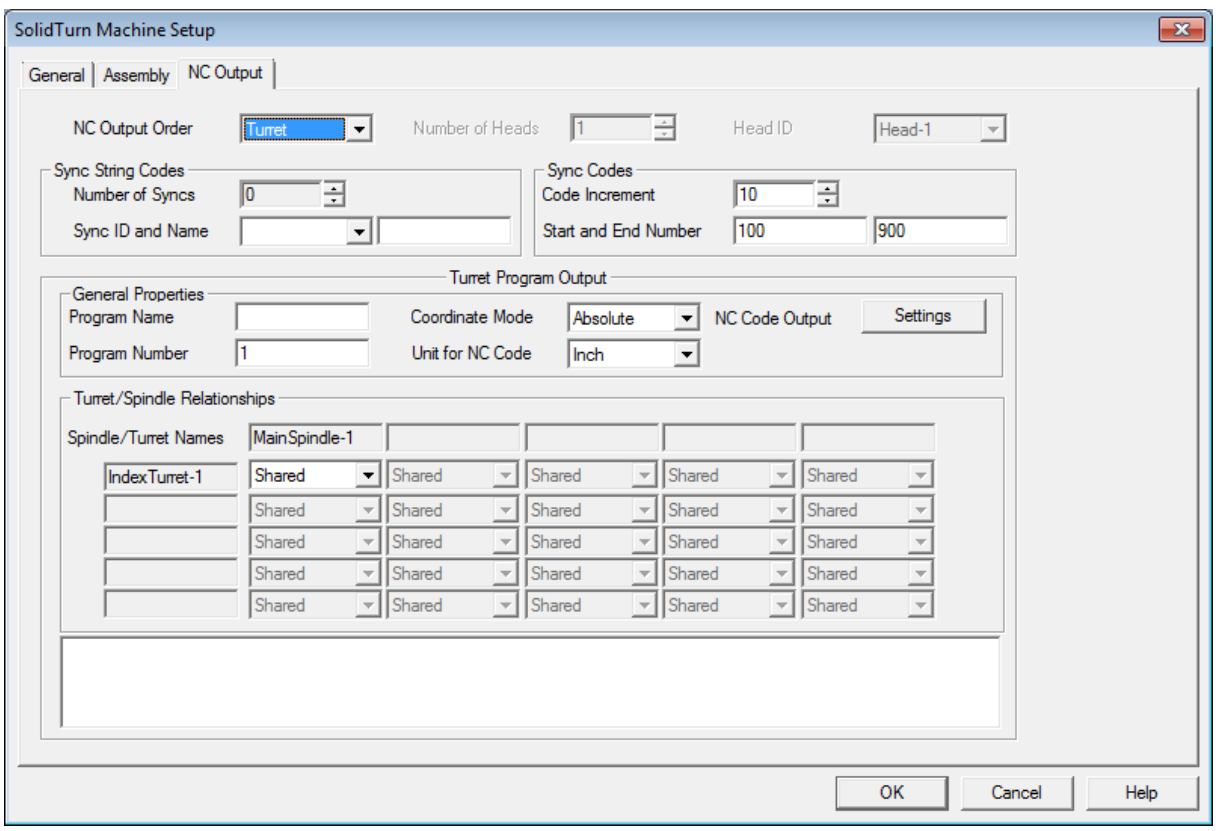

End of SolidTurn Machine Setup for WPI SL10 Lathe Tool in Esprit CAM Software

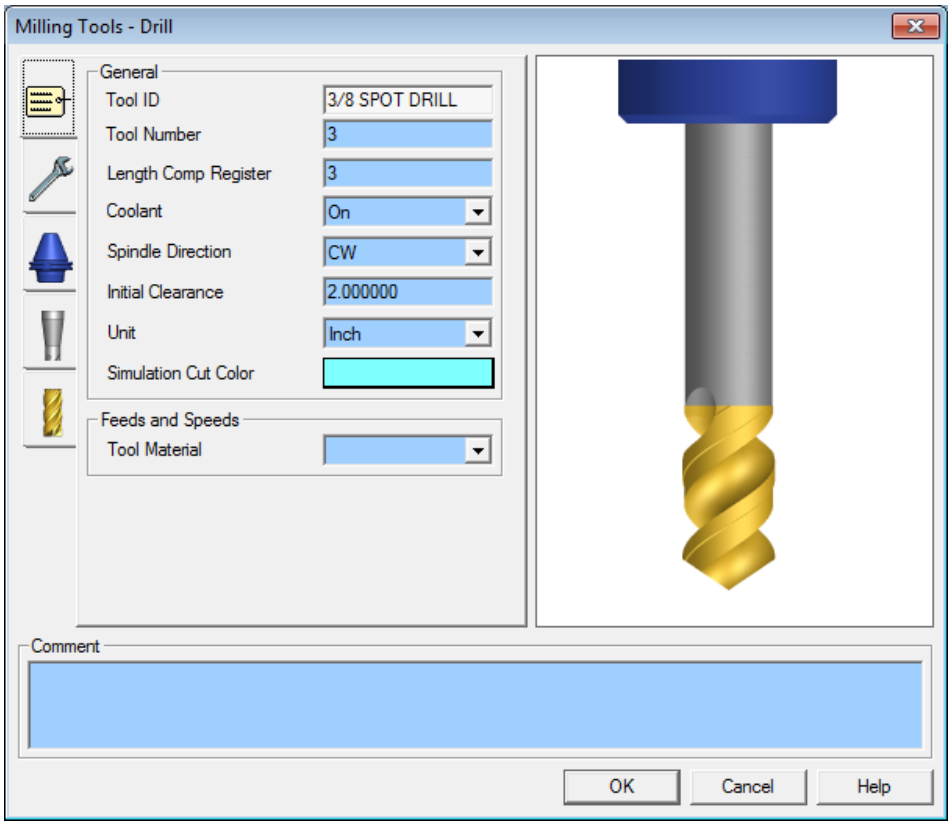

Tool 3 Setup, 3/8” Spot Drill, for WPI SL10 Lathe Tool in Esprit CAM Software

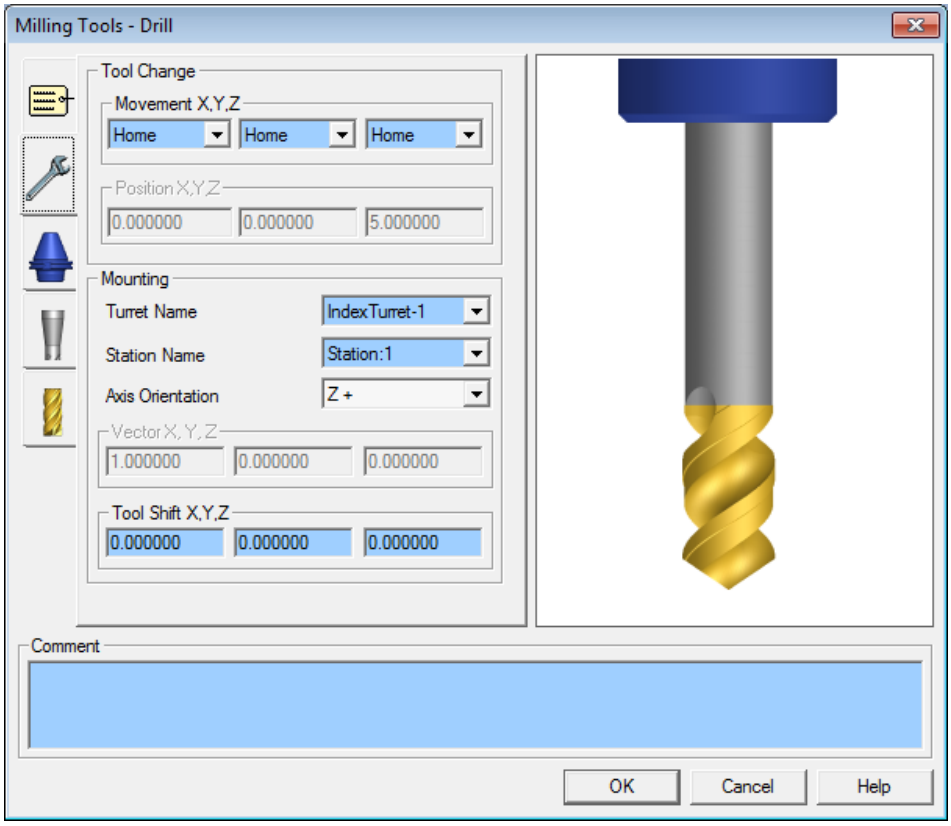

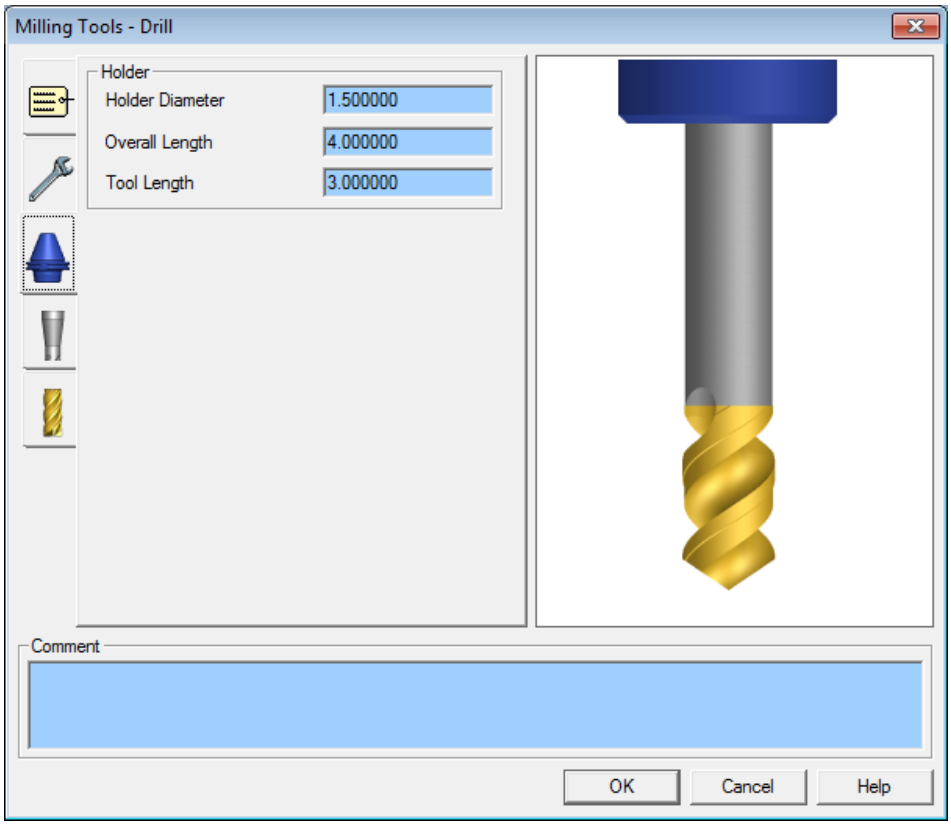
Milling Tools - Drill
Holder
Holder Diameter
1.500000
Overall Length
4.000000
Tool Length
3.000000
Comment
OK
Cancel
Help

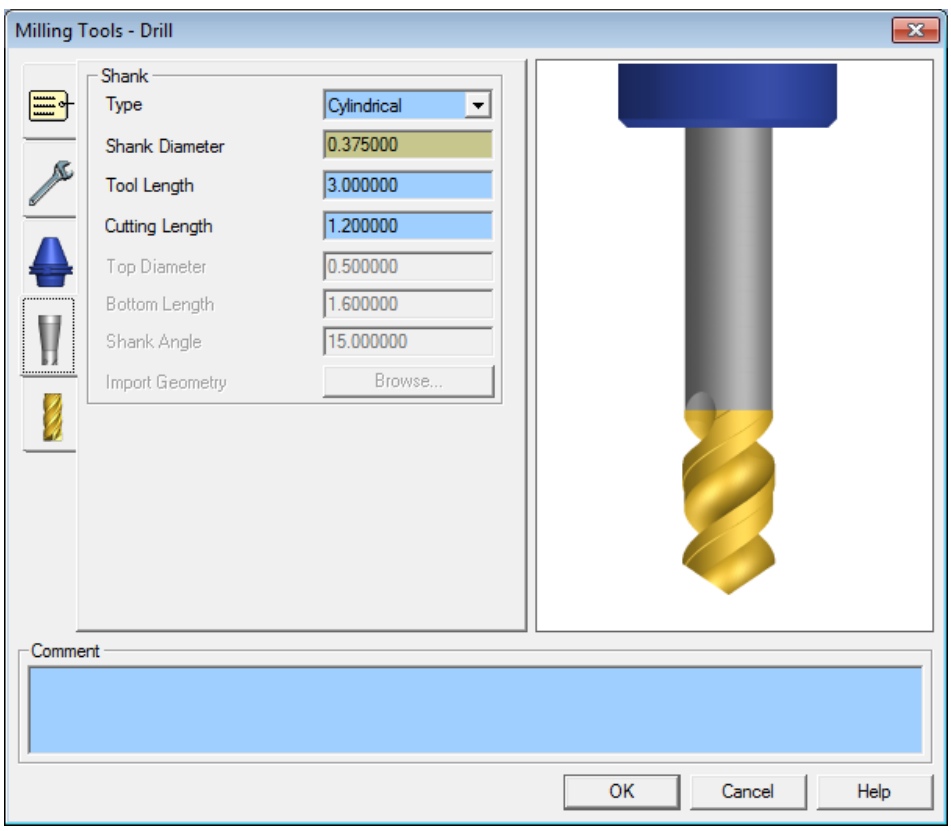
Milling Tools - Drill
Shank
Type
Cylindrical
Shank Diameter
0.375000
Tool Length
3.000000
Cutting Length
1.200000
Top Diameter
0.500000
Bottom Length
1.600000
Shank Angle
15.000000
Import Geometry
Browse...
Comment
OK
Cancel
Help

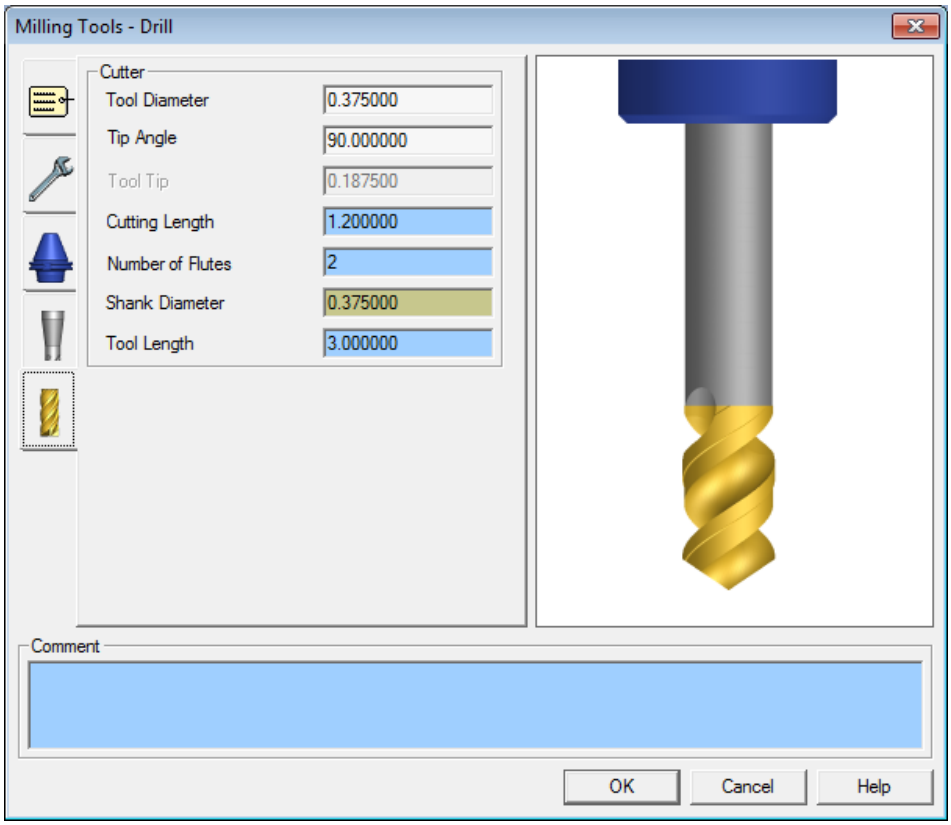

End of Tool 3 Setup, 3/8” Spot Drill, for WPI SL10 Lathe Tool in Esprit CAM Software

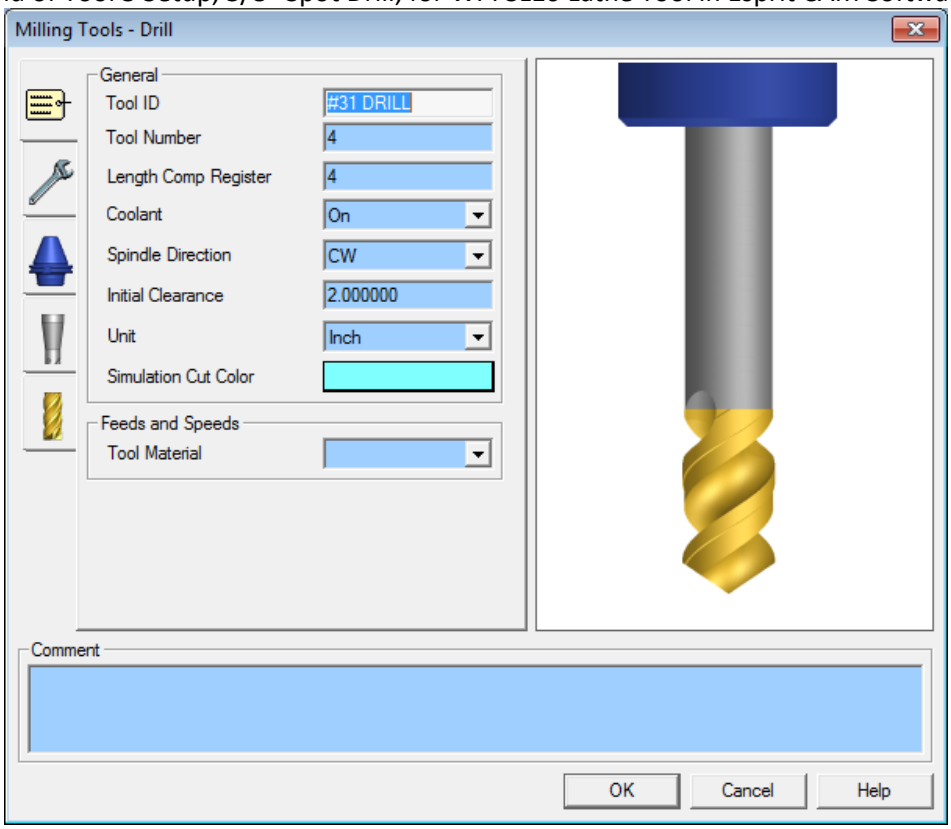

Tool 4 Setup, #31 Drill, for WPI SL10 Lathe Tool in Esprit CAM Software

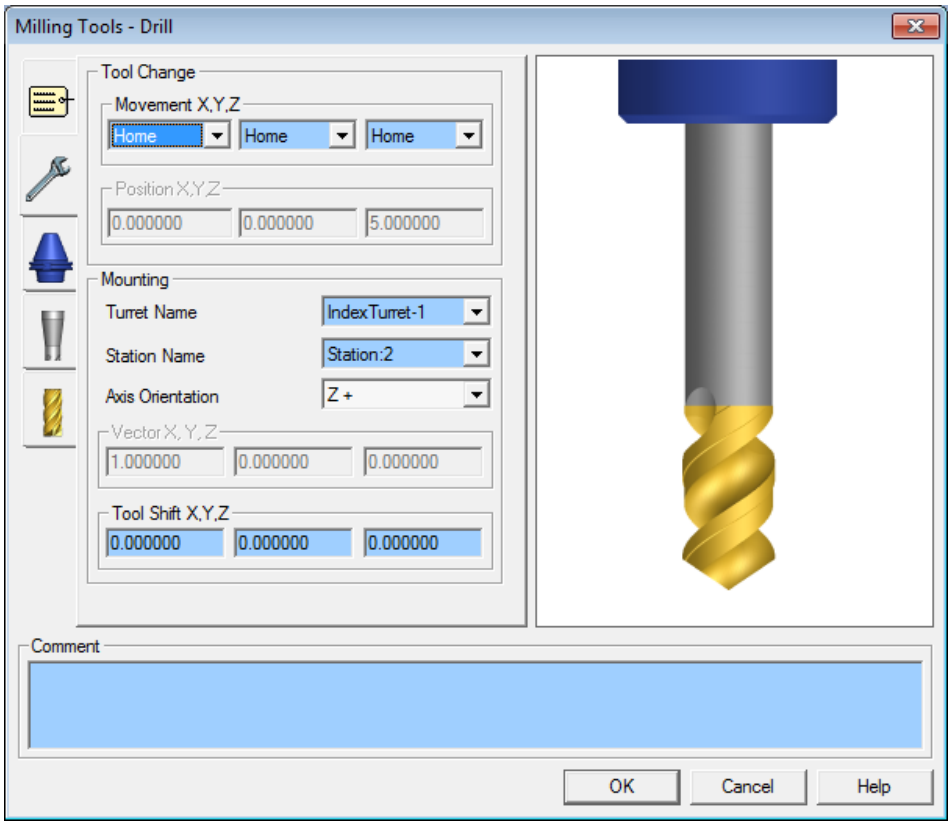
Milling Tools - Drill
Tool Change
Movement X,Y,Z
Home
Home
Home
Position X,Y,Z
0.000000
0.000000
5.000000
Mounting
Turret Name
IndexTurret-1
Station Name
Station:2
Axis Orientation
Z +
Vector X, Y, Z
1.000000
0.000000
0.000000
Tool Shift X,Y,Z
0.000000
0.000000
0.000000
Comment
OK
Cancel
Help

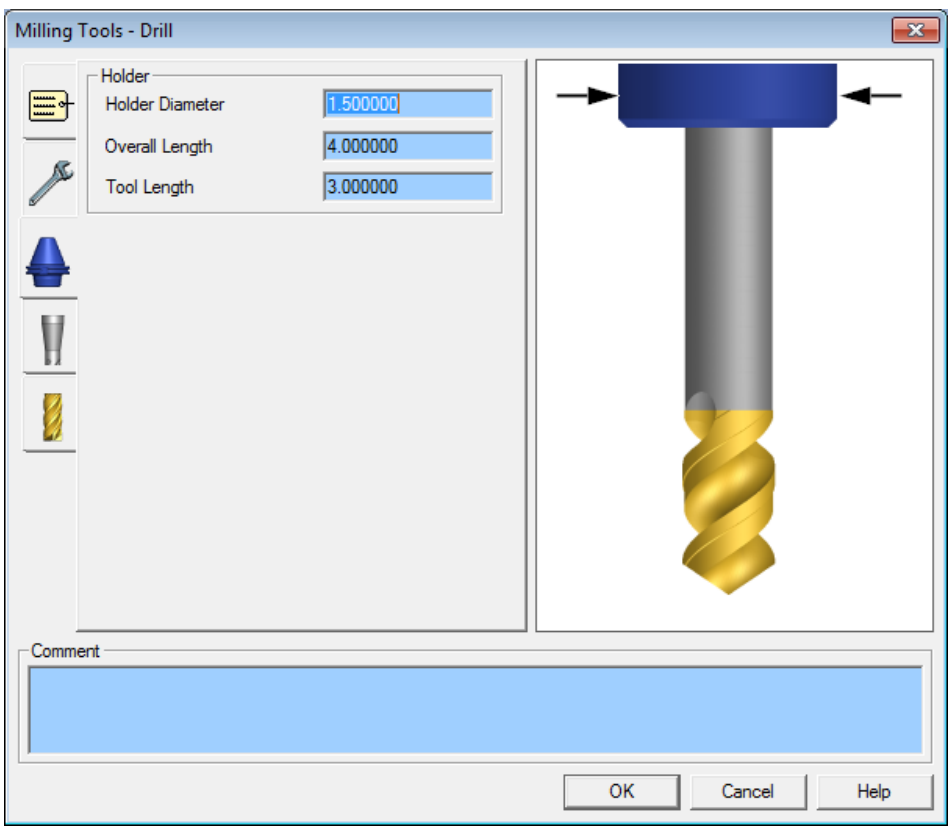
Milling Tools - Drill
Holder
Holder Diameter
1.500000
Overall Length
4.000000
Tool Length
3.000000
Comment
OK
Cancel
Help

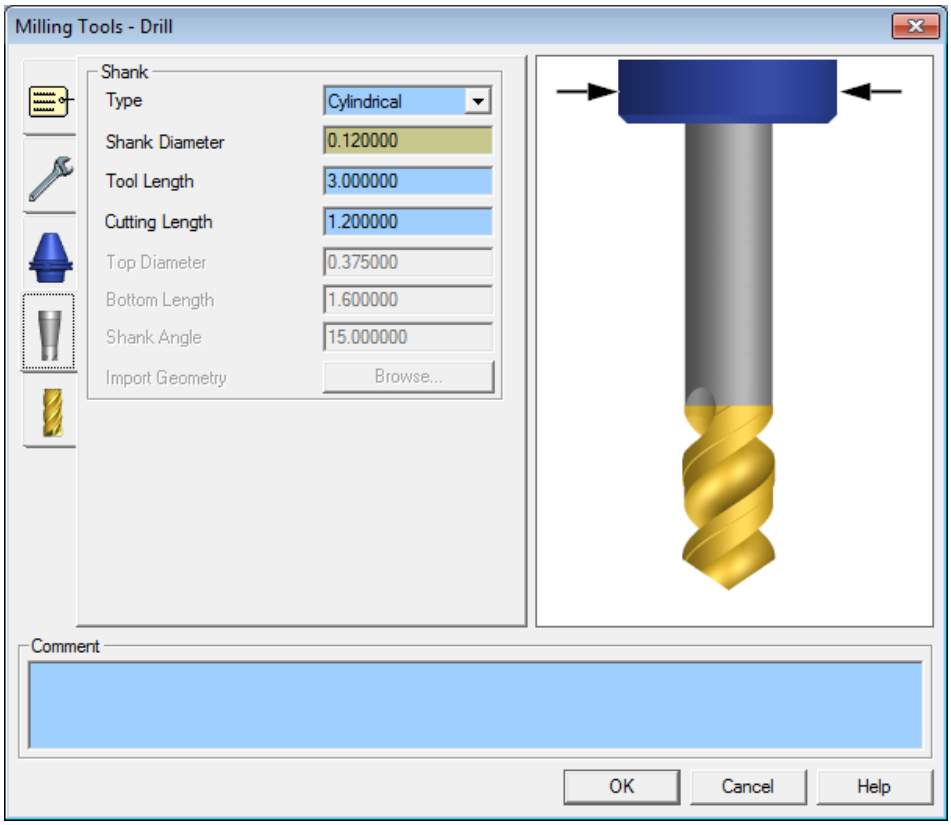

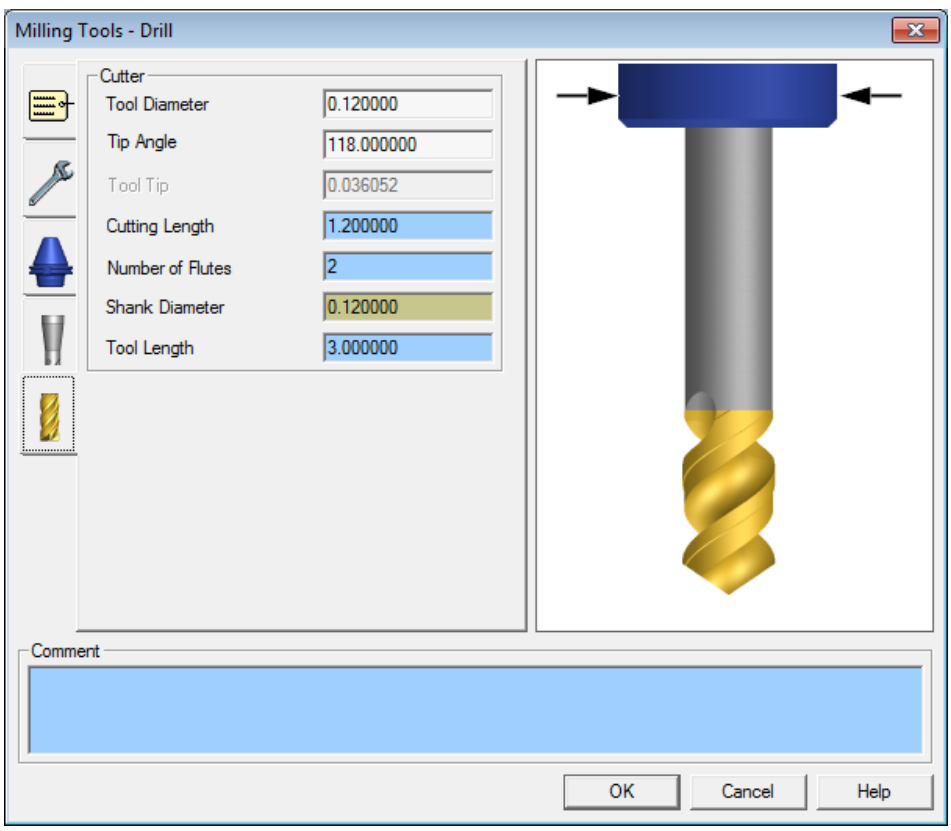

End of Tool 4 Setup, #31 Drill, for WPI SL10 Lathe Tool in Esprit CAM Software

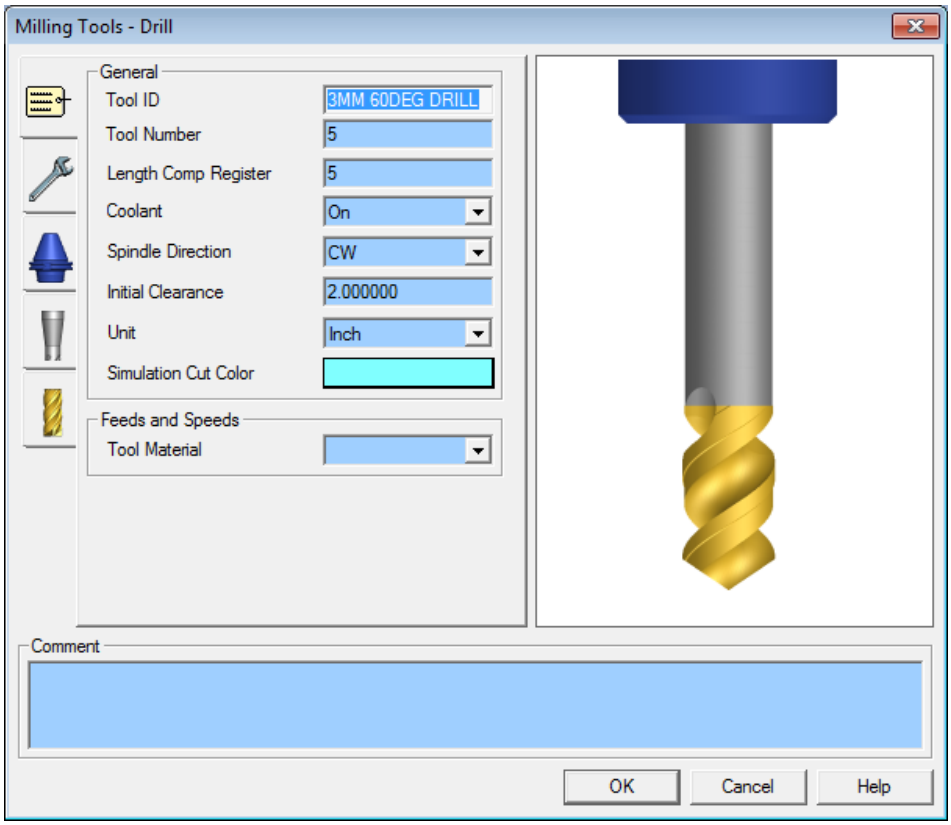

Tool 5 Setup, 3mm 60 Degree Drill, for WPI SL10 Lathe Tool in Esprit CAM Software

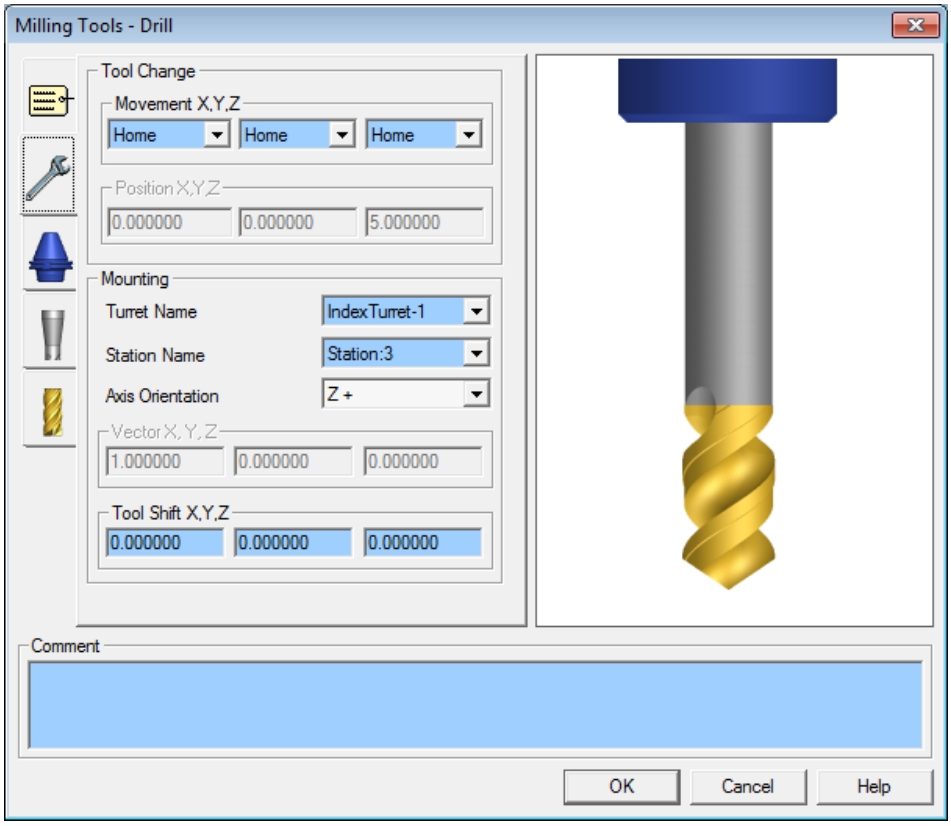

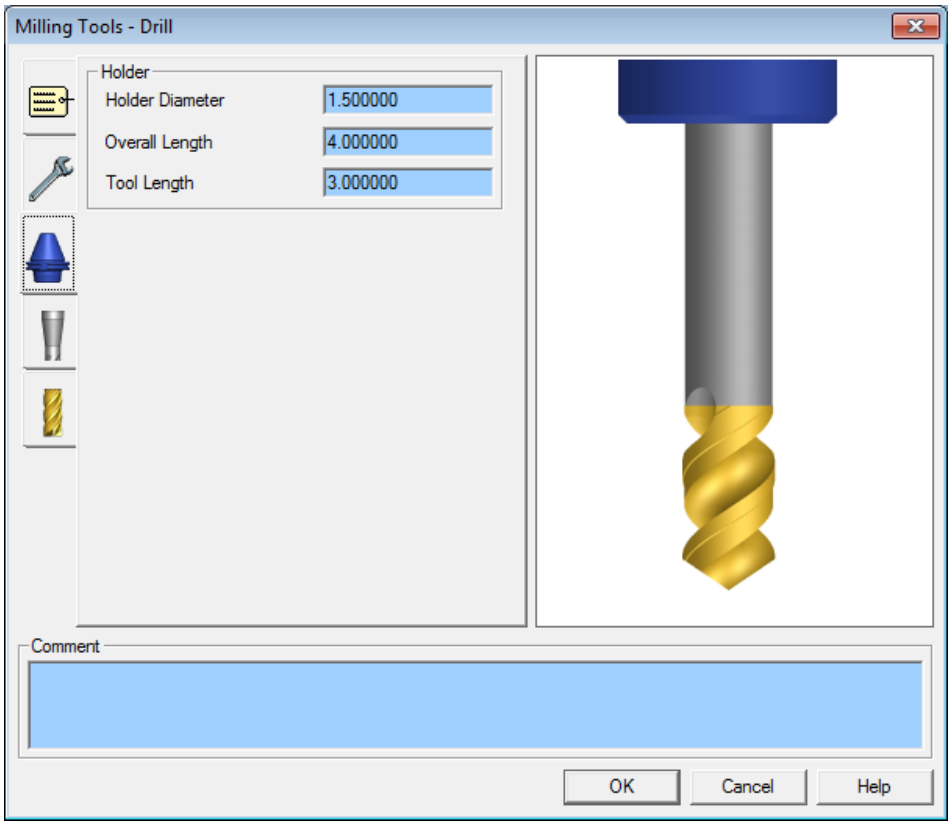
Milling Tools - Drill
Holder
Holder Diameter
1.500000
Overall Length
4.000000
Tool Length
3.000000
Comment
OK
Cancel
Help

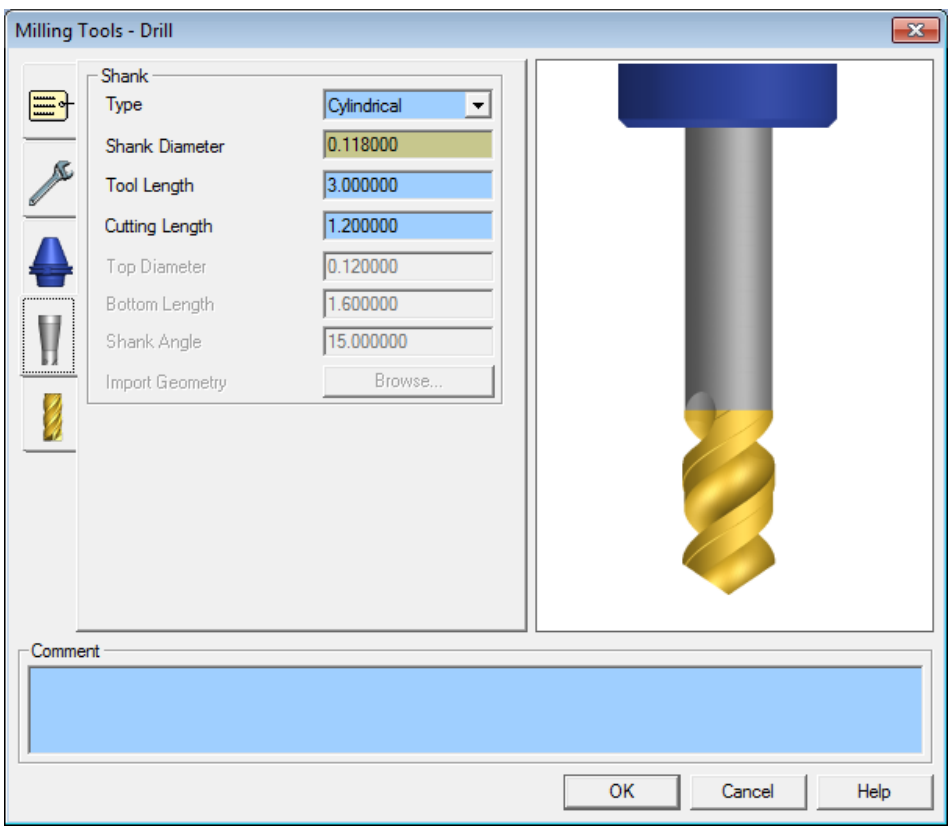
Milling Tools - Drill
Shank
Type
Cylindrical
Shank Diameter
0.118000
Tool Length
3.000000
Cutting Length
1.200000
Top Diameter
0.120000
Bottom Length
1.600000
Shank Angle
15.000000
Import Geometry
Browse...
Comment
OK
Cancel
Help

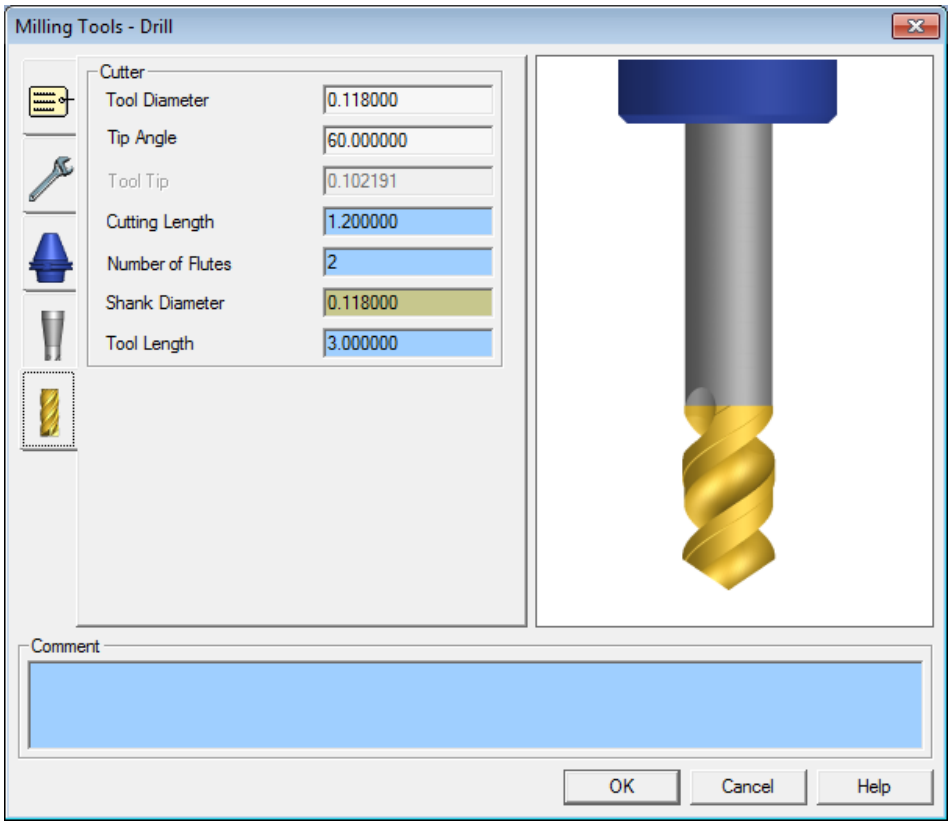

End of Tool 5 Setup, 3mm 60 Degree Drill, for WPI SL10 Lathe Tool in Esprit CAM Software

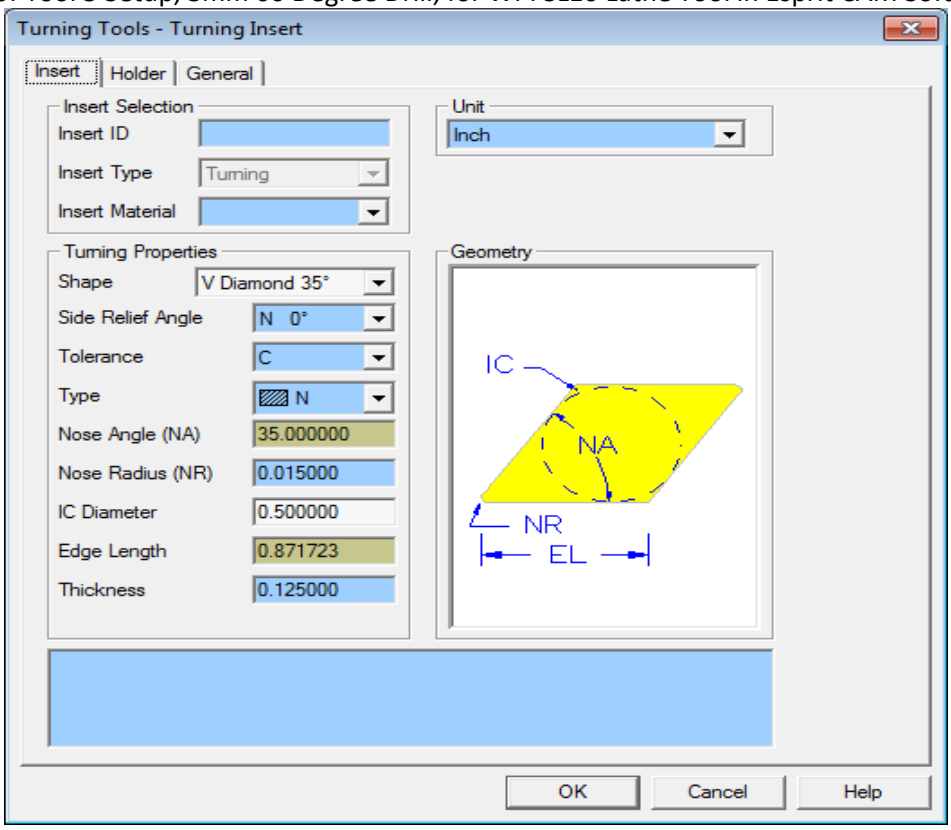

Tool 6 Setup, 35 Degree Diamond Cutting Tool, for WPI SL10 Lathe Tool in Esprit CAM Software

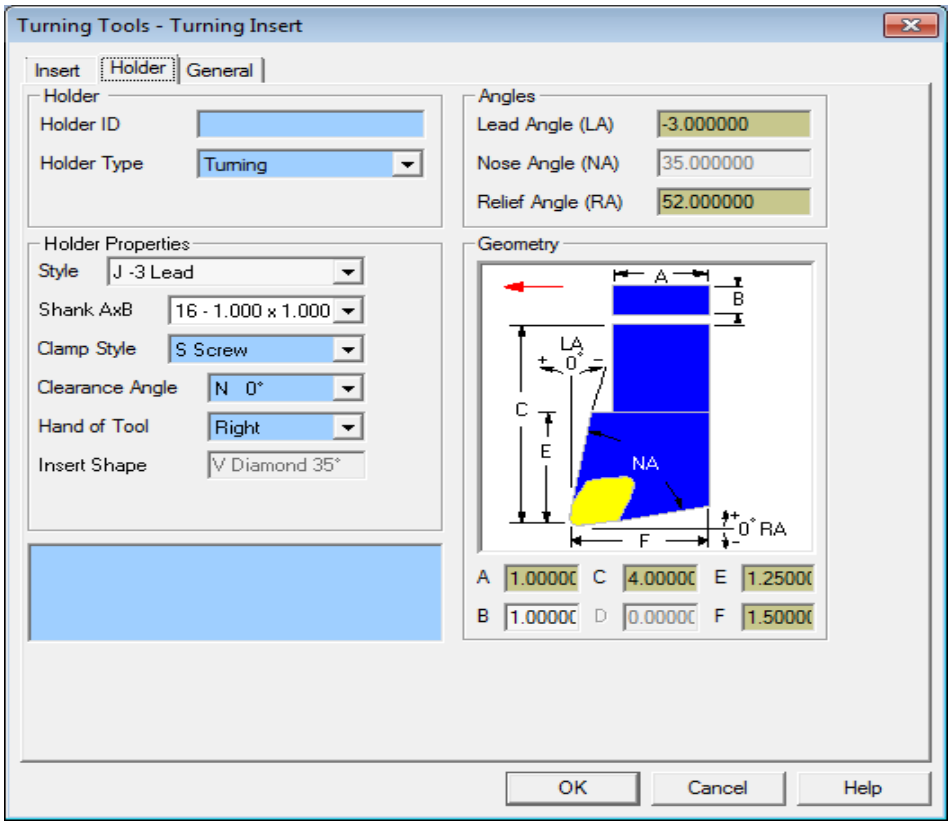

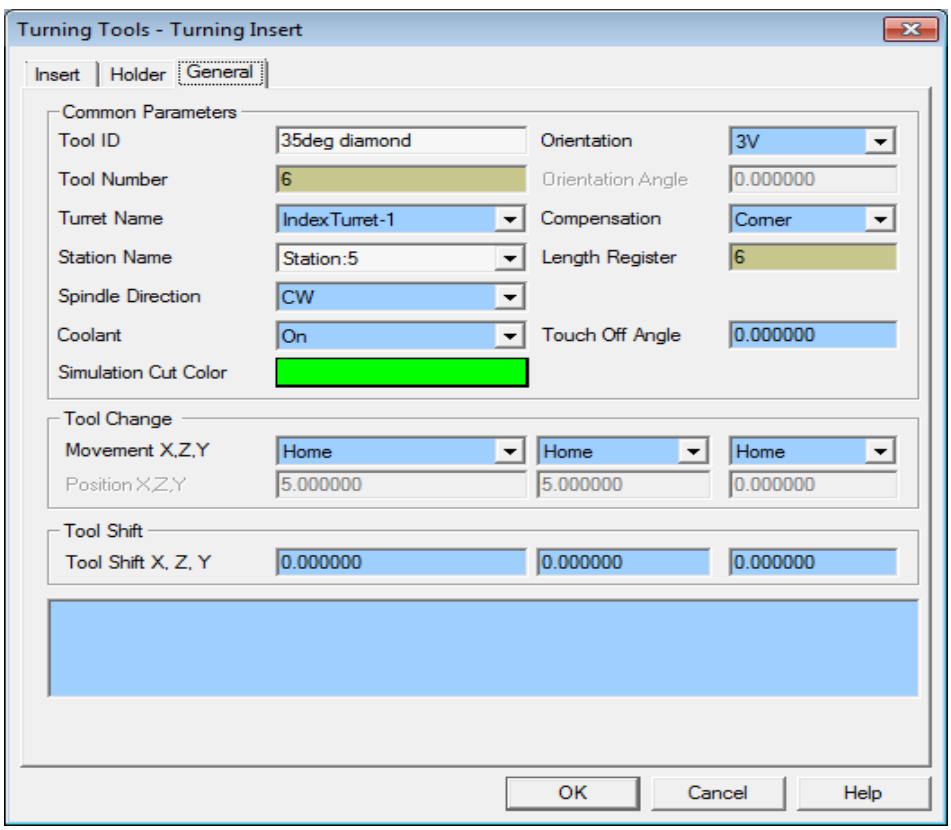

End of Tool 6 Setup, 35 Degree Diamond Cutting Tool, for WPI SL10 Lathe Tool in Esprit CAM Software

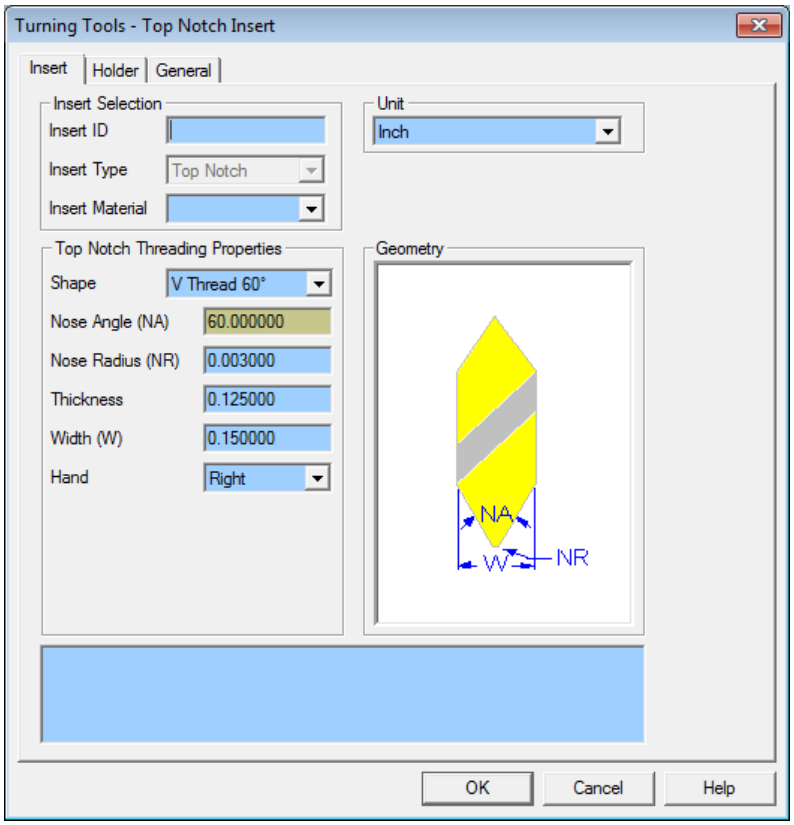

Tool 7 Setup, 60 Degree V-Threading Tool, for WPI SL10 Lathe Tool in Esprit CAM Software

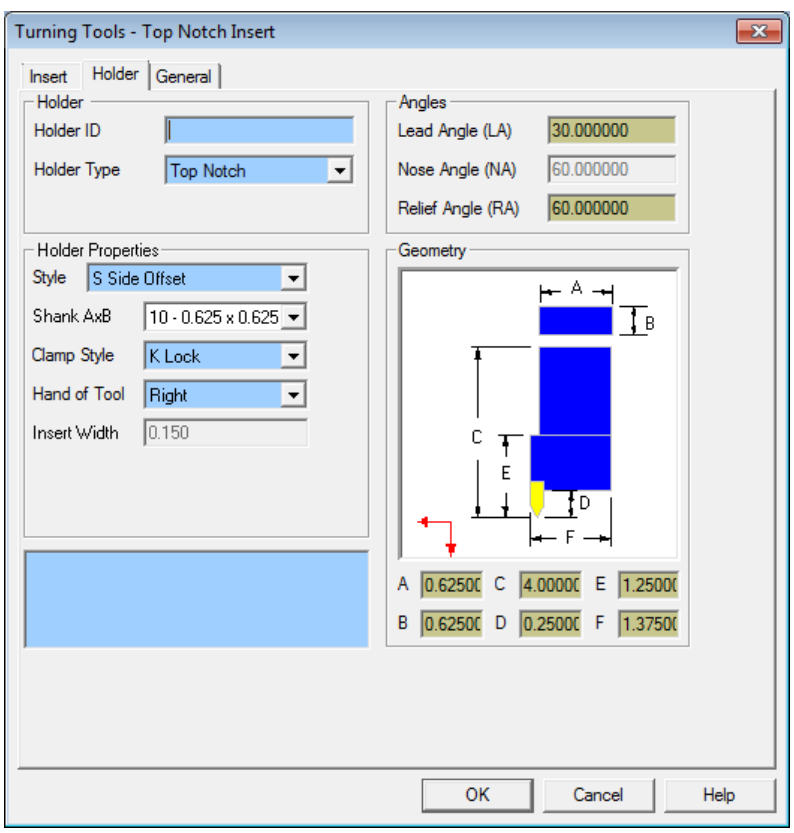

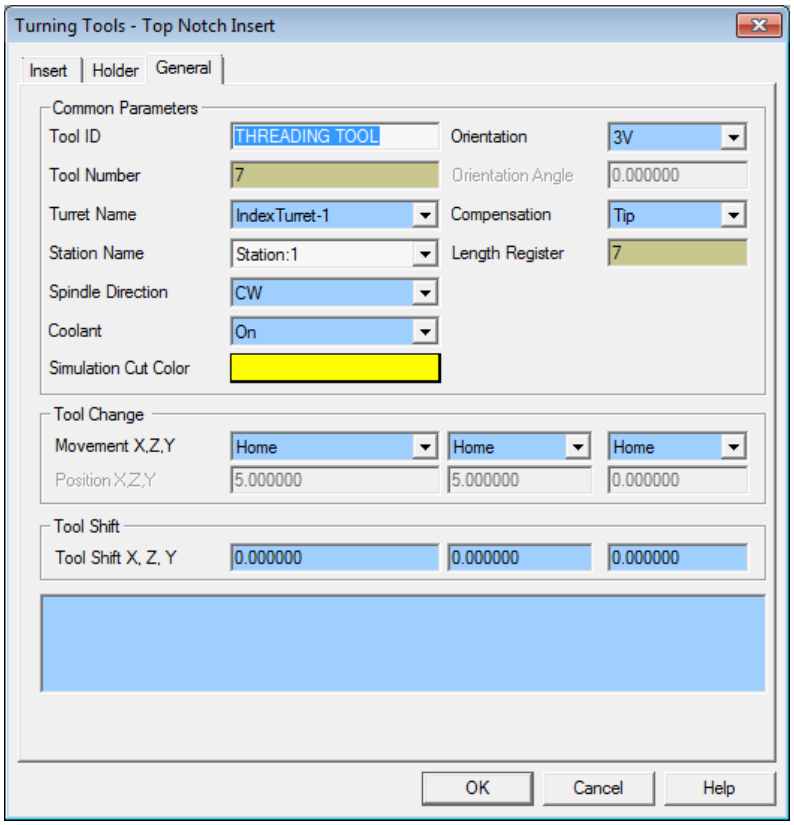

End of Tool 7 Setup, 60 Degree V-Threading Tool, for WPI SL10 Lathe Tool in Esprit CAM Software

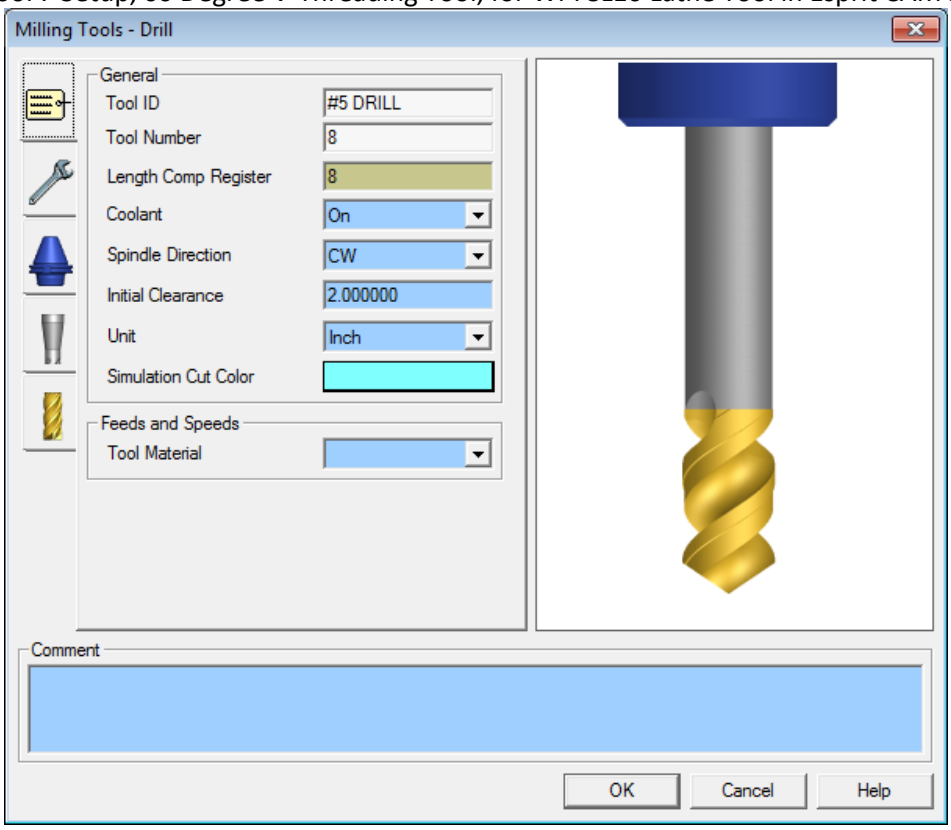

Tool 8 Setup, #5 Drill, for WPI SL10 Lathe Tool in Esprit CAM Software

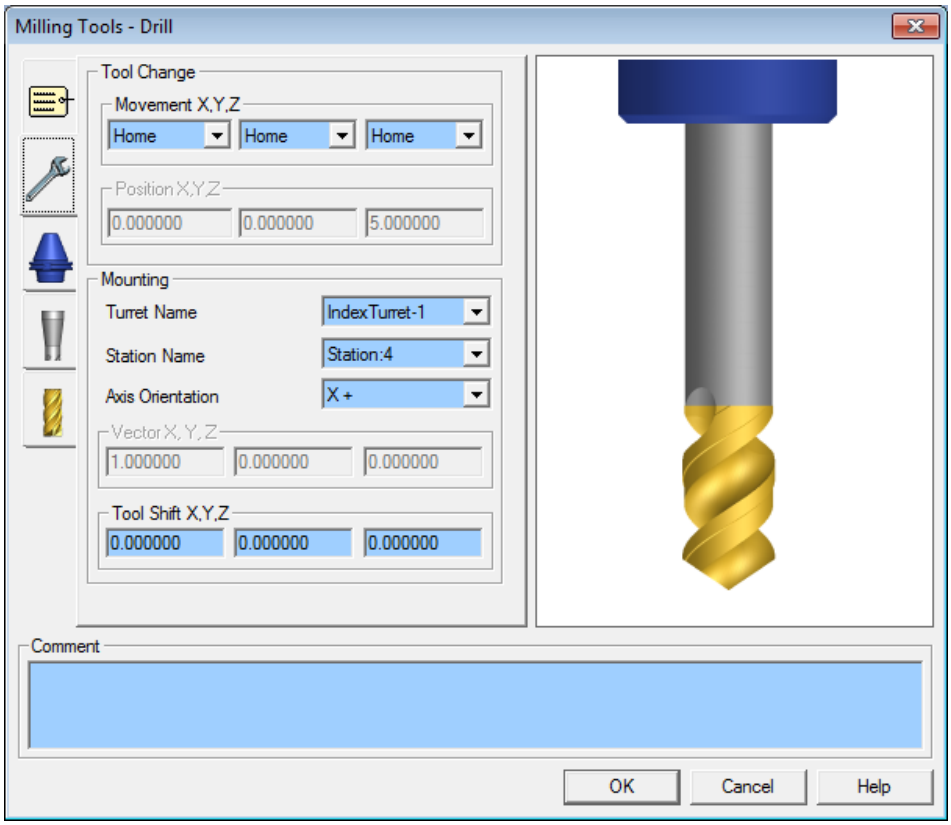
Milling Tools - Drill
Tool Change
Movement X,Y,Z
Home
Home
Home
Position X,Y,Z
0.000000
0.000000
5.000000
Mounting
Turret Name
IndexTurret-1
Station Name
Station:4
Axis Orientation
X +
Vector X, Y, Z
1.000000
0.000000
0.000000
Tool Shift X,Y,Z
0.000000
0.000000
0.000000
Comment
OK
Cancel
Help

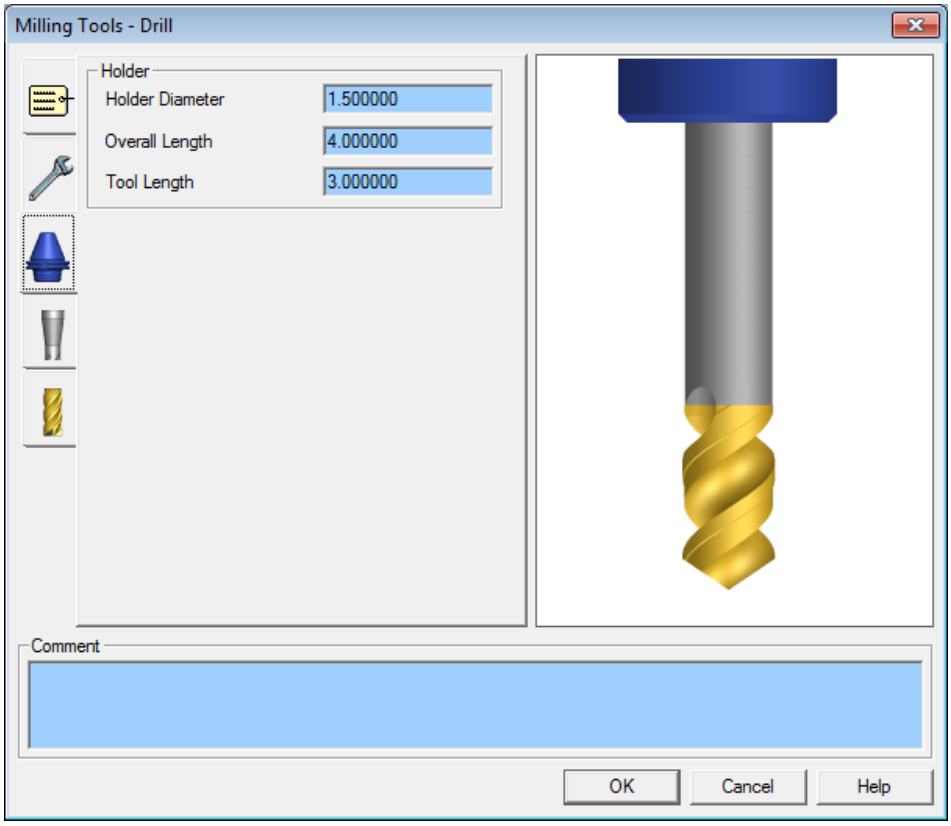
Milling Tools - Drill
Holder
Holder Diameter
1.500000
Overall Length
4.000000
Tool Length
3.000000
Comment
OK
Cancel
Help

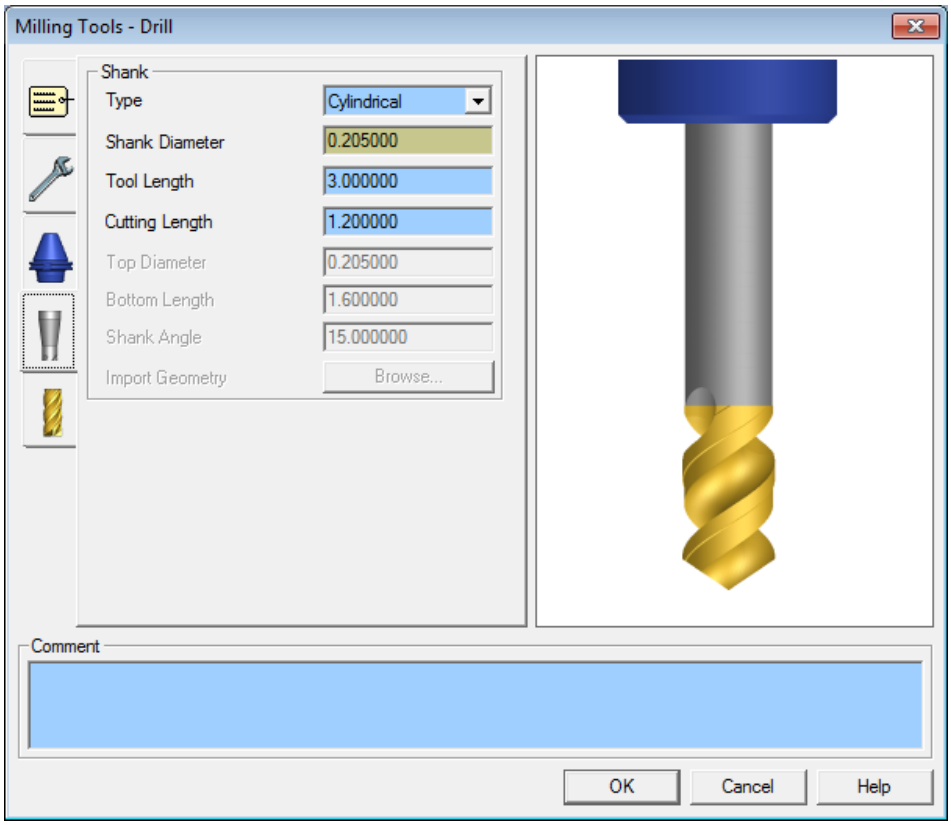

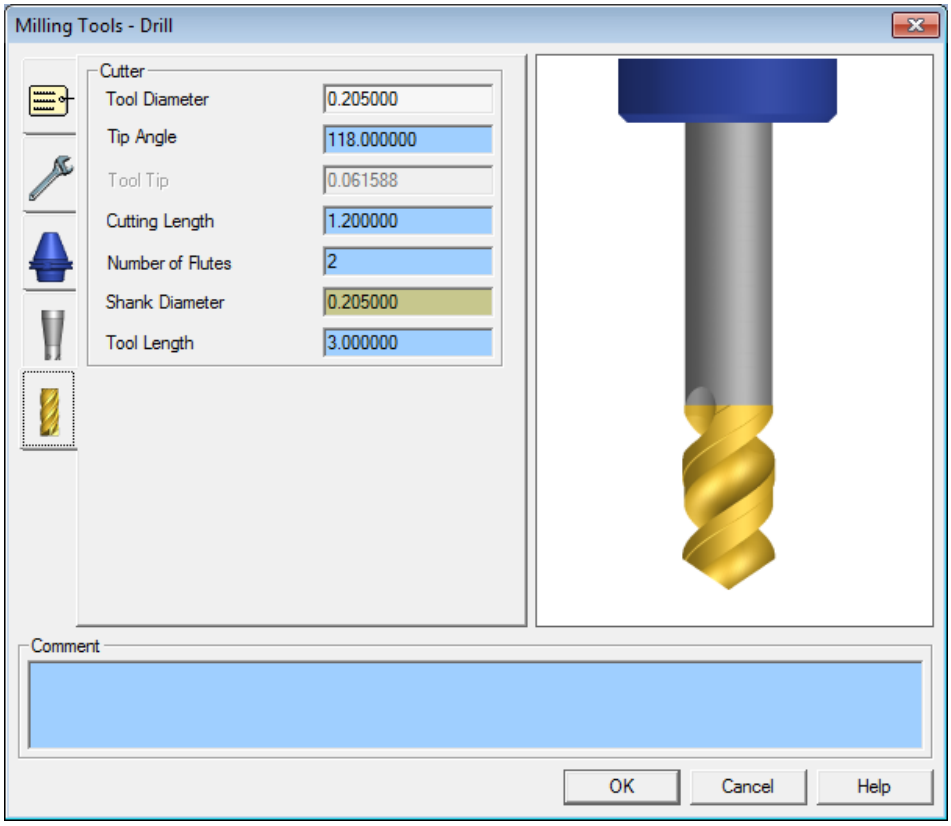

End of Tool 8 Setup, #5 Drill, for WPI SL10 Lathe Tool in Esprit CAM Software

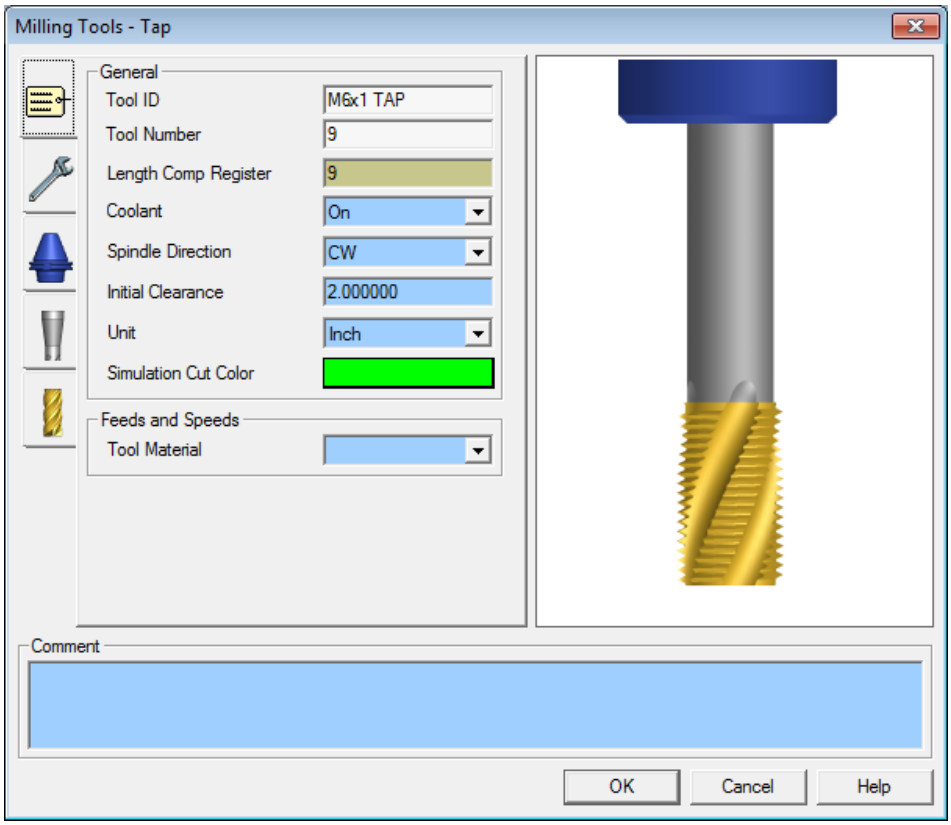

Tool 9 Setup, M6x1 Thread Tap Tool, for WPI SL10 Lathe Tool in Esprit CAM Software

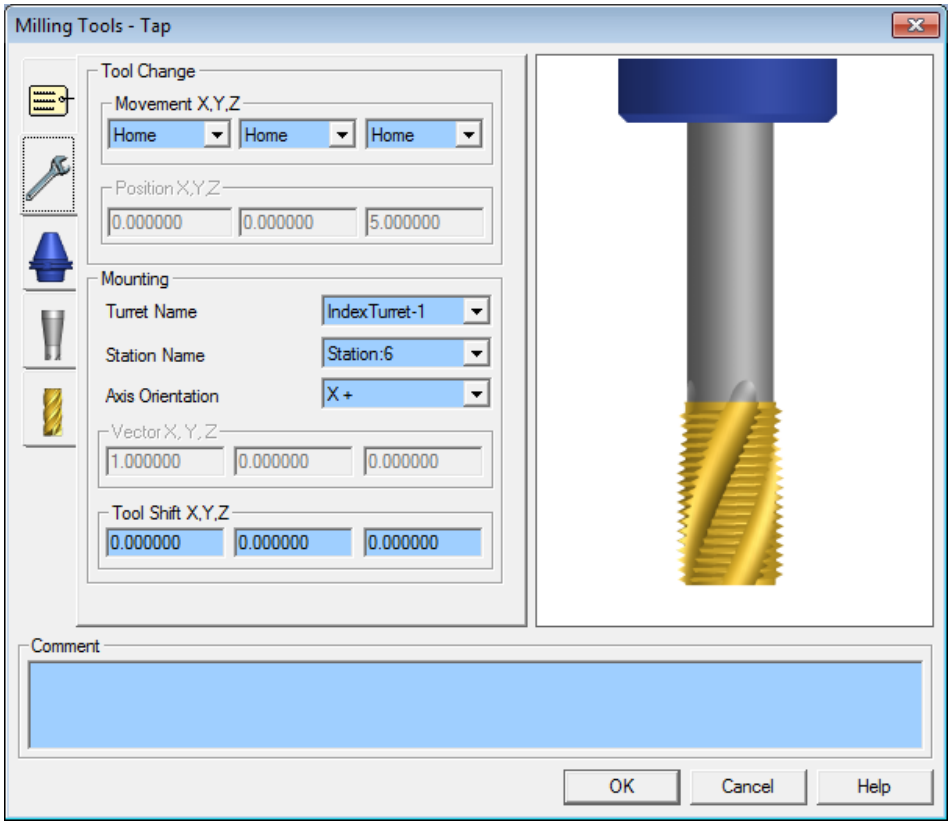

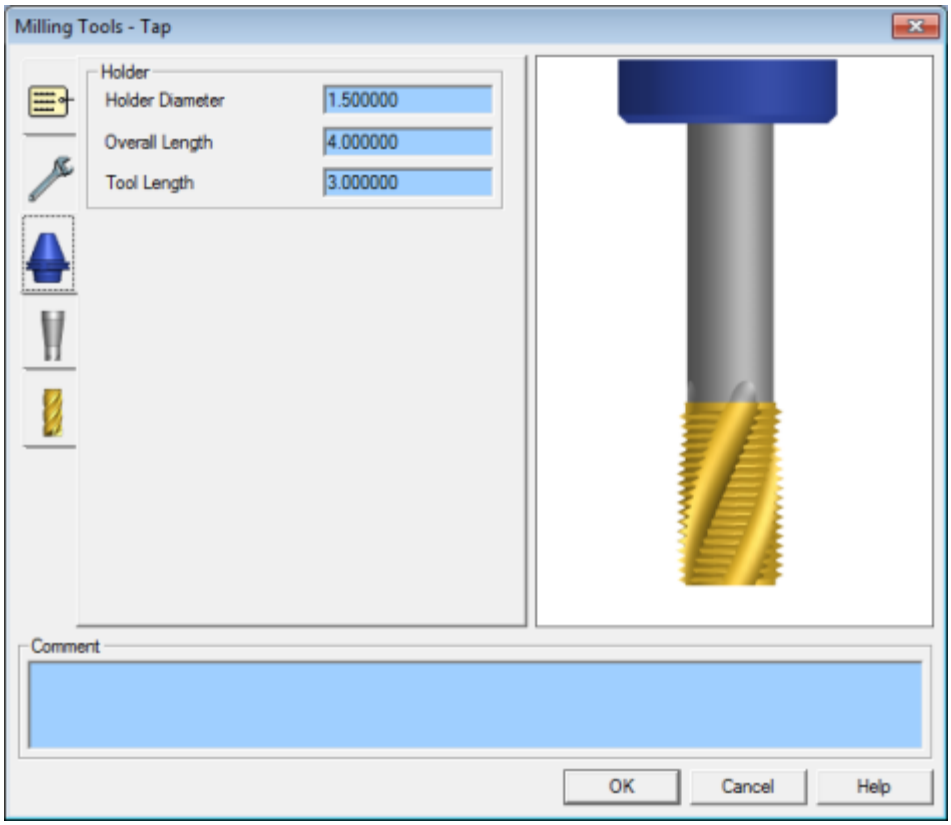
Milling Tools - Tap
Holder
Holder Diameter
1.500000
Overall Length
4.000000
Tool Length
3.000000
Comment
OK
Cancel
Help

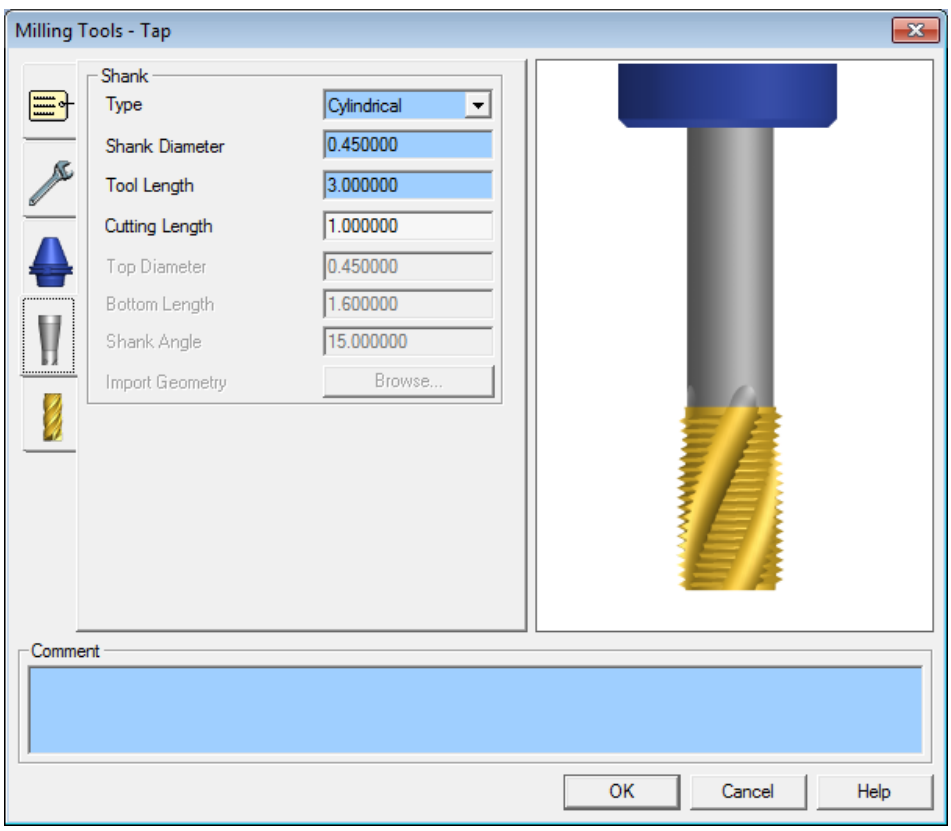
Milling Tools - Tap
Shank
Type
Cylindrical
Shank Diameter
0.450000
Tool Length
3.000000
Cutting Length
1.000000
Top Diameter
0.450000
Bottom Length
1.600000
Shank Angle
15.000000
Import Geometry
Browse...
Comment
OK
Cancel
Help

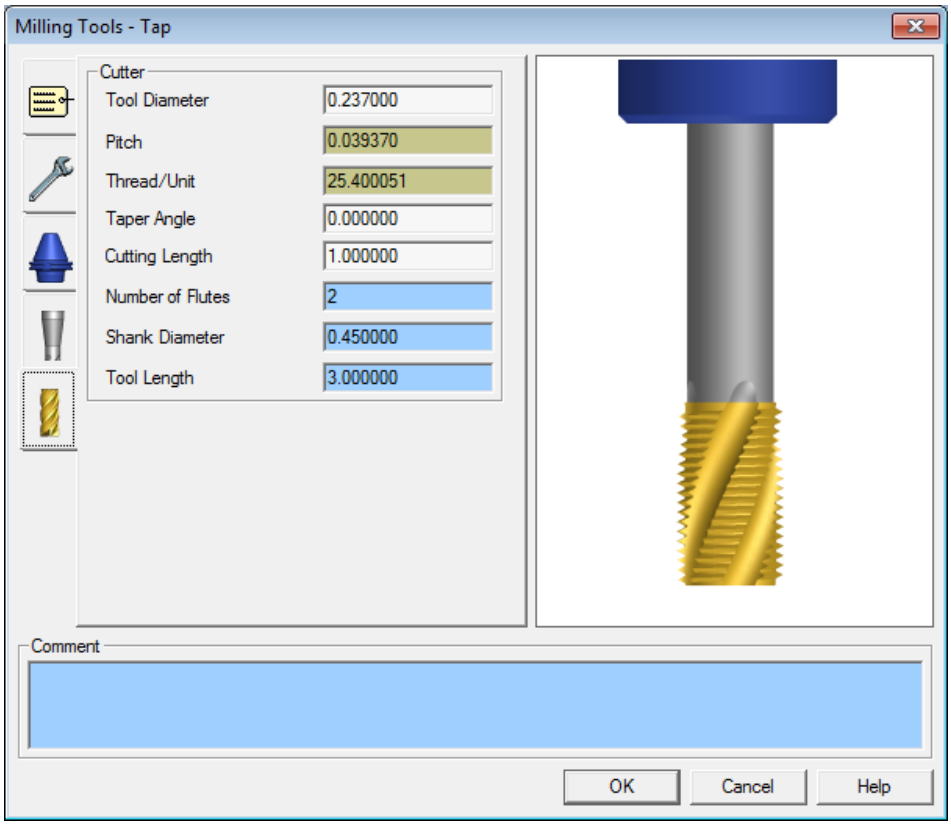

End of Tool 9 Setup, M6x1 Thread Tap Tool, for WPI SL10 Lathe Tool in Esprit CAM Software

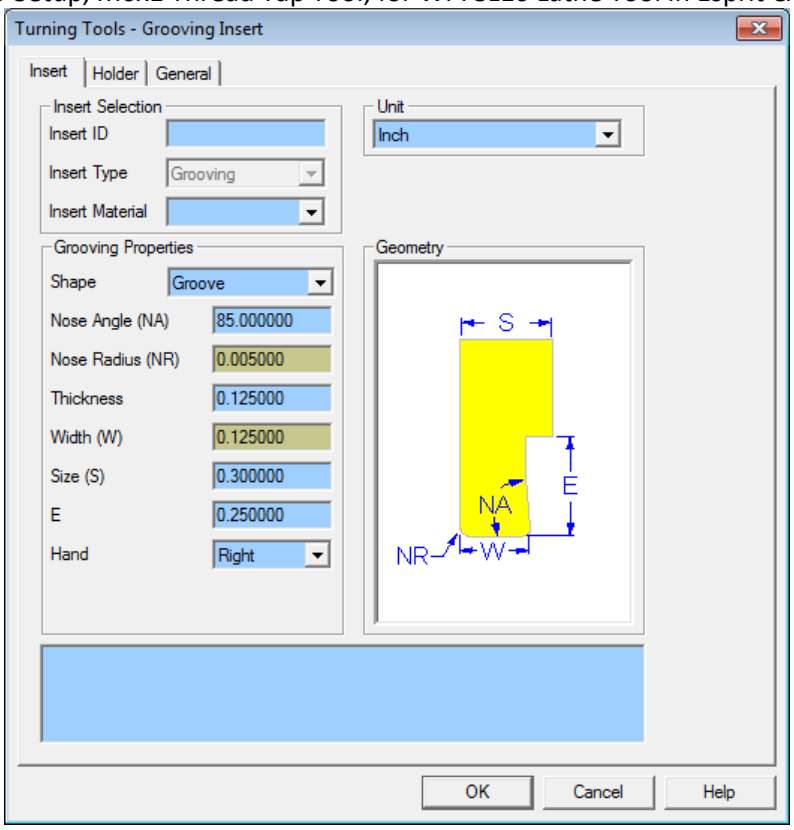

Tool 10 Setup, Grooving Cutoff Tool, for WPI SL10 Lathe Tool in Esprit CAM Software

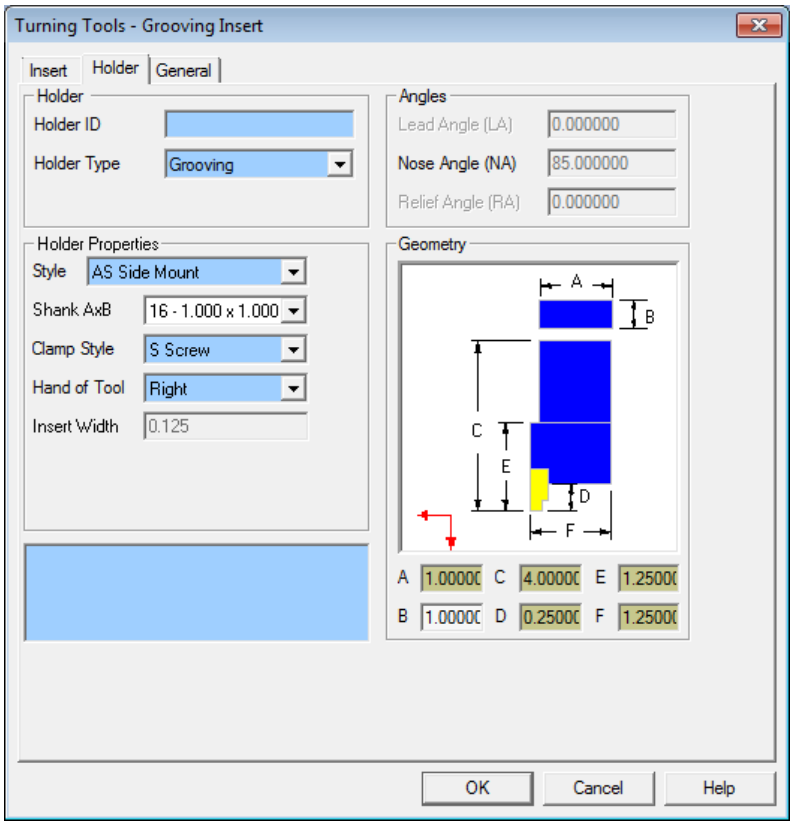

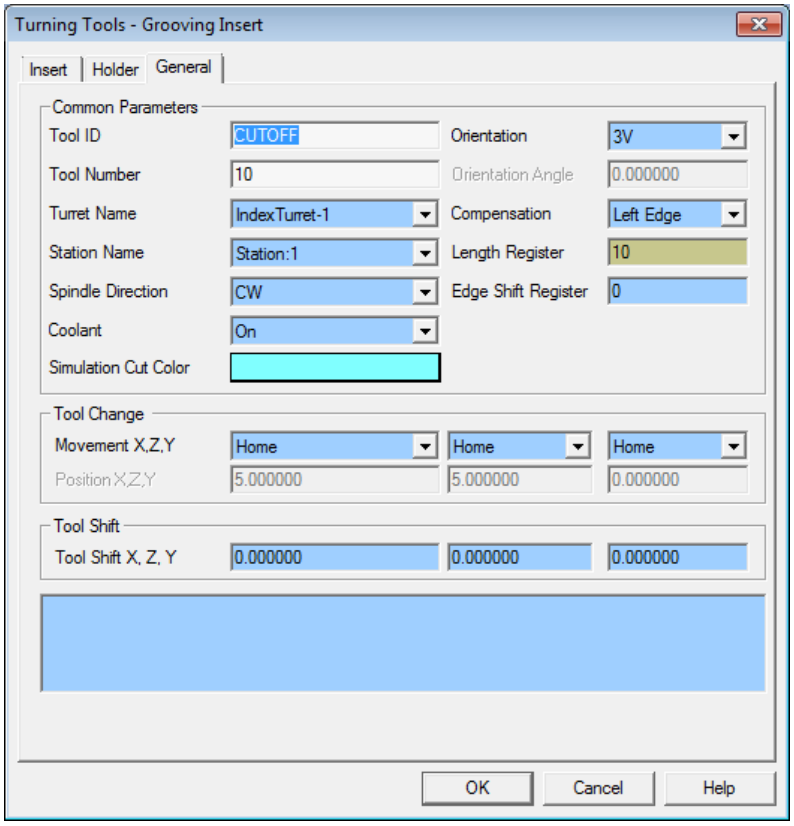

End of Tool 10 Setup, Grooving Cutoff Tool, for WPI SL10 Lathe Tool in Esprit CAM Software

Completed Esprit setup, now begin to program machining operations to manufacture custom nozzles.

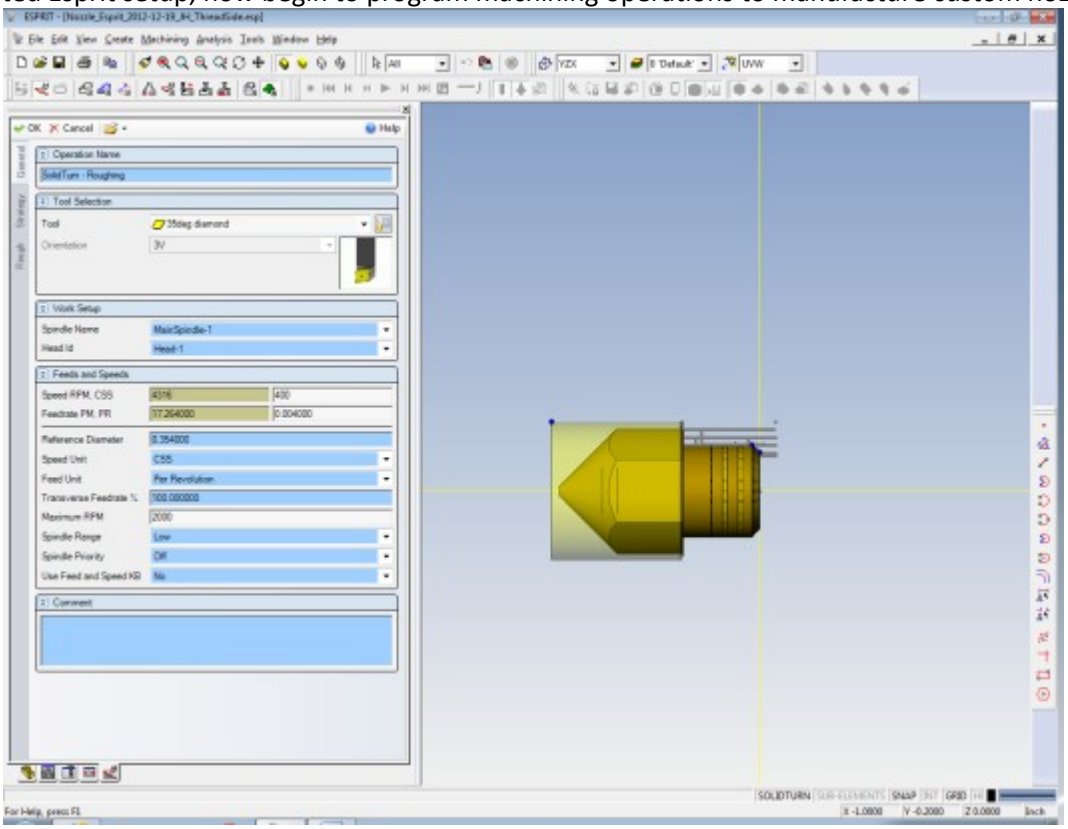

Using Brass Hex Stock from WPI Machine Shop Setup Rough Turning Operation For Thread End of Nozzle

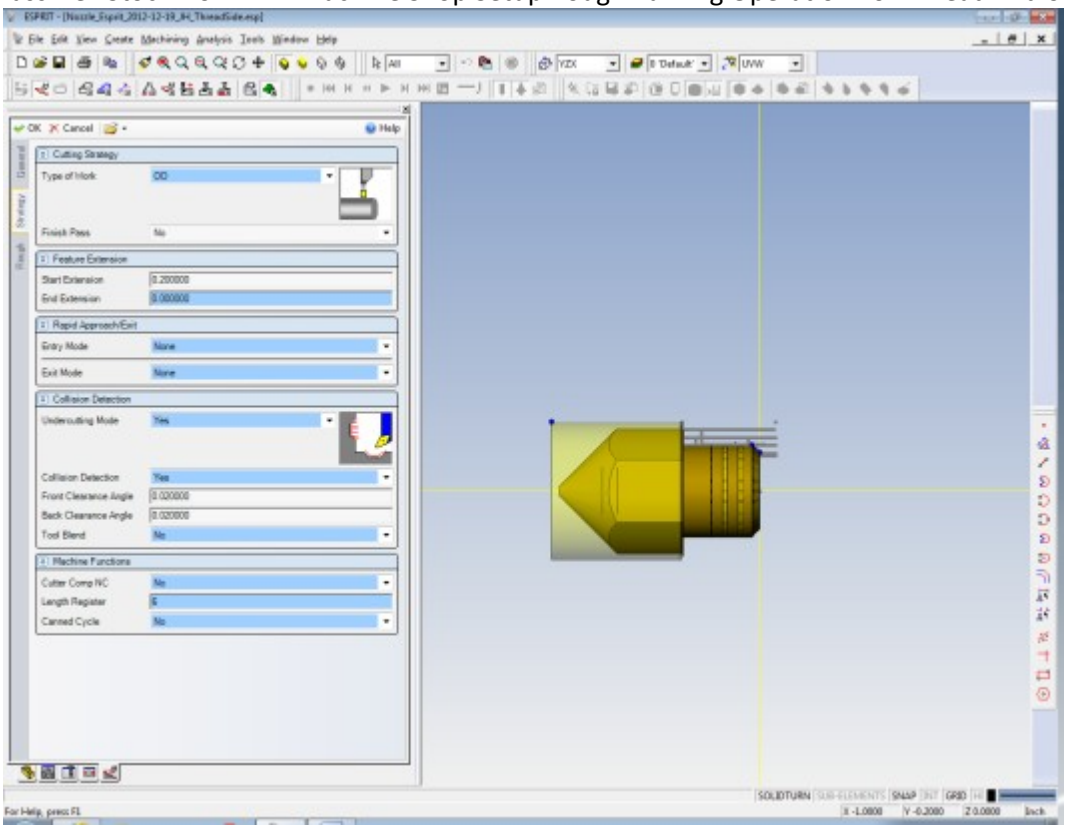

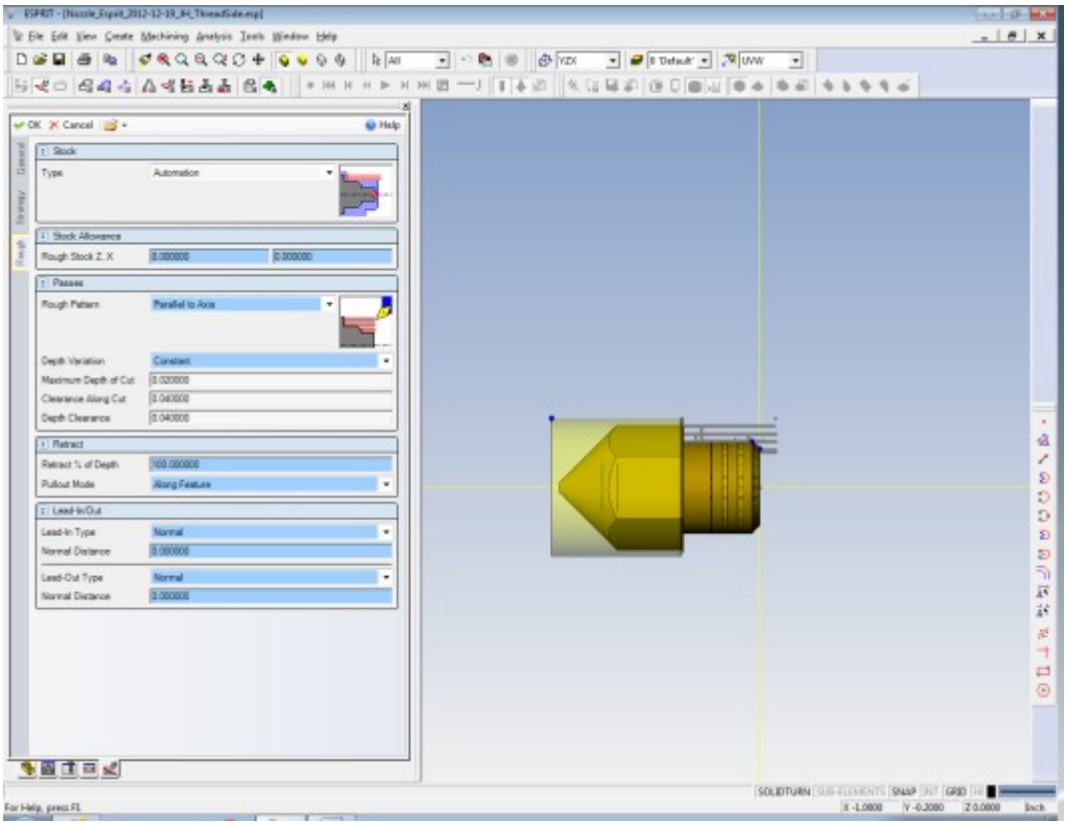

Completed Rough Turning Operation Settings For Thread End of Nozzle

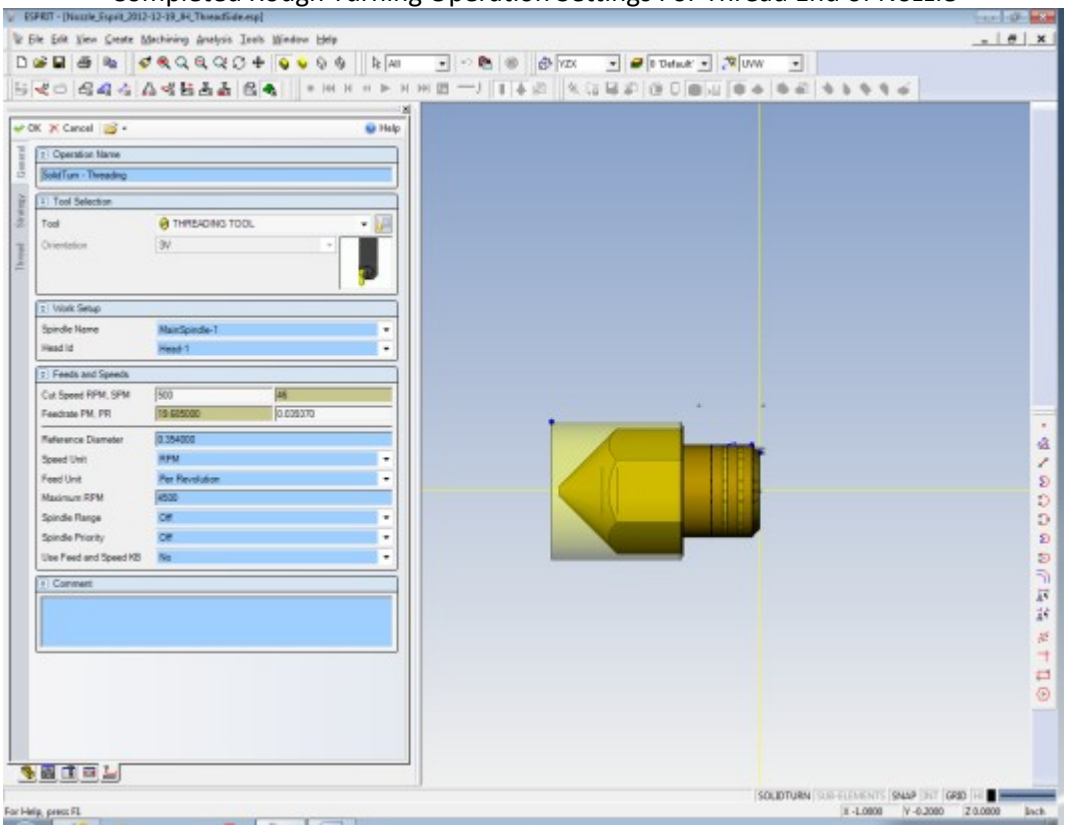

Setup Thread Cutting Operation For Thread End of Nozzle

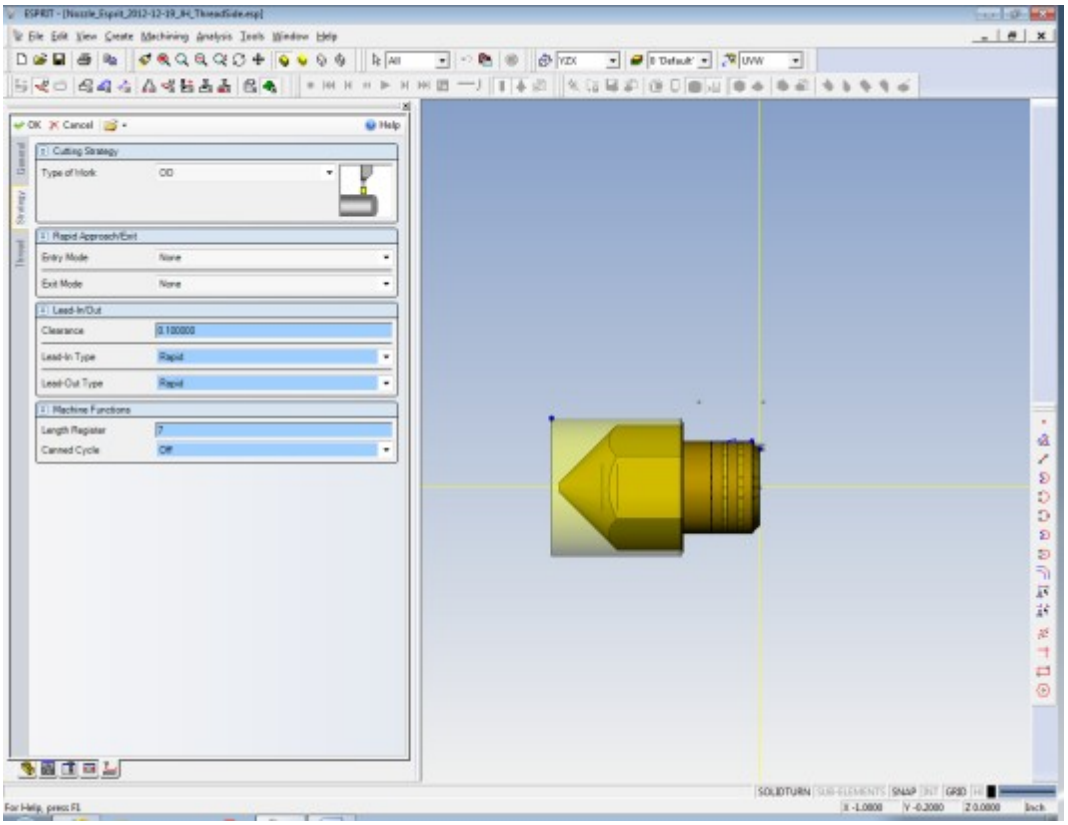

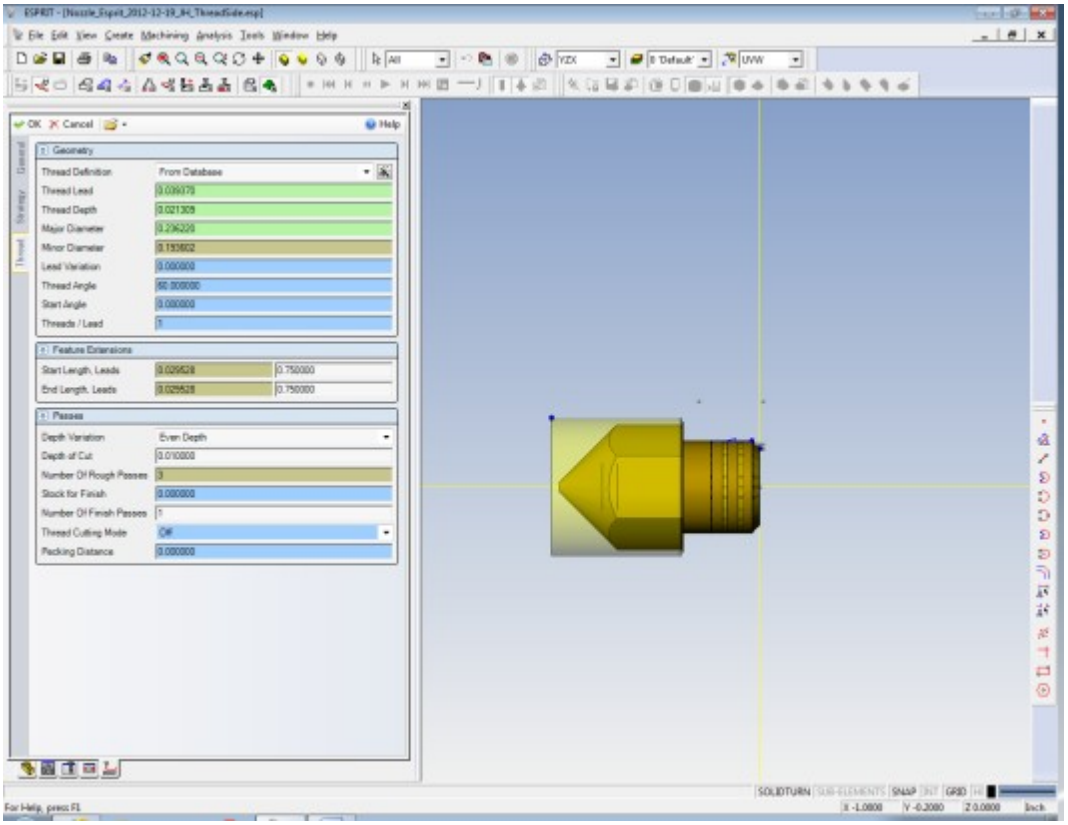

Completed Thread Cutting Operation Settings For Thread End of Nozzle

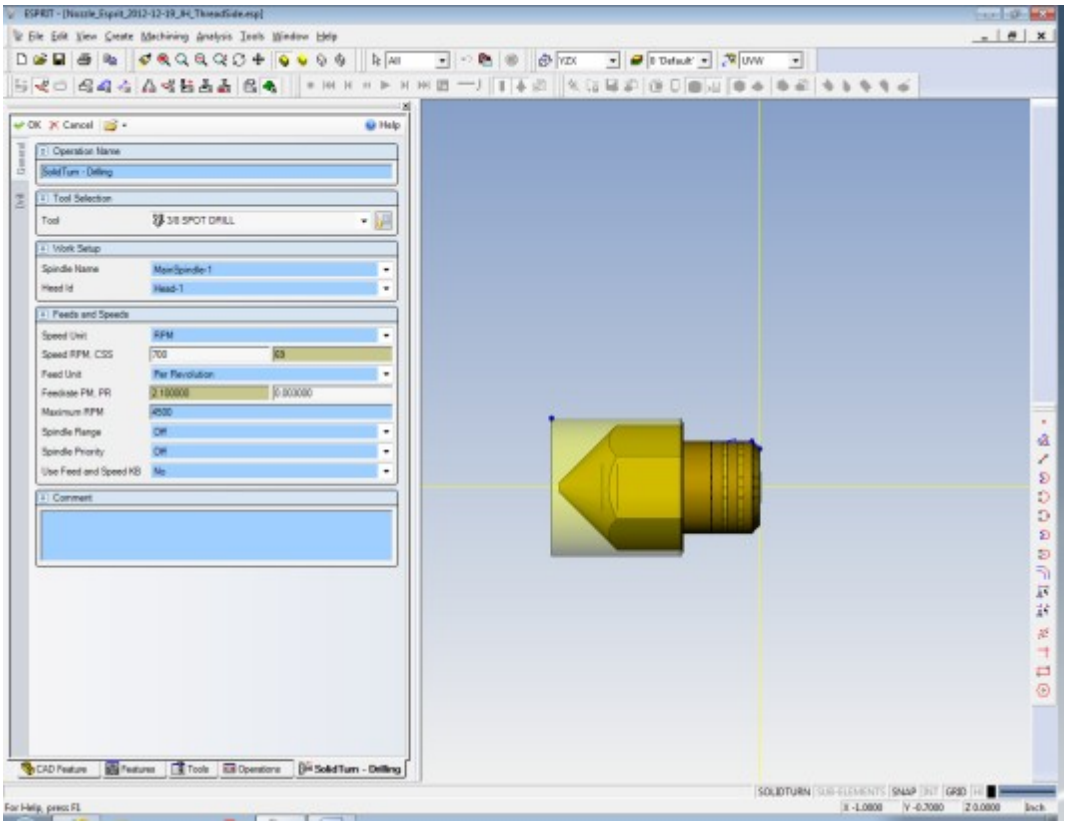

Setup Centering Spot Drill Operation For Thread End of Nozzle

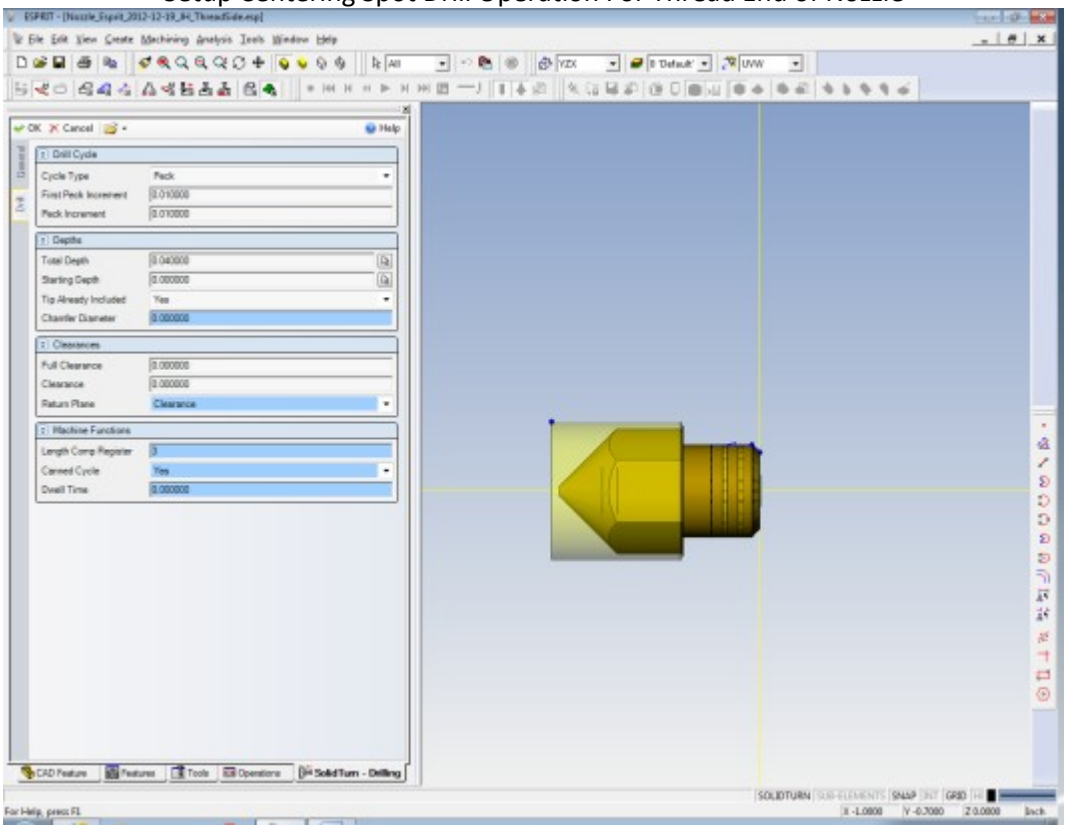

Completed Centering Spot Drill Operation Settings For Thread End of Nozzle

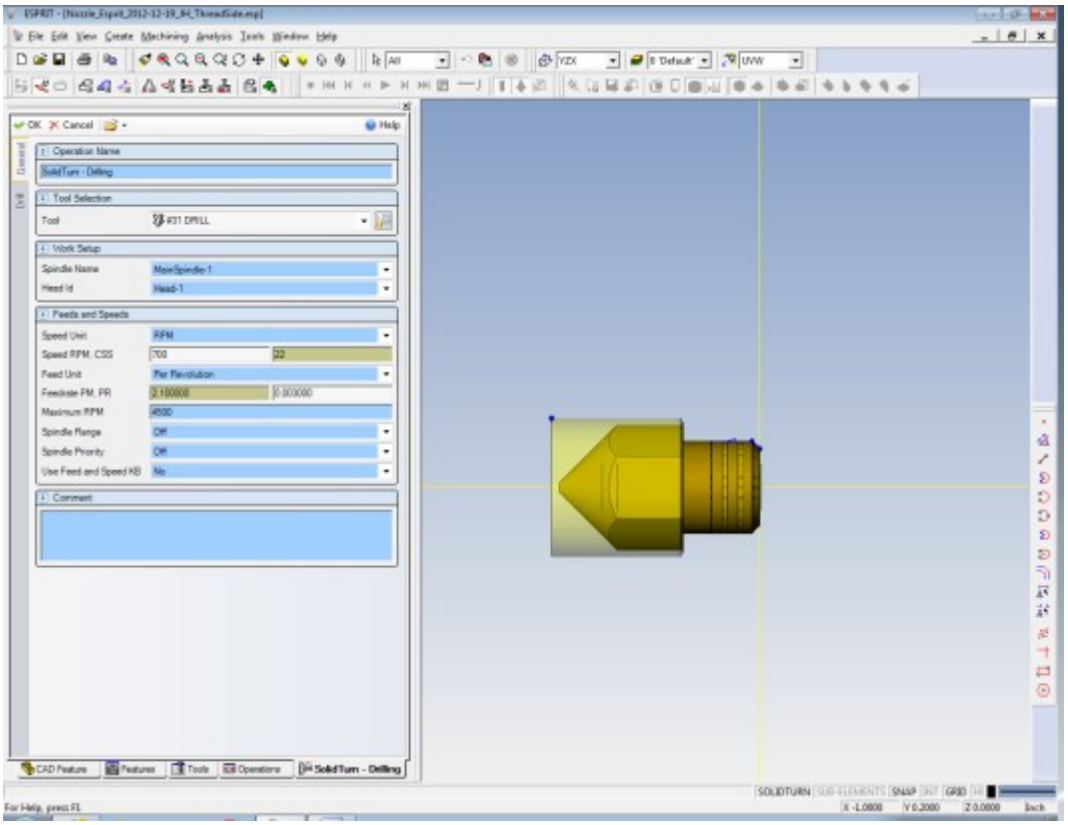

Setup #31 Drill Operation For Thread End of Nozzle

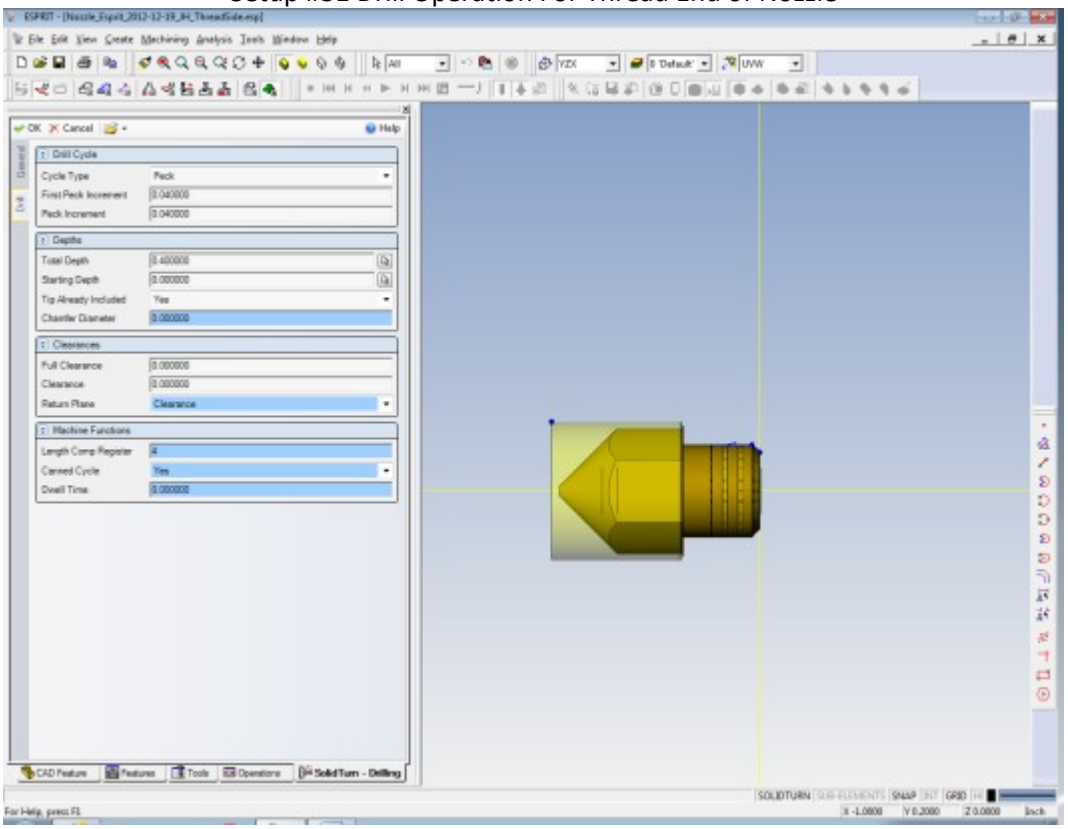

Completed #31 Drill Operation Settings For Thread End of Nozzle

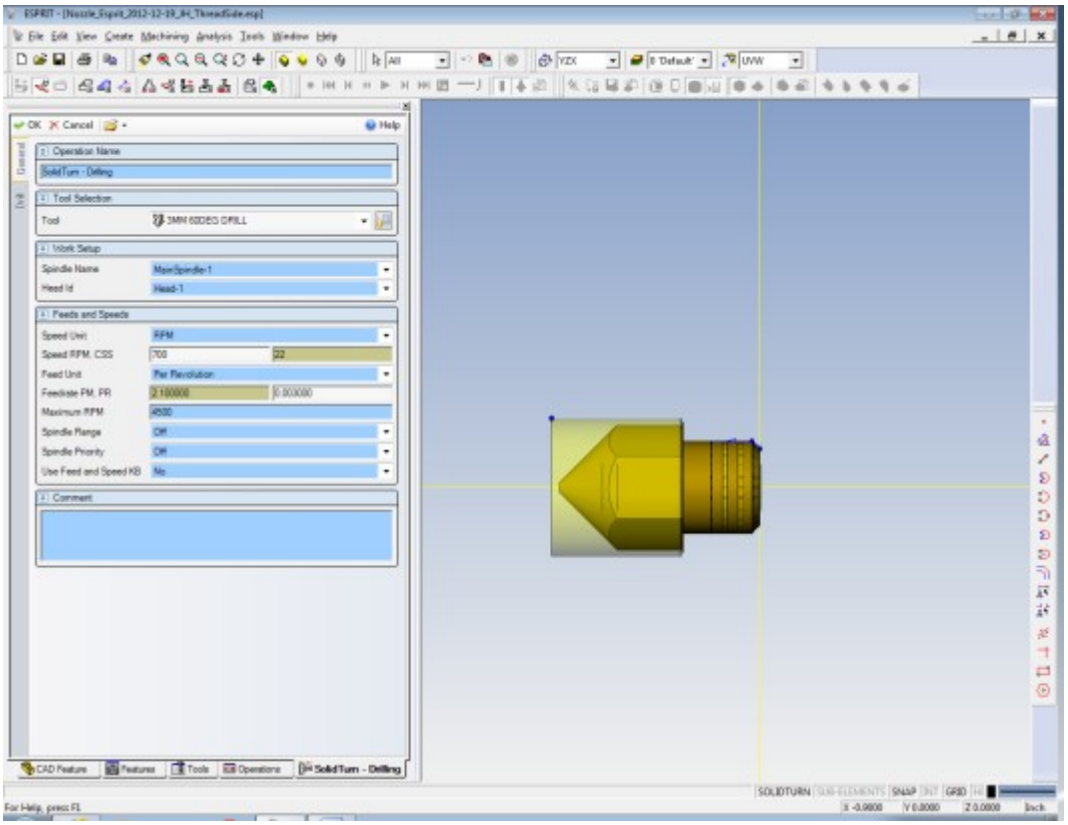

Setup Specialty 3mm 60 Degree Drilling Operation For Thread End of Nozzle

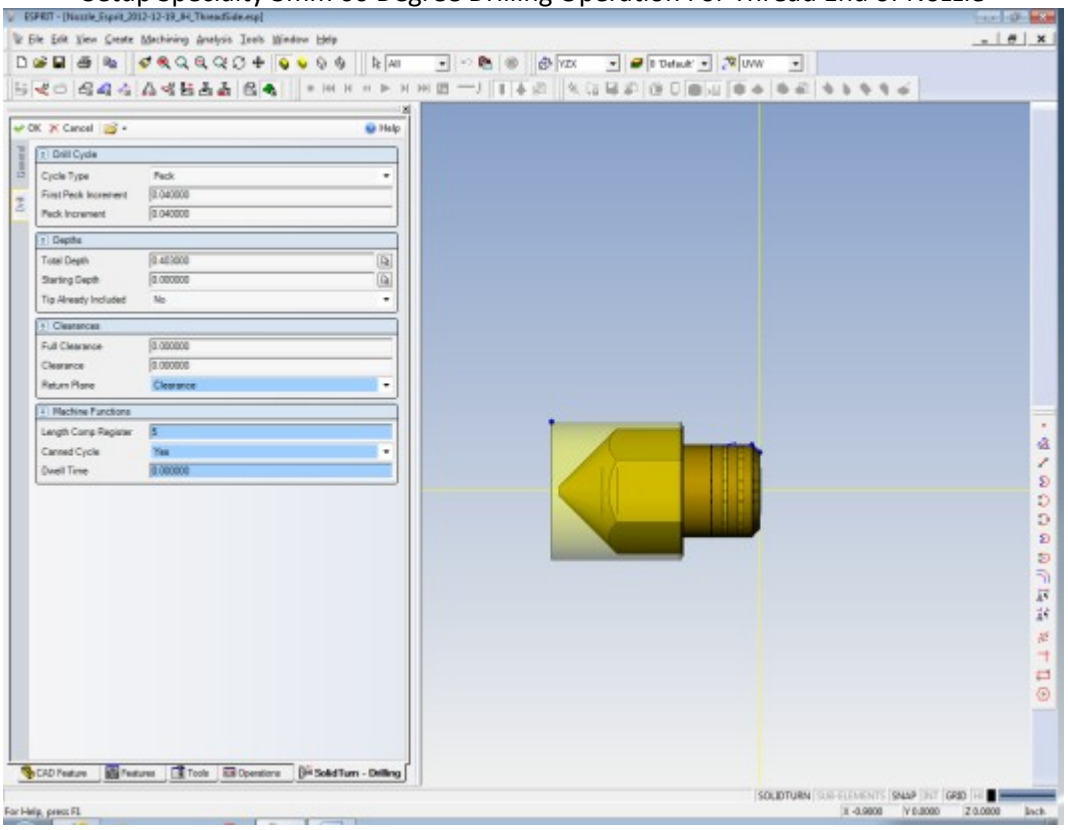

Completed Specialty 3mm 60 Degree Drilling Operation Settings For Thread End of Nozzle

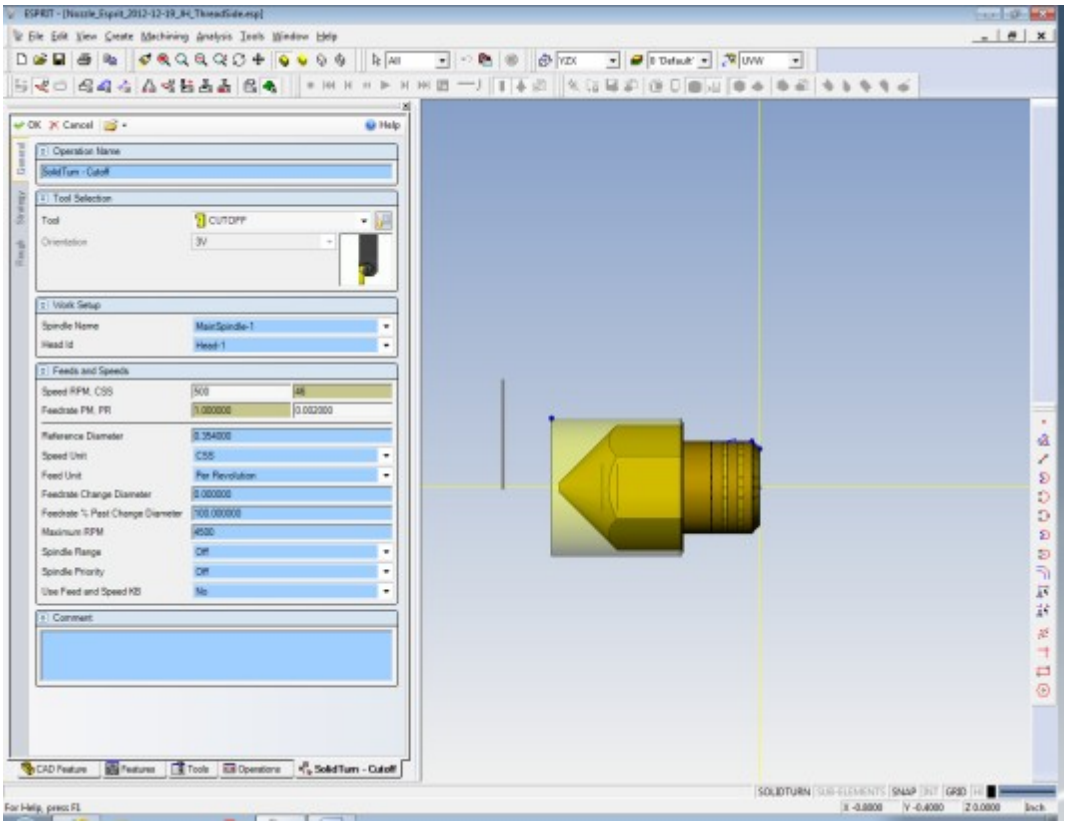

Setup Grooving Cutoff Tool Operation For Thread End of Nozzle

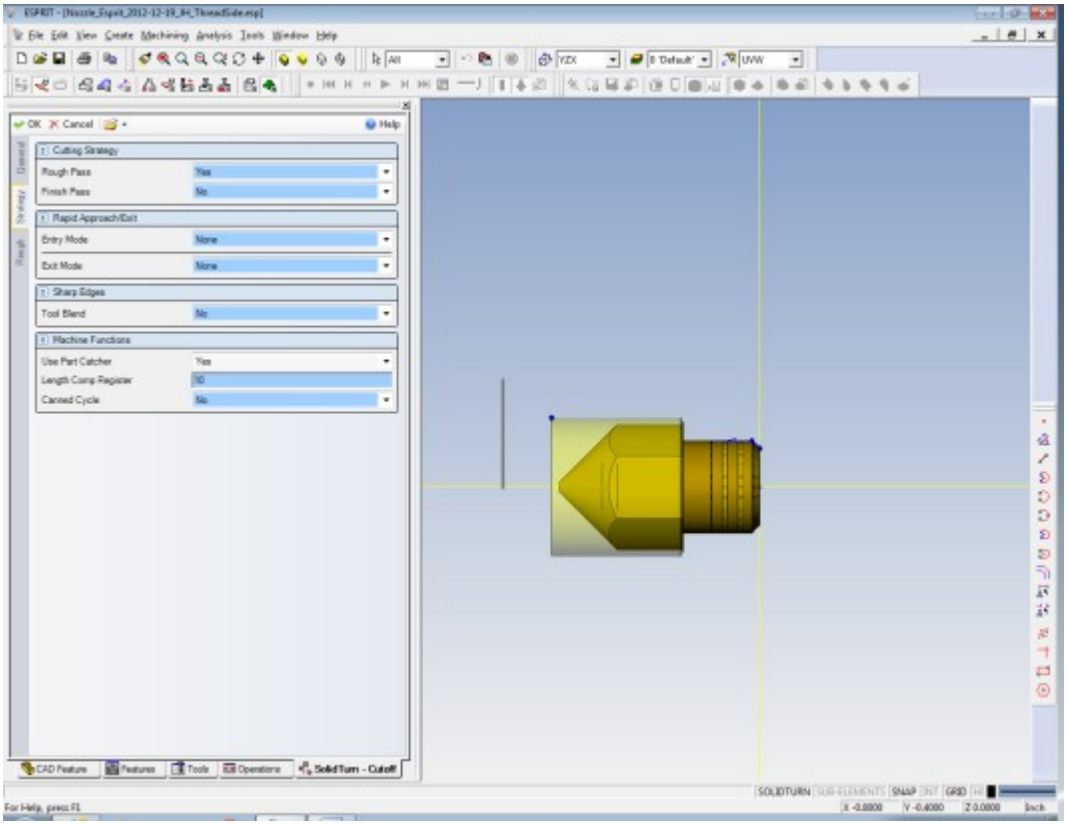

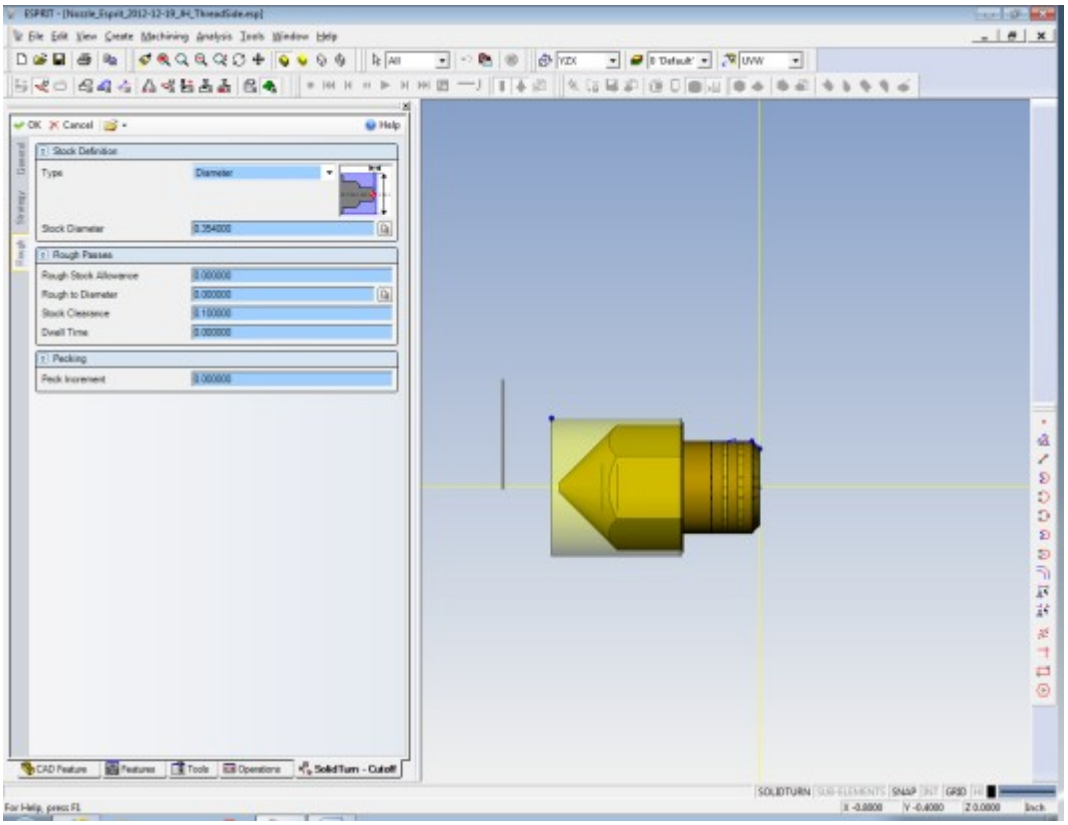

Completed Grooving Cutoff Tool Operation Settings For Thread End of Nozzle

MQP_DGF-111B_EspritCAM_CustomNozzleMachining_ThreadSide.wmv

Embedded Video File of Esprit Simulated Machining of the Above Operational Setup
(Double-Click Small wmv Icon Above to Play Video in Windows Media Player)

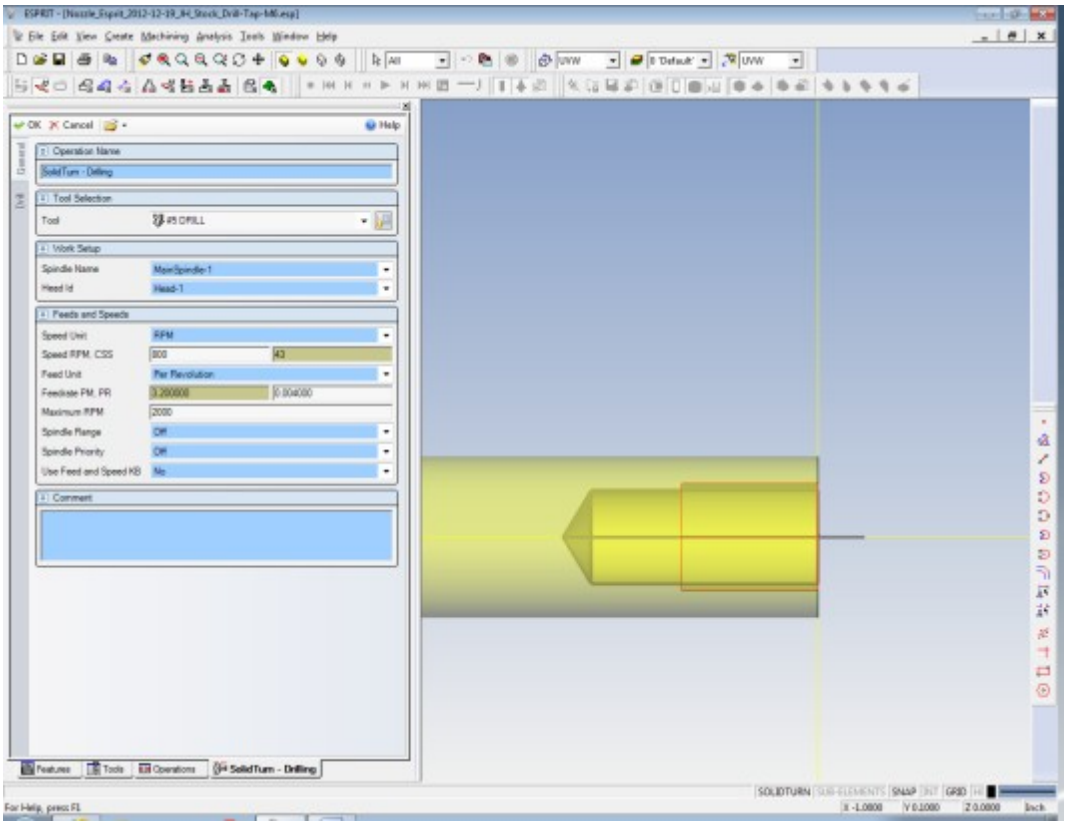

Setup #5 Drilling Operation in Stock for Mating Thread Part Holder for Cutoff Nozzle Blanks

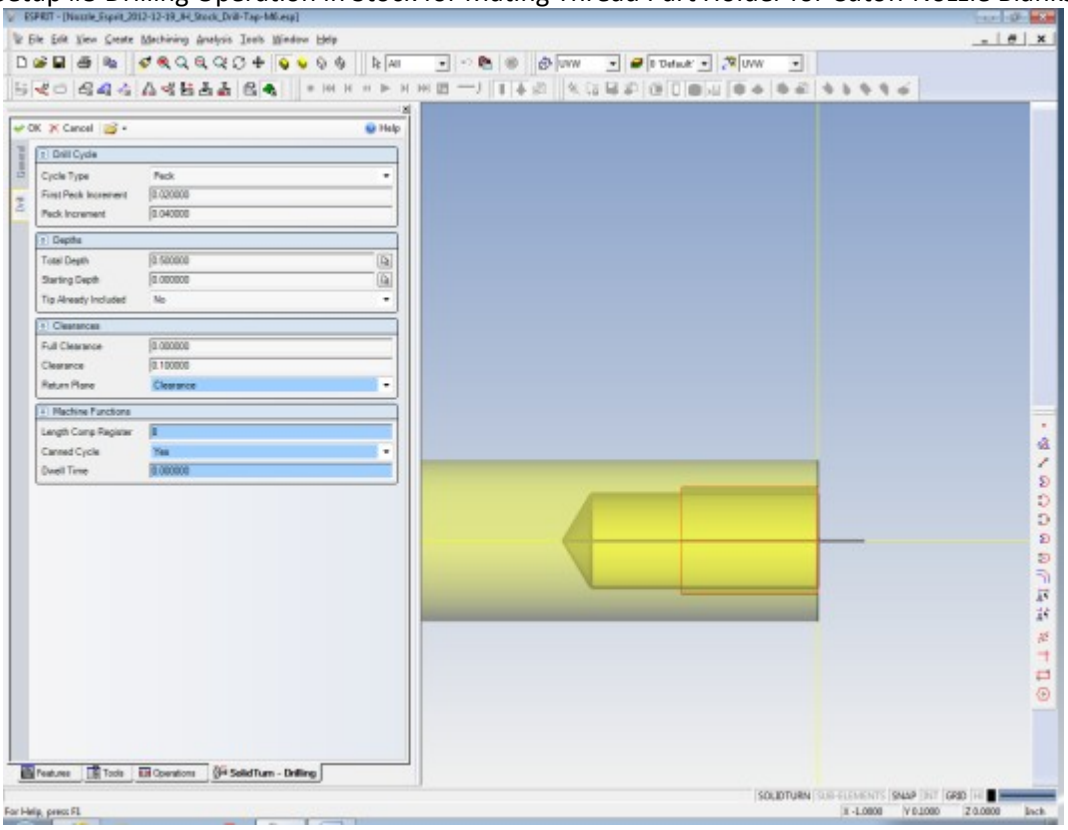

Completed #5 Drilling Operation Settings in Stock for Mating Thread Part Holder for Cutoff Nozzle Blanks

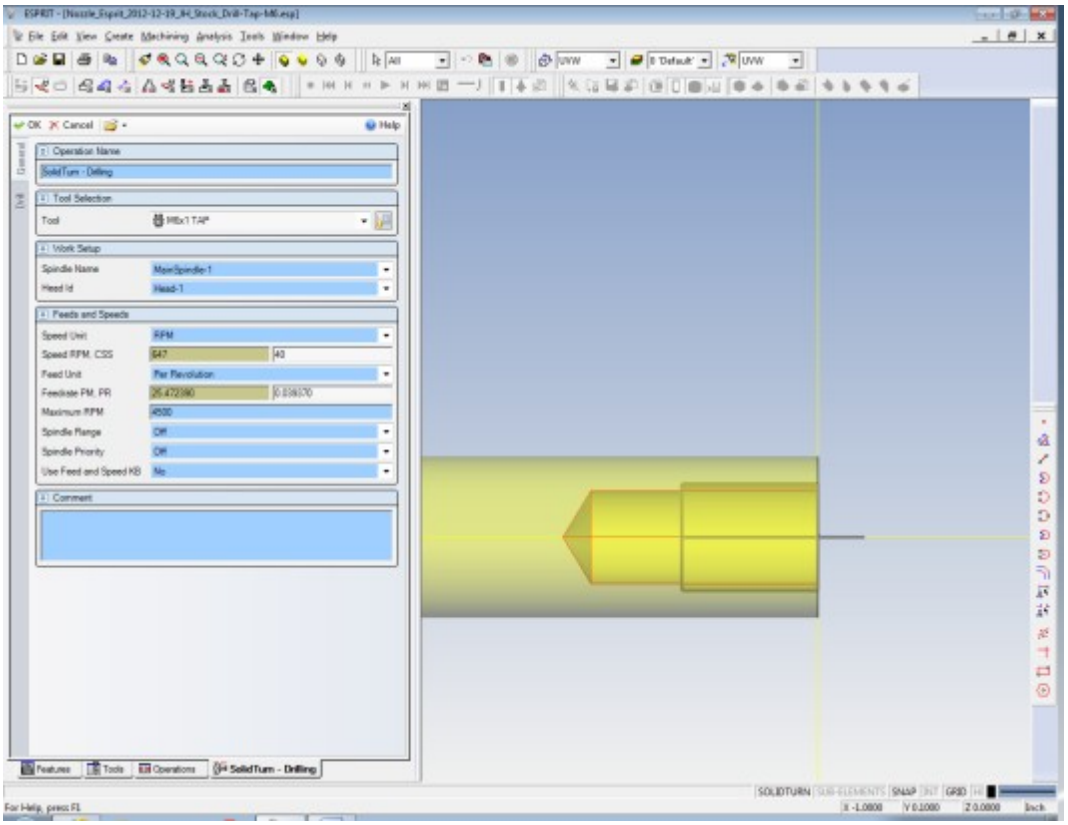

Setup M6x1 Tap Operation in Stock for Mating Thread Part Holder for Cutoff Nozzle Blanks

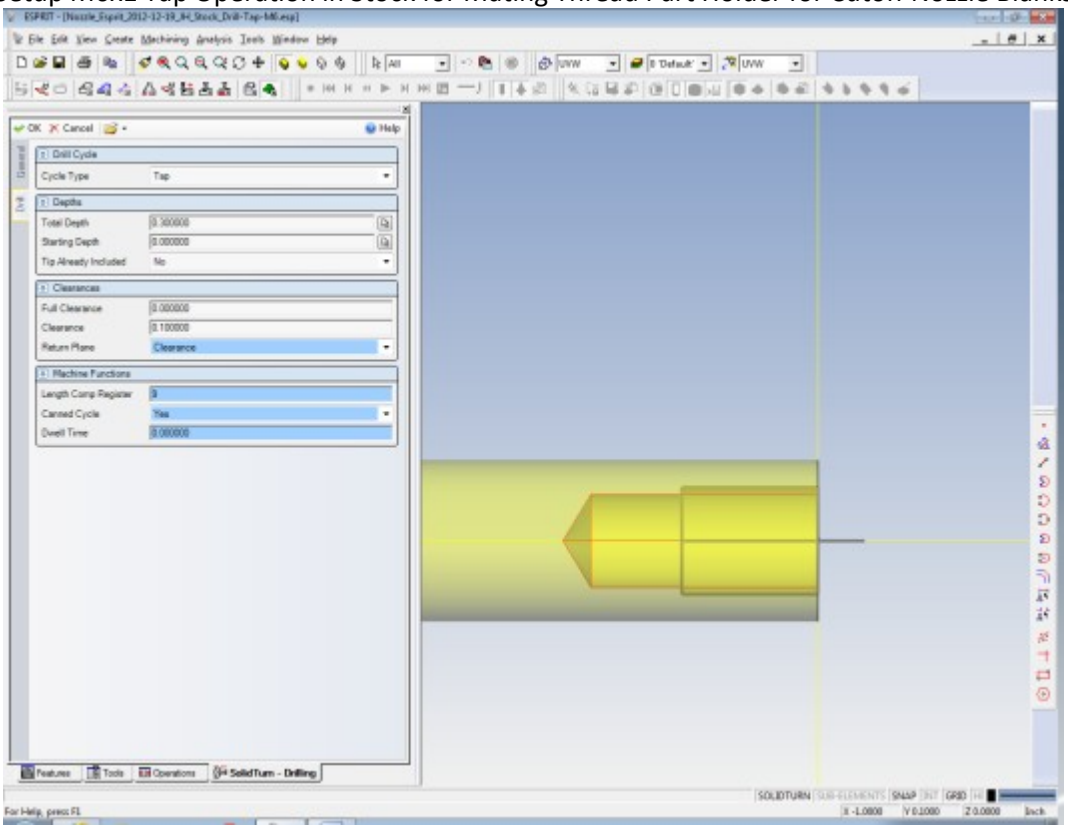

Completed M6x1 Tap Operation Settings in Stock for Mating Thread Part Holder for Cutoff Nozzle Blanks

MQP_DGF-111B_EspritCAM_CustomNozzleMachining_PartHolderThreadedStock.wmv

Embedded Video File of Esprit Simulated Machining of the Above Operational Setup
(Double-Click Small wmv Icon Above to Play Video in Windows Media Player)

Load Threaded Stock Part Holder into Machine & Thread on the Nozzle Blank Previously Cutoff

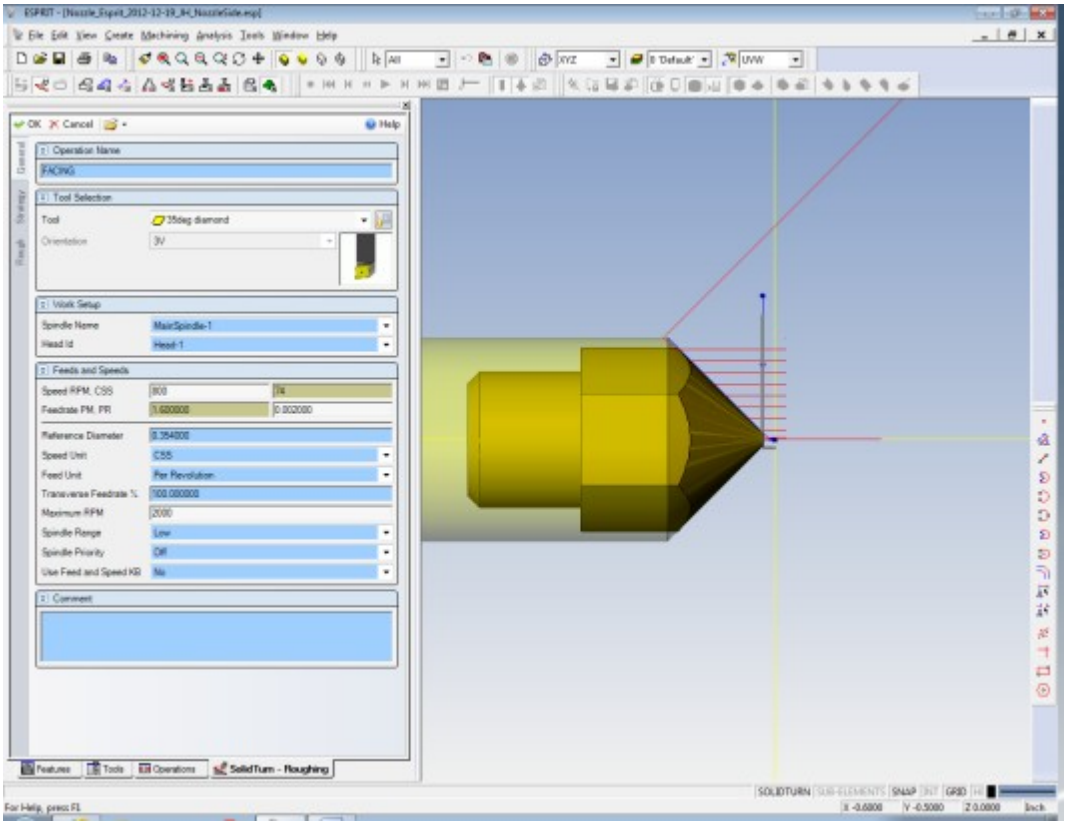

Setup Facing Operation for Front Nozzle End

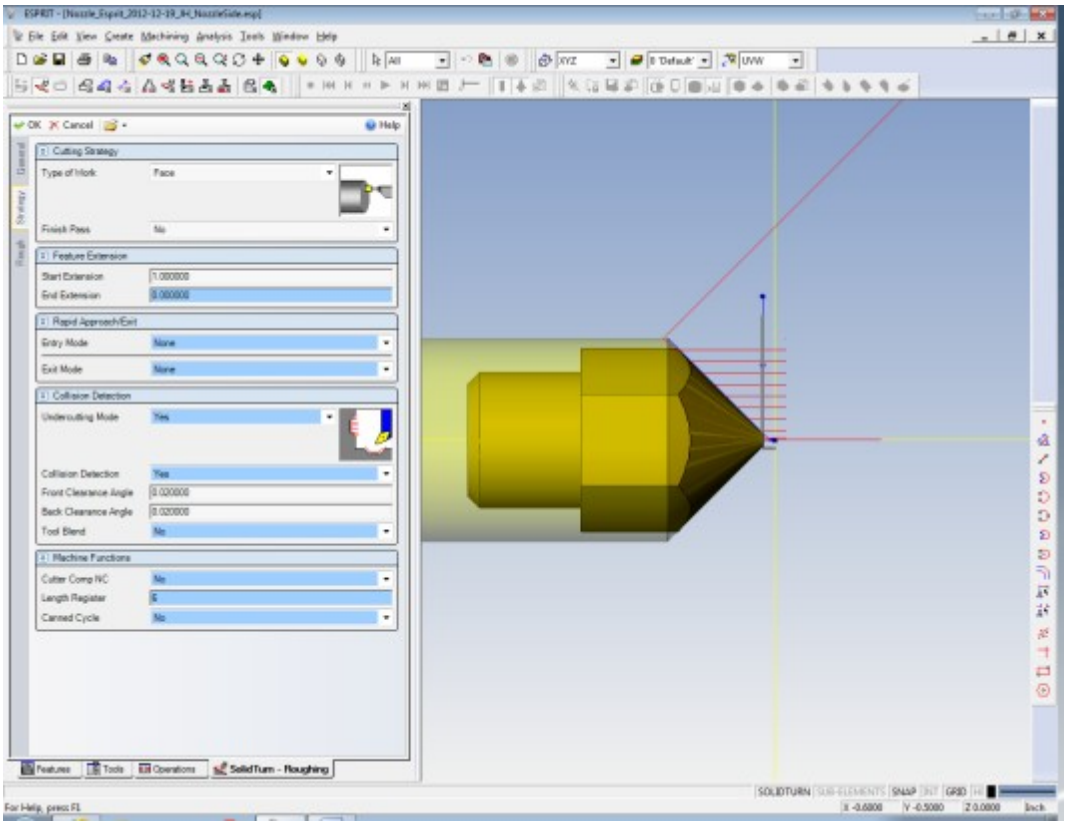

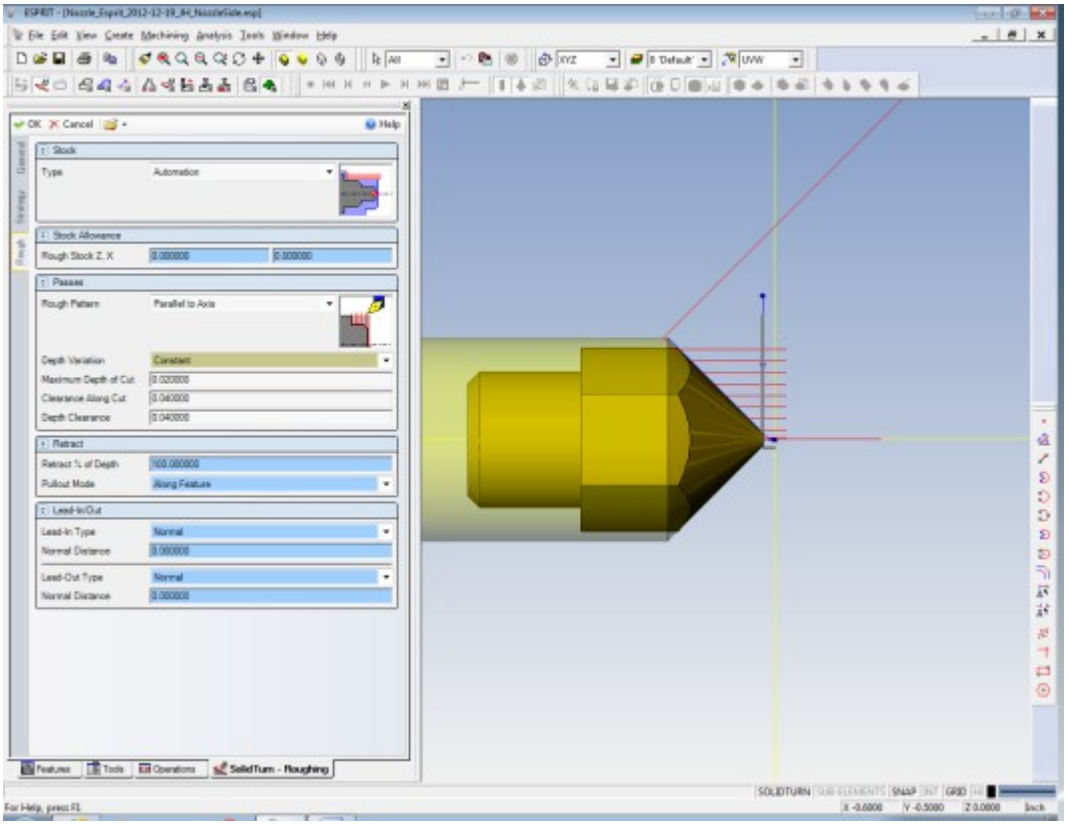

Completed Facing Operation Settings for Front Nozzle End

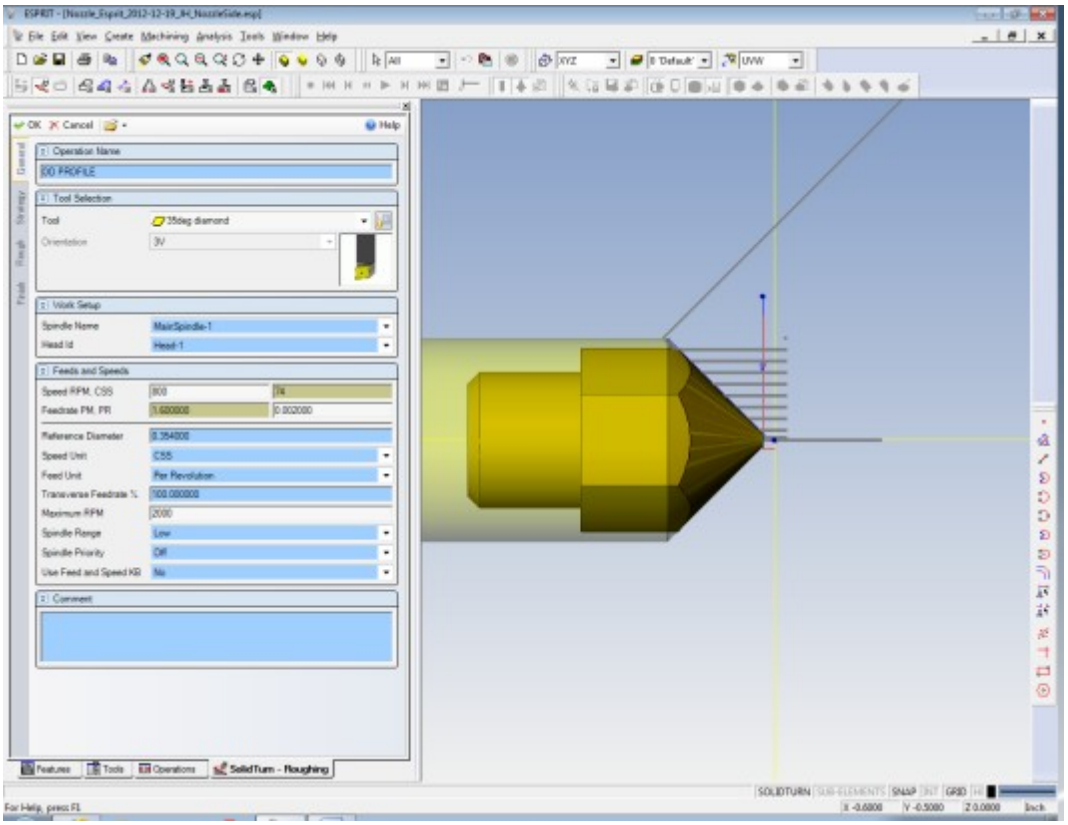

Setup OD Profile Turning Operation for Front Nozzle End

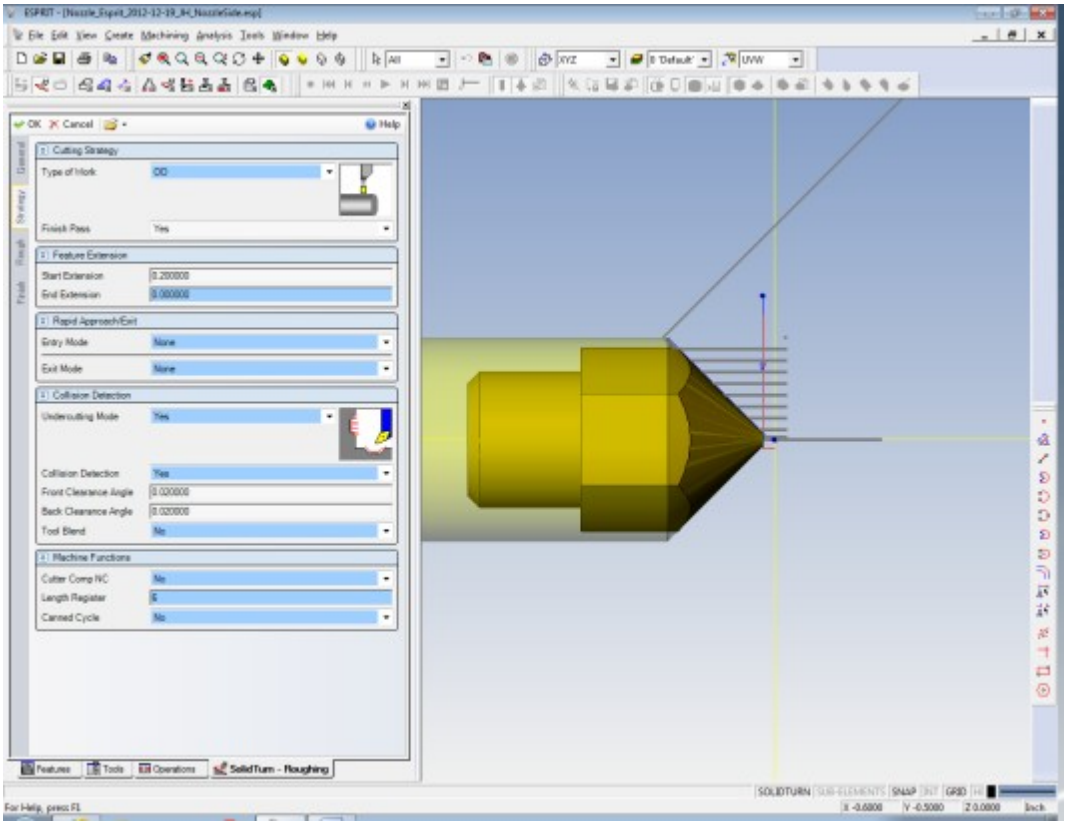

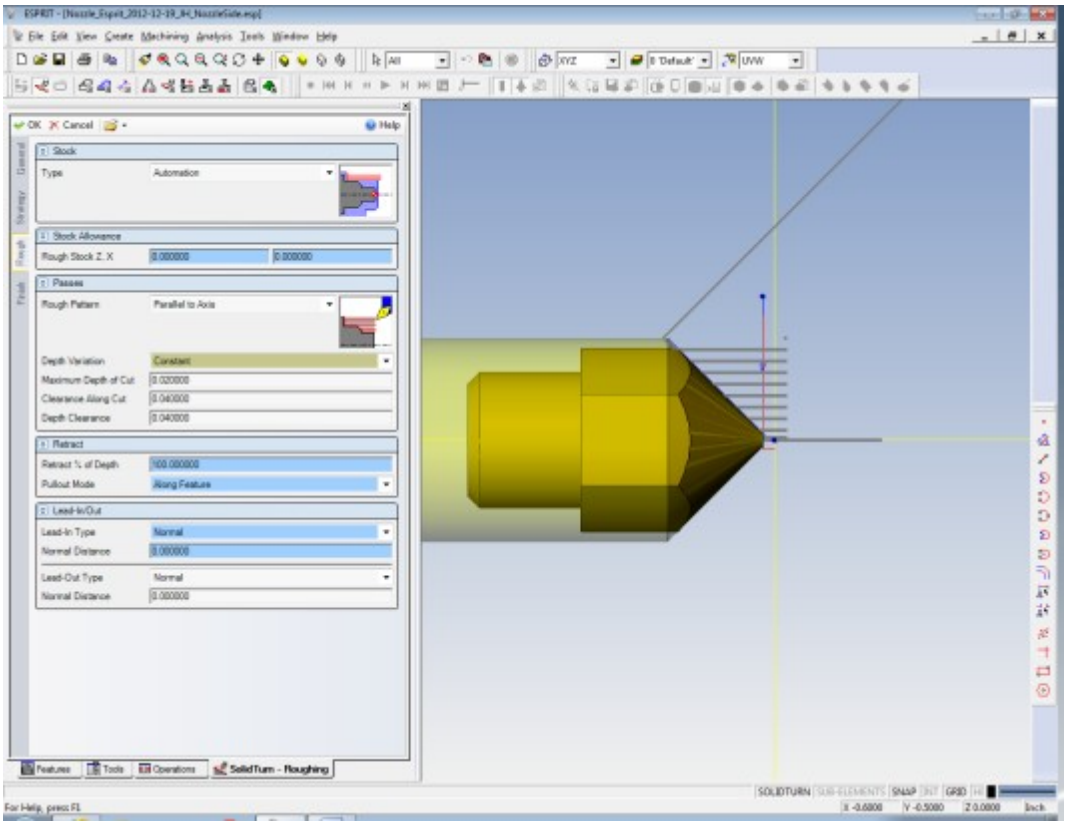

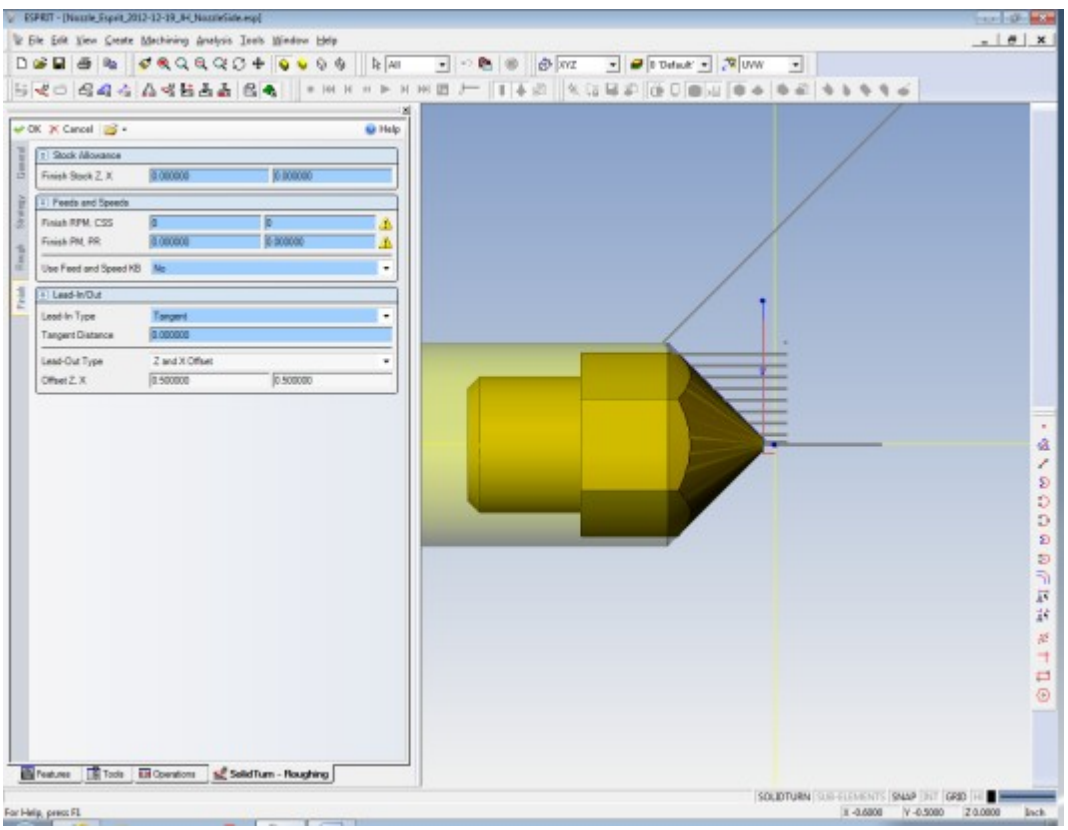

Completed OD Profile Turning Operation Settings for Front Nozzle End

MQP_DGF-111B_EspritCAM_CustomNozzleMachining_NozzleSide.wmv

Embedded Video File of Esprit Simulated Machining of the Above Operational Setup
(Double-Click Small wmv Icon Above to Play Video in Windows Media Player)

Completed Custom Nozzle Blank Manufacturing, Quantity 16, at WPI Machine Shop…
…Thanks to Adam Sears & Torbjorn Bergstrom For Guiding the Nozzle Blank Manufacturing Process.

Quantity 16 Nozzle Blanks Shipped to Experienced Machinists at Industrial Motions Engineering in Woburn MA for Final Remaining Step to Complete Custom Nozzles, Micro-drilling the Nozzle Bore Holes.

Industrial Motions Engineering of Woburn MA Donated Their Time & Machining Efforts for This MQP.
Thank You to Michael Mangum & Joe Fustolo of Industrial Motions Engineering for Donated Services.
http://www.industrialmotions.com/index.html
Industrial Motions Engineering
49R High Street
Woburn, MA 01801
Tel: 781.935.8800
Fax: 781.935.8849

Quantity 4 Completed Nozzles Each of 300μm & 250μm Sizes Back from Industrial Motions Engineering.

Quantity 3 Completed Nozzles Each of 200μm & 150μm Sizes Back from Industrial Motions Engineering.

Note 1: Only 1 Nozzle From Each Nozzle Size Passed Inspection Upon Receipt Back from Industrial Motions Engineering; Passing Nozzles Had Both Clean Bore Hole & Hole Centered in Nozzle Body.

Note2: Apparent Difficulties Machining with the Microdrills and/or the Machine Setup/Alignment.

Appendix G: Nozzle & Small Printing Test Measurement Images

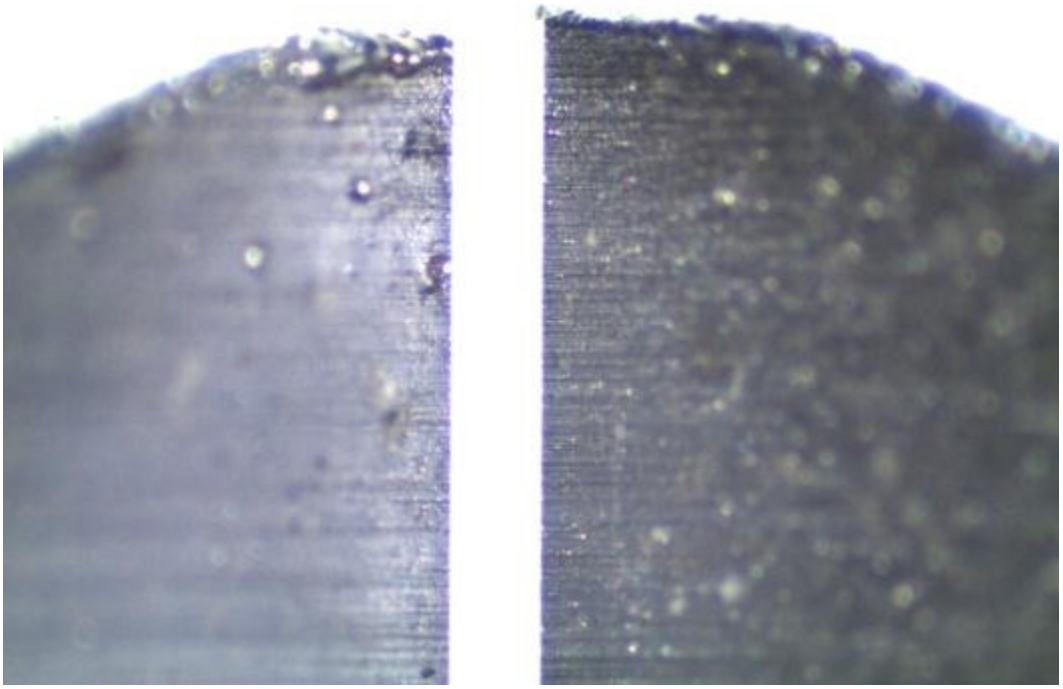

Vernier Caliper Microscope Calibration Image – Set to 0.010” (254µm) – Raw Image @ 35x

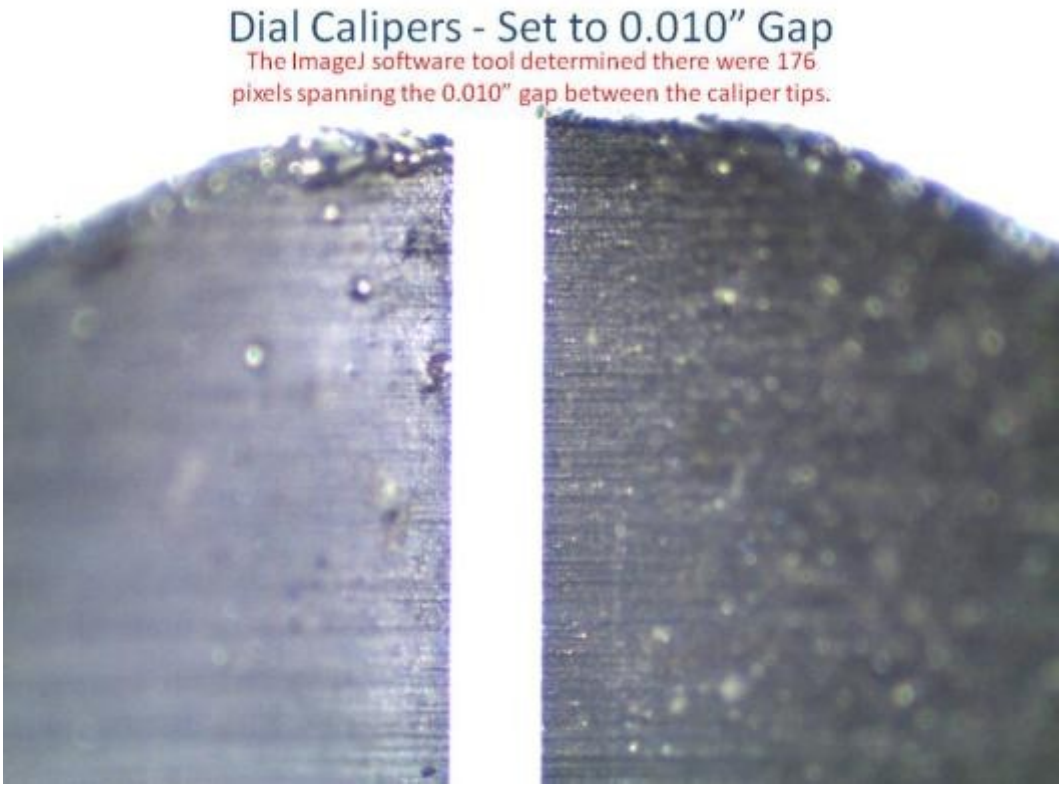

Measurements Using ImageJ Software – 176 Pixels = 0.010” – 1.44µm/pixel measurement resolution

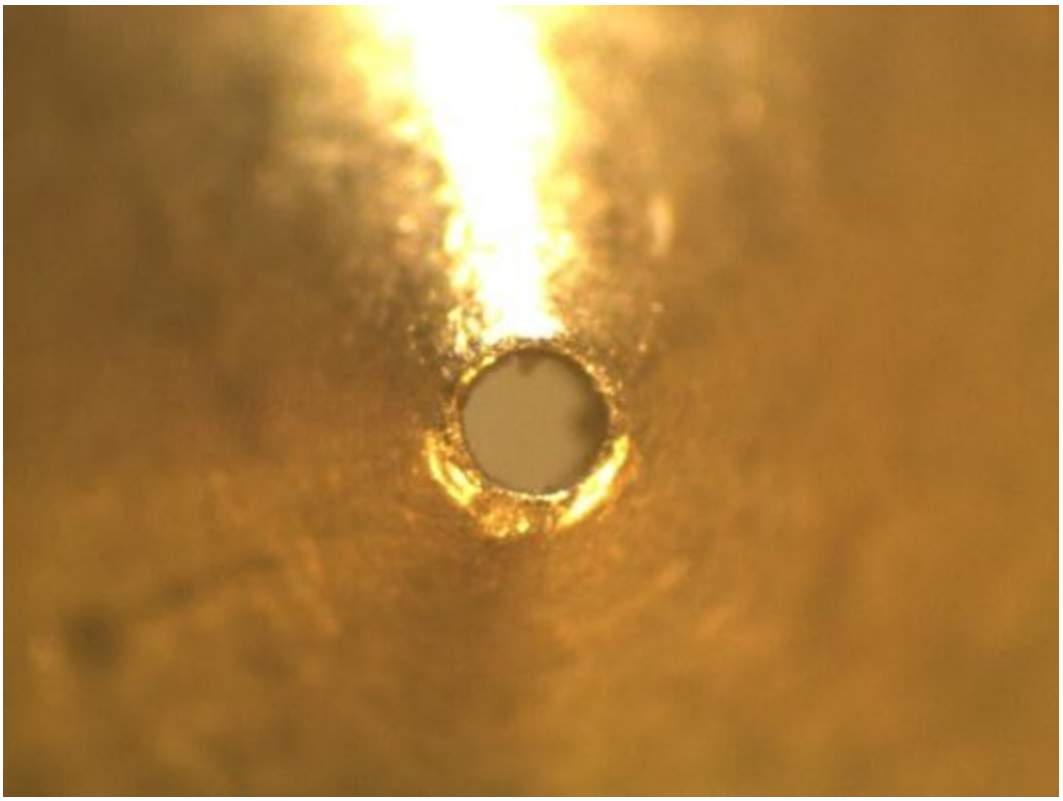

MakerBot Replicator Nozzle 1 – 400μm Nominal Bore – Raw Image @ 35x

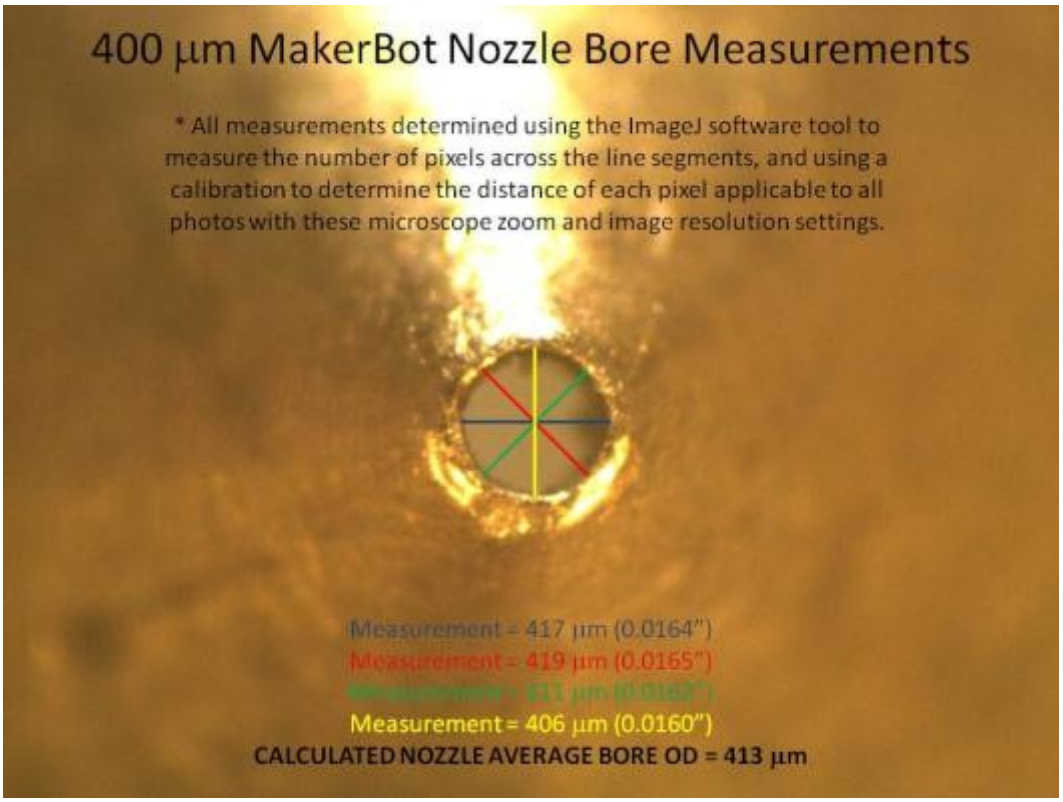

Measurements Using ImageJ Software – MakerBot Replicator Nozzle 1 – 400μm Nominal Bore

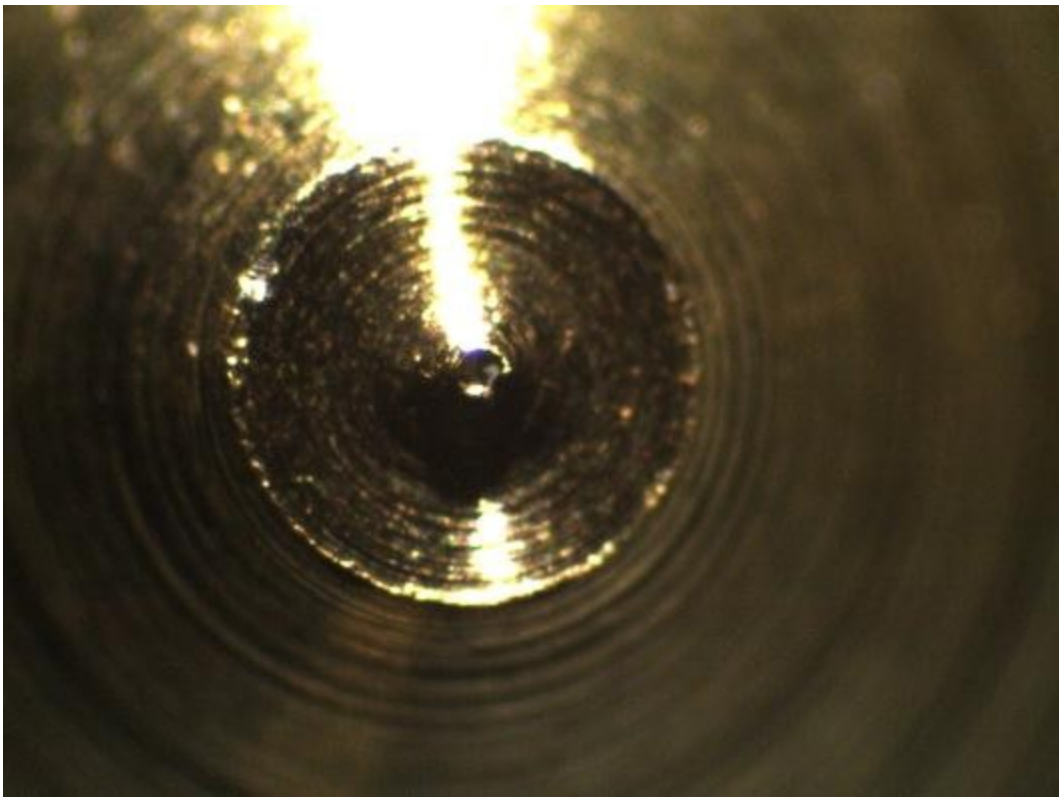

Custom 150µm Nominal Bore Nozzle # 1 – Raw Image @ 35x – Bad Nozzle, Not Used

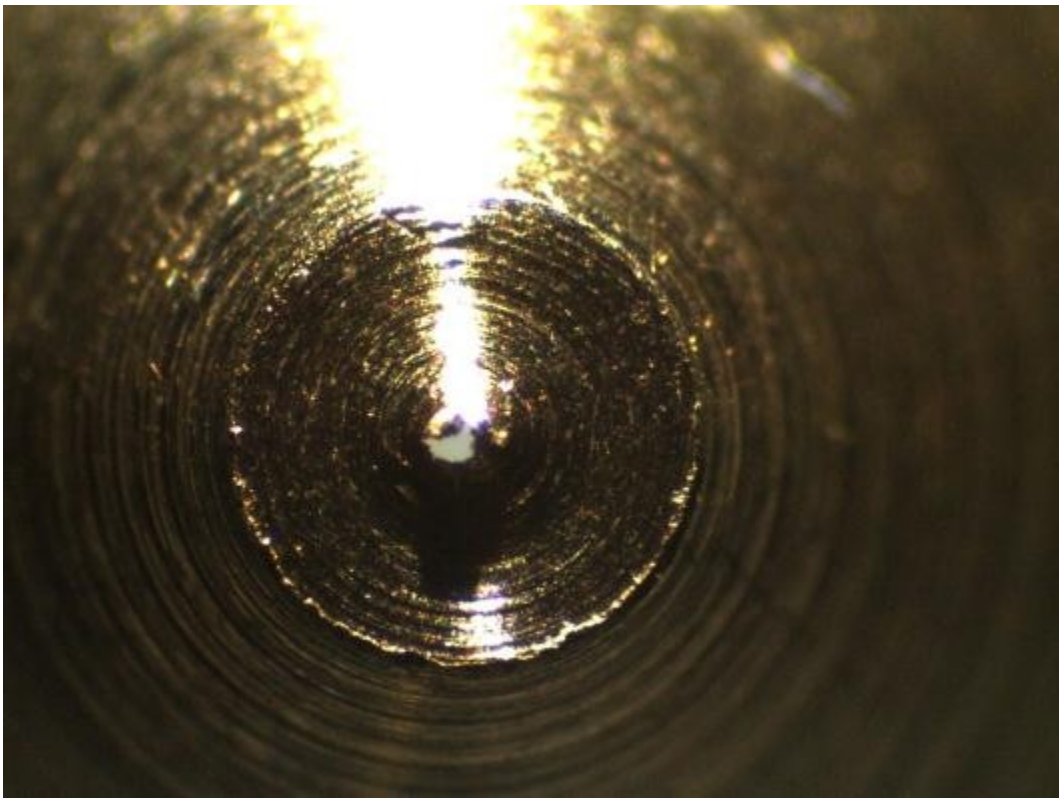

Custom 150µm Nominal Bore Nozzle # 2 – Raw Image @ 35x – Bad Nozzle, Not Used

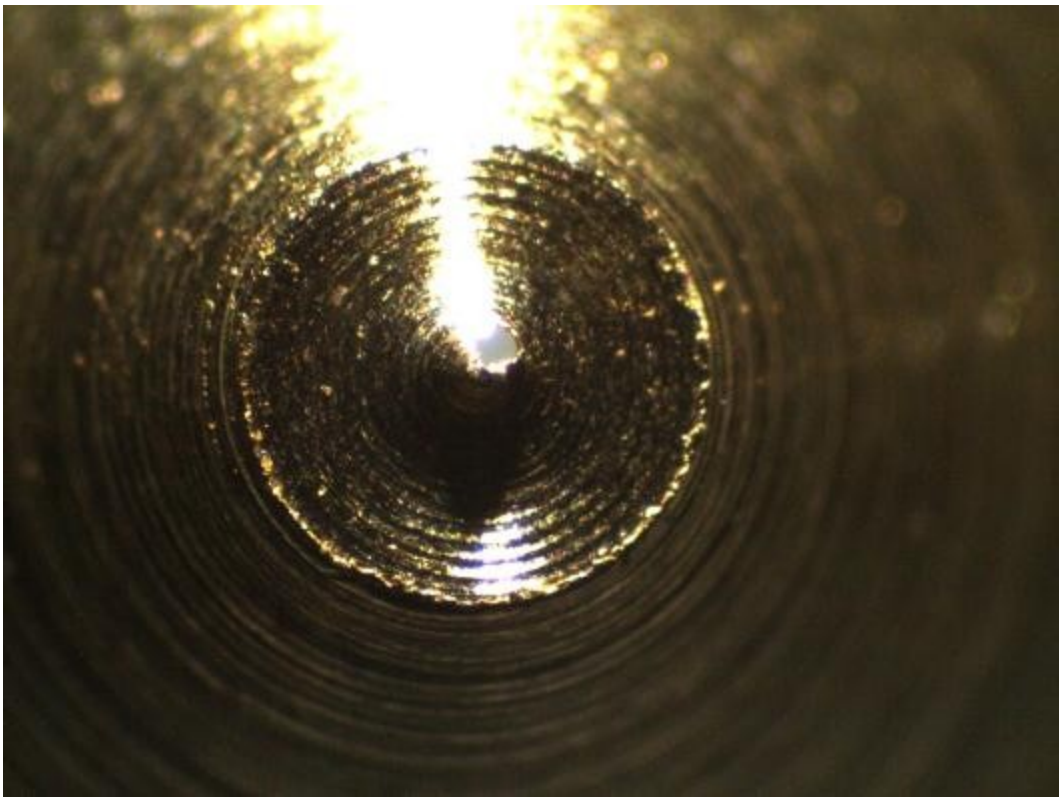

Custom 150µm Nominal Bore Nozzle # 3 – Raw Image @ 35x – Good Nozzle For Testing

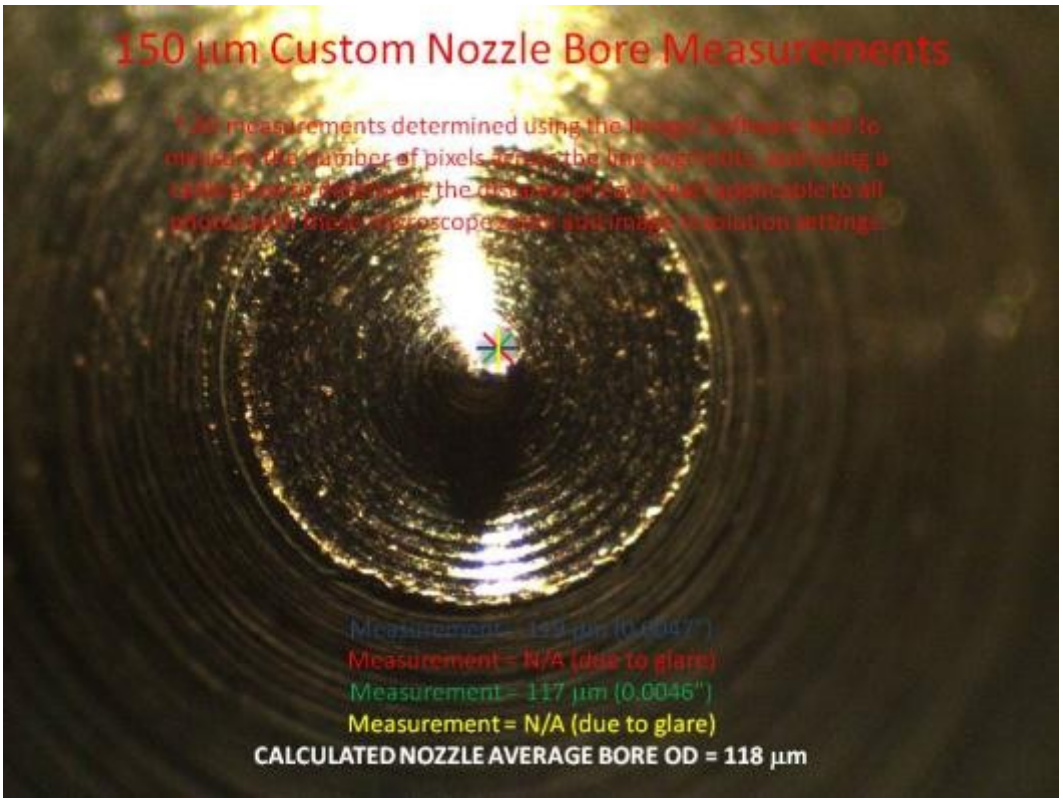

Measurements Using ImageJ Software – Custom 150µm Nominal Bore Nozzle # 3

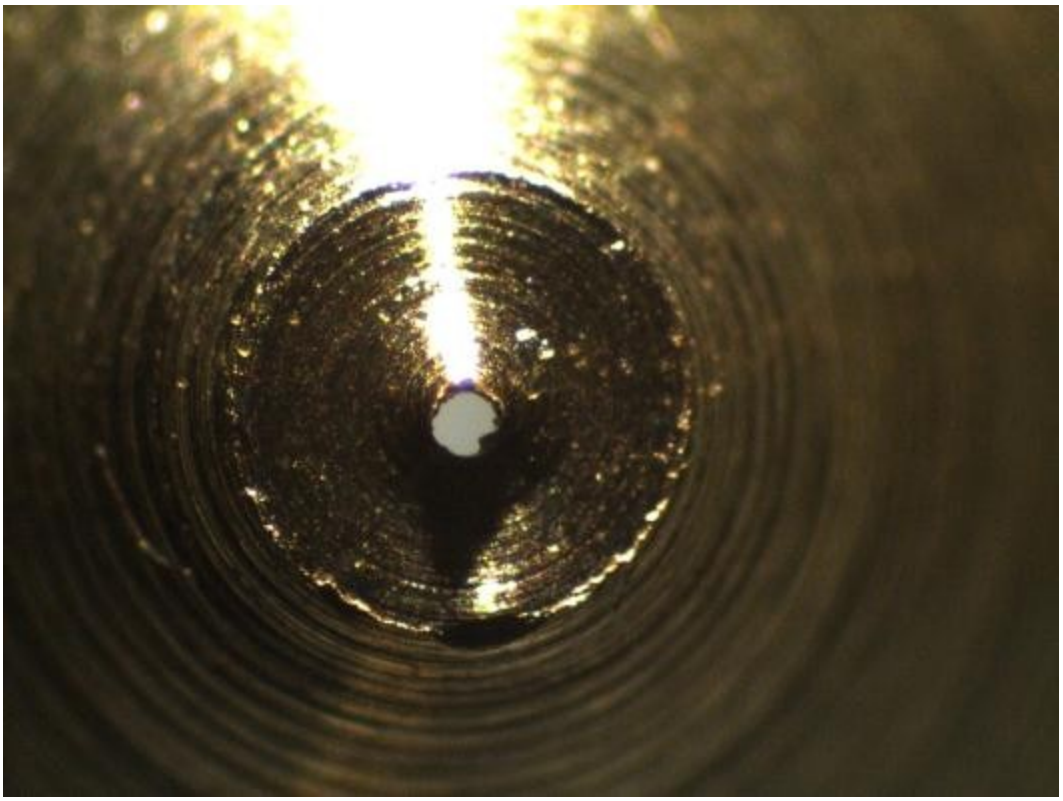

Custom 200µm Nominal Bore Nozzle # 1 – Raw Image @ 35x – Good Nozzle For Testing

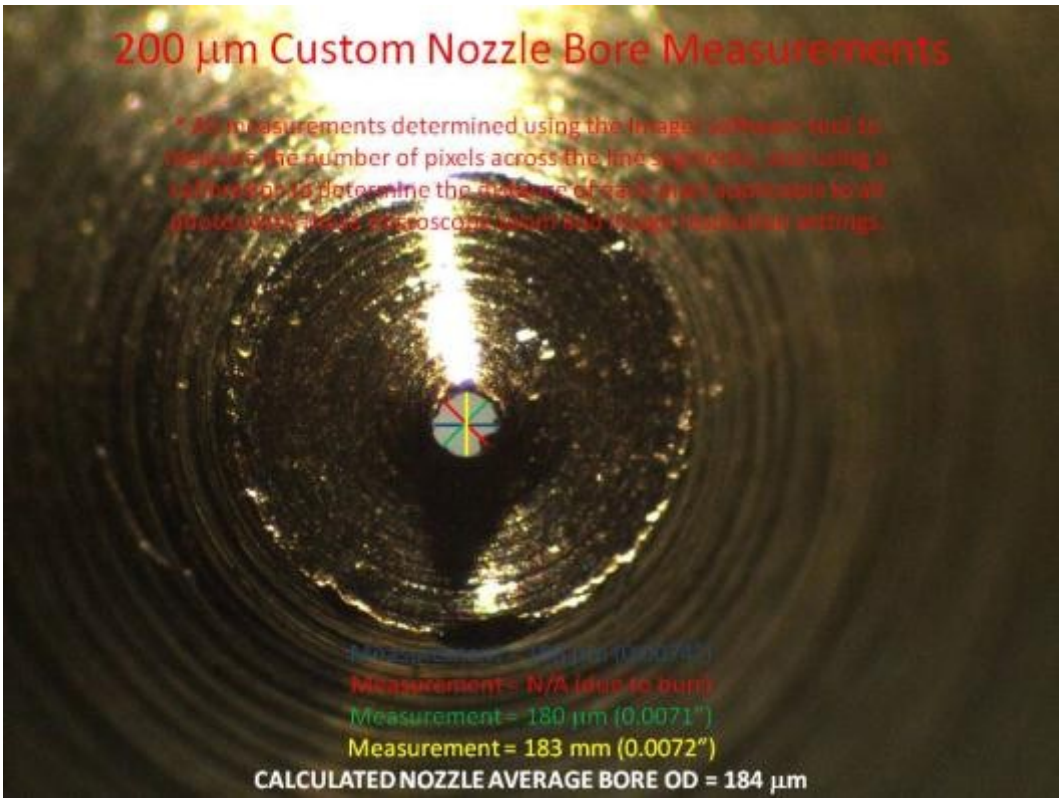

Measurements Using ImageJ Software – Custom 200µm Nominal Bore Nozzle # 1

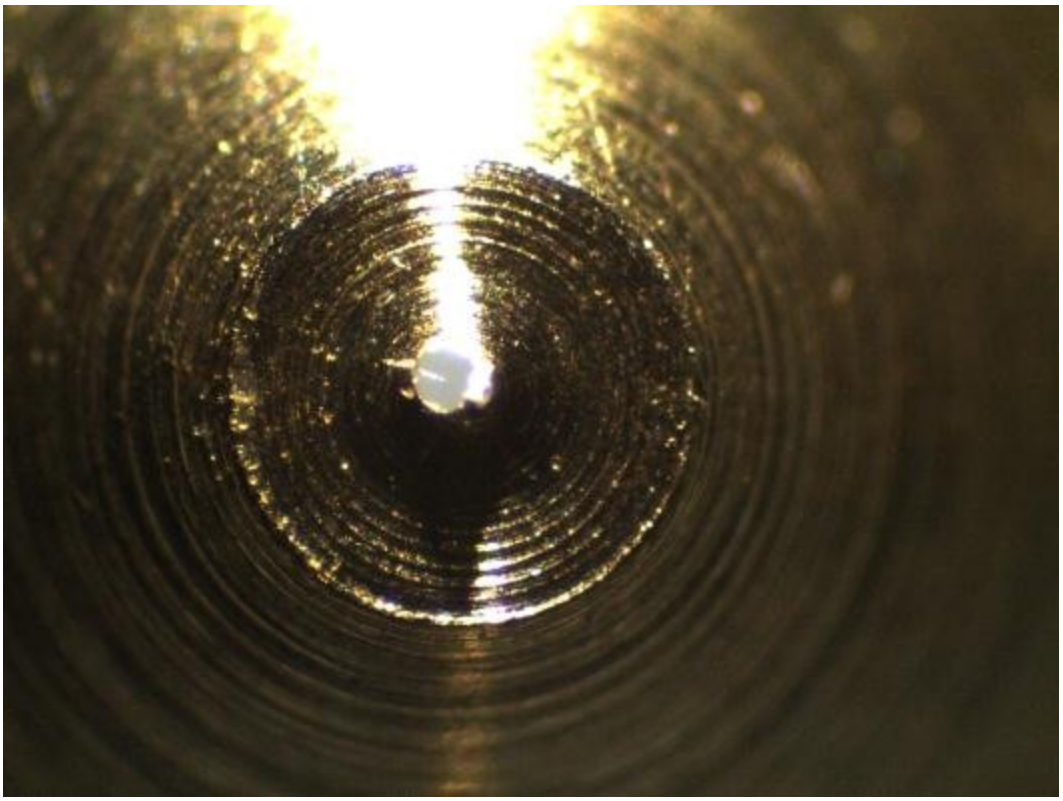

Custom 200µm Nominal Bore Nozzle # 2 – Raw Image @ 35x – Bad Nozzle, Not Used

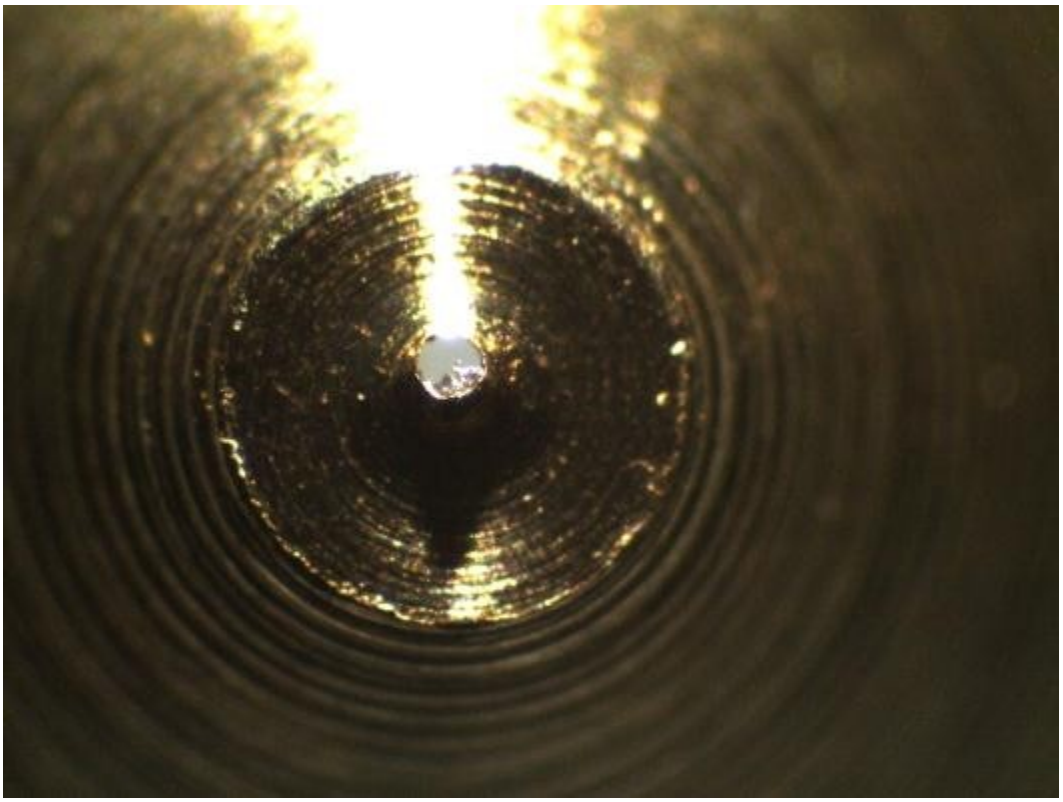

Custom 200µm Nominal Bore Nozzle # 3 – Raw Image @ 35x – Bad Nozzle, Not Used

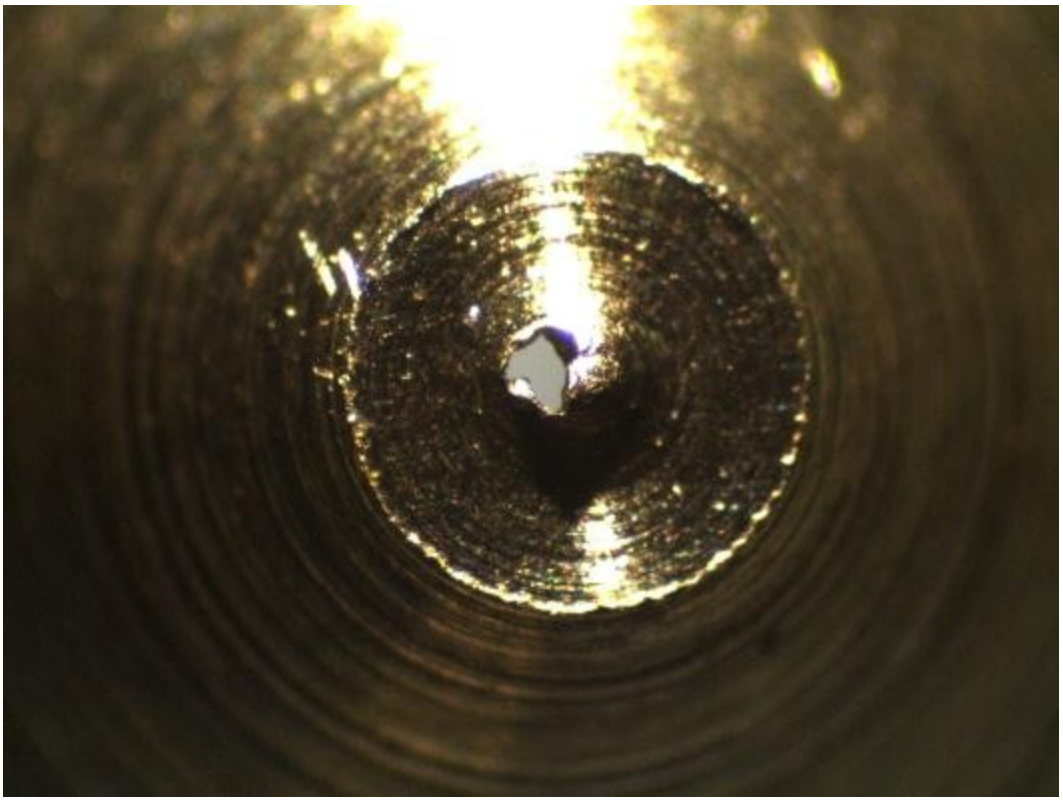

Custom 250µm Nominal Bore Nozzle # 1 – Raw Image @ 35x – Bad Nozzle, Not Used

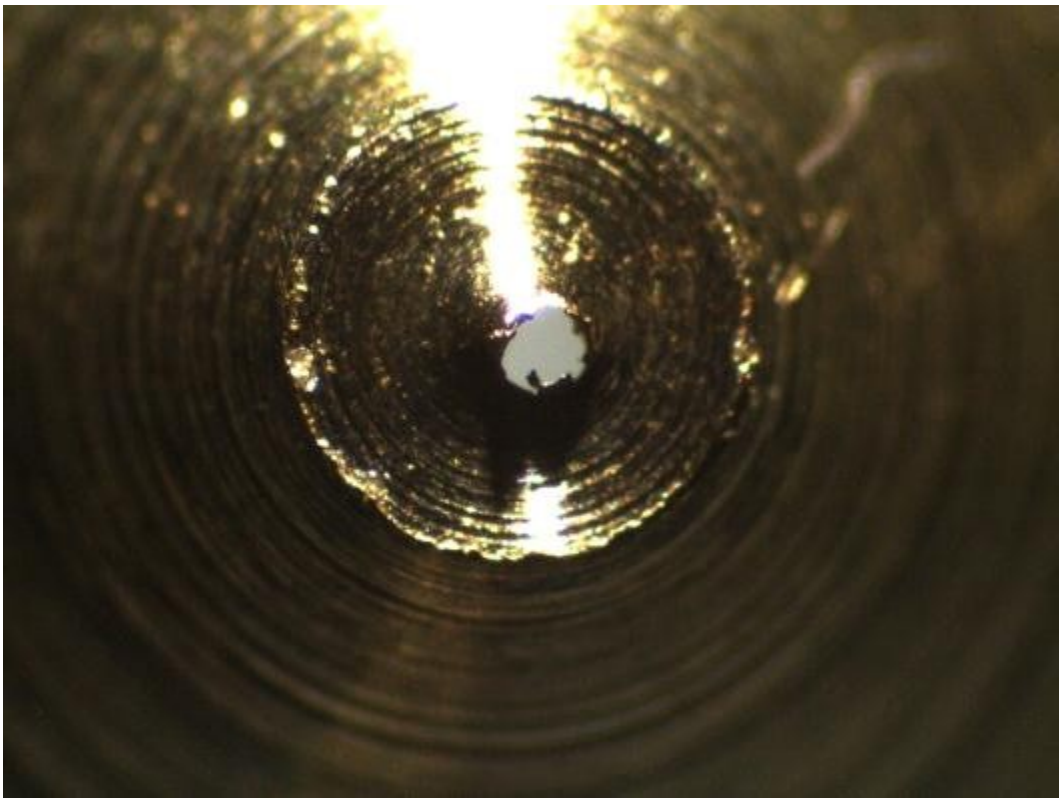

Custom 250µm Nominal Bore Nozzle # 2 – Raw Image @ 35x – Bad Nozzle, Not Used

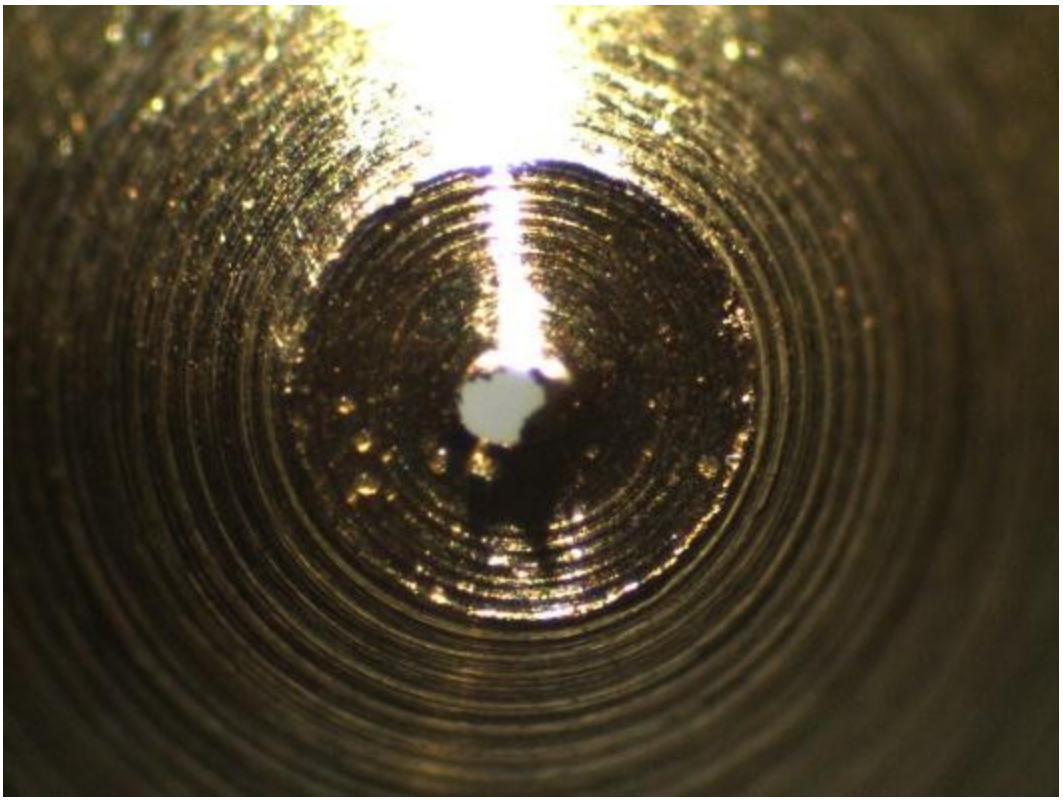

Custom 250µm Nominal Bore Nozzle # 3 – Raw Image @ 35x – Bad Nozzle, Not Used

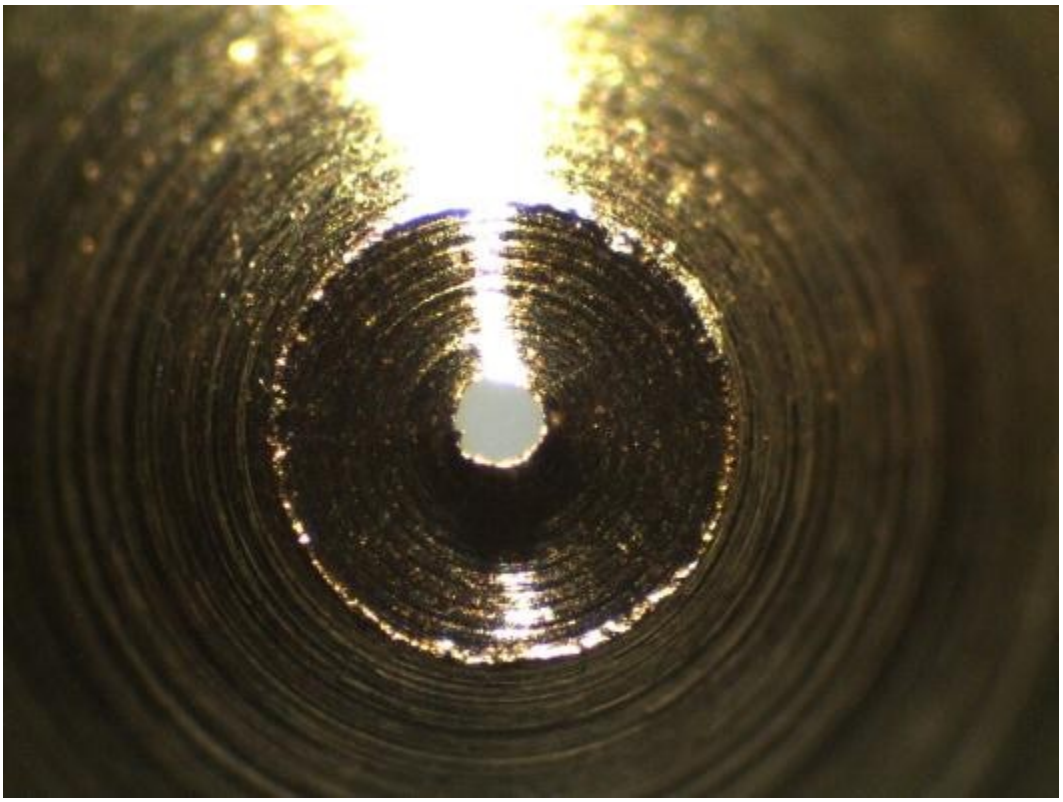

Custom 250µm Nominal Bore Nozzle # 4 – Raw Image @ 35x – Good Nozzle For Testing

Measurements Using ImageJ Software – Custom 250µm Nominal Bore Nozzle # 4

Custom 300µm Nominal Bore Nozzle # 1 – Raw Image @ 35x – Bad Nozzle, Not Used

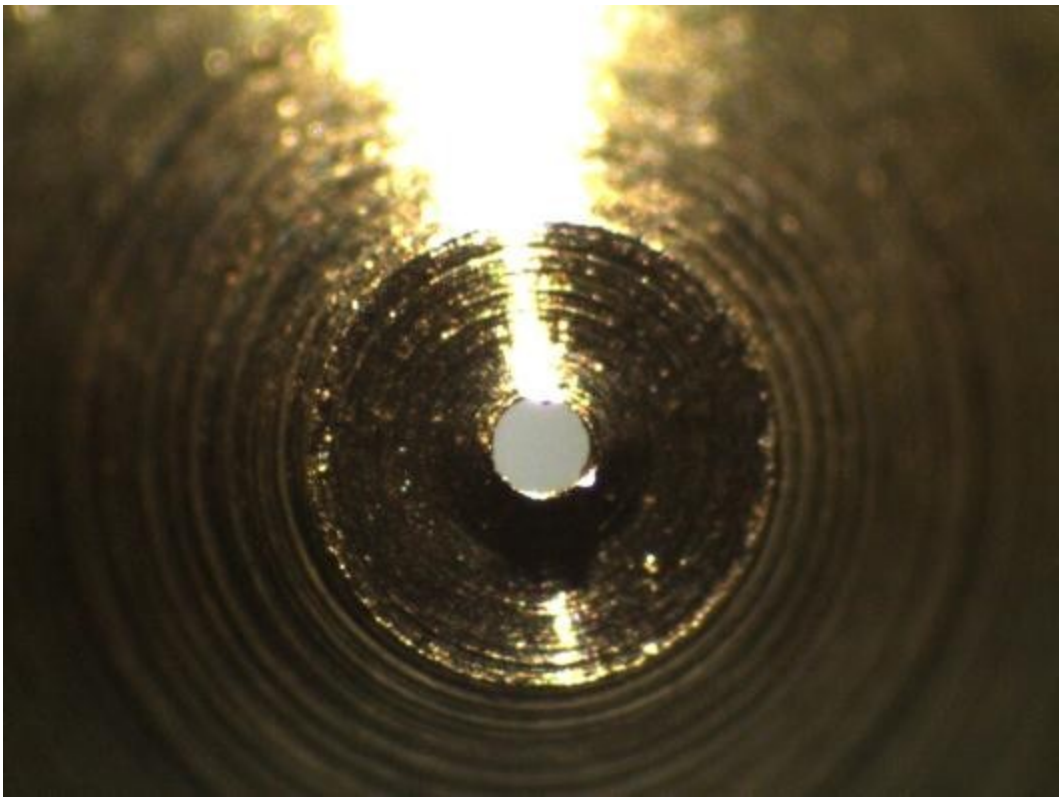

Custom 300µm Nominal Bore Nozzle # 2 – Raw Image @ 35x – Good Nozzle For Testing

Measurements Using ImageJ Software – Custom 300µm Nominal Bore Nozzle # 2

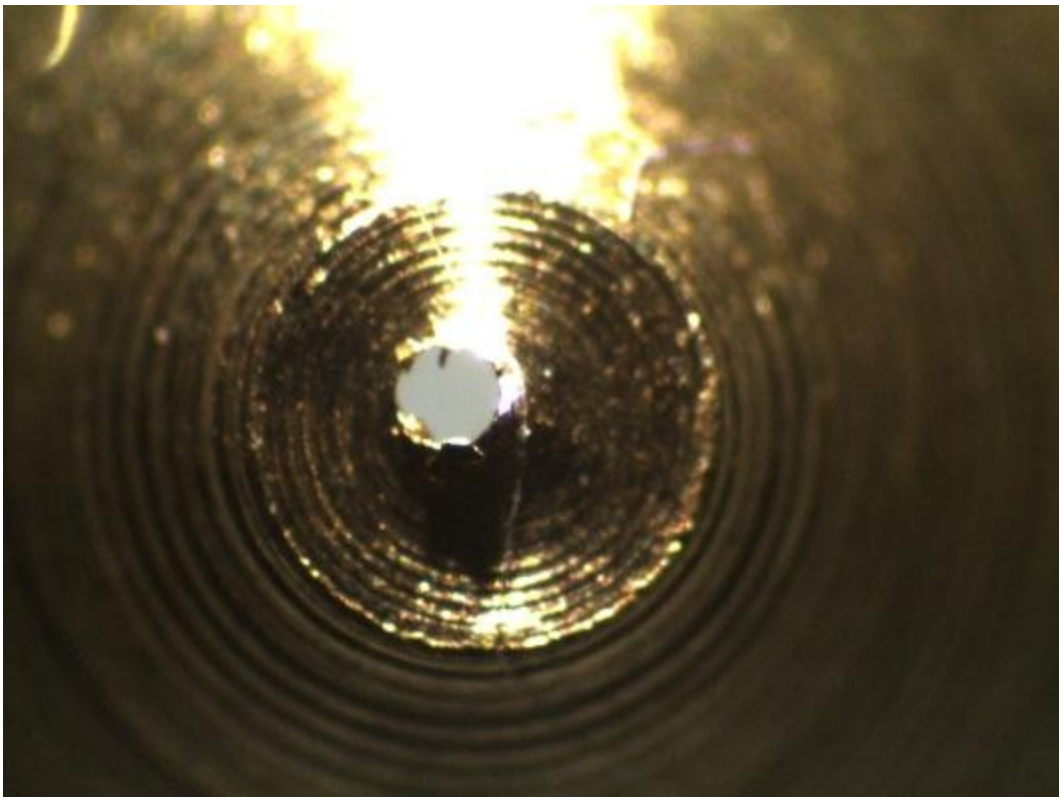

Custom 300μm Nominal Bore Nozzle # 3 – Raw Image @ 35x – Bad Nozzle, Not Used

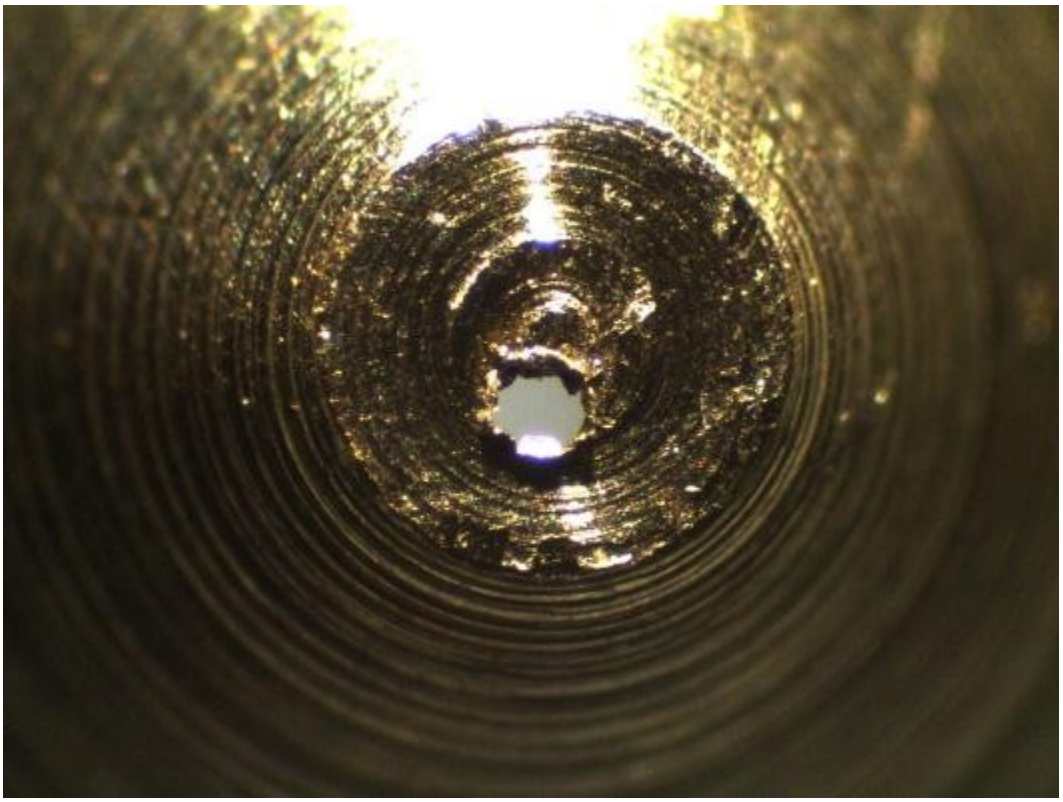

Custom 300μm Nominal Bore Nozzle # 4 – Raw Image @ 35x – Bad Nozzle, Not Used

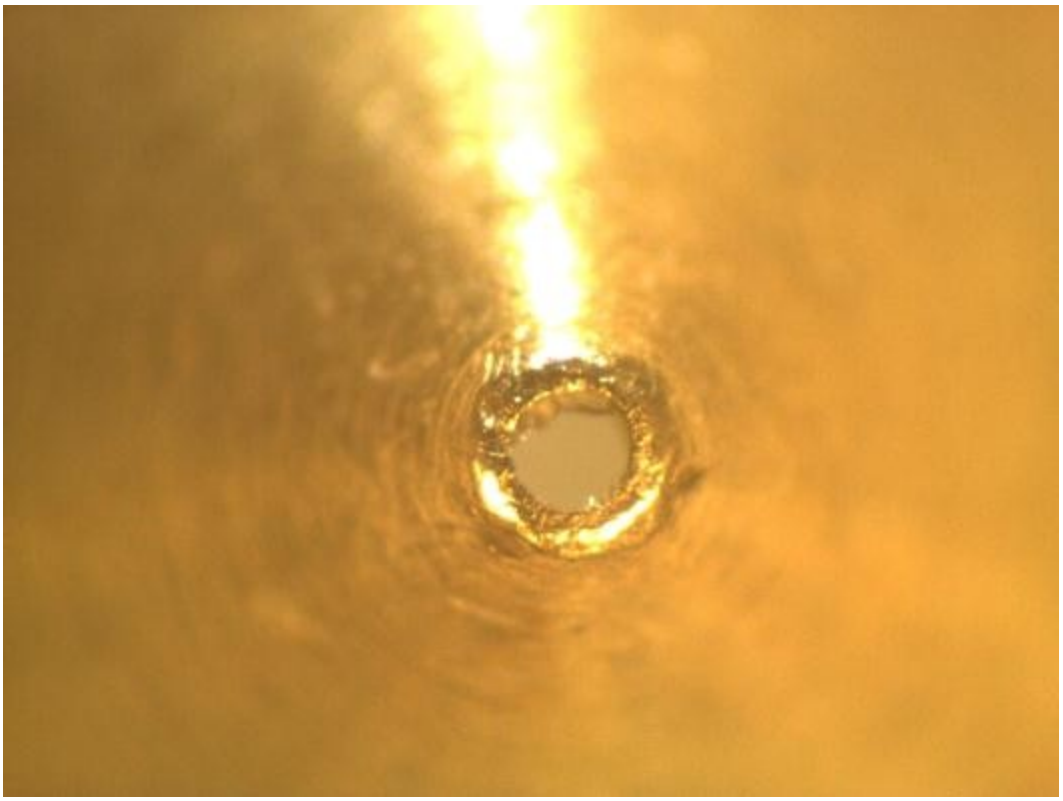

QU-BD MakerBot Compatible 350µm Nominal Bore Nozzle # 1 – Raw Image @ 35x – Not Used

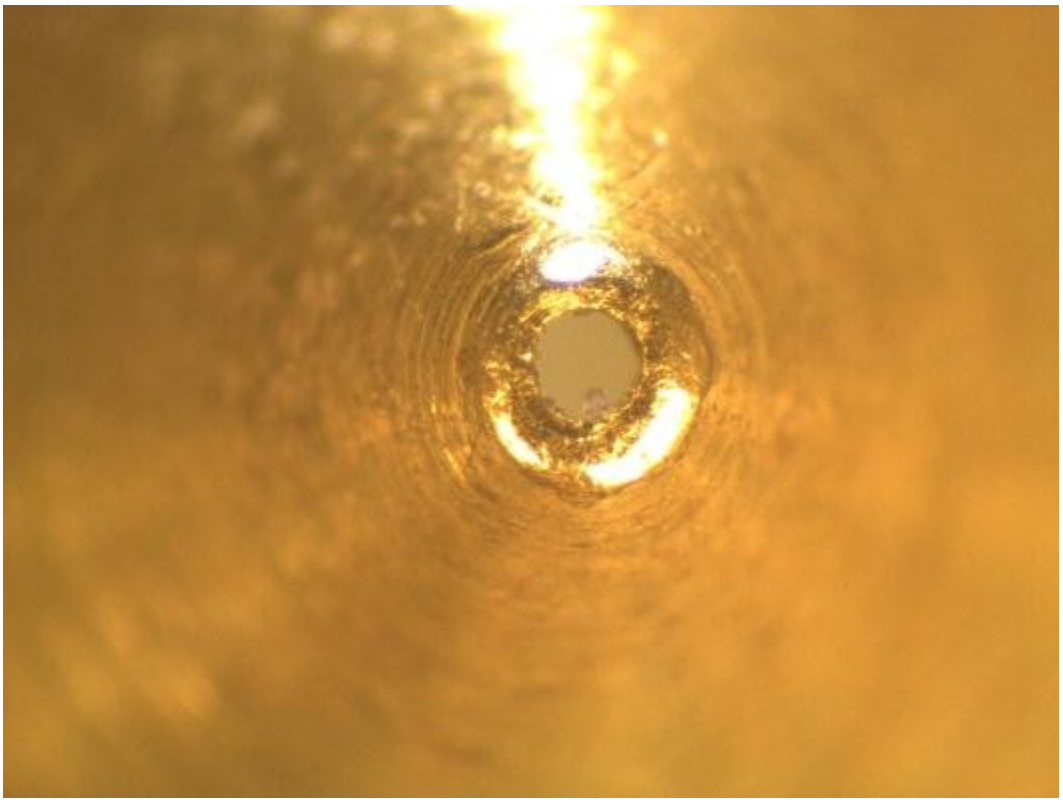

QU-BD MakerBot Compatible 350µm Nominal Bore Nozzle # 2 – Raw Image @ 35x – Not Used

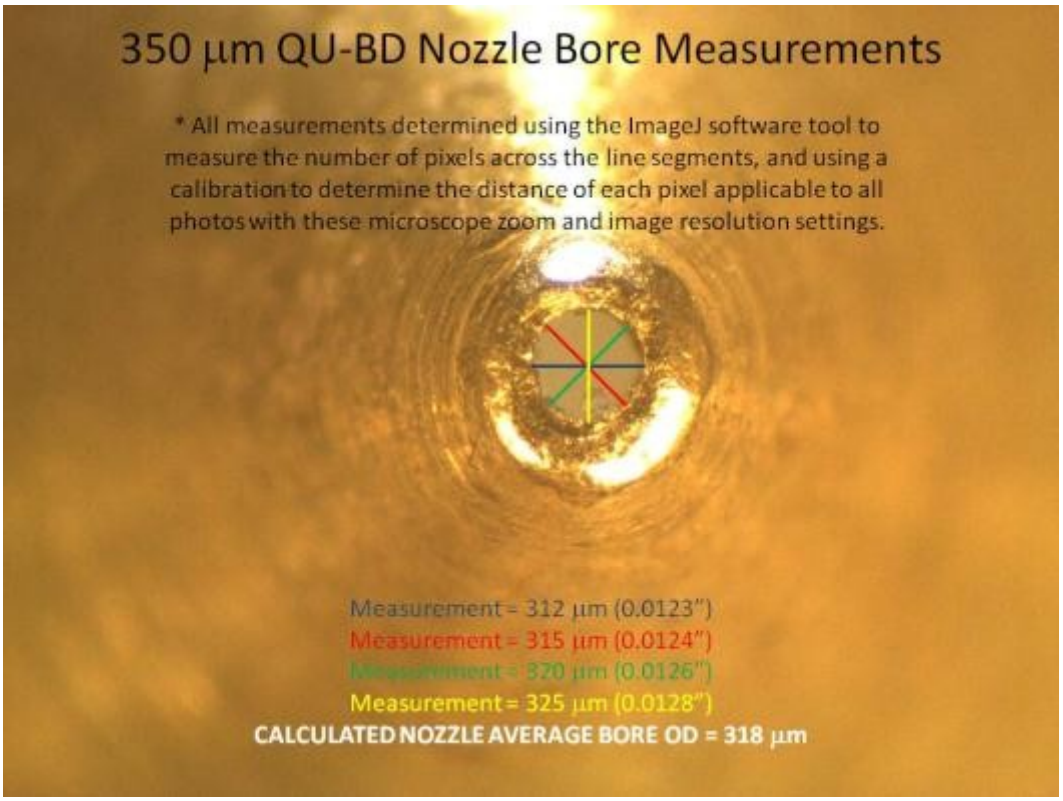

Measurements Using ImageJ Software – QU-BD MakerBot Compatible 350µm Nominal Bore Nozzle # 2

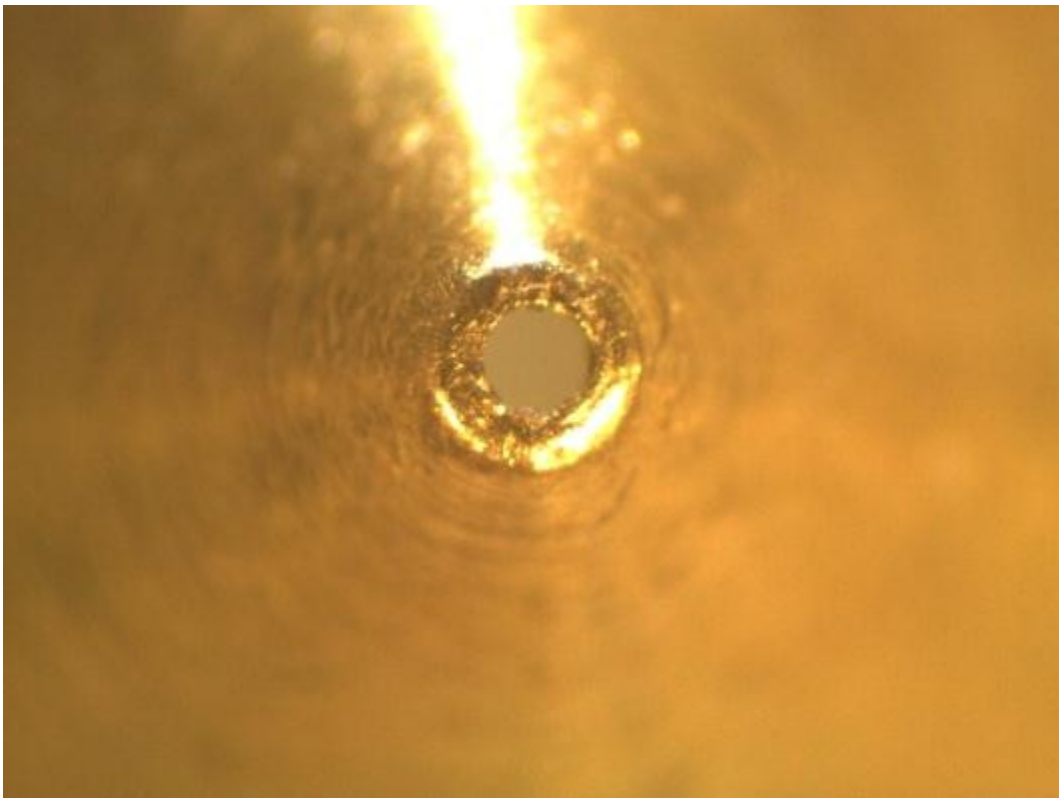

QU-BD MakerBot Compatible 350µm Nominal Bore Nozzle # 3 – Raw Image @ 35x – Not Used

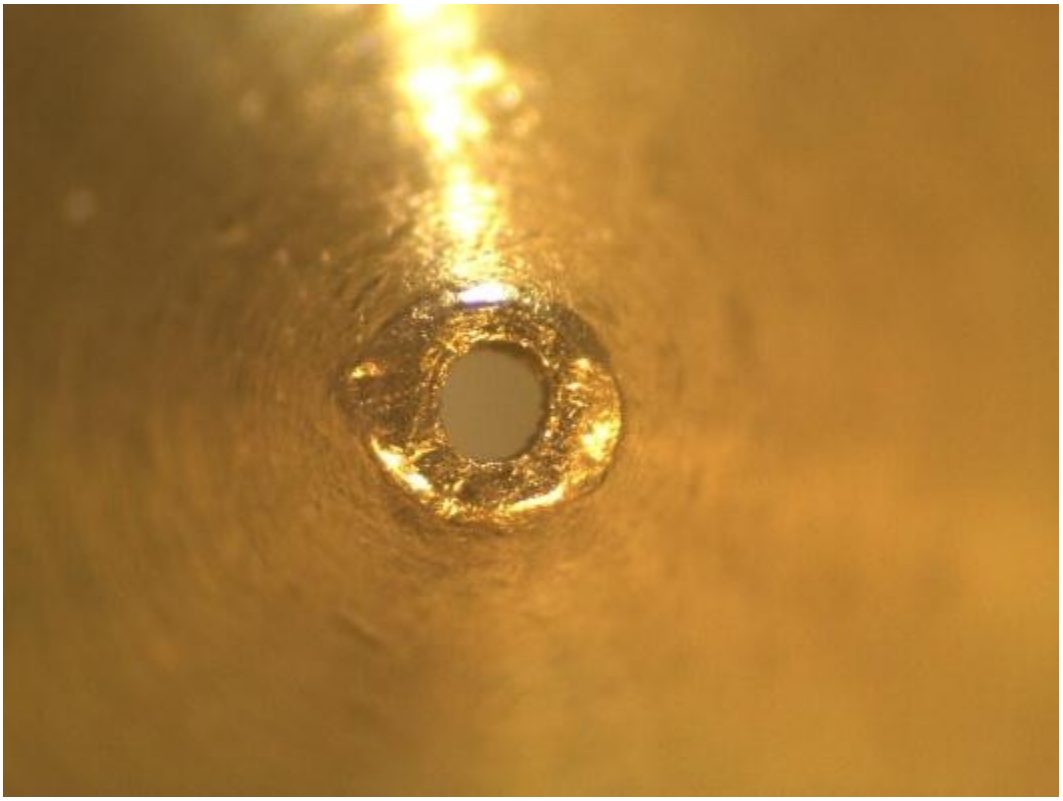

QU-BD MakerBot Compatible 350μm Nominal Bore Nozzle # 4 – Raw Image @ 35x – Not Used

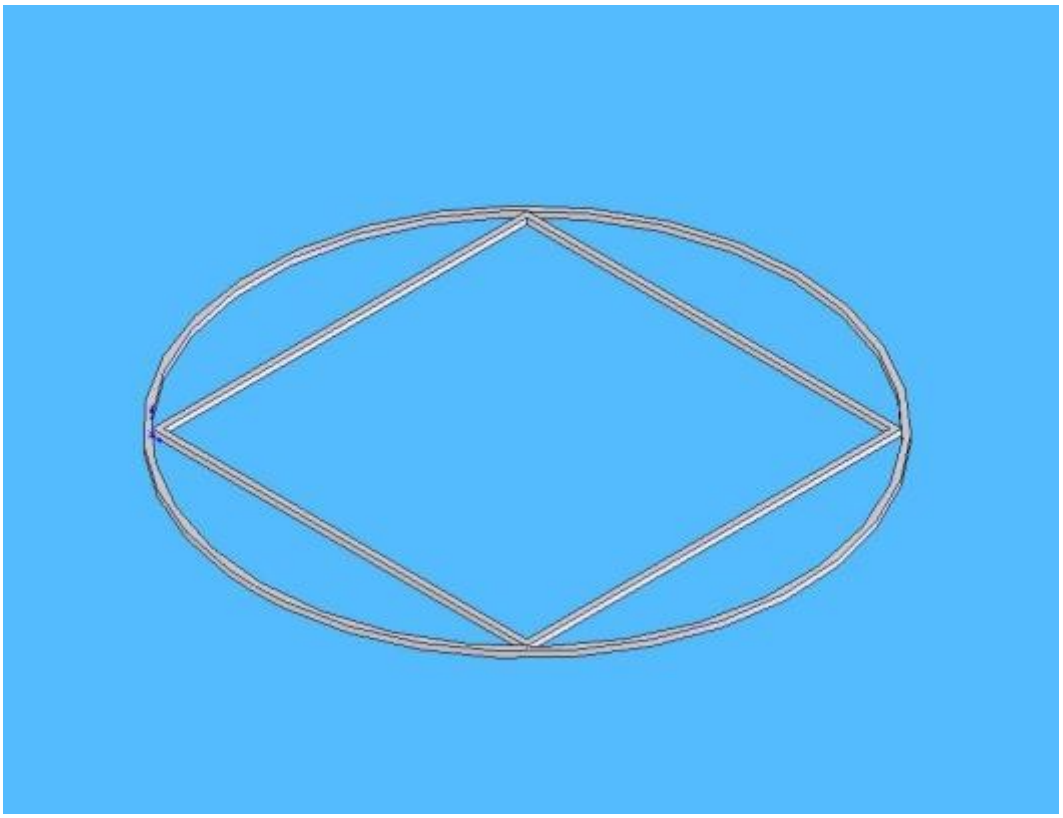

Image of SolidWorks CAD Part – Circle Square Test Pattern – 400μm Size Nozzle Test

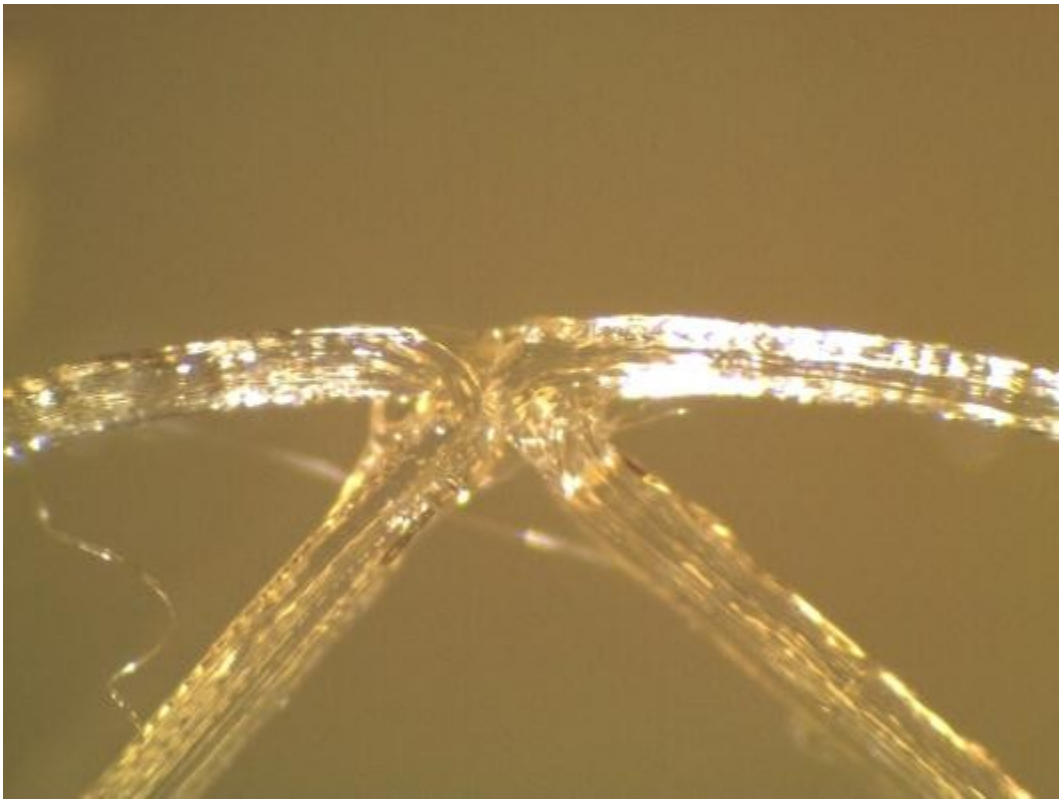

Circle Square Test Print – 150µm Nozzle - No Stretch – Raw Image @ 35x

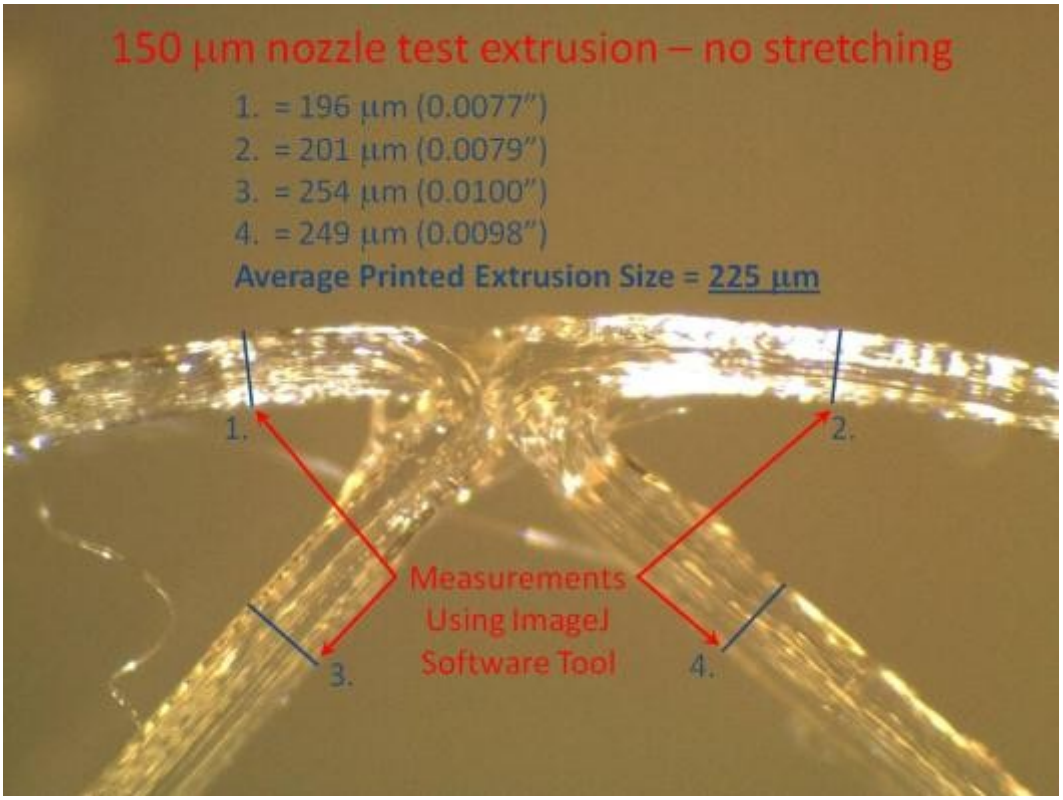

Measurements Using ImageJ Software - Circle Square Test Print – 150µm Nozzle - No Stretch

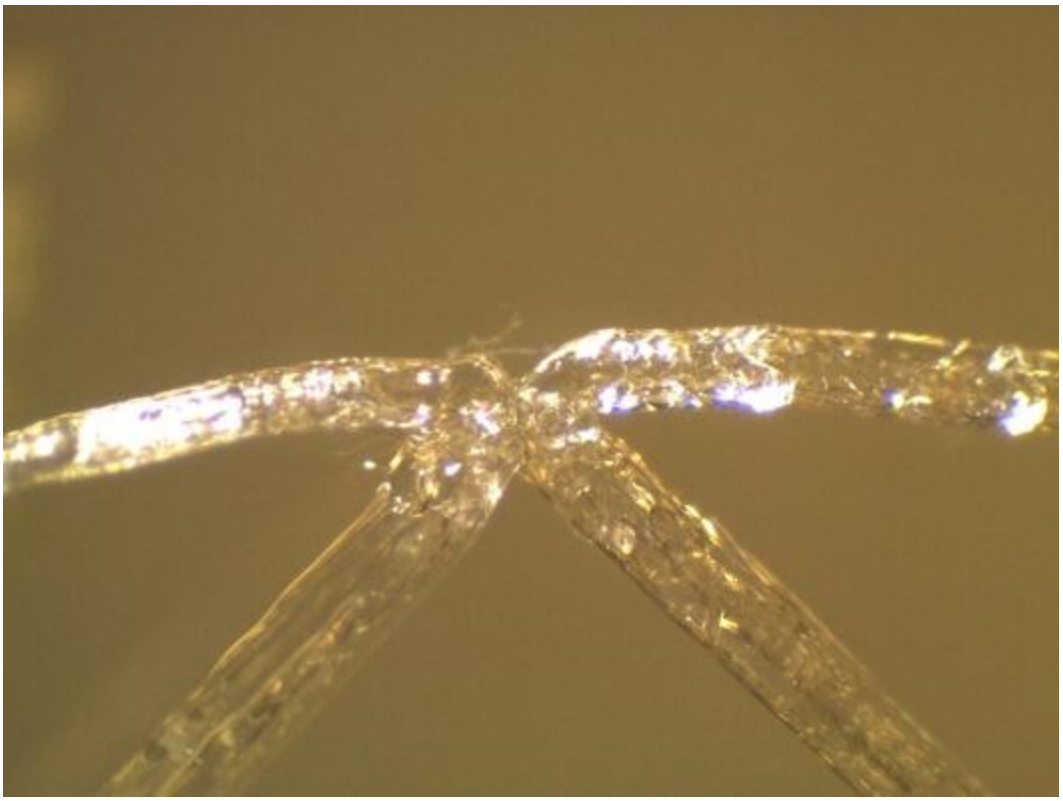

Circle Square Test Print – 150µm Nozzle - Stretched – Raw Image @ 35x

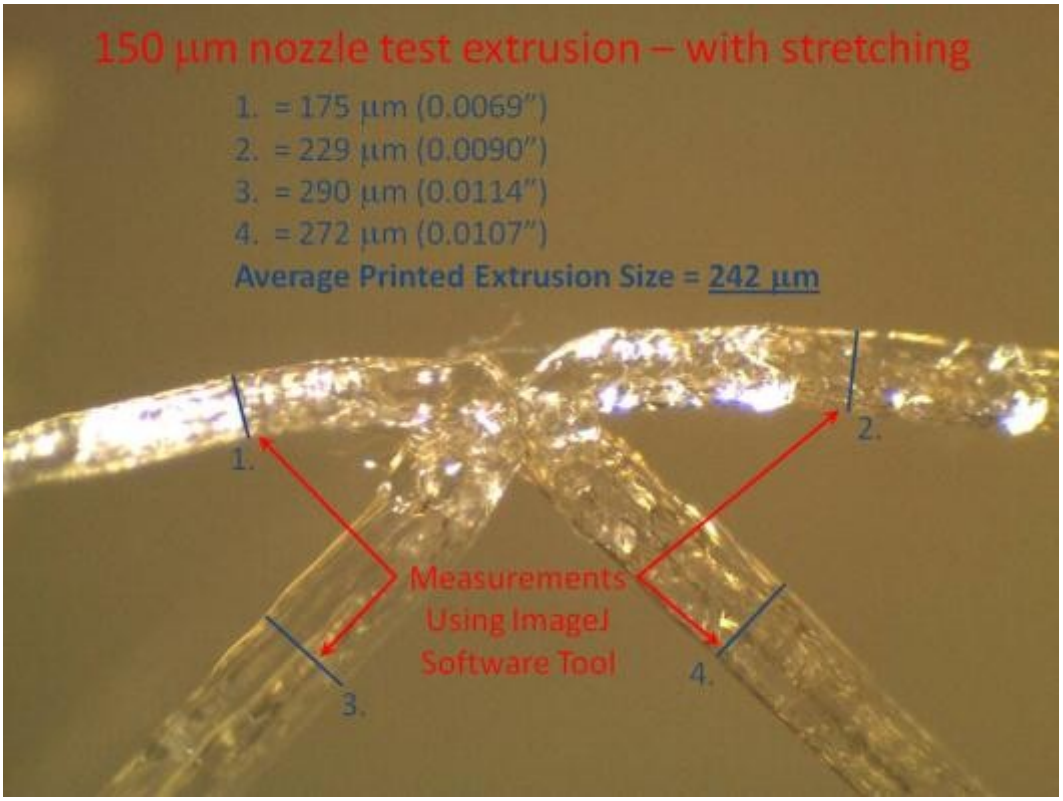

Measurements Using ImageJ Software - Circle Square Test Print – 150µm Nozzle – Stretched

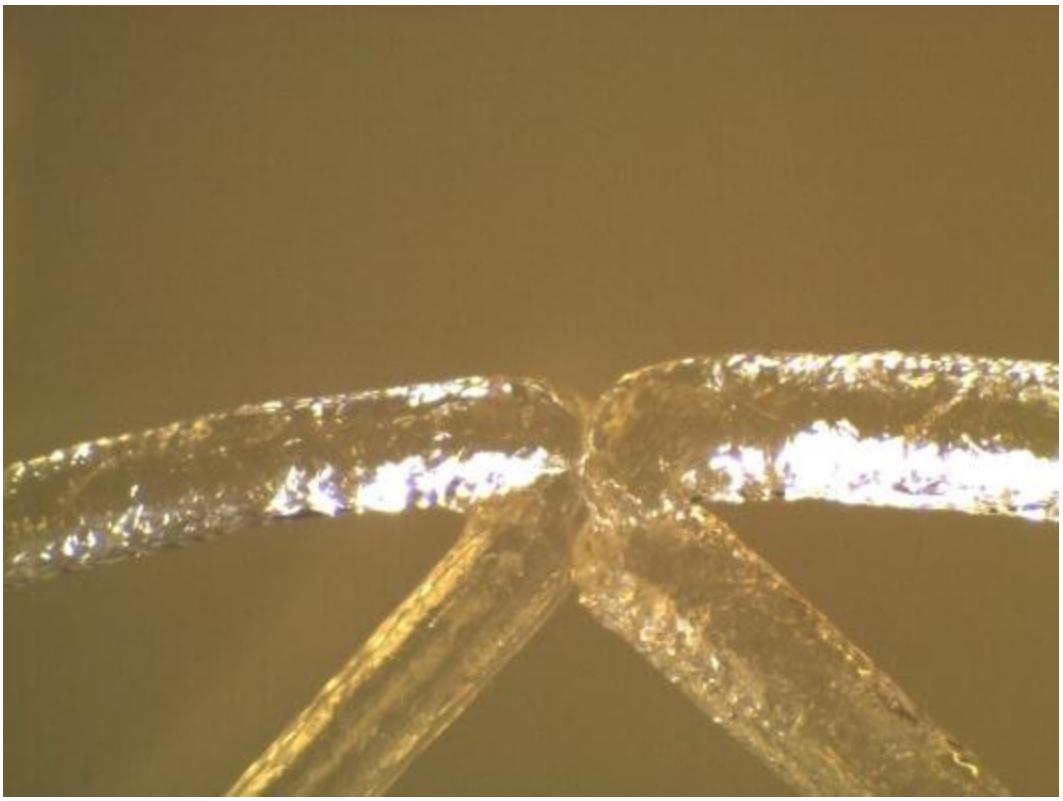

Circle Square Test Print – 200µm Nozzle - No Stretch – Raw Image @ 35x

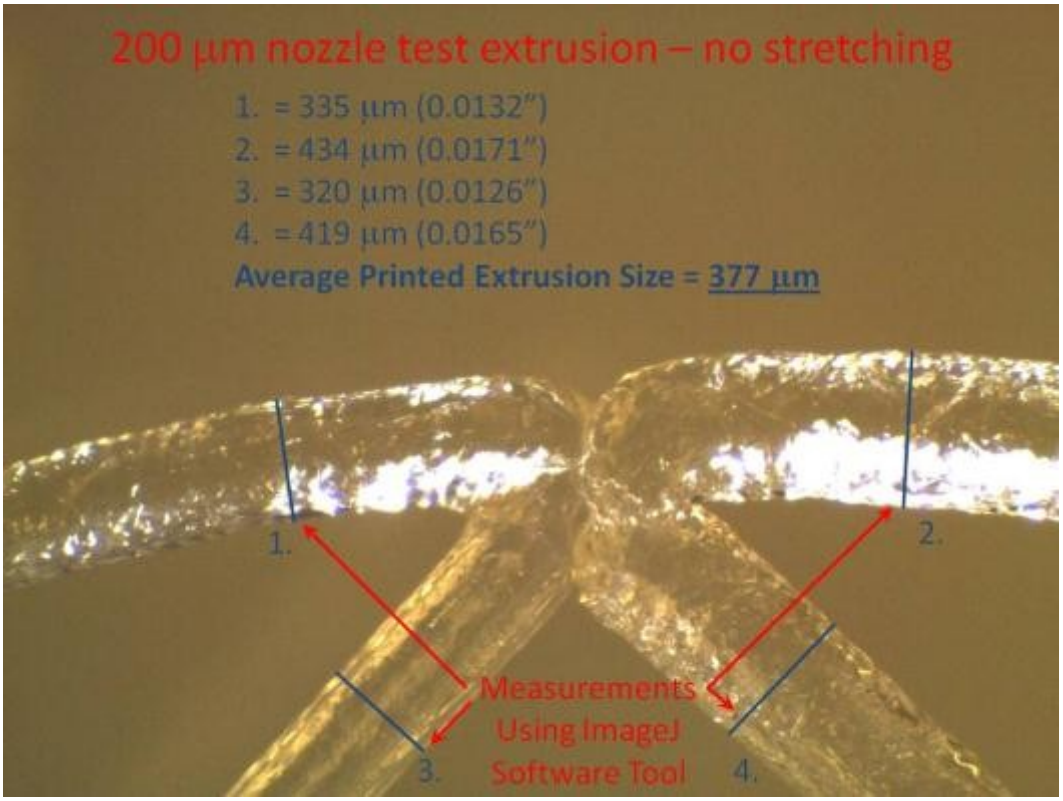

Measurements Using ImageJ Software - Circle Square Test Print – 200µm Nozzle - No Stretch

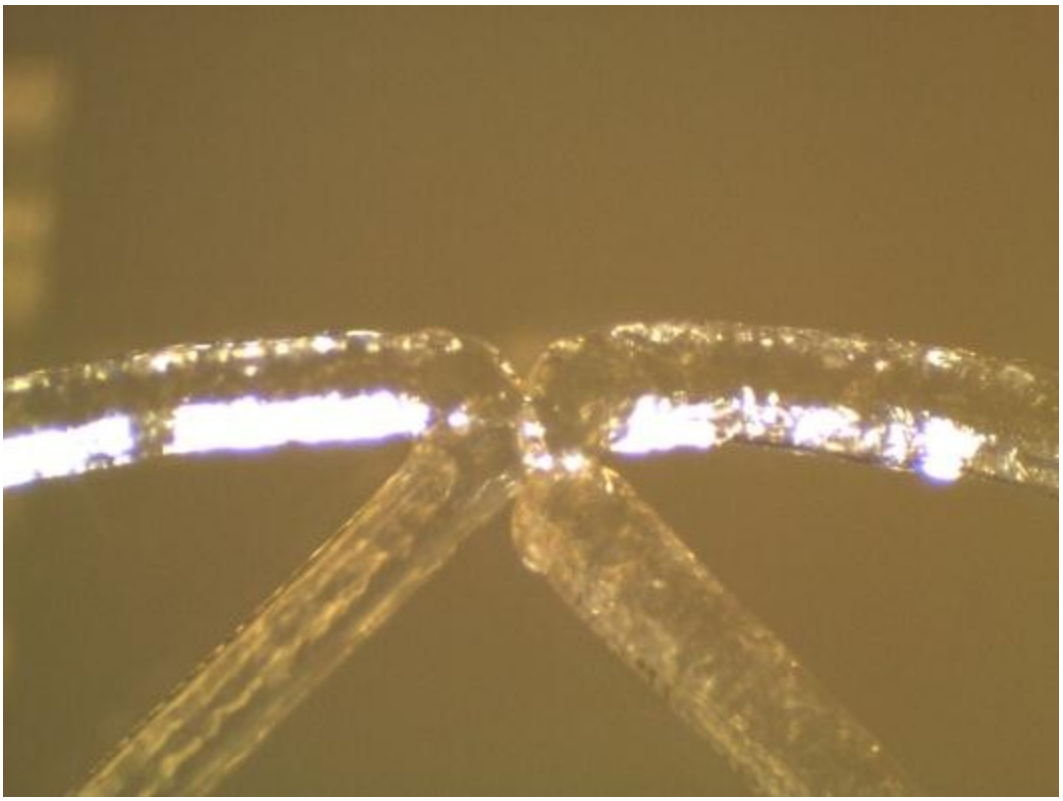

Circle Square Test Print – 200μm Nozzle - Stretched – Raw Image @ 35x

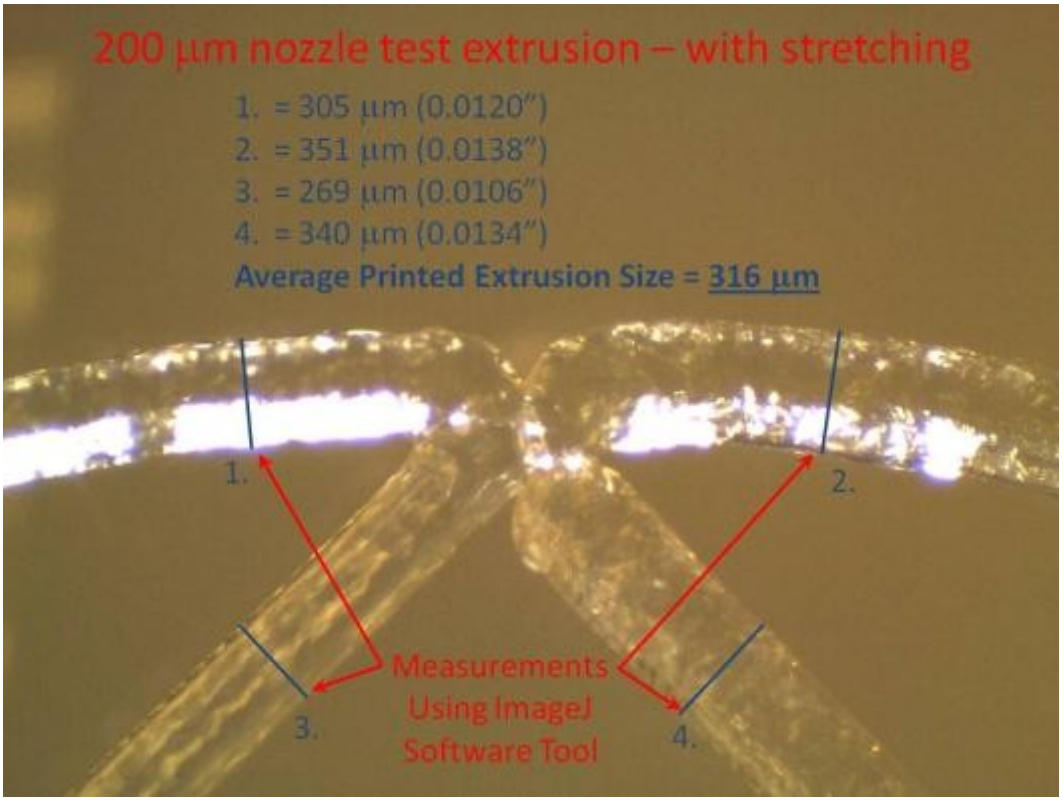

Measurements Using ImageJ Software - Circle Square Test Print – 200μm Nozzle – Stretched

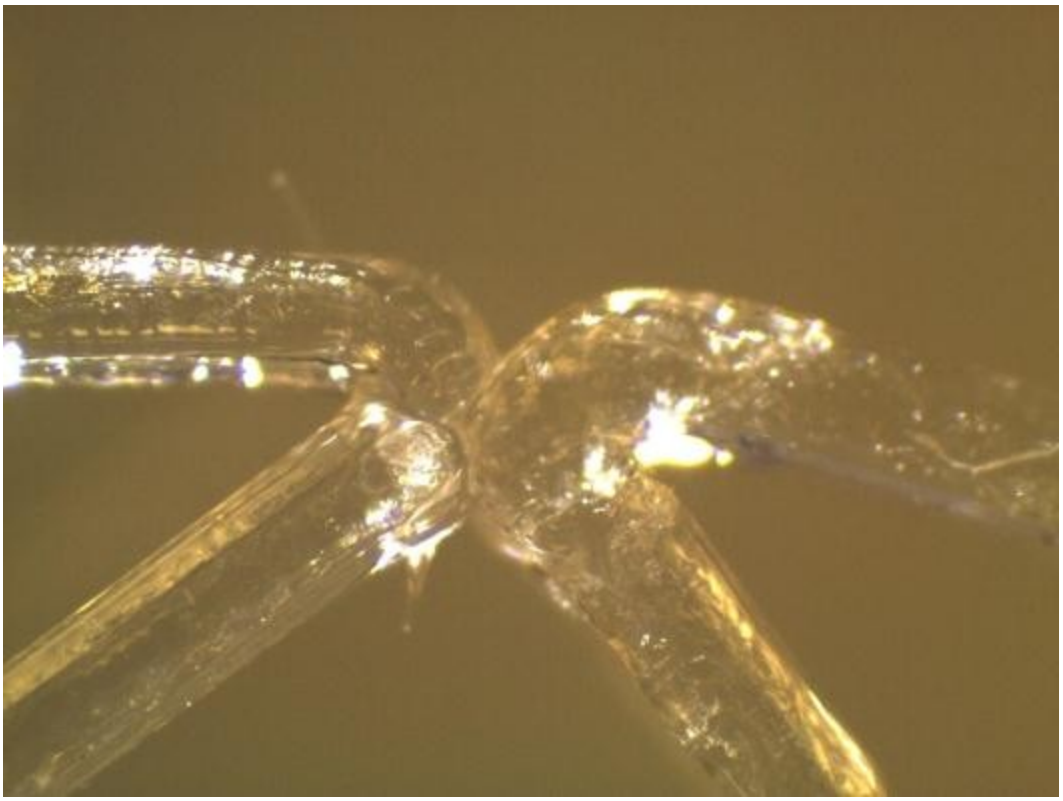

Circle Square Test Print – 250µm Nozzle - No Stretch – Raw Image @ 35x

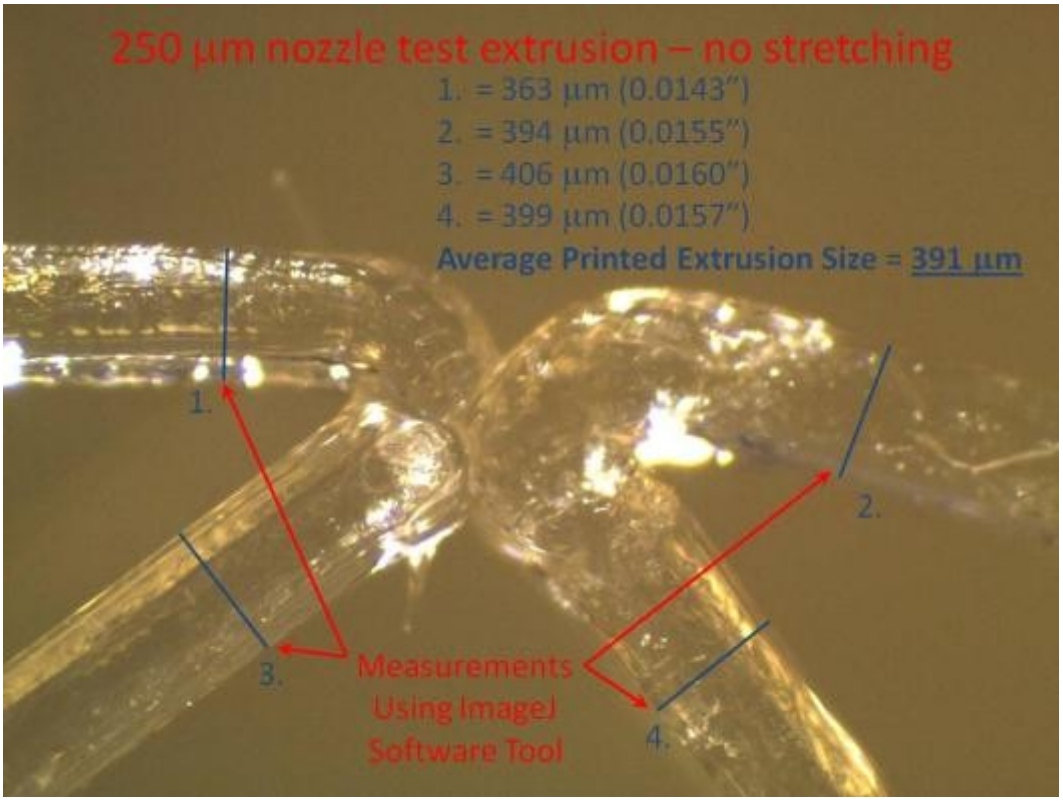

Measurements Using ImageJ Software - Circle Square Test Print – 250µm Nozzle - No Stretch

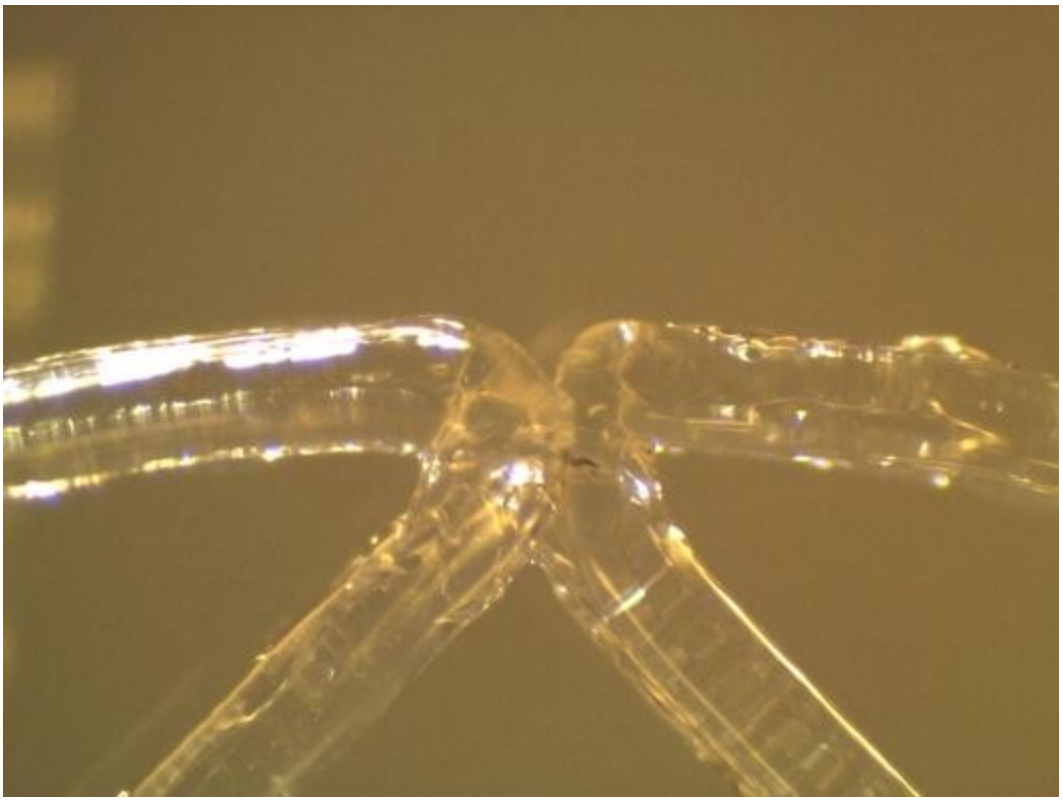

Circle Square Test Print – 250μm Nozzle - Stretched – Raw Image @ 35x

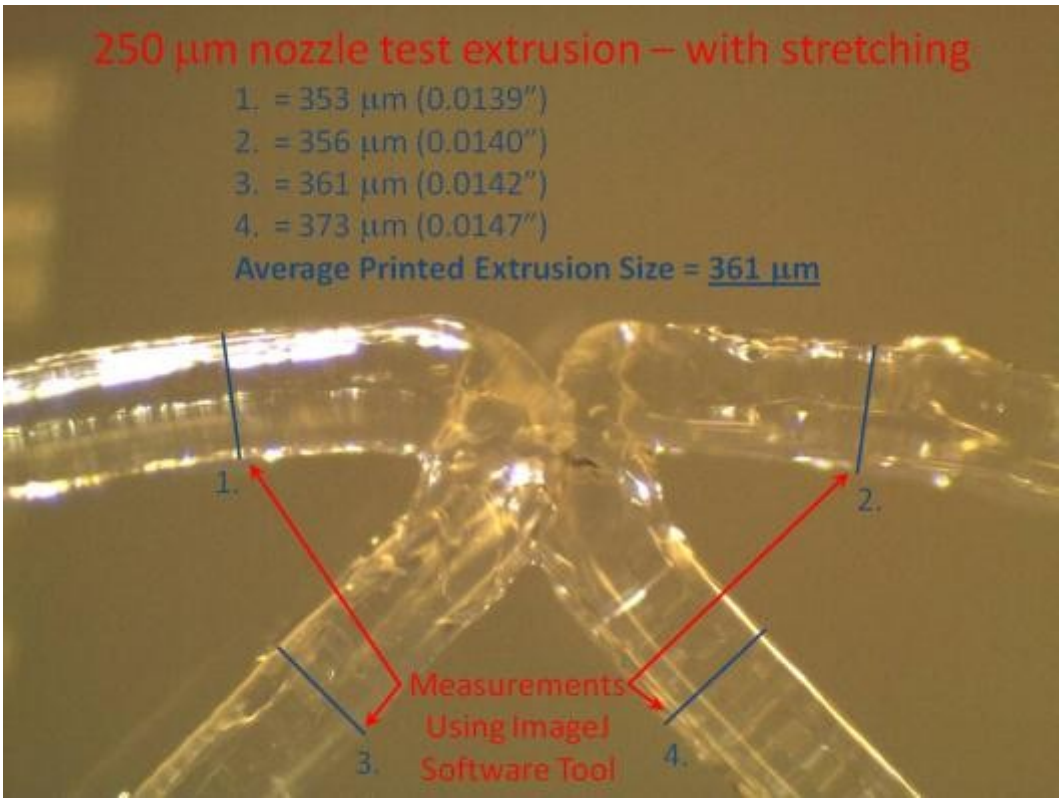

Measurements Using ImageJ Software - Circle Square Test Print – 250μm Nozzle – Stretched

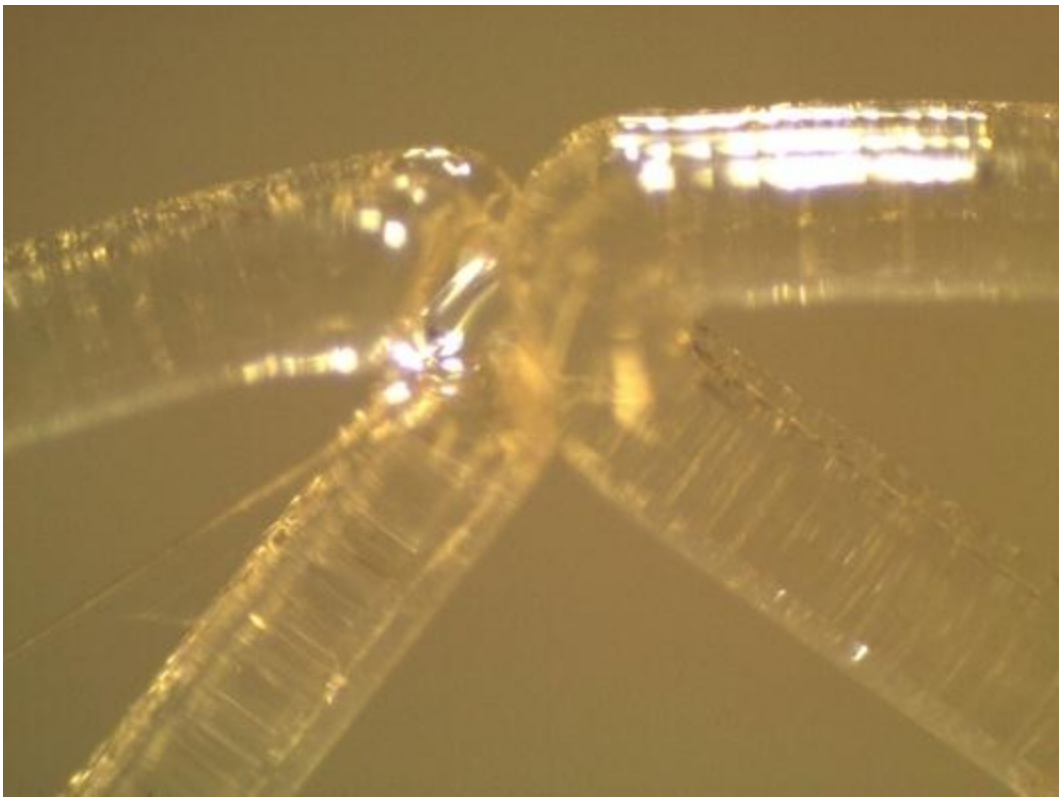

Circle Square Test Print – 300µm Nozzle - No Stretch – Raw Image @ 35x

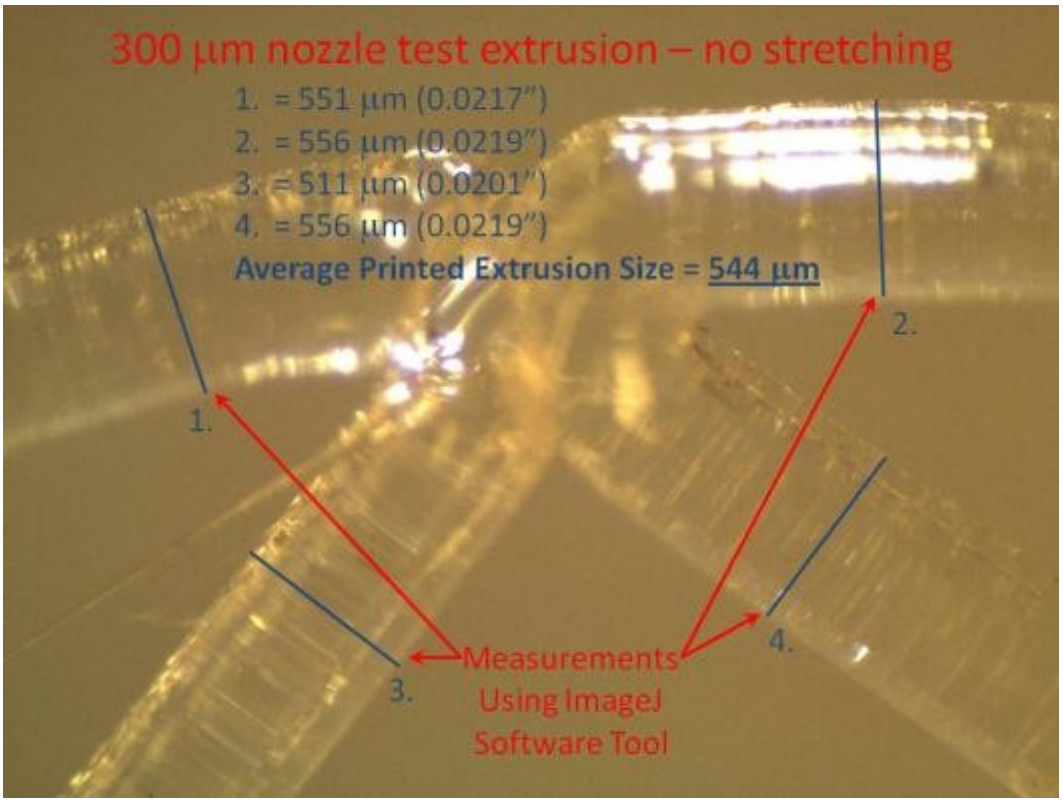

Measurements Using ImageJ Software - Circle Square Test Print – 300µm Nozzle - No Stretch

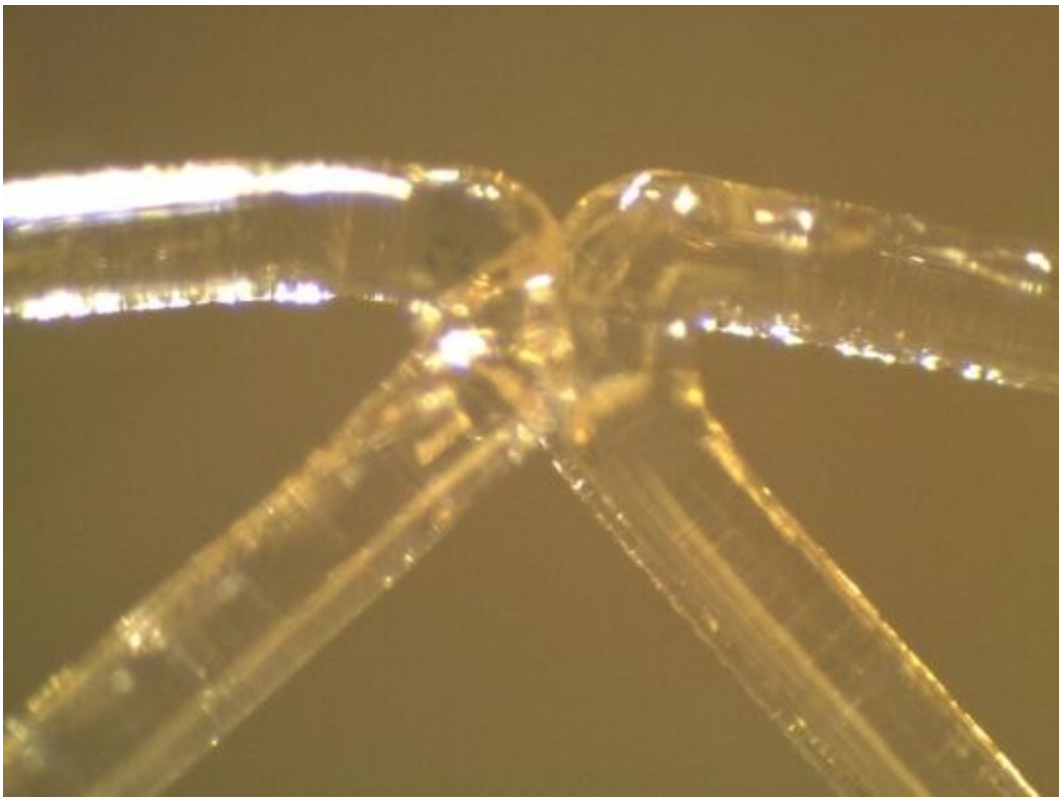

Circle Square Test Print – 300µm Nozzle - Stretched – Raw Image @ 35x

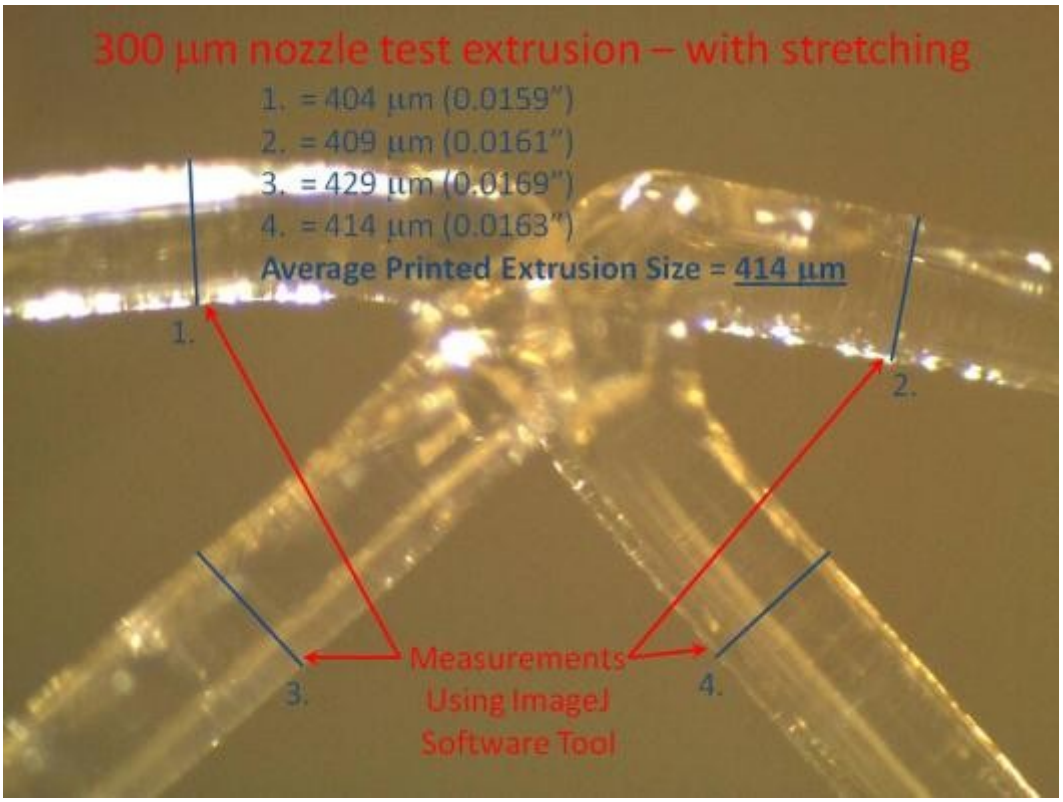

Measurements Using ImageJ Software - Circle Square Test Print – 300µm Nozzle – Stretched

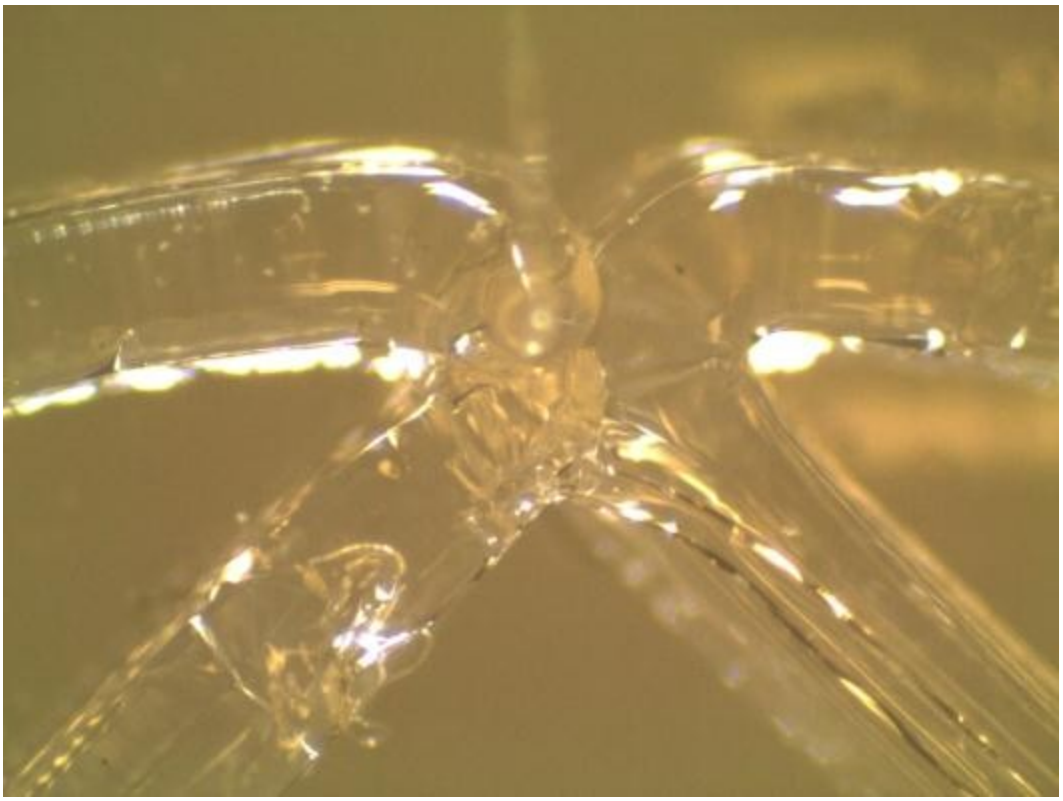

Circle Square Test Print – 400µm Nozzle - No Stretch – Raw Image @ 35x

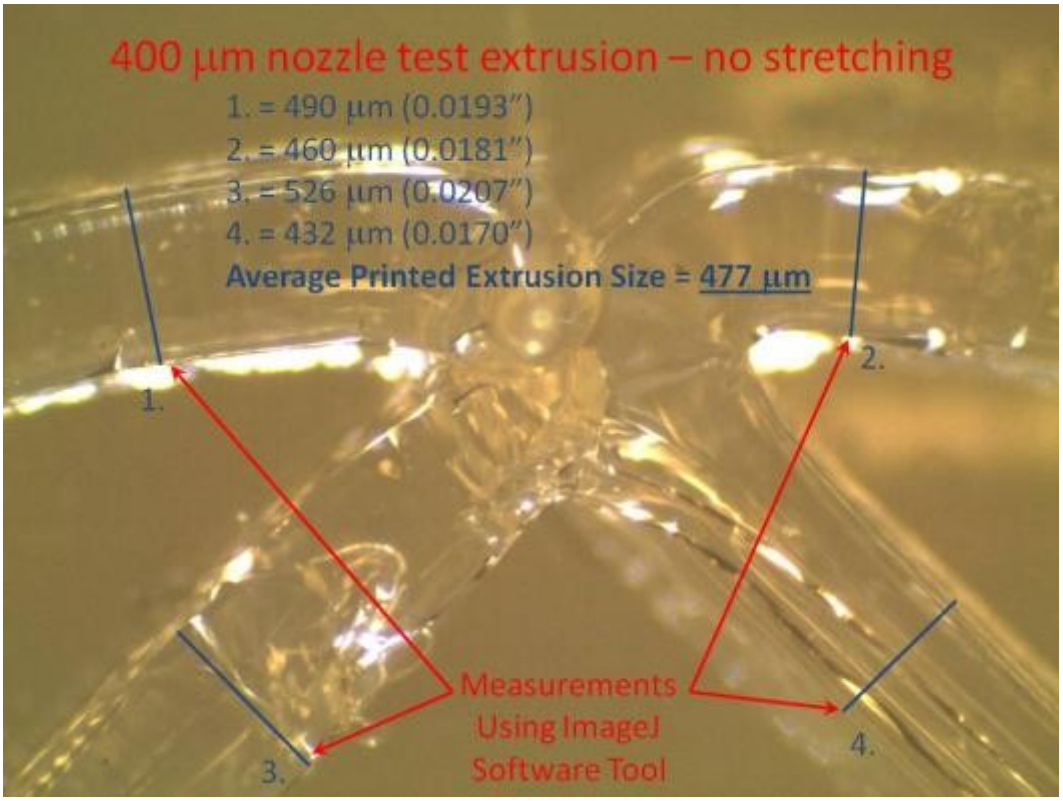

Measurements Using ImageJ Software - Circle Square Test Print – 400µm Nozzle - No Stretch

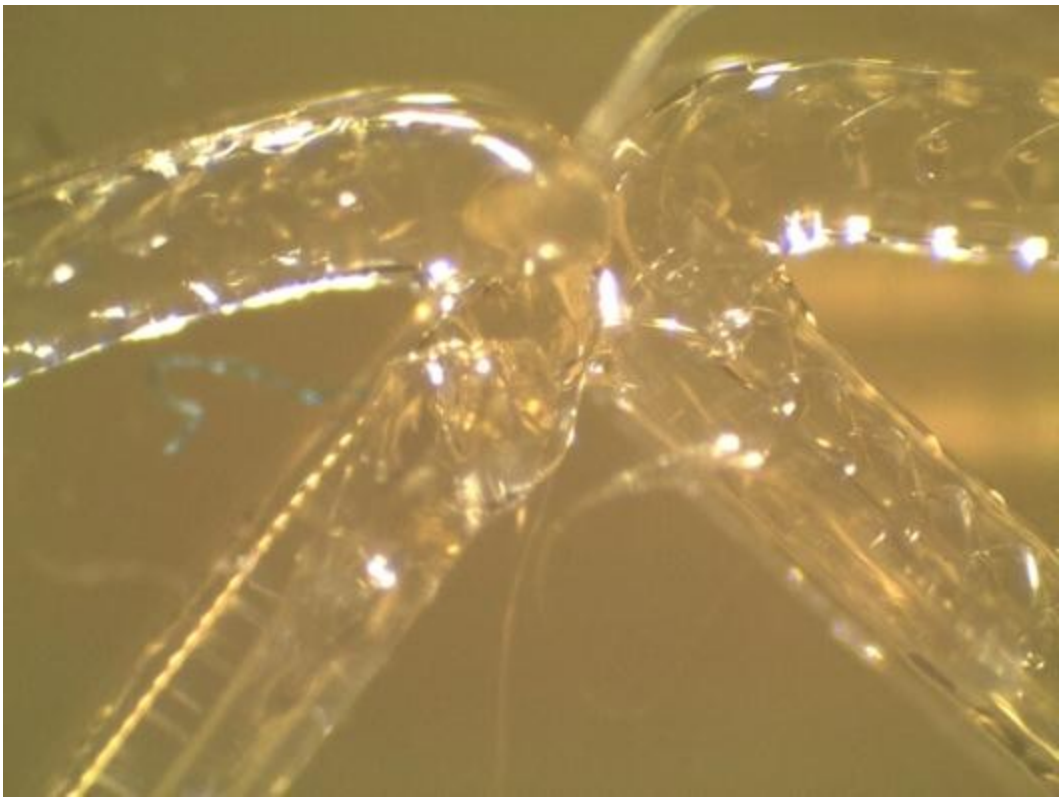

Circle Square Test Print – 400μm Nozzle - Stretched – Raw Image @ 35x

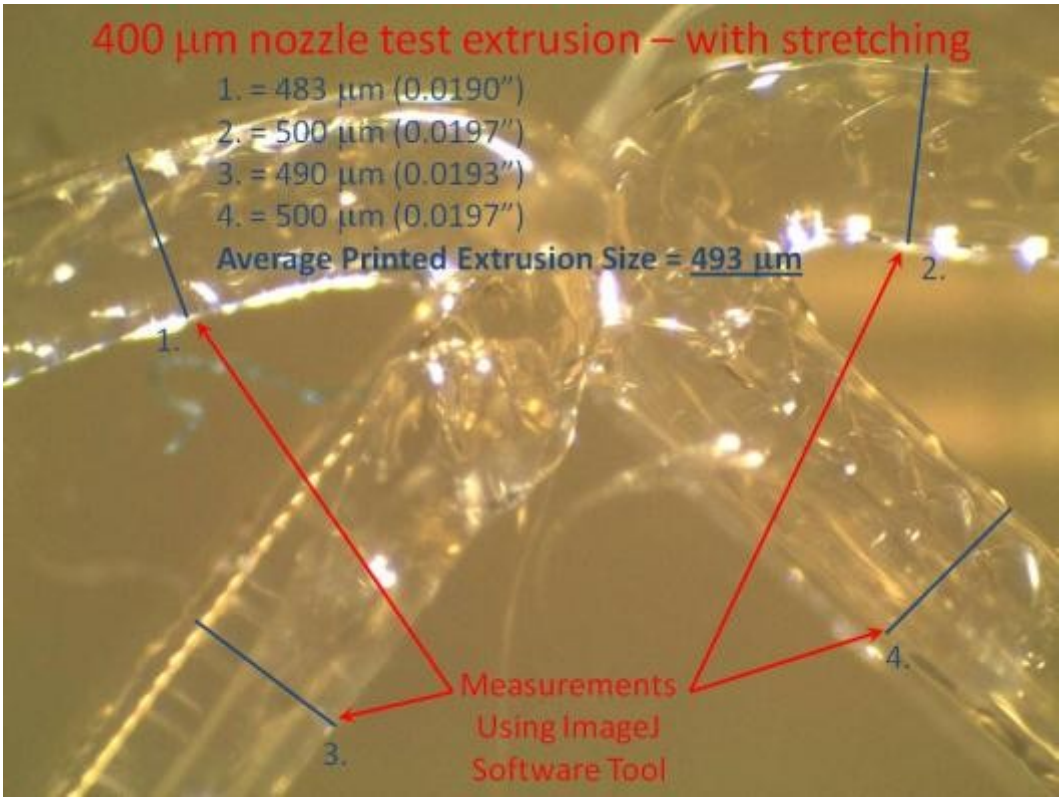

Measurements Using ImageJ Software - Circle Square Test Print – 400μm Nozzle – Stretched